nature
https://doi.org/10.1038/s41586-020-2491-6

Supplementary information

The timing and effect of the earliest human arrivals in North America

In the format provided by the authors and unedited

Lorena Becerra-Valdivia ✉ & Thomas Higham

SUPPLEMENTARY INFORMATION

The timing and effect of the earliest human arrivals in North America

Lorena Becerra-Valdivia[1,2] and Thomas Higham[1]

[1]Oxford Radiocarbon Accelerator Unit, Research Laboratory for Archaeology and History of Art, University of Oxford, Dyson Perrins Building, South Parks Road, OX1 3QY, Oxford, United Kingdom.
[2]Chronos ^{14}C-Cycle Facility, SSEAU, Mark Wainwright Analytical Centre Room G61, Chemical Sciences Building (F10), UNSW, Sydney, NSW 2052, Australia.

Table of Contents

1. Archaeological traditions discussed

1.1. Clovis

Clovis is the earliest, widespread cultural tradition of North America[1–4], dated in 2007 to 13,250-12,800 cal BP[5]. It is most commonly recognized by the presence of the Clovis projectile point, a fluted biface[6]. Clovis forms the basis of the 'Clovis-first' model, which stipulates that a group of big-game hunters initially entered North America from Asia ~13,5000 years ago via Beringia, moving southward through an ice-free corridor between the Laurentide and Cordilleran ice sheets. The technological origin of Clovis is yet unknown and it is generally believed to have developed in situ[7].

1.2. Western Stemmed tradition

Found in the Paleoindian record of the Intermountain West of North America, the Western Stemmed tradition (WST) is a non-fluted lithic technology dominated by large, generally narrow bifacial points with sloping shoulders and contracting, stem-like bases[8–12]. Through the dating of sites like Bonneville Estates, Cooper's Ferry, and Paisley Caves, this tradition is considered to be roughly coeval with or earlier than Clovis[8,9,13].

1.3. Beringian tradition

Reflecting the high degree of variability present in Beringia during the Pleistocene-Holocene transition, the Beringian tradition encompasses three main lithic industries[14–17]. Found in eastern Beringia, these include the Nenana, a non-microblade, biface-and-blade industry with Chindadn points (small and teardrop-shaped); the Denali, a distinctive microblade technology that generally postdates the Nenana; and the Northern Paleoindian, with bifacial, unfluted lanceolate points. Technology found at western Beringian sites, Ushki (component 7) and Berelekh, share similarities with Nenana[14].

2. Archaeological sites included

The 42 archaeological sites included in the analysis are listed alphabetically, according to category, and briefly described. Coordinates [noted in parentheses as 'latitude', 'longitude'; following the World Geodetic System (WGS84)], Bayesian age modelling notes and CQL code are provided for each. The latter can be copied into OxCal to replicate models. For multiple-phase sequences, brief notes are made regarding the degree of cultural association for the chronometric data included. Multimodal or highly imprecise start boundaries are highlighted and discussed. Generally, these features are caused by taphonomic issues, sampling/radiocarbon dating biases and/or unreliable chronometric data. The latter is a possibility given that, for objectivity, dates deemed problematic in the literature were not manually excluded. Instead, as noted in the Methods section, we relied on outlier analysis to objectively identify and down-weight outliers within the models. With the exception of five dates from Broken Mammoth (see section 2.1.2.) and Lubbock Lake (see section 2.3.3,), all dates were assigned a 0.05 probability of being an outlier.

2.1. Beringian tradition

2.1.1. Berelekh, eastern Siberia (Russia)

The Berelekh geoarchaeological complex (at 70.500000, 144.033333) contains a mammoth bone bed ("graveyard") and a stratified archaeological site[18–20]. Although there is no evidence of human contribution to the former, cut-marked faunal bones and lithic artifacts are found within the latter. In 2009, test excavations were performed in a number of terraces within the complex. In terrace 2 (T2; profile BA1), cultural material was found within layer 2 and dates obtained provide stratigraphic control. Using chronometric data from this section, the model created dates the start of the cultural component at Berelekh to 14,315-13,835 cal BP (Fig. S1). T2 BA1 was chosen as Beta-269470 and -269447 are the only two samples noted as belonging to a "culture-bearing layer"[19]. Directly dated human-modified osseous tools are noted as surface finds[19].

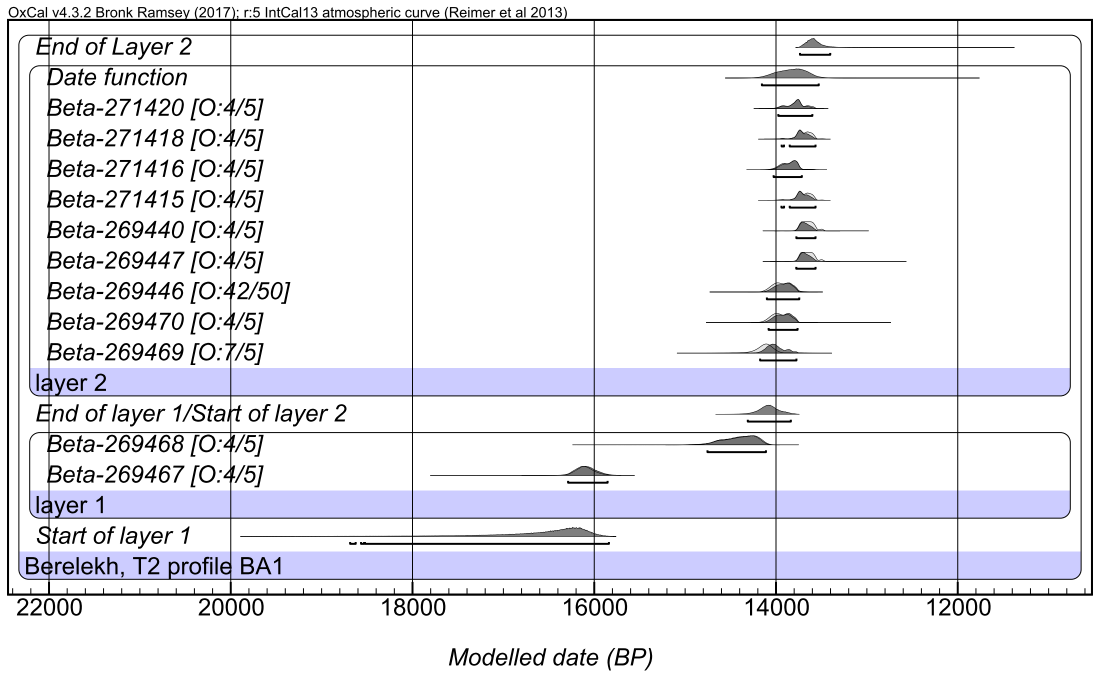

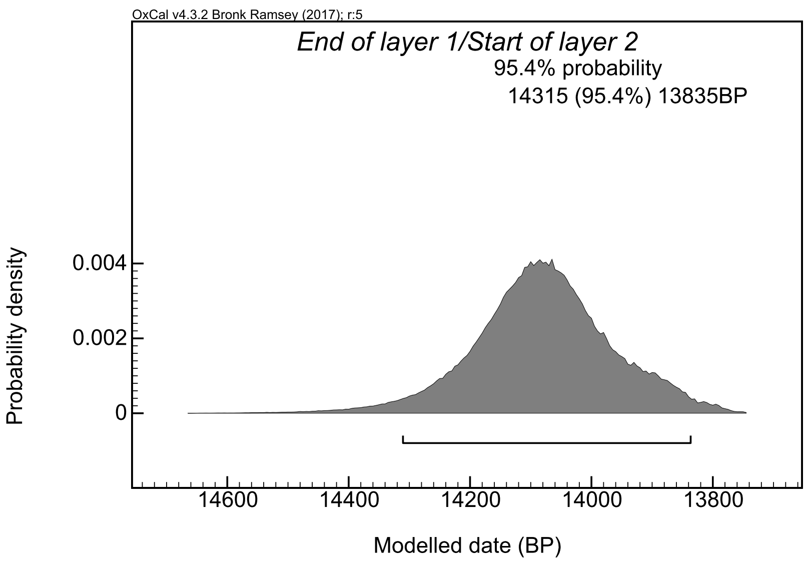

Fig. S1. Bayesian age model for Berelekh (T2; profile BA1; above), and start `Boundary` (below). Brackets beneath each age estimate show 95.4% confidence interval. 'O:prior/posterior probability' reflects the outlier analysis.

```
Plot()
{
 Outlier_Model("General",T(5),U(0,4),"t");
 Sequence("Berelehk, T2 profile BA1")
 {
  Boundary("Start of layer 1");
  Phase("layer 1")
  {
   R_Date("Beta-269467", 13390, 60)
   {
    Outlier("General", 0.05);
   };
   R_Date("Beta-269468", 12350, 60)
   {
    Outlier("General", 0.05);
   };
  };
  Boundary("End of layer 1/Start of layer 2");
  Phase("layer 2")
  {
   R_Date("Beta-269469", 12220, 60)
   {
    Outlier("General", 0.05);
   };
   R_Date("Beta-269470", 12100, 60)
   {
    Outlier("General", 0.05);
   };
   R_Date("Beta-269446", 12090, 60)
   {
    Outlier("General", 0.5);
   };
   R_Date("Beta-269447", 11830, 60)
   {
    Outlier("General", 0.05);
   };
   R_Date("Beta-269440", 11830, 60)
   {
    Outlier("General", 0.05);
   };
   R_Date("Beta-271415", 11890, 60)
   {
    Outlier("General", 0.05);
   };
   R_Date("Beta-271416", 11990, 60)
   {
    Outlier("General", 0.05);
   };
   R_Date("Beta-271418", 11890, 60)
   {
    Outlier("General", 0.05);
   };
   R_Date("Beta-271420", 11940, 60)
   {
    Outlier("General", 0.05);
   };
   Date("Date function");
  };
  Boundary("End of Layer 2");
 };
};
```

2.1.2. Broken Mammoth, Alaska (U.S.A.)

Broken Mammoth (XBD-131; at 64.266667, -146.116667) is a stratified archaeological site containing four Cultural Zones, with Cultural Zone 4 (C and B) representing the earliest human occupation[16,17,21–24]. Dates obtained provide stratigraphic control or date cultural features directly, e.g., hearth charcoal. Using these data, the model created places the start of Cultural Zone 4 at 14,130-13,255 cal BP (Fig. S2). CAMS-9898, within Cultural Zone 4 and deemed as an old ivory date by the archaeologists, was given an outlier probability of 1.

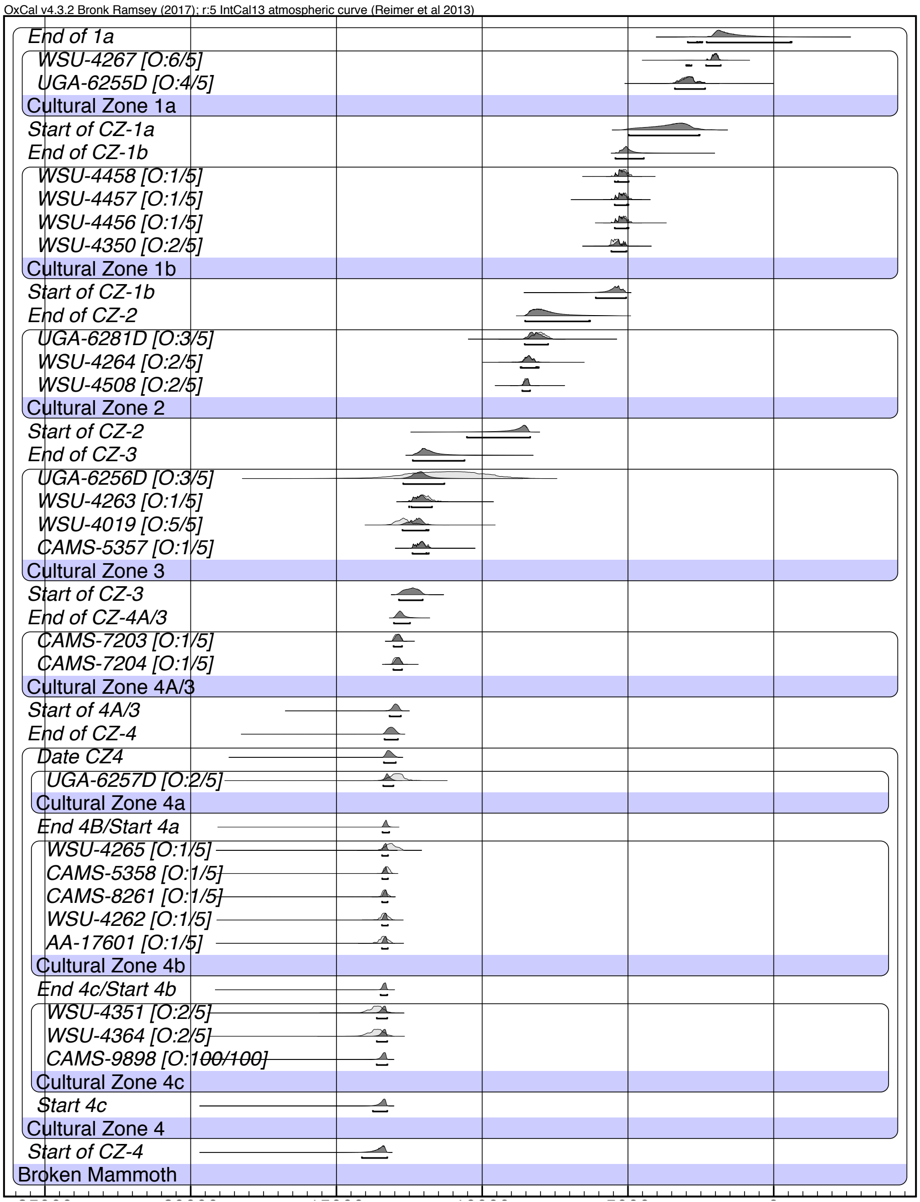

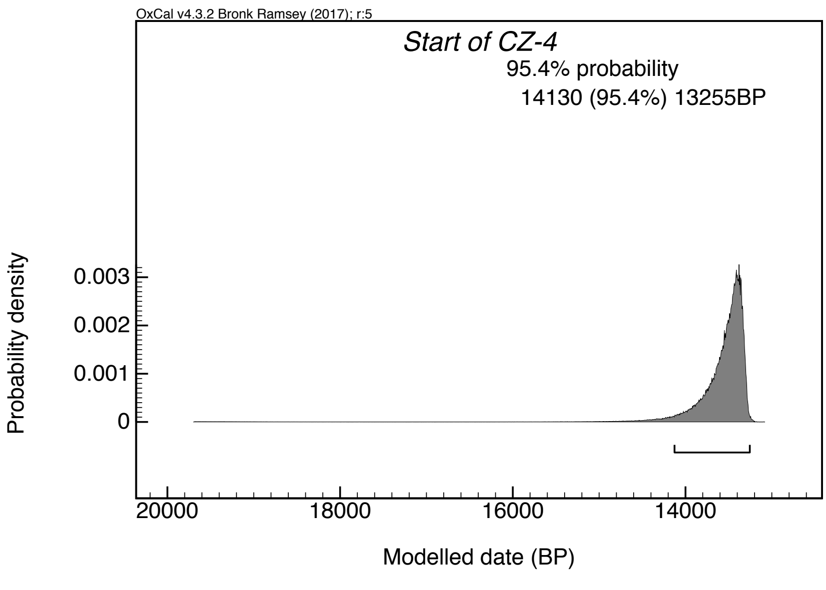

Fig. S2. Bayesian age model for Broken Mammoth (above), and start `Boundary` (below). Brackets beneath each age estimate show 95.4% confidence interval. 'O:prior/posterior probability' reflects the outlier analysis.

```
Plot()
{
Outlier_Model("General",T(5),U(0,4),"t");
Sequence("Broken Mammoth")
 {
 Boundary("Start of CZ-4");
 Sequence("Cultural Zone 4")
  {
  Boundary("Start 4c");
  Phase("Cultural Zone 4c")
   {
   R_Date("CAMS-9898", 15830, 70)
    {
    Outlier("General", 1.00);
    };
   R_Date("WSU-4364", 11770, 220)
    {
    Outlier("General", 0.05);
    };
   R_Date("WSU-4351", 11770, 210)
    {
    Outlier("General", 0.05);
    };
   };
  Boundary("End 4c/Start 4b");
  Phase("Cultural Zone 4b")
   {
   R_Date("AA-17601", 11540, 140)
    {
    Outlier("General", 0.05);
    };
   R_Date("WSU-4262", 11510, 120)
    {
    Outlier("General", 0.05);
    };
   R_Date("CAMS-8261", 11500, 80)
    {
    Outlier("General", 0.05);
    };
   R_Date("CAMS-5358", 11420, 70)
    {
    Outlier("General", 0.05);
    };
   R_Date("WSU-4265", 11280, 190)
    {
    Outlier("General", 0.05);
    };
   };
  Boundary("End 4B/Start 4a");
  Phase("Cultural Zone 4a")
   {
   R_Date("UGA-6257D", 11040, 260)
    {
    Outlier("General", 0.05);
    };
   };
  Date("Date CZ4");
  };
 Boundary("End of CZ-4 ");
 Boundary("Start of 4A/3");
 Phase("Cultural Zone 4A/3")
  {
  R_Date("CAMS-7204", 11060, 90)
   {
   Outlier("General", 0.05);
   };
  R_Date("CAMS-7203", 11040, 80)
   {
   Outlier("General", 0.05);
   };
  };
 Boundary("End of CZ-4A/3");
 Boundary("Start of CZ-3");
 Phase("Cultural Zone 3")
  {
  R_Date("CAMS-5357", 10290, 70)
   {
   Outlier("General", 0.05);
   };
  R_Date("WSU-4019", 10790, 230)
   {
   Outlier("General", 0.05);
   };
  R_Date("WSU-4263", 10270, 110)
   {
   Outlier("General", 0.05);
   };
  R_Date("UGA-6256D", 9690, 960)
   {
   Outlier("General", 0.05);
   };
  };
 Boundary("End of CZ-3");
 Boundary("Start of CZ-2");
 Phase("Cultural Zone 2")
  {
  R_Date("WSU-4508", 7700, 80)
   {
   Outlier("General", 0.05);
   };
  R_Date("WSU-4264", 7600, 140)
   {
   Outlier("General", 0.05);
   };
  R_Date("UGA-6281D", 7200, 205)
   {
   Outlier("General", 0.05);
   };
  };
 Boundary("End of CZ-2");
 Boundary("Start of CZ-1b");
 Phase("Cultural Zone 1b")
  {
  R_Date("WSU-4350", 4690, 110)
   {
   Outlier("General", 0.05);
   };
  R_Date("WSU-4456", 4540, 90)
   {
   Outlier("General", 0.05);
   };
  R_Date("WSU-4457", 4545, 90)
   {
   Outlier("General", 0.05);
   };
  R_Date("WSU-4458", 4525, 90)
   {
   Outlier("General", 0.05);
   };
  };
 Boundary("End of CZ-1b");
 Boundary("Start of CZ-1a");
 Phase("Cultural Zone 1a")
  {
  R_Date("UGA-6255D", 2815, 180)
   {
   Outlier("General", 0.05);
   };
  R_Date("WSU-4267", 2040, 65)
   {
   Outlier("General", 0.05);
   };
  };
 Boundary("End of 1a");
 };
};
```

2.1.3. Dry Creek, Alaska (U.S.A.)

Dry Creek (HEA-005; at 63.883333, -149.033333) is a stratified site containing four cultural components, with I and II representing the earliest occupations[25–33]. Based on lithic technology and antiquity, Component I has been assigned to the Nenana complex, whilst Component II to the Denali. Using the latest chronometric data obtained from cultural features, e.g., hearth charcoal[33], the model created places the start of Component I at 13,700-13,350 cal BP (Fig. S3).

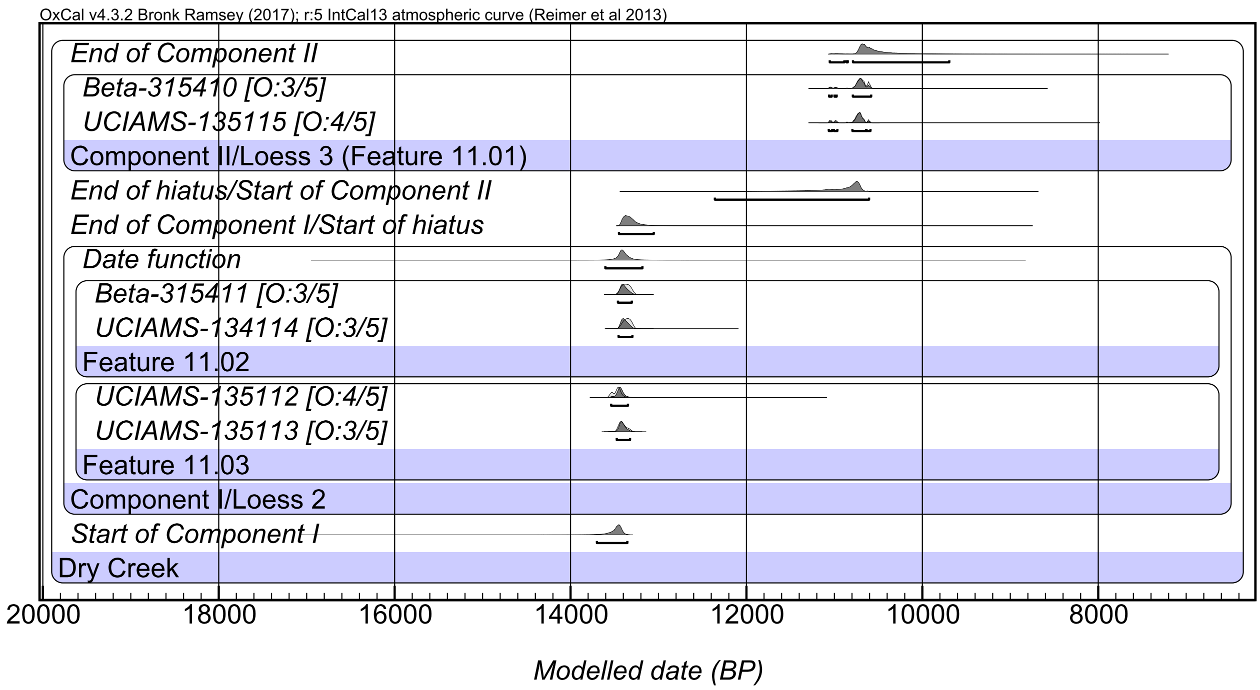

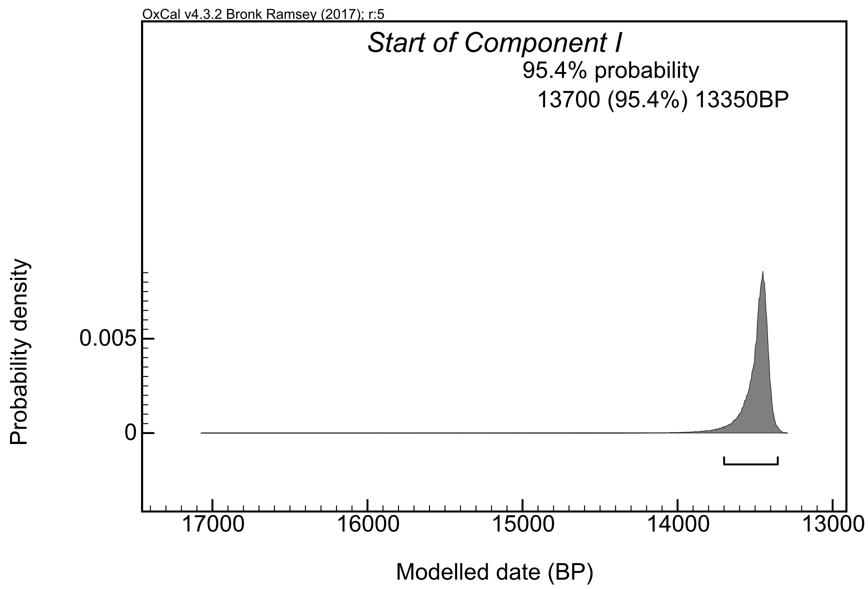

Fig. S3. Bayesian age model for Dry Creek (above), and start `Boundary` (below). Brackets beneath each age estimate show 95.4% confidence interval. 'O:prior/posterior probability' reflects the outlier analysis.

```
Plot()
{
 Outlier_Model("General",T(5),U(0,4),"t");
 Sequence("Dry Creek")
 {
  Boundary("Start of Component I");
  Phase("Component I/Loess 2")
  {
   Phase("Feature 11.03")
   {
    R_Date("UCIAMS-135113", 11580, 40)
```

```
  {
   Outlier("General", 0.05);
  };
  R_Date("UCIAMS-135112", 11635, 40)
  {
   Outlier("General", 0.05);
  };
 };
 Phase("Feature 11.02")
 {
  R_Date("UCIAMS-134114", 11510, 40)
  {
   Outlier("General", 0.05);
  };
  R_Date("Beta-315411", 11530, 50)
  {
   Outlier("General", 0.05);
  };
 };
 Date("Date function");
};
Boundary("End of Component I/Start of hiatus");
Boundary("End of hiatus/Start of Component II");
Phase("Component II/Loess 3 (Feature 11.01)")
{
 R_Date("UCIAMS-135115", 9480, 35)
 {
  Outlier("General", 0.05);
 };
 R_Date("Beta-315410", 9460, 40)
 {
  Outlier("General", 0.05);
 };
};
Boundary("End of Component II");
};
};
```

2.1.4. Mead, Alaska (U.S.A.)

Mead (XBD-071; at approximately 64.271001, -146.075173) is a stratified site containing five Cultural Zones (CZ), with CZ-4 representing the earliest human occupation[16,17,21,34,35]. Using the latest chronometric data obtained for the 2009/2011 excavations[17,34,35], which provide stratigraphic control or date cultural features directly, e.g., hearth charcoal, the model created places the start of CZ-4 at 13,520-13,010 cal BP (Fig. S4).

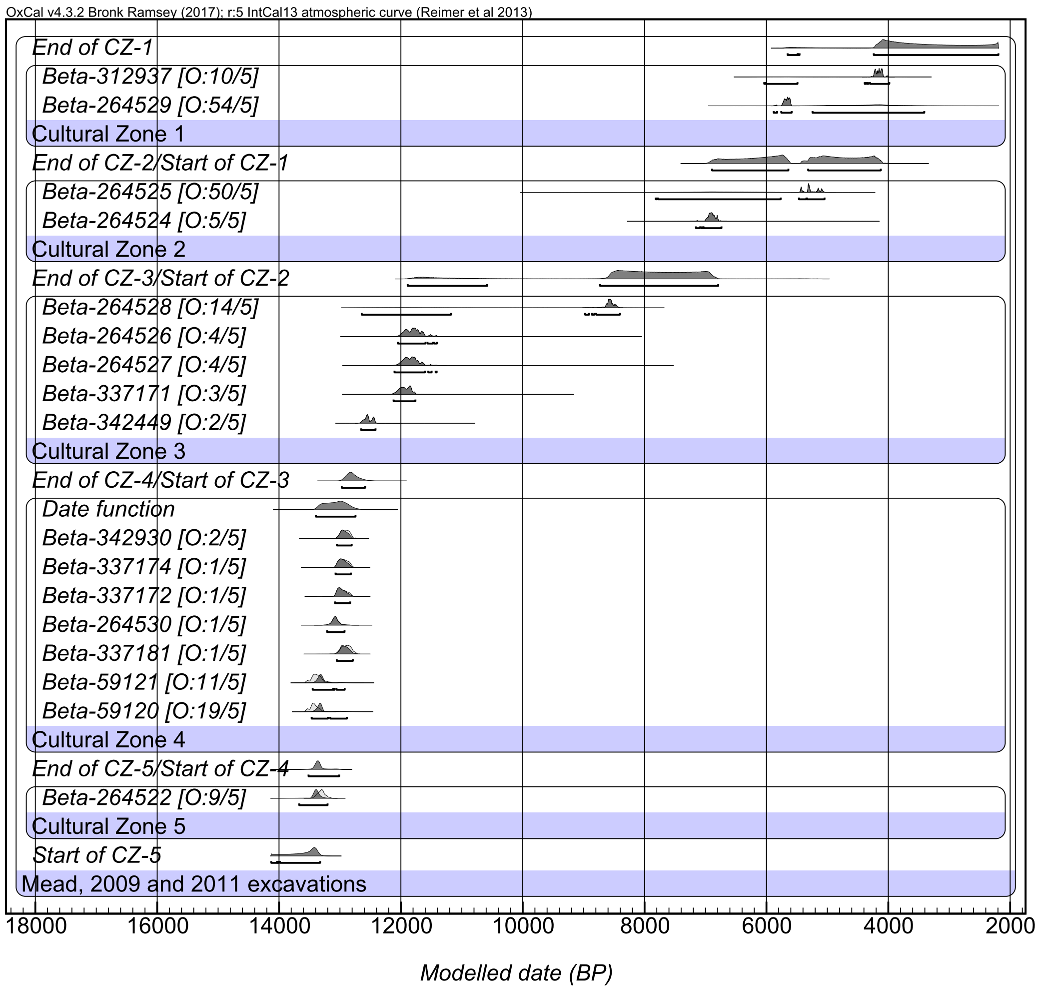

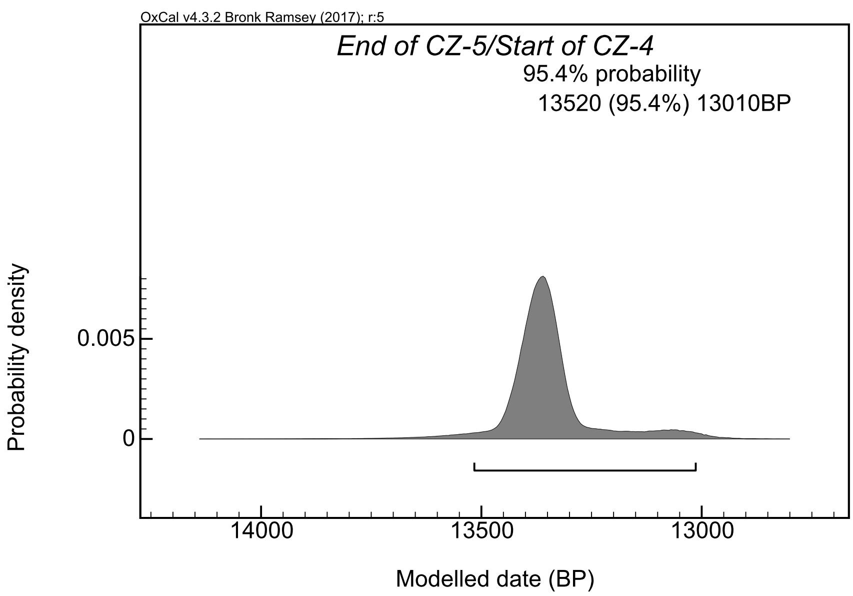

Fig. S4. Bayesian age model for Mead (above), and start `Boundary` (below). Brackets beneath each age estimate show 95.4% confidence interval. 'O:prior/posterior probability' reflects the outlier analysis.

```
Plot()
{
 Outlier_Model("General",T(5),U(0,4),"t");
 Sequence("Mead, 2009 and 2011 excavations")
 {
  Boundary("Start of CZ-5");
  Phase("Cultural Zone 5")
  {
   R_Date("Beta-264522", 11460, 50)
   {
    Outlier("General", 0.05);
```

```
   };
  };
  Boundary("End of CZ-5/Start of CZ-4");
  Phase("Cultural Zone 4")
  {
   R_Date("Beta-59120", 11600, 60)
   {
    Outlier("General", 0.05);
   };
   R_Date("Beta-59121", 11560, 80)
   {
    Outlier("General", 0.05);
   };
   R_Date("Beta-337181", 11030, 50)
   {
    Outlier("General", 0.05);
   };
   R_Date("Beta-264530", 11210, 60)
   {
    Outlier("General", 0.05);
   };
   R_Date("Beta-337172", 11100, 50)
   {
    Outlier("General", 0.05);
   };
   R_Date("Beta-337174", 11080, 50)
   {
    Outlier("General", 0.05);
   };
   R_Date("Beta-342930", 11050, 40)
   {
    Outlier("General", 0.05);
   };
   Date("Date function");
  };
  Boundary("End of CZ-4/Start of CZ-3");
  Phase("Cultural Zone 3")
  {
   R_Date("Beta-342449", 10560, 40)
   {
    Outlier("General", 0.05);
   };
   R_Date("Beta-337171", 10220, 40)
   {
    Outlier("General", 0.05);
   };
   R_Date("Beta-264527", 10160, 50)
   {
    Outlier("General", 0.05);
   };
   R_Date("Beta-264526", 10140, 50)
   {
    Outlier("General", 0.05);
   };
   R_Date("Beta-264528", 7790, 50)
   {
    Outlier("General", 0.05);
   };
  };
  Boundary("End of CZ-3/Start of CZ-2");
  Phase("Cultural Zone 2")
  {
   R_Date("Beta-264524", 6050, 40)
   {
    Outlier("General", 0.05);
   };
   R_Date("Beta-264525", 4580, 40)
   {
    Outlier("General", 0.05);
   };
  };
  Boundary("End of CZ-2/Start of CZ-1");
  Phase("Cultural Zone 1")
  {
   R_Date("Beta-264529", 4940, 40)
   {
    Outlier("General", 0.05);
   };
   R_Date("Beta-312937", 3780, 30)
   {
    Outlier("General", 0.05);
   };
  };
  Boundary("End of CZ-1");
 };
};
```

2.1.5. Mesa, Alaska (U.S.A.)

Mesa (KIR-102; at approximately 68.439857, -155.813683) is a multi-cluster site containing over fifteen hearths with associated Northern Paleoindian and microblade lithic industries[36–40]. All but one measurement obtained date cultural features directly, e.g., hearth charcoal. The exception was measured from "soil charcoal" (Beta-36805/ETH-6570) and provides stratigraphic control. Using these data, a single `Phase` model was built, dating the cultural component to 13,910-9,355 cal BP (`Date` function; Fig. S5).

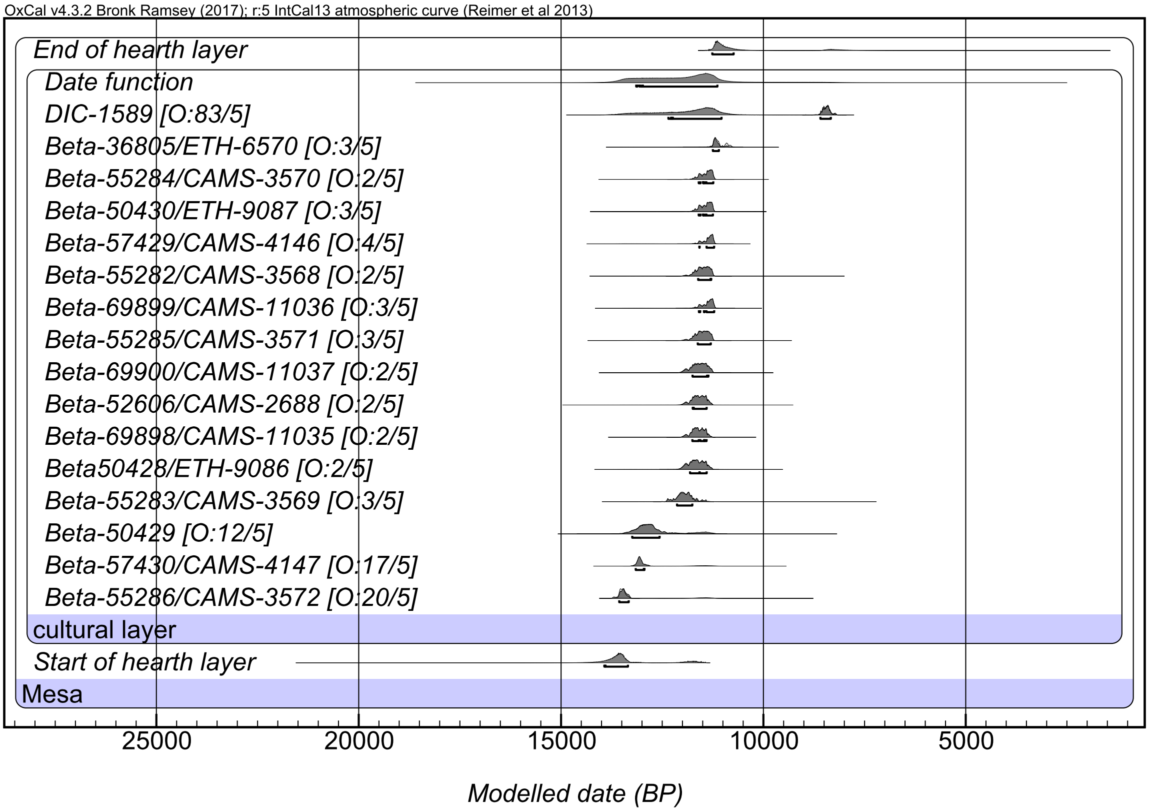

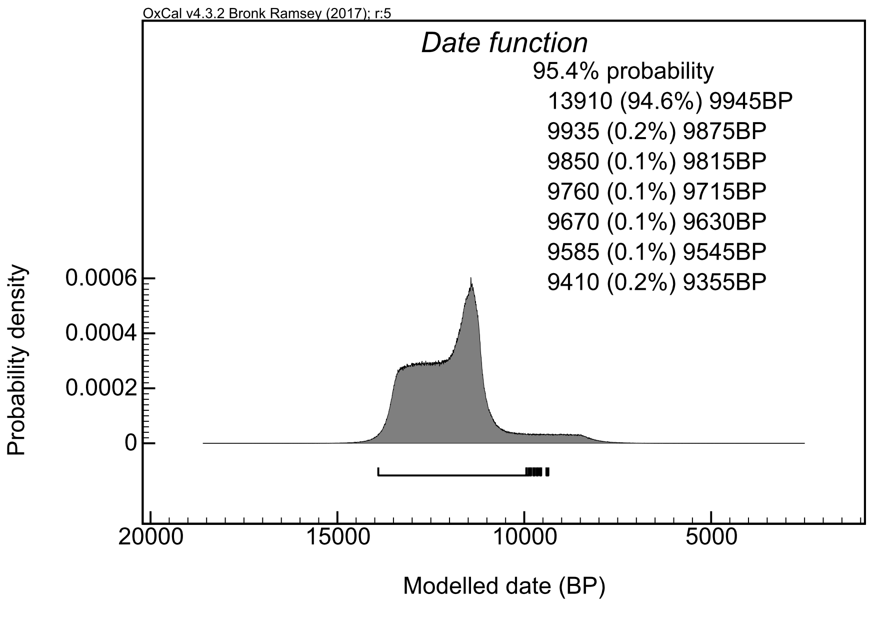

Fig. S5. Bayesian age model for Mesa (above), and `Date` function (below). Brackets beneath each age estimate show 95.4% confidence interval. 'O:prior/posterior probability' reflects the outlier analysis.

```
Plot()
{
 Outlier_Model("General",T(5),U(0,4),"t");
 Sequence("Mesa")
 {
  Boundary("Start of hearth layer");
  Phase("cultural layer")
  {
   R_Date("Beta-55286/CAMS-3572", 11660, 80)
   {
    Outlier("General", 0.05);
   };
   R_Date("Beta-57430/CAMS-4147", 11190, 70)
   {
    Outlier("General", 0.05);
   };
   R_Date("Beta-50429", 10980, 280)
   {
    Outlier("General", 0.05);
   };
   R_Date("Beta-55283/CAMS-3569", 10240, 80)
   {
    Outlier("General", 0.05);
```

```
  };
  R_Date("Beta50428/ETH-9086", 10090, 85)
  {
   Outlier("General", 0.05);
  };
  R_Date("Beta-69898/CAMS-11035", 10070, 60)
  {
   Outlier("General", 0.05);
  };
  R_Date("Beta-52606/CAMS-2688", 10060, 70)
  {
   Outlier("General", 0.05);
  };
  R_Date("Beta-69900/CAMS-11037", 10050, 90)
  {
   Outlier("General", 0.05);
  };
  R_Date("Beta-55285/CAMS-3571", 10000, 80)
  {
   Outlier("General", 0.05);
  };
  R_Date("Beta-69899/CAMS-11036", 9900, 80)
  {
   Outlier("General", 0.05);
  };
  R_Date("Beta-55282/CAMS-3568", 9990, 80)
  {
   Outlier("General", 0.05);
  };
  R_Date("Beta-57429/CAMS-4146", 9900, 70)
  {
   Outlier("General", 0.05);
  };
  R_Date("Beta-50430/ETH-9087", 9945, 75)
  {
   Outlier("General", 0.05);
  };
  R_Date("Beta-55284/CAMS-3570", 9930, 80)
  {
   Outlier("General", 0.05);
  };
  R_Date("Beta-36805/ETH-6570", 9730, 80)
  {
   Outlier("General", 0.05);
  };
  R_Date("DIC-1589", 7620, 95)
  {
   Outlier("General", 0.05);
  };
  Date("Date function");
 };
 Boundary("End of hearth layer");
 };
};
```

2.1.6. Moose Creek, Alaska (USA)

Moose Creek (FAI-206; at 64.066667, -149.100000) is a stratified site containing four cultural components[28,30,41–43]. Based on lithic technology and antiquity, Component I has been assigned to the Nenana complex, Component II to Denali I, and Component III to Denali II[41]. Only three dates obtained are considered to date cultural features directly (measured from hearth charcoal), whilst the rest are soil organics (in this case, located between Components I and II) and provide stratigraphic control. Using these data, the model created places the start of Component I at 15,195-12,865 cal BP or 13,735-12,980 cal BP (68.2% CI; Fig. S6). Given the results of the outlier analysis, however, further chronometric work is required to better define the chronology at this site.

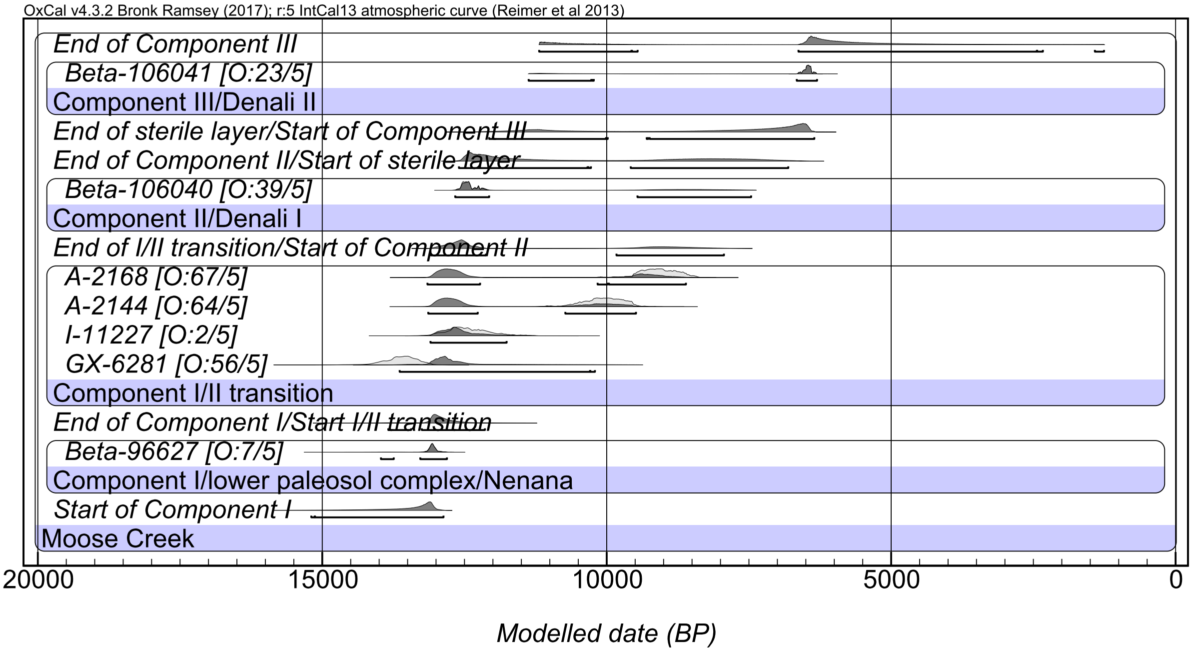

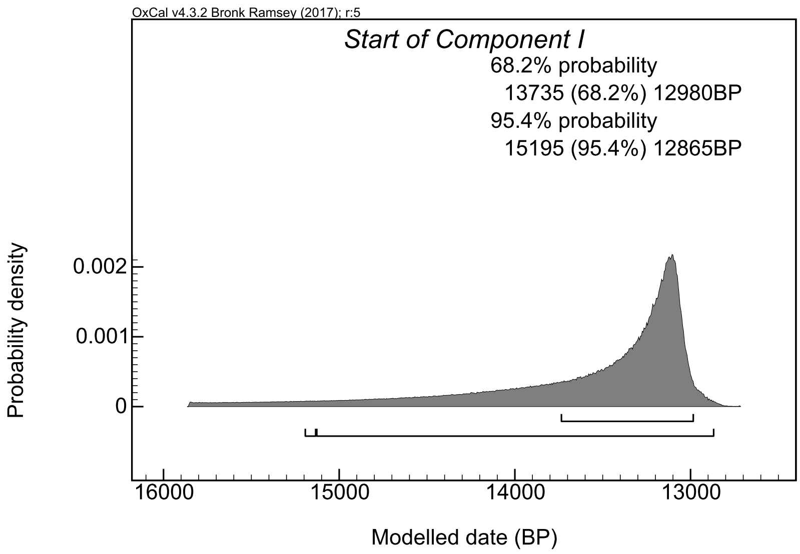

Fig. S6. Bayesian age model for Moose Creek (above), and start `Boundary` (below). Brackets beneath each age estimate show 95.4% and 68.2% confidence intervals. 'O:prior/posterior probability' reflects the outlier analysis.

```
Plot()
{
 Outlier_Model("General",T(5),U(0,4),"t");
 Sequence("Moose Creek")
 {
  Boundary("Start of Component I");
  Phase("Component I/lower paleosol complex/Nenana")
  {
   R_Date("Beta-96627", 11190, 60)
   {
    Outlier("General", 0.05);
   };
  };
  Boundary("End of Component I/Start I/II transition");
  Phase("Component I/II transition")
  {
   R_Date("GX-6281", 11730, 250)
   {
    Outlier("General", 0.05);
   };
   R_Date("I-11227", 10640, 280)
   {
    Outlier("General", 0.05);
   };
   R_Date("A-2144", 8940, 270)
   {
    Outlier("General", 0.05);
   };
   R_Date("A-2168", 8160, 260)
   {
    Outlier("General", 0.05);
   };
  };
  Boundary("End of I/II transition/Start of Component II");
  Phase("Component II/Denali I")
  {
   R_Date("Beta-106040", 10500, 60)
   {
    Outlier("General", 0.05);
```

```
   };
  };
  Boundary("End of Component II/Start of sterile layer");
  Boundary("End of sterile layer/Start of Component III");
  Phase("Component III/Denali II")
  {
   R_Date("Beta-106041", 5680, 50)
   {
    Outlier("General", 0.05);
   };
  };
  Boundary("End of Component III");
 };
};
```

2.1.7. Owl Ridge, Alaska (U.S.A.)

Owl Ridge (FAI-91; at 64.0125, -149.556944) is a stratified archaeological site containing three cultural components[30,44–46]. Based on lithic technology and antiquity, Component 1 has been assigned to the Nenana complex, whilst Component 2-3 to the Denali[46]. Using the latest chronometric data obtained for the 2007/2009/2010 excavations[46] (those clearly denoted from Components 1-3), the model created places the start of Component 1 at 14,315-12,745 cal BP (Fig. S7). Only two dates obtained are considered to directly date a cultural feature (hearth F10.01; Beta-289379 and -330172), whilst the rest are wood charcoals that provide stratigraphic control[46].

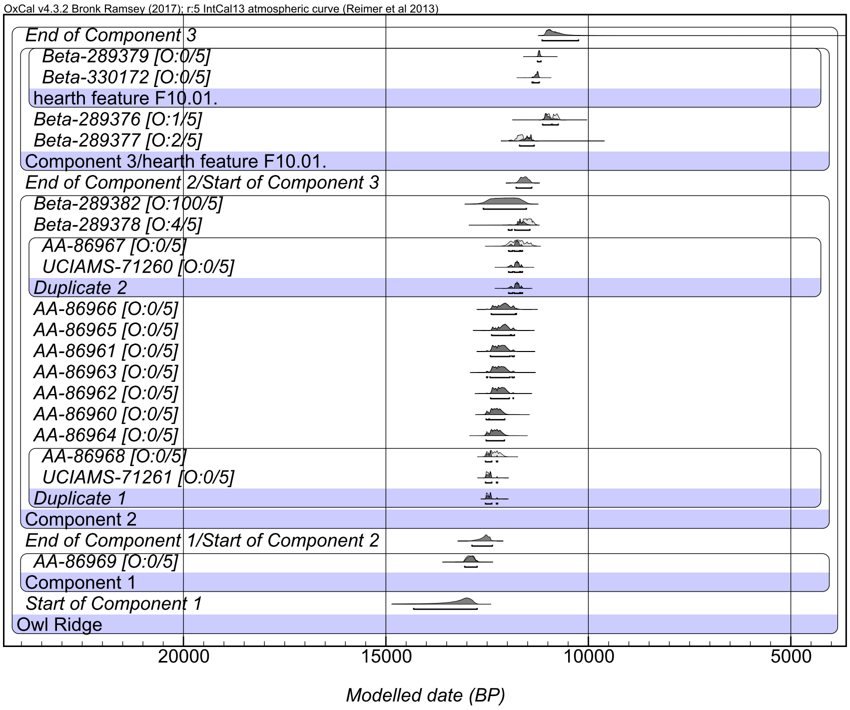

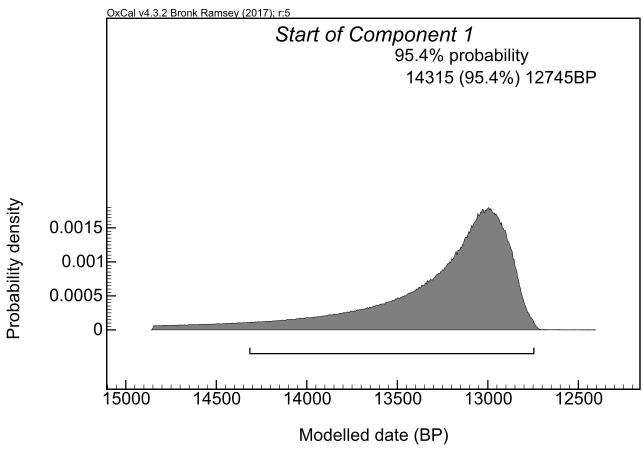

Fig. S7. Bayesian age model for Owl Ridge (above), and start `Boundary` (below). Brackets beneath each age estimate show 95.4% confidence interval. 'O:prior/posterior probability' reflects the outlier analysis.

```
Plot()
{
 Outlier_Model("General",T(5),U(0,4),"t");
 Outlier_Model("SSimple",N(0,2),0,"s");
 Sequence("Owl Ridge")
 {
  Boundary("Start of Component 1");
  Phase("Component 1")
  {
   R_Date("AA-86969", 11060, 60)
   {
    Outlier("General", 0.05);
   };
  };
  Boundary("End of Component 1/Start of Component 2");
  Phase("Component 2")
  {
   Combine("Duplicate 1")
   {
    R_Date("UCIAMS-71261", 10485, 25)
    {
     Outlier("SSimple", 0.05);
    };
    R_Date("AA-86968", 10440, 60)
    {
     Outlier("SSimple", 0.05);
    };
    Outlier("General", 0.05);
   };
   R_Date("AA-86964", 10420, 60)
   {
    Outlier("General", 0.05);
   };
   R_Date("AA-86960", 10415, 60)
   {
    Outlier("General", 0.05);
   };
   R_Date("AA-86962", 10335, 60)
   {
    Outlier("General", 0.05);
   };
   R_Date("AA-86963", 10340, 75)
   {
    Outlier("General", 0.05);
   };
   R_Date("AA-86961", 10330, 70)
   {
    Outlier("General", 0.05);
   };
   R_Date("AA-86965", 10295, 60)
   {
    Outlier("General", 0.05);
   };
   R_Date("AA-86966", 10290, 75)
   {
    Outlier("General", 0.05);
   };
   Combine("Duplicate 2")
   {
    R_Date("UCIAMS-71260", 10125, 20)
    {
     Outlier("SSimple", 0.05);
    };
    R_Date("AA-86967", 10120, 75)
    {
     Outlier("SSimple", 0.05);
    };
    Outlier("General", 0.05);
   };
   R_Date("Beta-289378", 10020, 40)
   {
    Outlier("General", 0.05);
   };
   R_Date("Beta-289382", 80, 40)
   {
    Outlier("General", 0.05);
   };
  };
  Boundary("End of Component 2/Start of Component 3");
  Phase("Component 3/hearth feature F10.01.")
  {
   R_Date("Beta-289377", 10080, 40)
   {
    Outlier("General", 0.05);
   };
   R_Date("Beta-289376", 9550, 40)
   {
    Outlier("General", 0.05);
   };
   Phase("hearth feature F10.01.")
   {
    R_Date("Beta-330172", 9880, 40)
    {
     Outlier("General", 0.05);
    };
    R_Date("Beta-289379", 9790, 40)
    {
     Outlier("General", 0.05);
    };
   };
  };
  Boundary("End of Component 3");
 };
};
```

2.1.8. Swan Point, Alaska (U.S.A.)

Swan Point (XBD-156; at 63.300000, -146.033333) is a stratified archaeological site containing four Cultural Zones [16,30,47–50]. Cultural Zone 4b, the earliest occupational layer, contains microblade technology that has been linked[51] to the Siberian Diuktai culture[52]. Dates obtained provide stratigraphic control or date cultural features directly, e.g., hearth charcoal. Using these data, the model created places its start at 14,650-14,150 cal BP (Fig. S8).

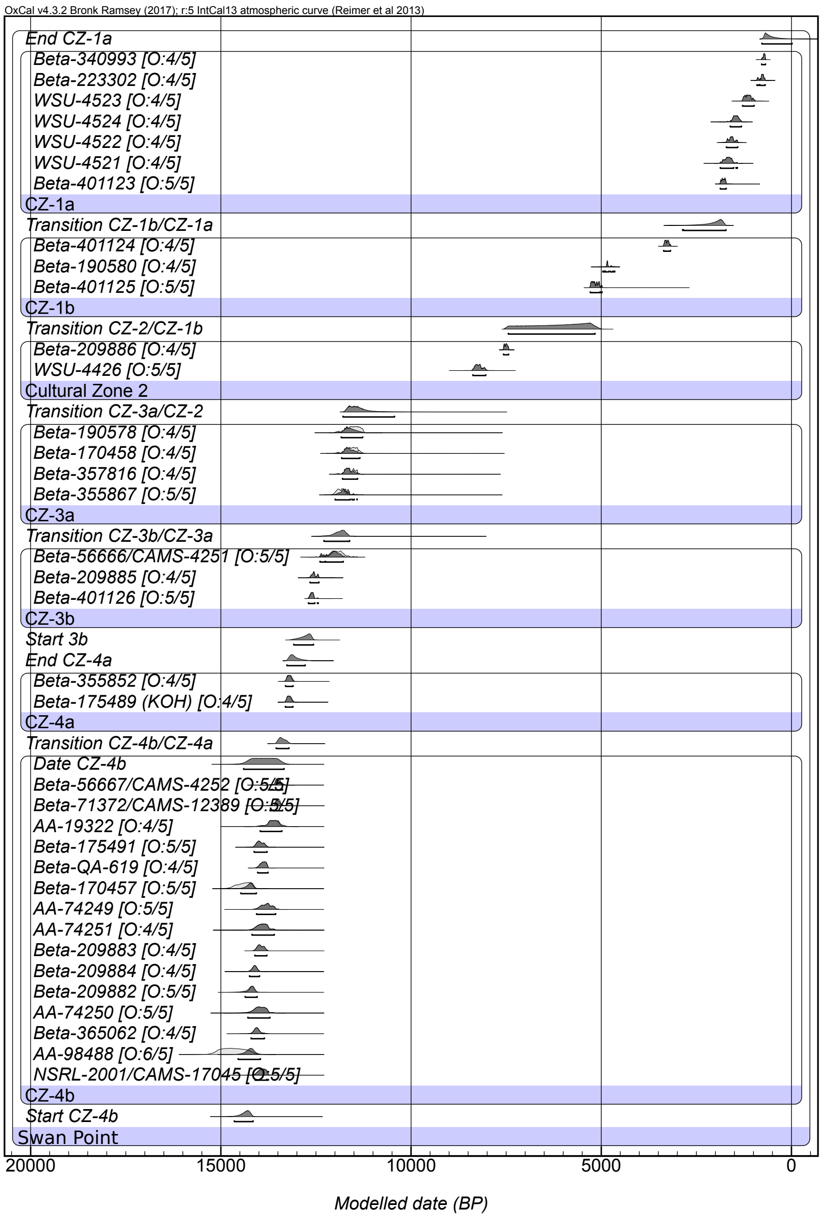

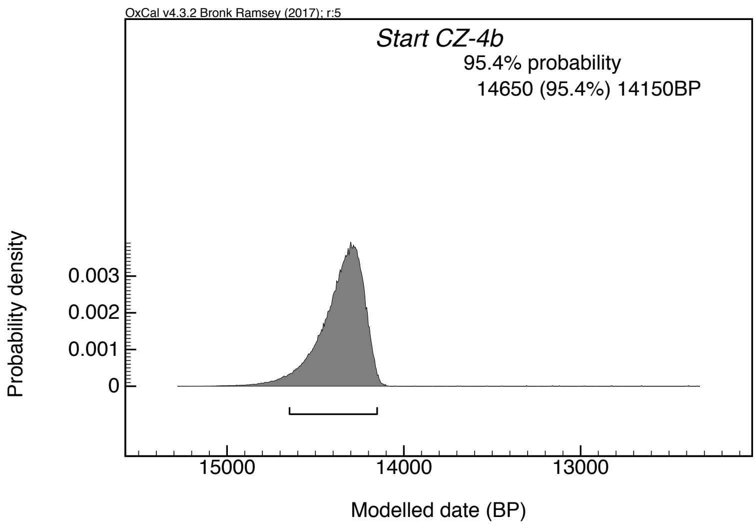

Fig. S8. Bayesian age model for Swan Point (above), and start `Boundary` (below). Brackets beneath each age estimate show 95.4% confidence interval. 'O:prior/posterior probability' reflects the outlier analysis.

```
Plot()
{
 Outlier_Model("General",T(5),U(0,4),"t");
 Sequence()
 {
  Boundary("Start CZ-4b");
  Phase("CZ-4b")
  {
   R_Date("NSRL-2001/CAMS-17045", 12060, 70)
   {
    Outlier("General", 0.05);
   };
   R_Date("AA-98488", 12500, 150)
   {
    Outlier("General", 0.05);
   };
   R_Date("Beta-365062", 12170, 50)
   {
    Outlier("General", 0.05);
   };
   R_Date("AA-74250", 12110, 120)
   {
    Outlier("General", 0.05);
   };
   R_Date("Beta-209882", 12290, 40)
   {
    Outlier("General", 0.05);
   };
   R_Date("Beta-209884", 12220, 40)
   {
    Outlier("General", 0.05);
   };
   R_Date("Beta-209883", 12100, 40)
   {
    Outlier("General", 0.05);
   };
   R_Date("AA-74251", 12050, 120)
   {
    Outlier("General", 0.05);
   };
   R_Date("AA-74249", 11950, 100)
   {
    Outlier("General", 0.05);
   };
   R_Date("Beta-170457", 12360, 60)
   {
    Outlier("General", 0.05);
   };
   R_Date("Beta-QA-619", 12040, 40)
   {
    Outlier("General", 0.05);
   };
   R_Date("Beta-175491", 12110, 50)
   {
    Outlier("General", 0.05);
   };
   R_Date("AA-19322", 11770, 140)
   {
    Outlier("General", 0.05);
   };
   R_Date("Beta-71372/CAMS-12389", 11660, 60)
   {
    Outlier("General", 0.05);
   };
   R_Date("Beta-56667/CAMS-4252", 11660, 70)
   {
    Outlier("General", 0.05);
   };
   Date("Date CZ-4b");
  };
  Boundary("Transition CZ-4b/CZ-4a");
  Phase("CZ-4a")
  {
   R_Date("Beta-175489 (KOH)", 11360, 50)
   {
    Outlier("General", 0.05);
   };
   R_Date("Beta-355852", 11350, 50)
   {
    Outlier("General", 0.05);
   };
  };
  Boundary("End CZ-4a");
  Boundary("Start 3b");
  Phase("CZ-3b")
  {
   R_Date("Beta-401126", 10620, 40)
   {
    Outlier("General", 0.05);
   };
   R_Date("Beta-209885", 10570, 40)
   {
    Outlier("General", 0.05);
   };
   R_Date("Beta-56666/CAMS-4251", 10230, 80)
   {
    Outlier("General", 0.05);
   };
  };
  Boundary("Transition CZ-3b/CZ-3a");
  Phase("CZ-3a")
  {
   R_Date("Beta-355867", 10160, 50)
   {
    Outlier("General", 0.05);
   };
   R_Date("Beta-357816", 10070, 40)
   {
    Outlier("General", 0.05);
   };
   R_Date("Beta-170458", 10050, 60)
   {
    Outlier("General", 0.05);
   };
   R_Date("Beta-190578", 10010, 90)
   {
    Outlier("General", 0.05);
   };
  };
  Boundary("Transition CZ-3a/CZ-2");
  Phase("Cultural Zone 2")
  {
   R_Date("WSU-4426", 7400, 80)
   {
    Outlier("General", 0.05);
   };
   R_Date("Beta-209886", 6610, 40)
   {
    Outlier("General", 0.05);
   };
  };
  Boundary("Transition CZ-2/CZ-1b");
  Phase("CZ-1b")
  {
   R_Date("Beta-401125", 4480, 30)
   {
    Outlier("General", 0.05);
   };
   R_Date("Beta-190580", 4260, 40)
   {
    Outlier("General", 0.05);
   };
   R_Date("Beta-401124", 3060, 30)
```

```
   {
    Outlier("General", 0.05);
   };
  };
  Boundary("Transition CZ-1b/CZ-1a");
  Phase("CZ-1a")
  {
   R_Date("Beta-401123", 1860, 30)
   {
    Outlier("General", 0.05);
   };
   R_Date("WSU-4521", 1750, 80)
   {
    Outlier("General", 0.05);
   };
   R_Date("WSU-4522", 1670, 60)
   {
    Outlier("General", 0.05);
   };
   R_Date("WSU-4524", 1570, 70)
   {
    Outlier("General", 0.05);
   };
   R_Date("WSU-4523", 1220, 70)
   {
    Outlier("General", 0.05);
   };
   R_Date("Beta-223302", 860, 40)
   {
    Outlier("General", 0.05);
   };
   R_Date("Beta-340993", 810, 30)
   {
    Outlier("General", 0.05);
   };
  };
  Boundary("End CZ-1a");
 };
};
```

2.1.9. Ushki, Kamchatka (Russia)

Ushki-1 and -5 (at approximately 56.206208, 159.994846) are archaeological sites containing two, stratified Paleoindian components—7 and 6[53]. Component 7 relates to the Nenana complex, whilst Component 6 has affinities with the Siberian Diuktai[52] culture and Denali. Dates obtained provide stratigraphic control or date cultural features directly, e.g., hearth charcoal. Using these data, the model created places the start of Component 7 at 13,435-12,855 cal BP (Fig. S9).

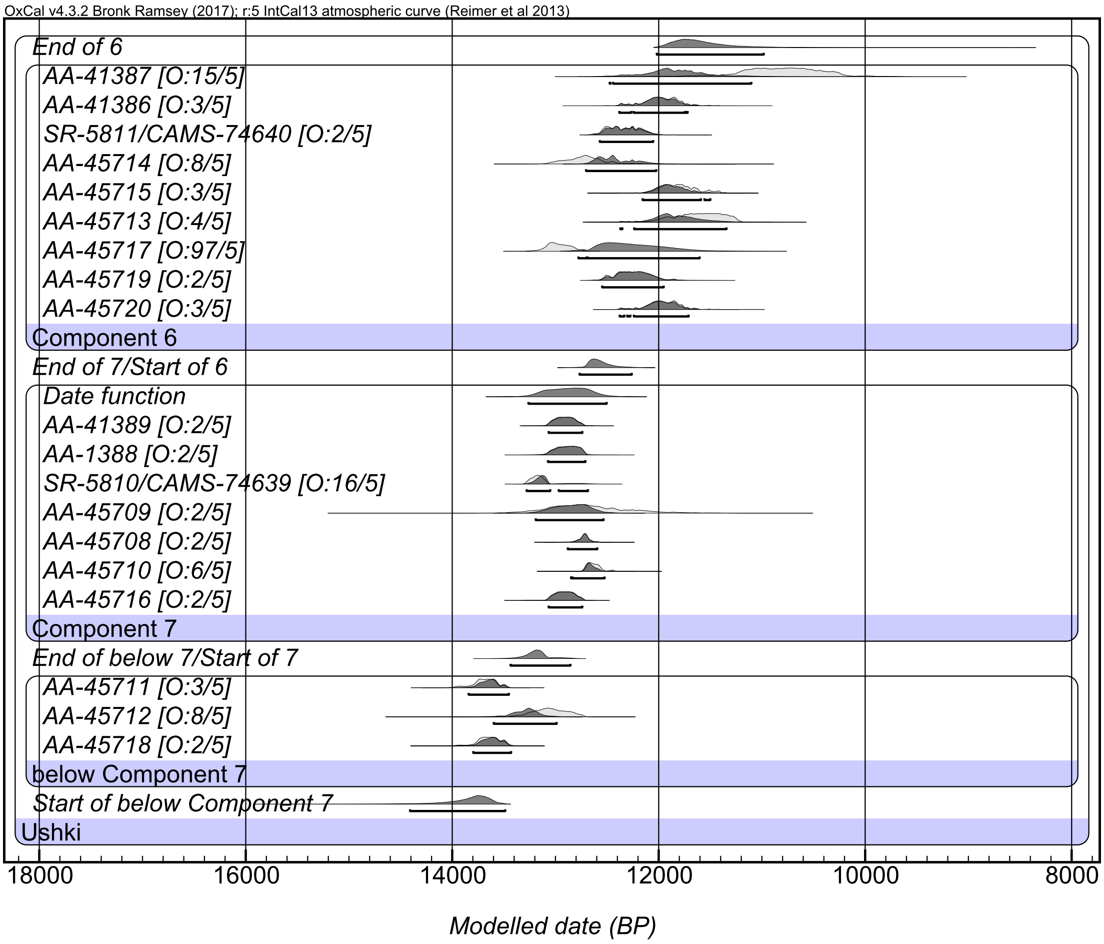

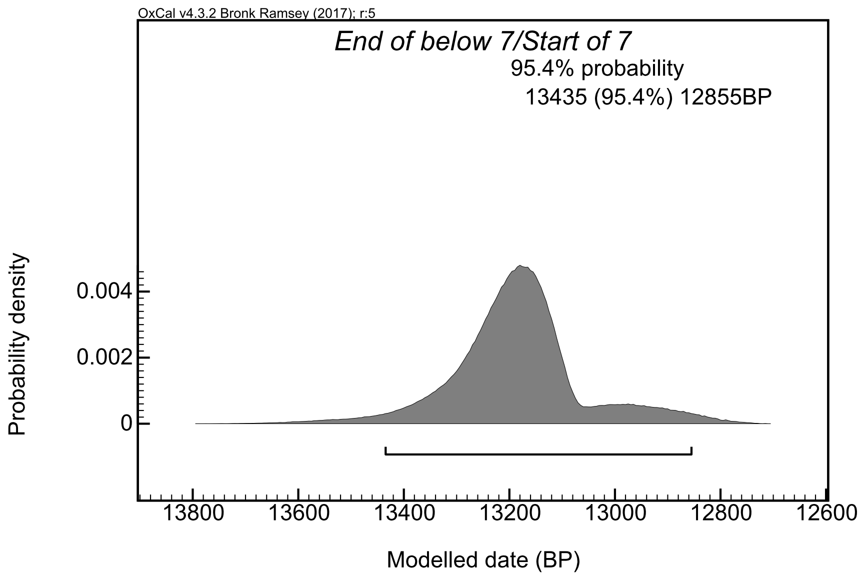

Fig. S9. Bayesian age model for Ushki (above), and start `Boundary` (below). Brackets beneath each age estimate show 95.4% confidence interval. ‘O:prior/posterior probability’ reflects the outlier analysis.

```
Plot()
{
 Outlier_Model("General",T(5),U(0,4),"t");
 Sequence("Ushki")
 {
  Boundary("Start of below Component 7");
  Phase("below Component 7")
  {
   R_Date("AA-45718", 11820, 100)
   {
    Outlier("General", 0.05);
   };
   R_Date("AA-45712", 11200, 160)
   {
    Outlier("General", 0.05);
```

```
  };
  R_Date("AA-45711", 11870, 90)
  {
   Outlier("General", 0.05);
  };
 };
 Boundary("End of below 7/Start of 7");
 Phase("Component 7")
 {
  R_Date("AA-45716", 11050, 75)
  {
   Outlier("General", 0.05);
  };
  R_Date("AA-45710", 10675, 75)
  {
   Outlier("General", 0.05);
  };
  R_Date("AA-45708", 10810, 75)
  {
   Outlier("General", 0.05);
  };
  R_Date("AA-45709", 10850, 320)
  {
   Outlier("General", 0.05);
  };
  R_Date("SR-5810/CAMS-74639", 11330, 50)
  {
   Outlier("General", 0.05);
  };
  R_Date("AA-1388", 11005, 115)
  {
   Outlier("General", 0.05);
  };
  R_Date("AA-41389", 11050, 75)
  {
   Outlier("General", 0.05);
  };
  Date("Date function");
 };
 Boundary("End of 7/Start of 6");
 Phase("Component 6")
 {
  R_Date("AA-45720", 10230, 70)
  {
   Outlier("General", 0.05);
  };
  R_Date("AA-45719", 10385, 90)
  {
   Outlier("General", 0.05);
  };
  R_Date("AA-45717", 11130, 100)
  {
   Outlier("General", 0.05);
  };
  R_Date("AA-45713", 10040, 130)
  {
   Outlier("General", 0.05);
  };
  R_Date("AA-45715", 10160, 75)
  {
   Outlier("General", 0.05);
  };
  R_Date("AA-45714", 10800, 175)
  {
   Outlier("General", 0.05);
  };
  R_Date("SR-5811/CAMS-74640", 10460, 80)
  {
   Outlier("General", 0.05);
  };
  R_Date("AA-41386", 10240, 75)
  {
   Outlier("General", 0.05);
  };
  R_Date("AA-41387", 9485, 275)
  {
   Outlier("General", 0.05);
  };
 };
 Boundary("End of 6");
 };
};
```

2.1.10. Walker Road, Alaska (U.S.A.)

Walker Road (HEA-130; at 63.966667, -149.083333) is a stratified site containing two cultural components, I and II. Based on lithic technology and antiquity, Component I has been assigned to the Nenana complex, whilst II is late Holocene[26,28,30,54]. Dates obtained provide stratigraphic control or date cultural features directly, e.g., hearth charcoal. Using these data, the model created places the start of Component I at 14,950-13,075 cal BP (Fig. S10).

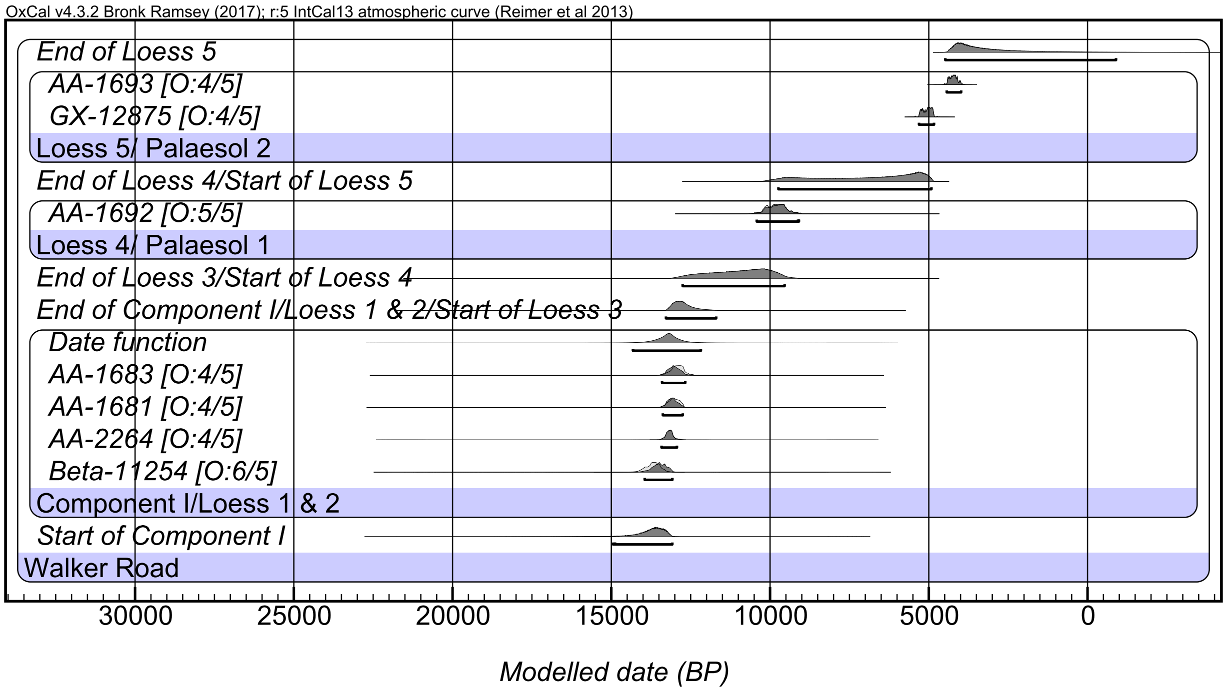

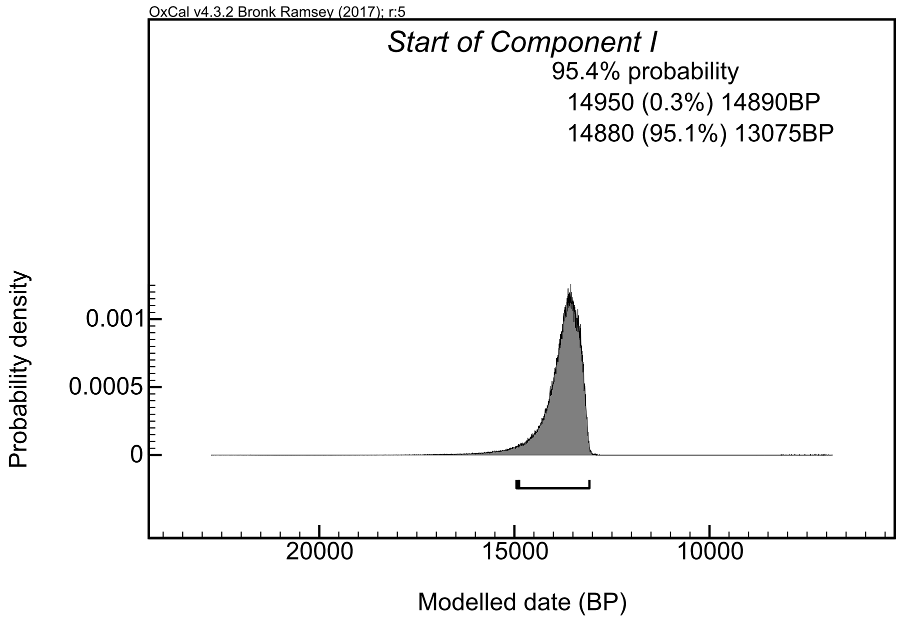

Fig. S10. Bayesian age model for Walker Road (above), and start `Boundary` (below). Brackets beneath each age estimate show 95.4% confidence interval. 'O:prior/posterior probability' reflects the outlier analysis.

```
Plot()
{
 Outlier_Model("General",T(5),U(0,4),"t");
 Sequence("Walker Road")
 {
  Boundary("Start of Component I");
  Phase("Component I/Loess 1 & 2")
  {
   R_Date("Beta-11254", 11820, 200)
   {
    Outlier("General", 0.05);
   };
   R_Date("AA-2264", 11300, 120)
   {
    Outlier("General", 0.05);
   };
   R_Date("AA-1681", 11170, 180)
   {
    Outlier("General", 0.05);
   };
   R_Date("AA-1683", 11010, 230)
   {
    Outlier("General", 0.05);
   };
   Date("Date function");
  };
  Boundary("End of Component I/Loess 1 & 2/Start of Loess 3");
  Boundary("End of Loess 3/Start of Loess 4");
  Phase("Loess 4/ Palaesol 1")
  {
```

```
    R_Date("AA-1692", 8720, 250)
    {
     Outlier("General", 0.05);
    };
   };
  Boundary("End of Loess 4/Start of Loess 5");
  Phase("Loess 5/ Palaesol 2")
  {
   R_Date("GX-12875", 4415, 95)
   {
    Outlier("General", 0.05);
   };
   R_Date("AA-1693", 3816, 79)
   {
    Outlier("General", 0.05);
   };
  };
  Boundary("End of Loess 5");
 };
};
```

2.2. Clovis tradition

<u>2.2.1. Anzick, Montana (U.S.A.)</u>

Anzick site (24PA506; at approximately 45.977128, -110.660209) contains the partial remains of a human individual (Anzick-1) with associated, and temporally coeval, Clovis osseous and lithic tool technology [5,55–62]. Although multiple dates have been obtained for the burial, HYP ages for Anzick-1 and the two Clovis antler rods are considered most reliable[62]. The incorporation of these into a single `Phase` model dates the Clovis component to 13,175-12,485 cal BP (`Date` function; Fig. S11).

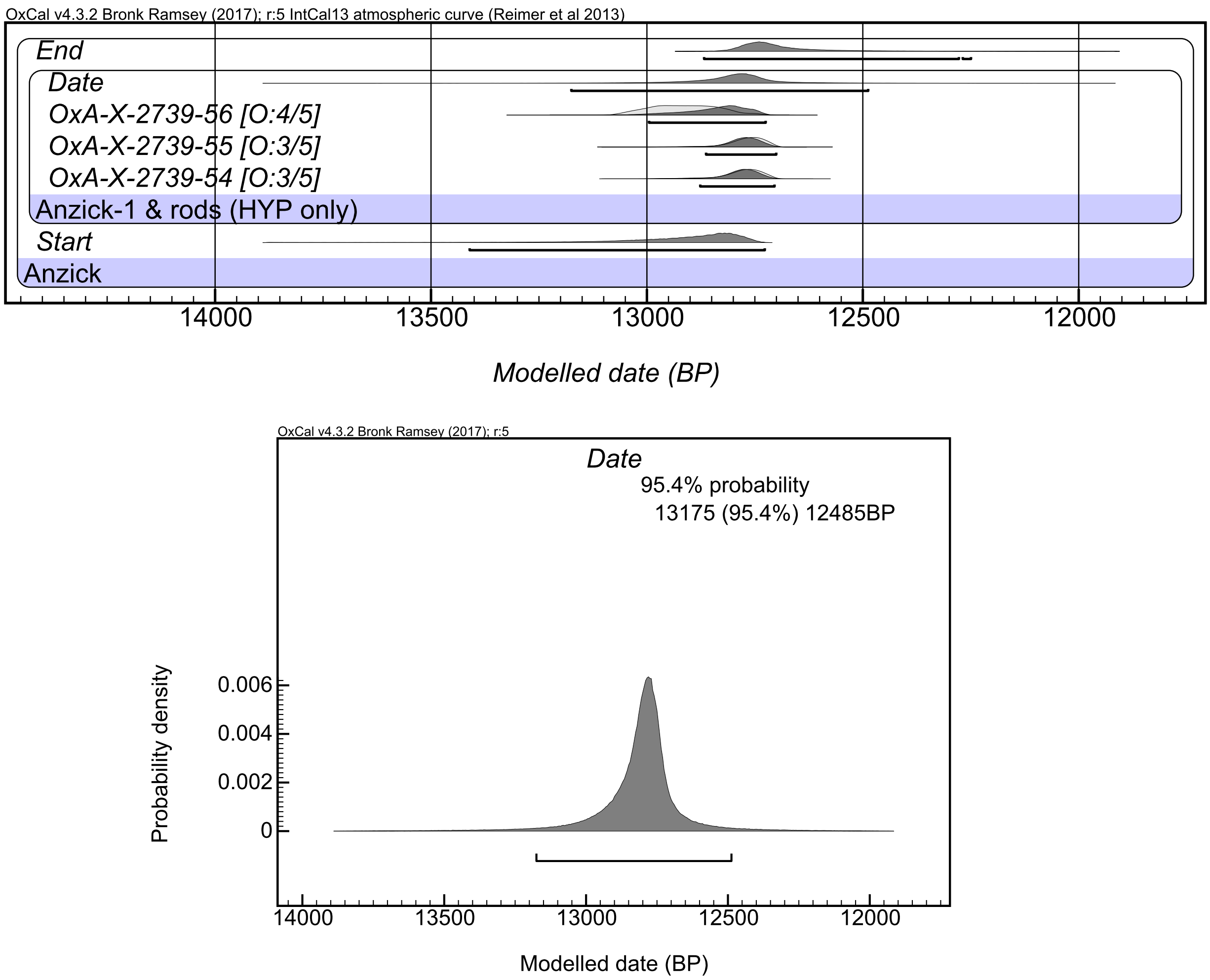

Fig. S11. Bayesian age model for Anzick (above), and `Date` function (below). Brackets beneath each age estimate show 95.4% confidence interval. 'O:prior/posterior probability' reflects the outlier analysis.

```
Sequence("Anzick")
{
 Outlier_Model("General",T(5),U(0,4),"t");
 Boundary("Start");
 Phase("Anzick-1 & rods (HYP only)")
 {
  R_Date("OxA-X-2739-54", 10915, 50)
  {
   Outlier("General", 0.05);
  };
  R_Date("OxA-X-2739-55", 10900, 50)
  {
   Outlier("General", 0.05);
  };
  R_Date("OxA-X-2739-56", 11050, 55)
  {
   Outlier("General", 0.05);
  };
  Date("Date");
 };
 Boundary("End");
};
```

2.2.2. Aubrey, Texas (U.S.A.)

Aubrey (41DN479; at approximately 33.353936, -97.087474) is a multi-cluster (e.g., Camp B and pond), stratified (units A-K) site containing Clovis lithic technology, hearths, and a well[63,64]. The Clovis component is found between units D and E. At Camp B, the Clovis occupation is dated by two charcoal dates from a hearth (AA-5271 and AA-5274) and further extrapolated from a dated pond deposit. Although both Camp B and the pond were modelled (see CQL code below), only the PDF belonging to the start of the Clovis camp (surface of unit A2) was incorporated into large-scale models, as the extrapolation introduces unnecessary uncertainty. The model created places the start of the Clovis component at 14,750-13,245 cal BP (Fig. S12).

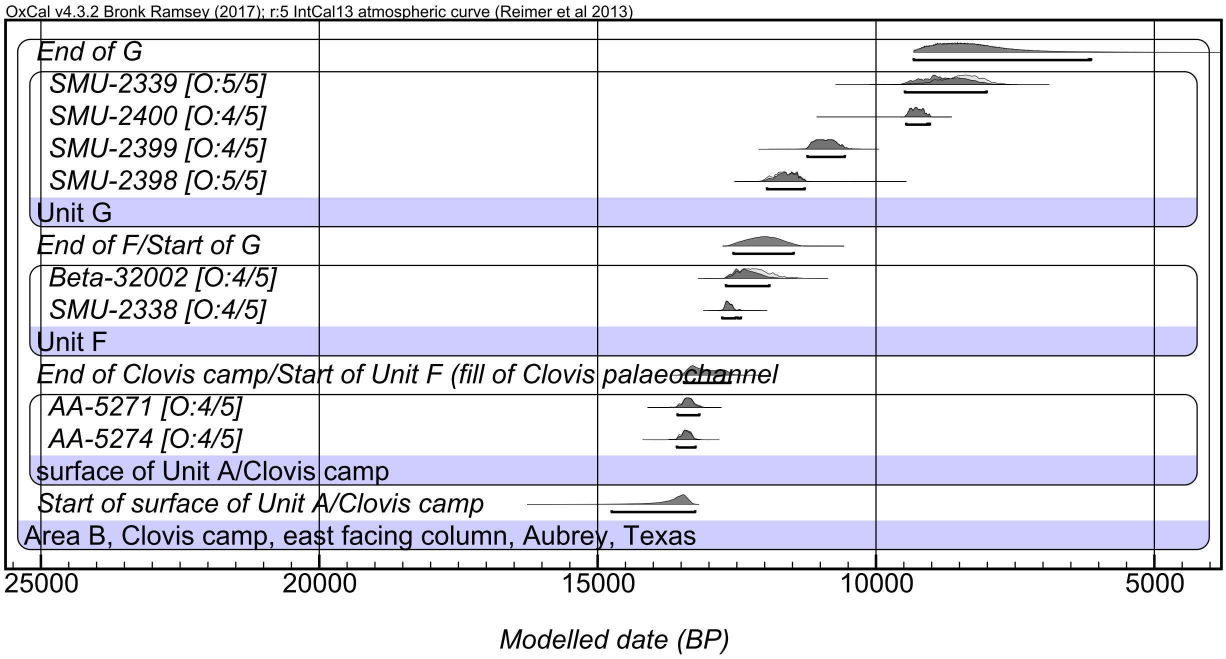

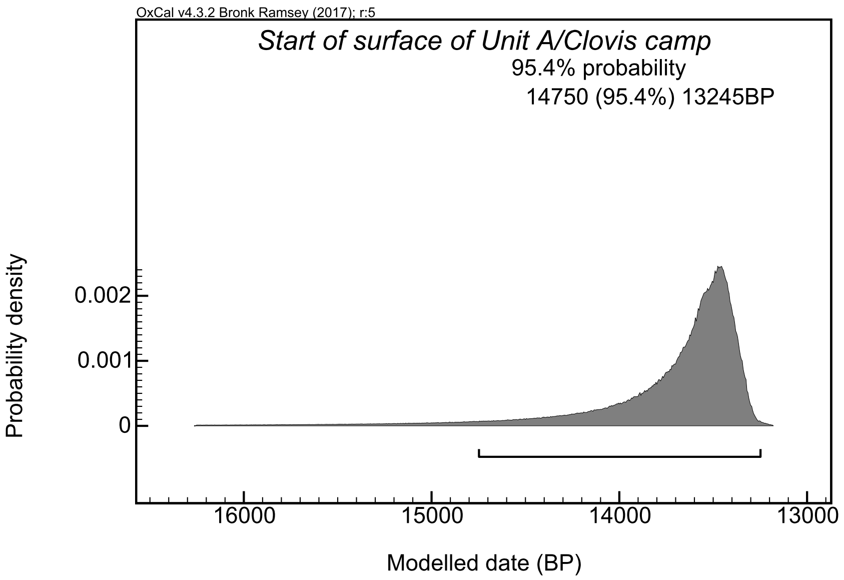

Fig. S12. Bayesian age model for Aubrey (Clovis camp; above), and start `Boundary` (below). Brackets beneath each age estimate show 95.4% confidence interval. 'O:prior/posterior probability' reflects the outlier analysis.

```
Plot()
 {
 Outlier_Model("General",T(5),U(0,4),"t");
 Sequence("Area B, Clovis camp, east facing column, Aubrey, Texas")
  {
  Boundary("Start of surface of Unit A/Clovis camp");
  Phase("surface of Unit A/Clovis camp")
   {
   R_Date("AA-5274", 11590, 93)
    {
    Outlier("General", 0.05);
    };
   R_Date("AA-5271", 11542, 111)
    {
    Outlier("General", 0.05);
    };
   };
  Boundary("End of Clovis camp/Start of Unit F (fill of Clovis palaeochannel");
  Phase("Unit F")
   {
   R_Date("SMU-2338", 10718, 90)
    {
    Outlier("General", 0.05);
    };
   R_Date("Beta-32002", 10360, 150)
    {
    Outlier("General", 0.05);
    };
   };
  Boundary("End of F/Start of G");
```

```
   Phase("Unit G")
   {
    R_Date("SMU-2398", 10084, 80)
    {
     Outlier("General", 0.05);
    };
    R_Date("SMU-2399", 9572, 130)
    {
     Outlier("General", 0.05);
    };
    R_Date("SMU-2400", 8275, 70)
    {
     Outlier("General", 0.05);
    };
    R_Date("SMU-2339", 7582, 320)
    {
     Outlier("General", 0.05);
    };
   };
   Boundary("End of G");
  };
 };
Plot()
{
 Outlier_Model("General",T(5),U(0,4),"t");
 Sequence("Area A pond, west facing column, Aubrey, Texas")
 {
  Boundary("Start of B");
  Sequence("Unit B")
  {
   Phase("B1")
   {
    R_Date("SMU-2236", 14202, 220)
    {
     Outlier("General", 0.05);
    };
    R_Date("SMU-2304", 13569, 400)
    {
     Outlier("General", 0.05);
    };
   };
   Phase("B2")
   {
    R_Date("SMU-2303", 13575, 100)
    {
     Outlier("General", 0.05);
    };
    R_Date("SMU-2302", 13665, 170)
    {
     Outlier("General", 0.05);
    };
    R_Date("SMU-2202", 13344, 410)
    {
     Outlier("General", 0.05);
    };
    R_Date("SMU-2305", 13263, 105)
    {
     Outlier("General", 0.05);
    };
   };
  };
  Boundary("End of B/Start of C");
  Phase("Unit C")
  {
   R_Date("SMU-2478", 12334, 170)
   {
    Outlier("General", 0.05);
   };
  };
  Boundary("End of C/Start of D");
  Boundary("End of D/Start of E");
  Phase("Unit E")
  {
   R_Date("SMU-2194", 10937, 80)
   {
    Outlier("General", 0.05);
   };
   R_Date("SMU-2406", 10390, 80)
   {
    Outlier("General", 0.05);
   };
  };
  Boundary("End of E");
 };
};
```

2.2.3. Blackwater Locality No. 1, New Mexico (U.S.A.)

Blackwater Locality No. 1 (29RV2; at 34.276686, -103.322134), the type-site for Clovis, is a stratified (units A-G) site containing Clovis, Folsom, Midland, and Agate Basin material, as well as evidence for mammoth butchering[65–69]. The Clovis component is found within Unit C. Although no bone dates exist (the first author attempted to extract collagen from one human-modified bone sample without success), the geochronology at the site is well established[65,66]. Using these data, the model created places the start of the Clovis component at 13,440-12,675 cal BP (Fig. S13).

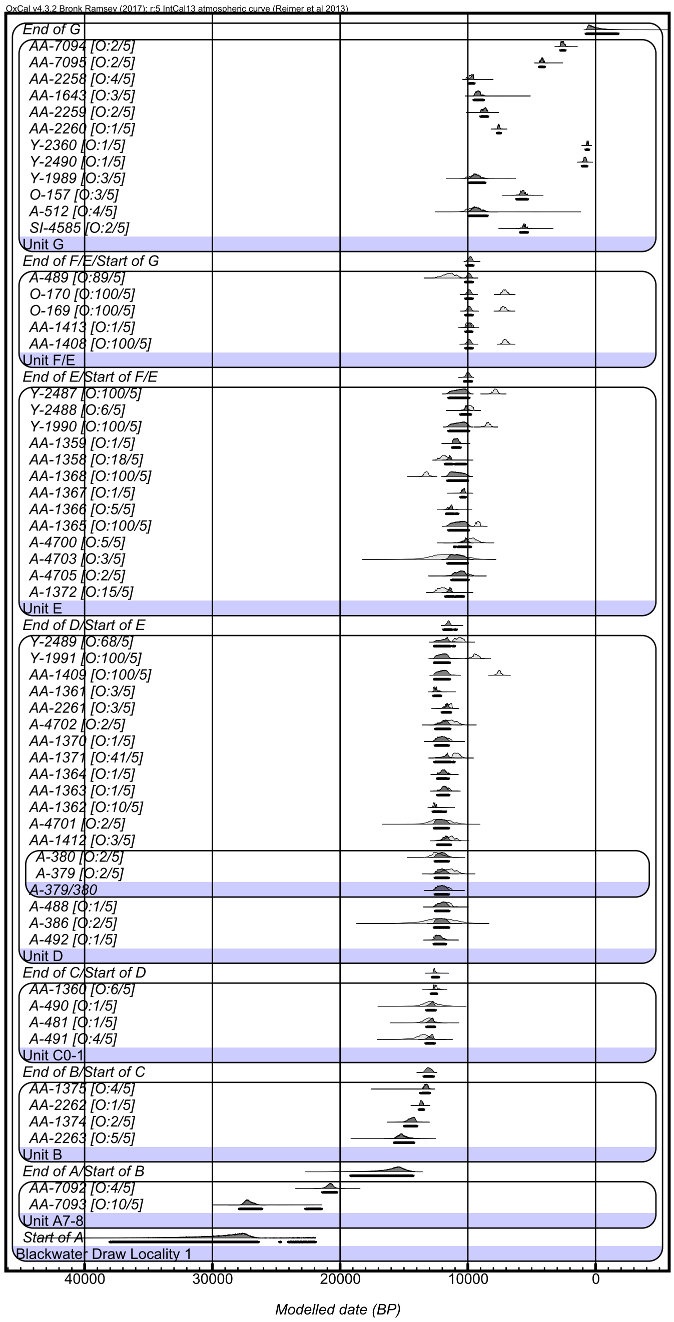

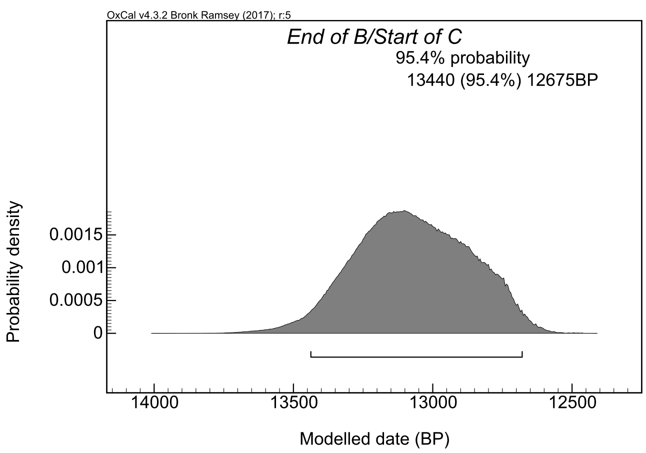

Fig. S13. Bayesian age model for Blackwater Locality No. 1 (above), and start `Boundary` (below). Brackets beneath each age estimate show 95.4% confidence interval. 'O:prior/posterior probability' reflects the outlier analysis.

```
Plot()
{
 Outlier_Model("General",T(5),U(0,4),"t");
 Outlier_Model("SSimple",N(0,2),0,"s");
 Sequence("Blackwater Draw Locality 1")
 {
  Boundary("Start of A");
  Phase("Unit A7-8")
  {
   R_Date("AA-7093", 22930, 290)
   {
    Outlier("General", 0.05);
   };
   R_Date("AA-7092", 17220, 170)
   {
    Outlier("General", 0.05);
   };
  };
  Boundary("End of A/Start of B");
  Phase("Unit B")
  {
   R_Date("AA-2263", 12790, 160)
   {
    Outlier("General", 0.05);
   };
   R_Date("AA-1374", 12330, 110)
   {
    Outlier("General", 0.05);
   };
   R_Date("AA-2262", 11810, 90)
   {
    Outlier("General", 0.05);
   };
   R_Date("AA-1375", 11380, 150)
   {
    Outlier("General", 0.05);
   };
  };
  Boundary("End of B/Start of C");
  Phase("Unit C0-1")
  {
   R_Date("A-491", 11630, 400)
   {
    Outlier("General", 0.05);
   };
   R_Date("A-481", 11170, 360)
   {
    Outlier("General", 0.05);
   };
   R_Date("A-490", 11040, 500)
   {
    Outlier("General", 0.05);
   };
   R_Date("AA-1360", 10580, 100)
   {
    Outlier("General", 0.05);
   };
  };
  Boundary("End of C/Start of D");
  Phase("Unit D")
  {
   R_Date("A-492", 10490, 200)
   {
    Outlier("General", 0.05);
   };
   R_Date("A-386", 10490, 900)
   {
    Outlier("General", 0.05);
   };
   R_Date("A-488", 10170, 260)
   {
    Outlier("General", 0.05);
   };
   R_Combine("A-379/380")
   {
    R_Date("A-379", 9900, 320)
    {
     Outlier("SSimple", 0.05);
    };
    R_Date("A-380", 10600, 320)
    {
     Outlier("SSimple", 0.05);
    };
    Outlier("General", 0.05);
   };
   R_Date("AA-1412", 9860, 210)
   {
    Outlier("General", 0.05);
   };
   R_Date("A-4701", 10470, 580)
   {
    Outlier("General", 0.05);
   };
   R_Date("AA-1362", 10740, 100)
   {
    Outlier("General", 0.05);
   };
   R_Date("AA-1363", 10160, 120)
   {
    Outlier("General", 0.05);
   };
   R_Date("AA-1364", 10210, 110)
   {
    Outlier("General", 0.05);
   };
   R_Date("AA-1371", 9560, 180)
   {
    Outlier("General", 0.05);
   };
   R_Date("AA-1370", 10260, 230)
   {
    Outlier("General", 0.05);
   };
   R_Date("A-4702", 9870, 320)
   {
    Outlier("General", 0.05);
   };
   R_Date("AA-2261", 9950, 100)
   {
    Outlier("General", 0.05);
   };
   R_Date("AA-1361", 10640, 110)
   {
    Outlier("General", 0.05);
   };
   R_Date("AA-1409", 6660, 160)
   {
    Outlier("General", 0.05);
   };
   R_Date("Y-1991", 8430, 200)
   {
    Outlier("General", 0.05);
   };
   R_Date("Y-2489", 9400, 200)
   {
    Outlier("General", 0.05);
   };
  };
  Boundary("End of D/Start of E");
  Phase("Unit E")
  {
   R_Date("A-1372", 10250, 200)
   {
```

```
    Outlier("General", 0.05);
   };
   R_Date("A-4705", 9296, 320)
   {
    Outlier("General", 0.05);
   };
   R_Date("A-4703", 10000, 910)
   {
    Outlier("General", 0.05);
   };
   R_Date("A-4700", 8630, 310)
   {
    Outlier("General", 0.05);
   };
   R_Date("AA-1365", 8230, 100)
   {
    Outlier("General", 0.05);
   };
   R_Date("AA-1366", 9890, 100)
   {
    Outlier("General", 0.05);
   };
   R_Date("AA-1367", 9150, 90)
   {
    Outlier("General", 0.05);
   };
   R_Date("AA-1368", 11400, 190)
   {
    Outlier("General", 0.05);
   };
   R_Date("AA-1358", 10190, 130)
   {
    Outlier("General", 0.05);
   };
   R_Date("AA-1359", 9590, 120)
   {
    Outlier("General", 0.05);
   };
   R_Date("Y-1990", 7610, 160)
   {
    Outlier("General", 0.05);
   };
   R_Date("Y-2488", 8830, 160)
   {
    Outlier("General", 0.05);
   };
   R_Date("Y-2487", 7020, 180)
   {
    Outlier("General", 0.05);
   };
  };
  Boundary("End of E/Start of F/E");
  Phase("Unit F/E")
  {
   R_Date("AA-1408", 6190, 130)
   {
    Outlier("General", 0.05);
   };
   R_Date("AA-1413", 8830, 120)
   {
    Outlier("General", 0.05);
   };
   R_Date("O-169", 6300, 150)
   {
    Outlier("General", 0.05);
   };
   R_Date("O-170", 6230, 150)
   {
    Outlier("General", 0.05);
   };
   R_Date("A-489", 9890, 290)
   {
    Outlier("General", 0.05);
   };
  };
  Boundary("End of F/E/Start of G");
  Phase("Unit G")
  {
   R_Date("SI-4585", 4855, 90)
   {
    Outlier("General", 0.05);
   };
   R_Date("A-512", 8470, 350)
   {
    Outlier("General", 0.05);
   };
   R_Date("O-157", 4950, 150)
   {
    Outlier("General", 0.05);
   };
   R_Date("Y-1989", 8450, 280)
   {
    Outlier("General", 0.05);
   };
   R_Date("Y-2490", 910, 100)
   {
    Outlier("General", 0.05);
   };
   R_Date("Y-2360", 680, 80)
   {
    Outlier("General", 0.05);
   };
   R_Date("AA-2260", 6720, 80)
   {
    Outlier("General", 0.05);
   };
   R_Date("AA-2259", 7850, 110)
   {
    Outlier("General", 0.05);
   };
   R_Date("AA-1643", 8230, 140)
   {
    Outlier("General", 0.05);
   };
   R_Date("AA-2258", 8730, 90)
   {
    Outlier("General", 0.05);
   };
   R_Date("AA-7095", 3800, 60)
   {
    Outlier("General", 0.05);
   };
   R_Date("AA-7094", 2500, 60)
   {
    Outlier("General", 0.05);
   };
  };
  Boundary("End of G");
 };
};
```

2.2.4. Cactus Hill, Virginia (U.S.A.)

Cactus Hill (44SX202; at approximately 36.986668, -77.322360) is a multi-cluster, stratified (levels 1-7) archaeological site containing pre-Clovis and Clovis, Archaic, Woodland, and historic material[70–75]. Optically-stimulated luminescence (OSL) and radiocarbon dating methods have been used to date the deposits[71], providing stratigraphic control. Using these data, the model created places the start of the pre-Clovis component at 20,585-18,970 cal BP, and the start of Clovis at 13,605-11,390 cal BP (Fig. S14).

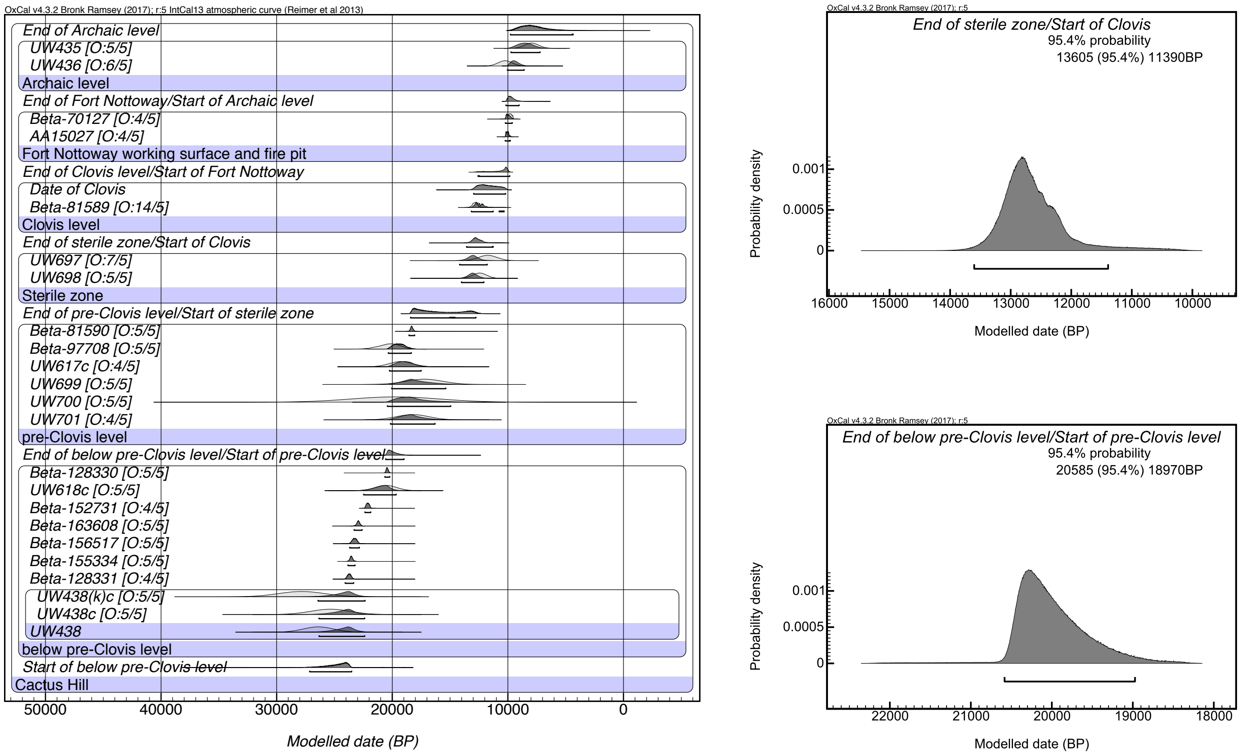

Fig. S14. Bayesian age model for Cactus Hill (left), and start boundaries for both pre-Clovis and Clovis components (adjacent). Brackets beneath each age estimate show 95.4% confidence interval. ‘O:prior/posterior probability’ reflects the outlier analysis.

```
Plot()
{
 Outlier_Model("General",T(5),U(0,4),"t");
 Outlier_Model("SSimple",N(0,2),0,"s");
 Sequence("Cactus Hill")
 {
  Boundary("Start of below pre-Clovis level");
  Phase("below pre-Clovis level")
  {
   Combine("UW438")
   {
    Date("UW438c", N(2010-25400, 1700))
    {
     Outlier("SSimple", 0.05);
    };
    Date("UW438(k)c", N(2010-27900, 2000))
    {
     Outlier("SSimple", 0.05);
    };
    Outlier("General", 0.05);
   };
   R_Date("Beta-128331", 19700, 130)
   {
    Outlier("General", 0.05);
   };
   R_Date("Beta-155334", 19540, 70)
   {
    Outlier("General", 0.05);
   };
   R_Date("Beta-156517", 19310, 150)
   {
    Outlier("General", 0.05);
   };
   R_Date("Beta-163608", 19050, 80)
   {
    Outlier("General", 0.05);
   };
   R_Date("Beta-152731", 18250, 80)
   {
    Outlier("General", 0.05);
   };
   Date("UW618c", N(2010-20600, 900))
   {
    Outlier("General", 0.05);
   };
   R_Date("Beta-128330", 16940, 50)
   {
    Outlier("General", 0.05);
   };
  };
  Boundary("End of below pre-Clovis level/Start of pre-Clovis level");
  Phase("pre-Clovis level")
  {
   Date("UW701", N(2010-18300, 1400))
   {
    Outlier("General", 0.05);
   };
   Date("UW700", N(2010-19800, 3800))
   {
    Outlier("General", 0.05);
```

```
  };
  Date("UW699", N(2010-17300, 1600))
  {
   Outlier("General", 0.05);
  };
  Date("UW617c", N(2010-19300, 1000))
  {
   Outlier("General", 0.05);
  };
  R_Date("Beta-97708", 16670, 730)
  {
   Outlier("General", 0.05);
  };
  R_Date("Beta-81590", 15070, 70)
  {
   Outlier("General", 0.05);
  };
 };
 Boundary("End of pre-Clovis level/Start of sterile zone");
 Phase("Sterile zone")
 {
  Date("UW698", N(2010-12500, 600))
  {
   Outlier("General", 0.05);
  };
  Date("UW697", N(2010-11800, 800))
  {
   Outlier("General", 0.05);
  };
 };
 Boundary("End of sterile zone/Start of Clovis");
 Phase("Clovis level")
 {
  R_Date("Beta-81589", 10920, 250)
  {
   Outlier("General", 0.05);
  };
 };
 Boundary("End of Clovis level/Start of Fort Nottoway");
 Phase("Fort Nottoway working surface and fire pit")
 {
  R_Date("AA15027", 8920, 65)
  {
   Outlier("General", 0.05);
  };
  R_Date("Beta-70127", 8800, 120)
  {
   Outlier("General", 0.05);
  };
 };
 Boundary("End of Fort Nottoway/Start of Archaic level");
 Phase("Archaic level")
 {
  Date("UW436", N(2010-10300, 600))
  {
   Outlier("General", 0.05);
  };
  Date("UW435", N(2010-8000, 600))
  {
   Outlier("General", 0.05);
  };
 };
 Boundary("End of Archaic level");
 };
};
```

2.2.5. Colby, Wyoming (U.S.A.)

Colby (48WA322; at approximately 44.020499, -107.854297) is a Clovis, mammoth-butchering site with associated lithic tool technology[5,76,77]. The incorporation of two XAD bone dates (UCIAMS-11342 and UCIAMS-11343) into a single `Phase`, dates the archaeological event to 13,165-12,350 cal BP (`Date` function; Fig. S15).

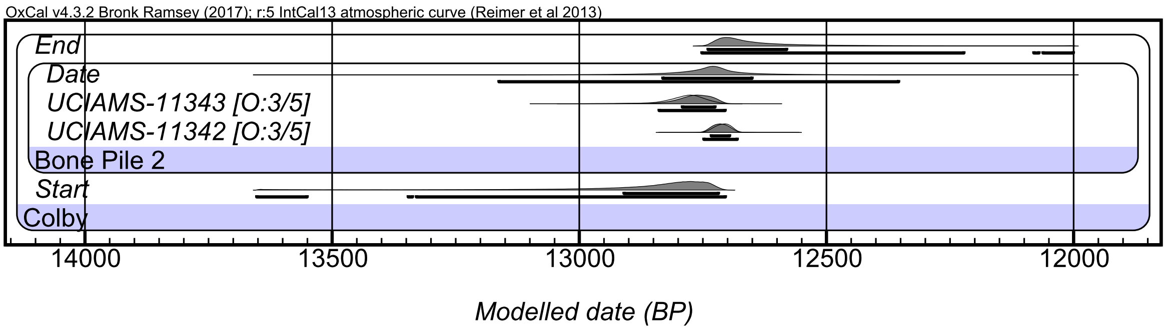

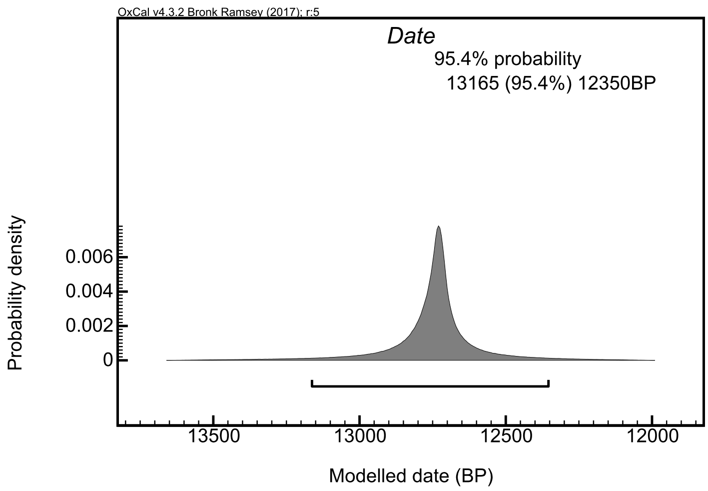

Fig. S15. Bayesian age model for Colby (above), and `Date` function (below). Brackets beneath each age estimate show 95.4% confidence interval. 'O:prior/posterior probability' reflects the outlier analysis.

```
Sequence("Colby")
{
 Outlier_Model("General",T(5),U(0,4),"t");
 Boundary("Start");
 Phase("Bone Pile 2")
  {
  R_Date("UCIAMS-11342", 10790, 30)
   {
   Outlier("General", 0.05);
   };
  R_Date("UCIAMS-11343", 10950, 30)
   {
   Outlier("General", 0.05);
   };
  Date("Date");
  };
 Boundary("End");
};
```

2.2.6. Debra L. Friedkin, Texas (U.S.A.)

The Debra L. Friedkin site (41BL1239; at approximately 30.892283, -97.709742) is a stratified, multicomponent site (blocks A and B) containing pre-Clovis ("Buttermilk complex"; but see ref 78), Clovis, Folsom, late Paleoindian, and Archaic material[79–82]. OSL has been used to date the deposits. Using the latest chronometric evidence[82], the model created places the start of the Buttermilk complex at 16,330-14,690 cal BP, and the start of Clovis at 14,755-13,120 cal BP (Fig. S16). This includes dates within "Boundary Date" categories in preceding phases. If incorporated in succeeding phases, the same date to 17,495-15,275 and 14,960-13,295 cal BP, correspondingly. CQL code for both models are provided below.

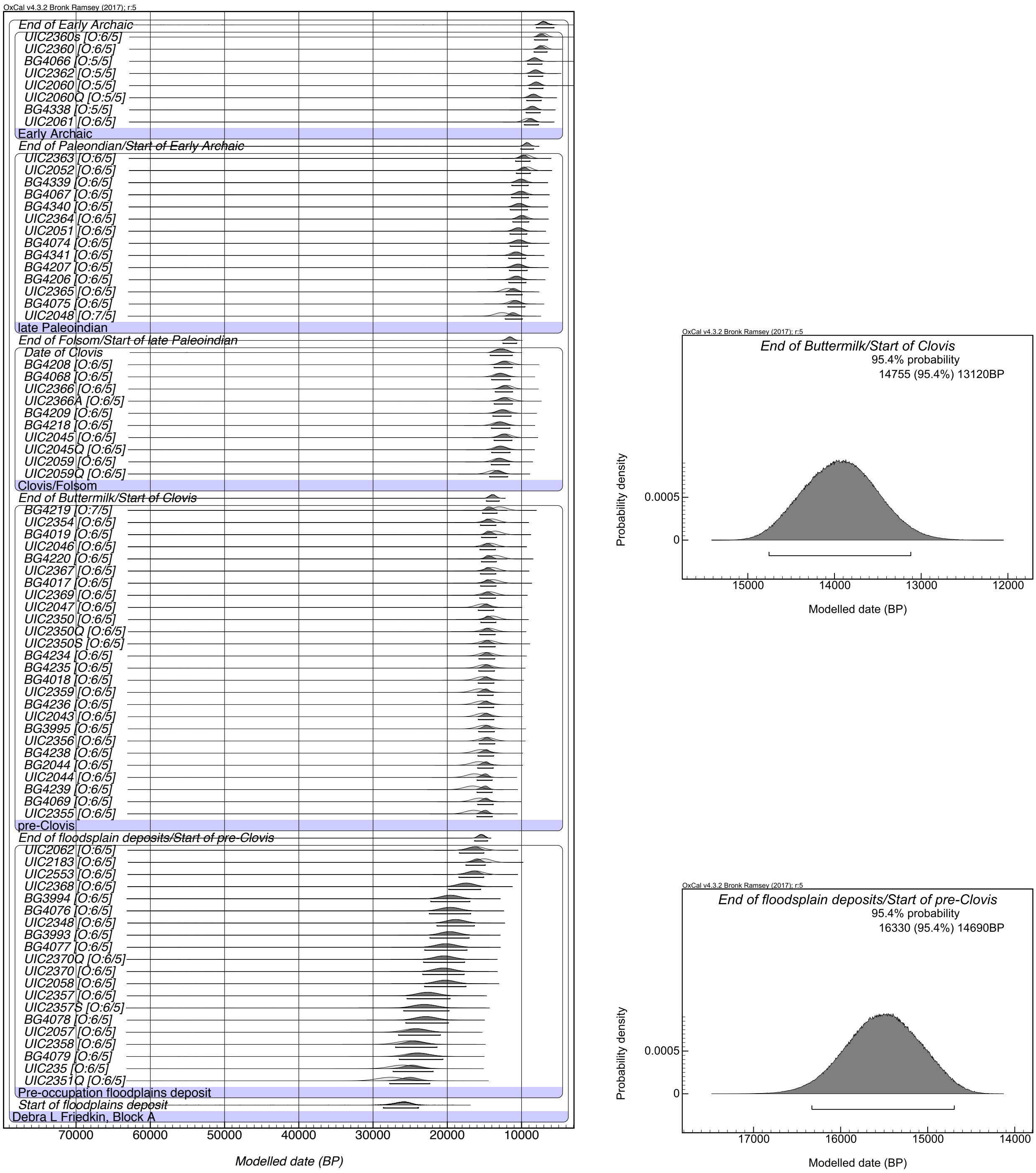

Fig. S16. Bayesian age model for Debra L. Friedkin (left), and start boundaries for both pre-Clovis and Clovis components (adjacent). Brackets beneath each age estimate show 95.4% confidence interval. 'O:prior/posterior probability' reflects the outlier analysis.

```
Plot()
{
Outlier_Model("General",T(5),U(0,4),"t");
 Sequence("Debra L Friedkin, Block A, dates in Boundary Date in preceding phases")
 {
 Boundary("Start of floodplains deposit");
 Phase("Pre-occupation floodplains deposit")
 {
  Date("UIC2351Q", N(2010-27650, 1800))
  {
   Outlier("General", 0.05);
  };
  Date("UIC235", N(2010-26090, 1670))
  {
   Outlier("General", 0.05);
  };
  Date("BG4079", N(2010-24145, 1635))
  {
   Outlier("General", 0.05);
  };
  Date("UIC2358", N(2010-25185, 1640))
  {
   Outlier("General", 0.05);
  };
  Date("UIC2057", N(2010-24420, 1580))
  {
   Outlier("General", 0.05);
  };
```

```
Date("BG4078", N(2010-22950, 1445))
{
Outlier("General", 0.05);
};
Date("UIC2357S", N(2010-23150, 1600))
{
Outlier("General", 0.05);
};
Date("UIC2357", N(2010-22710, 1450))
{
Outlier("General", 0.05);
};
Date("UIC2058", N(2010-20330, 1320))
{
Outlier("General", 0.05);
};
Date("UIC2370", N(2010-20565, 1325))
{
Outlier("General", 0.05);
};
Date("UIC2370Q", N(2010-20490, 1305))
{
Outlier("General", 0.05);
};
Date("BG4077", N(2010-20250, 1340))
{
Outlier("General", 0.05);
};
Date("BG3993", N(2010-19750, 1245))
{
Outlier("General", 0.05);
};
Date("UIC2348", N(2010-18930, 1210))
{
Outlier("General", 0.05);
};
Date("BG4076", N(2010-19680, 1320))
{
Outlier("General", 0.05);
};
Date("BG3994", N(2010-19650, 1230))
{
Outlier("General", 0.05);
};
Date("UIC2368", N(2010-17530, 1140))
{
Outlier("General", 0.05);
};
Date("UIC2553", N(2010-16270, 1040))
{
Outlier("General", 0.05);
};
Date("UIC2183", N(2010-15110, 960))
{
Outlier("General", 0.05);
};
Date("UIC2062", N(2010-16170, 1030))
{
Outlier("General", 0.05);
};
};
Boundary("End of floodsplain deposits/Start of pre-Clovis");
Phase("pre-Clovis")
{
Date("UIC2355", N(2010-16515, 1075))
{
Outlier("General", 0.05);
};
Date("BG4069", N(2010-15725, 1030))
{
Outlier("General", 0.05);
};
Date("BG4239", N(2010-16650, 1110))
{
Outlier("General", 0.05);
};
Date("UIC2044", N(2010-16400, 1040))
{
Outlier("General", 0.05);
};
Date("BG2044", N(2010-15800, 1080))
{
Outlier("General", 0.05);
};
Date("BG4238", N(2010-15500, 1020))
{
Outlier("General", 0.05);
};
Date("UIC2356", N(2010-14710, 940))
{
Outlier("General", 0.05);
};
Date("BG3995", N(2010-15020, 1010))
{
Outlier("General", 0.05);
};
Date("UIC2043", N(2010-15210, 960))
{
Outlier("General", 0.05);
};
Date("BG4236", N(2010-15400, 1015))
{
Outlier("General", 0.05);
};
Date("UIC2359", N(2010-15730, 1010))
{
Outlier("General", 0.05);
};
Date("BG4018", N(2010-15265, 1000))
{
Outlier("General", 0.05);
};
Date("BG4235", N(2010-14965, 985))
{
Outlier("General", 0.05);
};
Date("BG4234", N(2010-14790, 985))
{
Outlier("General", 0.05);
};
Date("UIC2350S", N(2010-14580, 1030))
{
Outlier("General", 0.05);
};
Date("UIC2350Q", N(2010-14480, 920))
{
Outlier("General", 0.05);
};
Date("UIC2350", N(2010-14000, 890))
{
Outlier("General", 0.05);
};
Date("UIC2047", N(2010-15270, 960))
{
Outlier("General", 0.05);
};
Date("UIC2369", N(2010-14370, 930))
{
Outlier("General", 0.05);
};
Date("BG4017", N(2010-13960, 965))
{
Outlier("General", 0.05);
};
Date("UIC2367", N(2010-14080, 920))
{
```

```
 Outlier("General", 0.05);
 };
 Date("BG4220", N(2010-13595, 930))
 {
 Outlier("General", 0.05);
 };
 Date("UIC2046", N(2010-14350, 910))
 {
 Outlier("General", 0.05);
 };
 Date("BG4019", N(2010-13620, 880))
 {
 Outlier("General", 0.05);
 };
 Date("UIC2354", N(2010-14070, 910))
 {
 Outlier("General", 0.05);
 };
 Date("BG4219", N(2010-13010, 905))
 {
 Outlier("General", 0.05);
 };
};
Boundary("End of Buttermilk/Start of Clovis");
Phase("Clovis/Folsom")
{
 Date("UIC2059Q", N(2010-13780, 885))
 {
 Outlier("General", 0.05);
 };
 Date("UIC2059", N(2010-13090, 830))
 {
 Outlier("General", 0.05);
 };
 Date("UIC2045Q", N(2010-12925, 845))
 {
 Outlier("General", 0.05);
 };
 Date("UIC2045", N(2010-12240, 800))
 {
 Outlier("General", 0.05);
 };
 Date("BG4218", N(2010-13020, 870))
 {
 Outlier("General", 0.05);
 };
 Date("BG4209", N(2010-12560, 830))
 {
 Outlier("General", 0.05);
 };
 Date("UIC2366A", N(2010-12100, 860))
 {
 Outlier("General", 0.05);
 };
 Date("UIC2366", N(2010-12000, 770))
 {
 Outlier("General", 0.05);
 };
 Date("BG4068", N(2010-12940, 855))
 {
 Outlier("General", 0.05);
 };
 Date("BG4208", N(2010-12170, 820))
 {
 Outlier("General", 0.05);
 };
 Date("Date of Clovis");
};
Boundary("End of Folsom/Start of late Paleoindian");
Phase("late Paleoindian")
{
 Date("UIC2048", N(2010-12690, 955))
 {
 Outlier("General", 0.05);
 };
 Date("BG4075", N(2010-11060, 735))
 {
 Outlier("General", 0.05);
 };
 Date("UIC2365", N(2010-11870, 760))
 {
 Outlier("General", 0.05);
 };
 Date("BG4206", N(2010-10785, 715))
 {
 Outlier("General", 0.05);
 };
 Date("BG4207", N(2010-10530, 750))
 {
 Outlier("General", 0.05);
 };
 Date("BG4341", N(2010-10830, 695))
 {
 Outlier("General", 0.05);
 };
 Date("BG4074", N(2010-10375, 740))
 {
 Outlier("General", 0.05);
 };
 Date("UIC2051", N(2010-10480, 675))
 {
 Outlier("General", 0.05);
 };
 Date("UIC2364", N(2010-9930, 640))
 {
 Outlier("General", 0.05);
 };
 Date("BG4340", N(2010-10360, 705))
 {
 Outlier("General", 0.05);
 };
 Date("BG4067", N(2010-10100, 695))
 {
 Outlier("General", 0.05);
 };
 Date("BG4339", N(2010-10095, 655))
 {
 Outlier("General", 0.05);
 };
 Date("UIC2052", N(2010-9250, 600))
 {
 Outlier("General", 0.05);
 };
 Date("UIC2363", N(2010-9405, 610))
 {
 Outlier("General", 0.05);
 };
};
Boundary("End of Paleondian/Start of Early Archaic");
Phase("Early Archaic")
{
 Date("UIC2061", N(2010-9215, 620))
 {
 Outlier("General", 0.05);
 };
 Date("BG4338", N(2010-8655, 550))
 {
 Outlier("General", 0.05);
 };
 Date("UIC2060Q", N(2010-8490, 560))
 {
 Outlier("General", 0.05);
 };
 Date("UIC2060", N(2010-8070, 520))
 {
 Outlier("General", 0.05);
```

```
  };
  Date("UIC2362", N(2010-8160, 540))
  {
   Outlier("General", 0.05);
  };
  Date("BG4066", N(2010-8315, 540))
  {
   Outlier("General", 0.05);
  };
  Date("UIC2360", N(2010-7160, 470))
  {
   Outlier("General", 0.05);
  };
  Date("UIC2360s", N(2010-7030, 470))
  {
   Outlier("General", 0.05);
  };
 };
 Boundary("End of Early Archaic");
 };
};

Plot()
{
 Outlier_Model("General",T(5),U(0,4),"t");
 Sequence("Debra L Friedkin, Block A, dates in Boundary Date in succeeding phases")
 {
 Boundary("Start of floodplains deposit");
 Phase("Pre-occupation floodplains deposit")
 {
  Date("UIC2351Q", N(2010-27650, 1800))
  {
   Outlier("General", 0.05);
  };
  Date("UIC235", N(2010-26090, 1670))
  {
   Outlier("General", 0.05);
  };
  Date("BG4079", N(2010-24145, 1635))
  {
   Outlier("General", 0.05);
  };
  Date("UIC2358", N(2010-25185, 1640))
  {
   Outlier("General", 0.05);
  };
  Date("UIC2057", N(2010-24420, 1580))
  {
   Outlier("General", 0.05);
  };
  Date("BG4078", N(2010-22950, 1445))
  {
   Outlier("General", 0.05);
  };
  Age("UIC2357S", N(2010-23150, 1600))
  {
   Outlier("General", 0.05);
  };
  Date("UIC2357", N(2010-22710, 1450))
  {
   Outlier("General", 0.05);
  };
  Date("UIC2058", N(2010-20330, 1320))
  {
   Outlier("General", 0.05);
  };
  Date("UIC2370", N(2010-20565, 1325))
  {
   Outlier("General", 0.05);
  };
  Date("UIC2370Q", N(2010-20490, 1305))
  {
   Outlier("General", 0.05);
  };
  Date("BG4077", N(2010-20250, 1340))
  {
   Outlier("General", 0.05);
  };
  Date("BG3993", N(2010-19750, 1245))
  {
   Outlier("General", 0.05);
  };
  Age("UIC2348", N(2010-18930, 1210))
  {
   Outlier("General", 0.05);
  };
  Date("BG4076", N(2010-19680, 1320))
  {
   Outlier("General", 0.05);
  };
  Date("BG3994", N(2010-19650, 1230))
  {
   Outlier("General", 0.05);
  };
 };
 Boundary("End of floodsplain deposits/Start of pre-Clovis");
 Phase("pre-Clovis")
 {
  Date("UIC2368", N(2010-17530, 1140))
  {
   Outlier("General", 0.05);
  };
  Date("UIC2553", N(2010-16270, 1040))
  {
   Outlier("General", 0.05);
  };
  Date("UIC2183", N(2010-15110, 960))
  {
   Outlier("General", 0.05);
  };
  Date("UIC2062", N(2010-16170, 1030))
  {
   Outlier("General", 0.05);
  };
  Date("UIC2355", N(2010-16515, 1075))
  {
   Outlier("General", 0.05);
  };
  Date("BG4069", N(2010-15725, 1030))
  {
   Outlier("General", 0.05);
  };
  Date("BG4239", N(2010-16650, 1110))
  {
   Outlier("General", 0.05);
  };
  Date("UIC2044", N(2010-16400, 1040))
  {
   Outlier("General", 0.05);
  };
  Date("BG2044", N(2010-15800, 1080))
  {
   Outlier("General", 0.05);
  };
  Date("BG4238", N(2010-15500, 1020))
  {
   Outlier("General", 0.05);
  };
  Date("UIC2356", N(2010-14710, 940))
  {
   Outlier("General", 0.05);
  };
  Date("BG3995", N(2010-15020, 1010))
  {
   Outlier("General", 0.05);
```

```
};
Date("UIC2043", N(2010-15210, 960))
{
 Outlier("General", 0.05);
};
Date("BG4236", N(2010-15400, 1015))
{
 Outlier("General", 0.05);
};
Date("UIC2359", N(2010-15730, 1010))
{
 Outlier("General", 0.05);
};
Date("BG4018", N(2010-15265, 1000))
{
 Outlier("General", 0.05);
};
Date("BG4235", N(2010-14965, 985))
{
 Outlier("General", 0.05);
};
Date("BG4234", N(2010-14790, 985))
{
 Outlier("General", 0.05);
};
Date("UIC2350S", N(2010-14580, 1030))
{
 Outlier("General", 0.05);
};
Date("UIC2350Q", N(2010-14480, 920))
{
 Outlier("General", 0.05);
};
Date("UIC2350", N(2010-14000, 890))
{
 Outlier("General", 0.05);
};
Date("UIC2047", N(2010-15270, 960))
{
 Outlier("General", 0.05);
};
Date("UIC2369", N(2010-14370, 930))
{
 Outlier("General", 0.05);
};
Date("BG4017", N(2010-13960, 965))
{
 Outlier("General", 0.05);
};
Date("UIC2367", N(2010-14080, 920))
{
 Outlier("General", 0.05);
};
Date("BG4220", N(2010-13595, 930))
{
 Outlier("General", 0.05);
};
};
Boundary("End of Buttermilk/Start of Clovis");
Phase("Clovis/Folsom")
{
Date("UIC2046", N(2010-14350, 910))
{
 Outlier("General", 0.05);
};
Date("BG4019", N(2010-13620, 880))
{
 Outlier("General", 0.05);
};
Date("UIC2354", N(2010-14070, 910))
{
 Outlier("General", 0.05);
};
Date("BG4219", N(2010-13010, 905))
{
 Outlier("General", 0.05);
};
Date("UIC2059Q", N(2010-13780, 885))
{
 Outlier("General", 0.05);
};
Date("UIC2059", N(2010-13090, 830))
{
 Outlier("General", 0.05);
};
Date("UIC2045Q", N(2010-12925, 845))
{
 Outlier("General", 0.05);
};
Date("UIC2045", N(2010-12240, 800))
{
 Outlier("General", 0.05);
};
Date("BG4218", N(2010-13020, 870))
{
 Outlier("General", 0.05);
};
Date("BG4209", N(2010-12560, 830))
{
 Outlier("General", 0.05);
};
Date("UIC2366A", N(2010-12100, 860))
{
 Outlier("General", 0.05);
};
Date("UIC2366", N(2010-12000, 770))
{
 Outlier("General", 0.05);
};
Date("BG4068", N(2010-12940, 855))
{
 Outlier("General", 0.05);
};
Date("BG4208", N(2010-12170, 820))
{
 Outlier("General", 0.05);
};
};
Boundary("End of Folsom/Start of late Paleoindian");
Phase("late Paleoindian")
{
Date("UIC2048", N(2010-12690, 955))
{
 Outlier("General", 0.05);
};
Date("BG4075", N(2010-11060, 735))
{
 Outlier("General", 0.05);
};
Date("UIC2365", N(2010-11870, 760))
{
 Outlier("General", 0.05);
};
Date("BG4206", N(2010-10785, 715))
{
 Outlier("General", 0.05);
};
Date("BG4207", N(2010-10530, 750))
{
 Outlier("General", 0.05);
};
Date("BG4341", N(2010-10830, 695))
{
 Outlier("General", 0.05);
};
Date("BG4074", N(2010-10375, 740))
```

```
{
 Outlier("General", 0.05);
};
Date("UIC2051", N(2010-10480, 675))
{
 Outlier("General", 0.05);
};
Date("UIC2364", N(2010-9930, 640))
{
 Outlier("General", 0.05);
};
Date("BG4340", N(2010-10360, 705))
{
 Outlier("General", 0.05);
};
Date("BG4067", N(2010-10100, 695))
{
 Outlier("General", 0.05);
};
Date("BG4339", N(2010-10095, 655))
{
 Outlier("General", 0.05);
};
Date("UIC2052", N(2010-9250, 600))
{
 Outlier("General", 0.05);
};
Date("UIC2363", N(2010-9405, 610))
{
 Outlier("General", 0.05);
};
};
Boundary("End of Paleondian/Start of Early Archaic");
Phase("Early Archaic")
{
Date("UIC2061", N(2010-9215, 620))
{
 Outlier("General", 0.05);
};
Date("BG4338", N(2010-8655, 550))
{
 Outlier("General", 0.05);
};
Date("UIC2060Q", N(2010-8490, 560))
{
 Outlier("General", 0.05);
};
Date("UIC2060", N(2010-8070, 520))
{
 Outlier("General", 0.05);
};
Date("UIC2362", N(2010-8160, 540))
{
 Outlier("General", 0.05);
};
Date("BG4066", N(2010-8315, 540))
{
 Outlier("General", 0.05);
};
Date("UIC2360", N(2010-7160, 470))
{
 Outlier("General", 0.05);
};
Date("UIC2360s", N(2010-7030, 470))
{
 Outlier("General", 0.05);
};
};
Boundary("End of Early Archaic");
};
};
```

2.2.7. Dent, Colorado (U.S.A.)

Dent (5WL269; at approximately 40.319080, -104.829562) is a Clovis, mammoth-butchering site with associated lithic tool technology[5,57,58,83–88]. Although multiple dates have been obtained for the site, two HYP dates (OxA-X-2736-11 and OxA-X-2736-12) produced from mammoth bone samples are considered most reliable[88]. The incorporation of these into a single `Phase` model dates the Clovis component to 13,545-12,415 cal BP (`Date` function; Fig. S17).

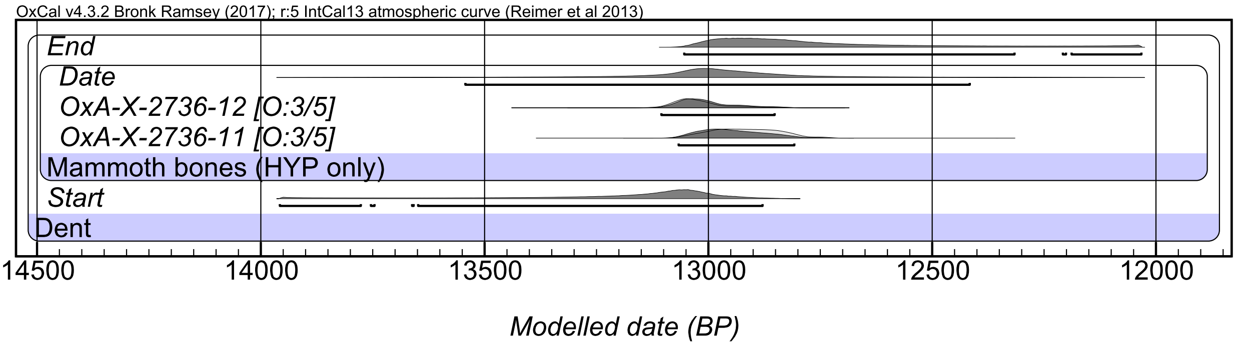

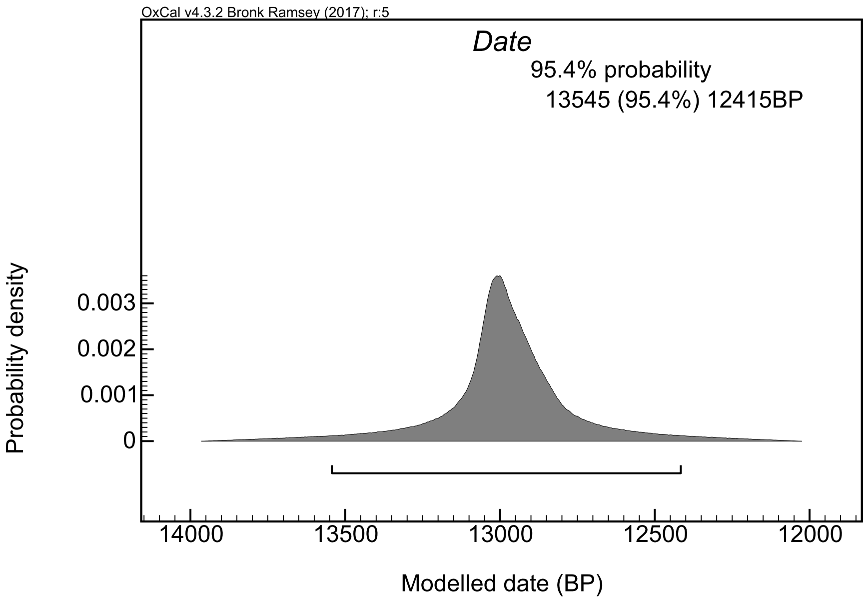

Fig. S17. Bayesian age model for Dent (above), and `Date` function (below). Brackets beneath each age estimate show 95.4% confidence interval. 'O:prior/posterior probability' reflects the outlier analysis.

```
Sequence("Dent")
{
 Outlier_Model("General",T(5),U(0,4),"t");
 Boundary("Start");
 Phase("Mammoth bones (HYP only)")
 {
  R_Date("OxA-X-2736-11", 11055, 50)
  {
   Outlier("General", 0.05);
  };
  R_Date("OxA-X-2736-12", 11155, 50)
  {
   Outlier("General", 0.05);
  };
  Date("Date");
 };
 Boundary("End");
};
```

2.2.8. Domebo, Oklahoma (U.S.A.)

Domebo (34CD50; at approximately 34.957529, -98.271482) is a Clovis, mammoth-butchering site with associated lithic tool technology[57,89,90]. Although multiple dates have been obtained for the site, an XAD date (UCIAMS-11341; 12,910-12,710 cal BP) produced from mammoth bone is considered the most reliable[5] and is here used.

2.2.9. El Fin del Mundo, Sonora (Mexico)

El Fin del Mundo (at approximately 29.733406, -111.760384) is a multi-cluster, stratified (units 2-4) site containing Clovis lithic technology and evidence for gomphothere butchering[91]. Within Locality 1, the Clovis component is found in stratum 3, member 3B. Although multiple dates have been obtained, "poor chronostratigraphic integrity best characterises the sequence exposed"[91]. Regardless, Sanchez et al.[91] assign the age of the Clovis component to AA-100181B (11,550±60 BP), a date obtained from a charcoal fleck among the same level as lithic flakes (gomphothere bone was not directly dated due to poor collagen preservation). Using these data, the model created places the start of the Clovis component at 14,135-13,470 cal BP (Fig. S18). Further chronometric work is required to better define the chronology at this site, however.

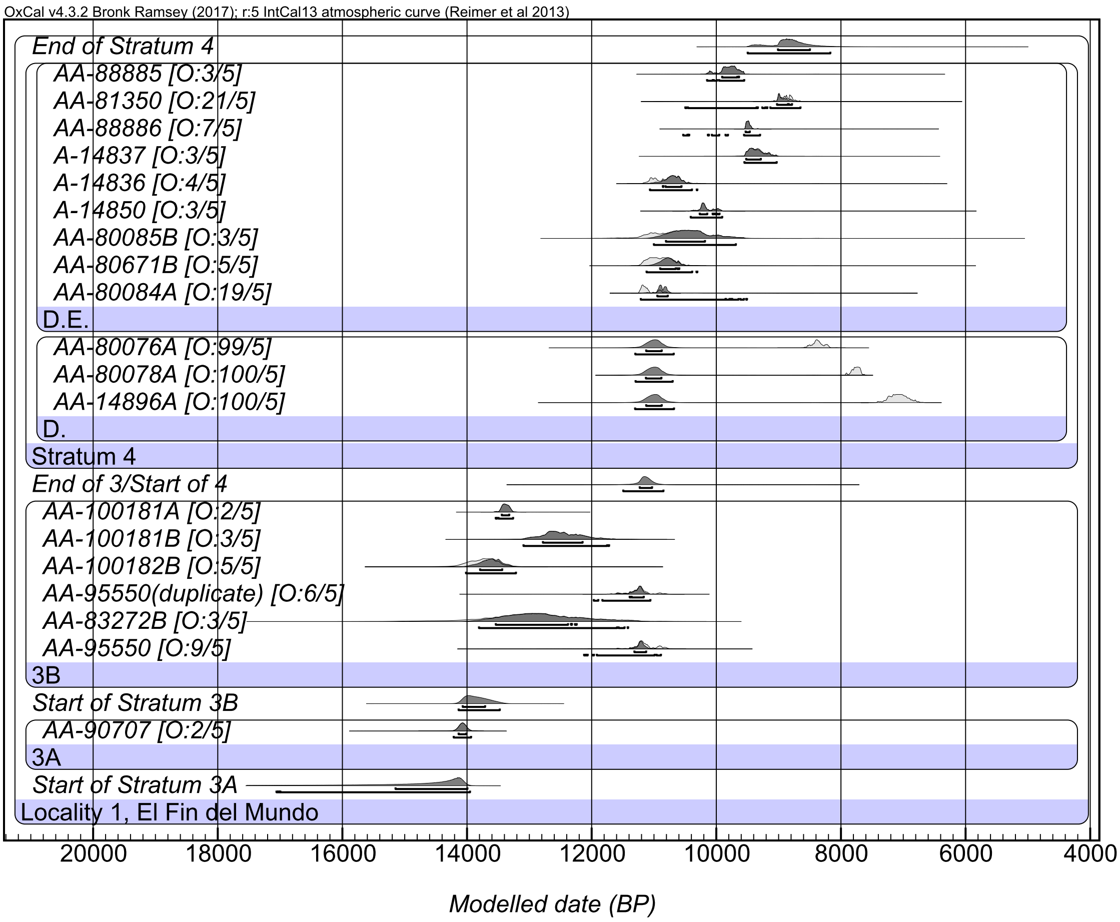

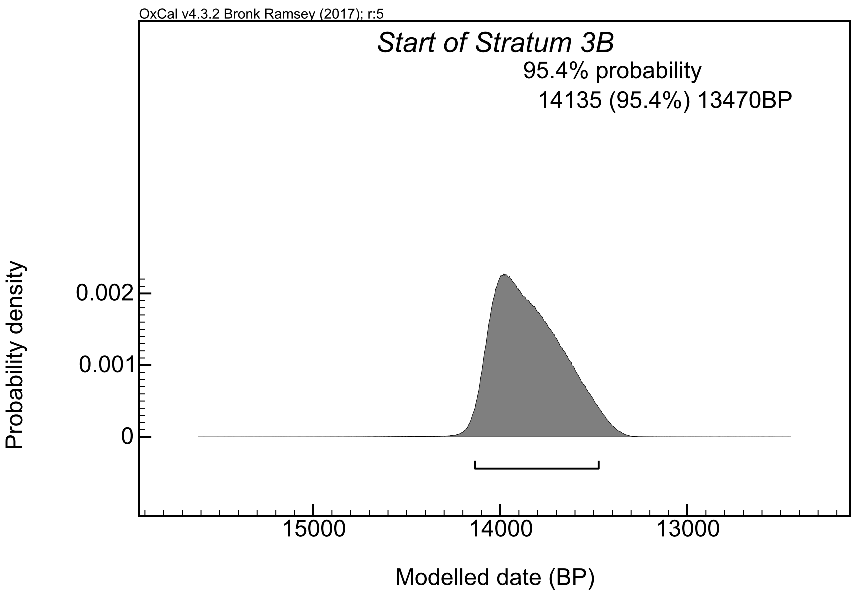

Fig. S18. Bayesian age model for El Fin del Mundo (above), and start `Boundary` (below). Brackets beneath each age estimate show 95.4% confidence interval. 'O:prior/posterior probability' reflects the outlier analysis.

```
Plot()
{
 Outlier_Model("General",T(5),U(0,4),"t");
 Sequence("Locality 1, El Fin del Mundo")
 {
  Boundary("Start of Stratum 3A");
  Phase("3A")
  {
   R_Date("AA-90707", 12180, 40)
   {
    Outlier("General", 0.05);
   };
  };
  Boundary("Start of Stratum 3B");
  Phase("3B")
  {
   R_Date("AA-95550", 9755, 92)
   {
    Outlier("General", 0.05);
   };
   R_Date("AA-83272B", 11040, 580)
   {
    Outlier("General", 0.05);
   };
   R_Date("AA-95550(duplicate)", 9804, 93)
   {
    Outlier("General", 0.05);
   };
   R_Date("AA-100182B", 11880, 200)
   {
    Outlier("General", 0.05);
   };
   R_Date("AA-100181B", 10650, 250)
   {
    Outlier("General", 0.05);
   };
   R_Date("AA-100181A", 11550, 60)
   {
    Outlier("General", 0.05);
   };
  };
  Boundary("End of 3/Start of 4");
  Sequence("Stratum 4")
  {
   Phase("D.")
   {
    R_Date("AA-14896A", 6185, 115)
    {
     Outlier("General", 0.05);
    };
    R_Date("AA-80078A", 6921, 58)
    {
     Outlier("General", 0.05);
    };
    R_Date("AA-80076A", 7570, 93)
    {
     Outlier("General", 0.05);
    };
   };
   Phase("D.E.")
   {
    R_Date("AA-80084A", 9715, 64)
    {
     Outlier("General", 0.05);
    };
    R_Date("AA-80671B", 9560, 120)
    {
     Outlier("General", 0.05);
    };
    R_Date("AA-80085B", 9290, 290)
    {
     Outlier("General", 0.05);
    };
    R_Date("A-14850", 9030, 75)
    {
     Outlier("General", 0.05);
    };
    R_Date("A-14836", 9465, 100)
    {
     Outlier("General", 0.05);
    };
    R_Date("A-14837", 8375, 110)
    {
     Outlier("General", 0.05);
    };
    R_Date("AA-88886", 8470, 50)
    {
     Outlier("General", 0.05);
    };
    R_Date("AA-81350", 8030, 50)
    {
     Outlier("General", 0.05);
    };
    R_Date("AA-88885", 8770, 60)
    {
     Outlier("General", 0.05);
    };
   };
  };
  Boundary("End of Stratum 4");
 };
};
```

2.2.10. Gault, Texas (U.S.A.)

Gault (41BL323; at 30.892283, -97.709742) is a multi-cluster, stratified (units 1-10) site containing pre-Clovis ("Gault Assemblage"), Clovis, Late Paleoindian, and Archaic material[92–97]. The pre-Clovis level is represented by small-projectile-point technology and a blade-and-core tradition. OSL was used to date the deposits[96,97]. Using these data, the model created places the start of the pre-Clovis (Gault Assemblage) component at 26,435-17,385 cal BP, and the start of Clovis at 16,895-12,705 cal BP (Fig. S19). The lack of precision in the model is largely due to the OSL measurements (with large error margins) and the few constraints from preceding dates. When we compare this model to that from the Debra L. Friedkin site (see Fig. S16), essentially the same archaeological location, we can see that the Clovis start boundary overlaps, but it is much more precise. Therefore, it is likely that more dates from phases constraining the start of the Clovis phase would result in a reduction in the span of the start boundary at this site.

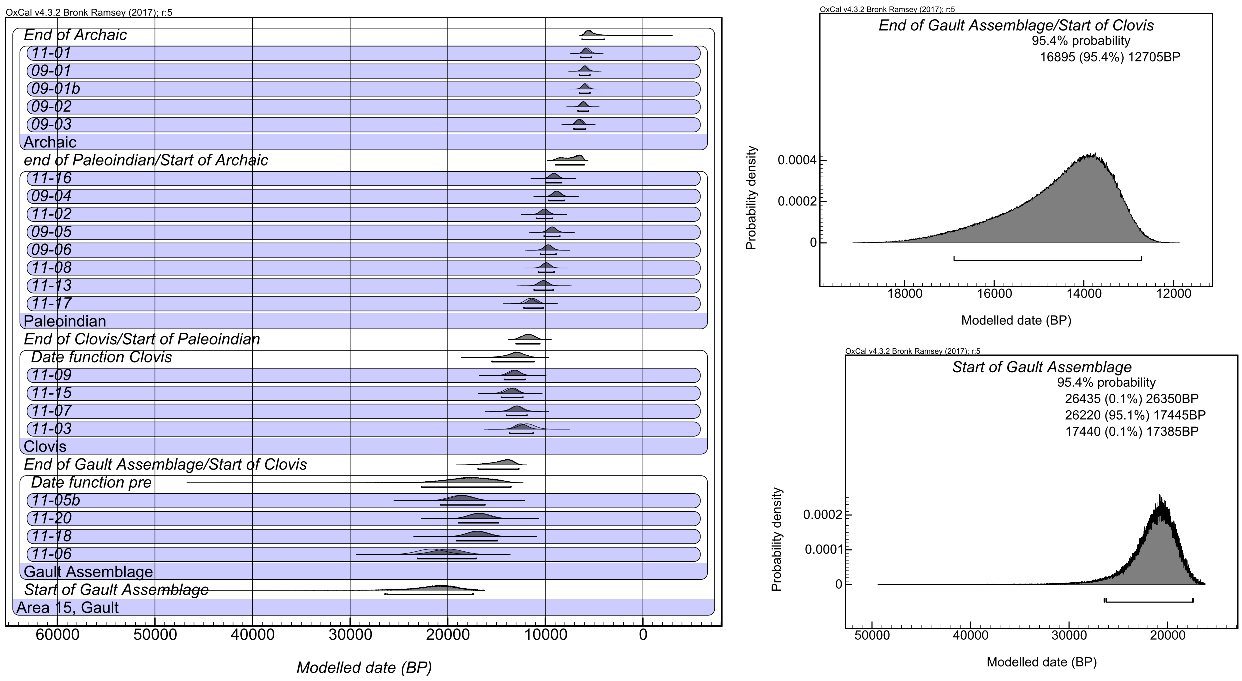

Fig. S19. Bayesian age model for Gault (above), and start boundaries for both pre-Clovis and Clovis components (adjacent). Brackets beneath each age estimate show 95.4% confidence interval. 'O:prior/posterior probability' reflects the outlier analysis.

```
Plot()
{
 Outlier_Model("General",T(5),U(0,4),"t");
 Sequence("Area 15, Gault")
 {
  Boundary("Start of Gault Assemblage");
  Phase("Gault Assemblage")
  {
   Age("11-06", N(21700, 1400))
   {
    Outlier("General", 0.05);
   };
   Age("11-18", N(16900, 1100))
   {
    Outlier("General", 0.05);
   };
   Age("11-20", N(16700, 1100))
   {
    Outlier("General", 0.05);
   };
   Age("11-05b", N(18700, 1200))
   {
    Outlier("General", 0.05);
   };
   Date("Date function pre");
  };
  Boundary("End of Gault Assemblage/Start of Clovis");
  Phase("Clovis")
  {
   Age("11-03", N(11900, 800))
   {
    Outlier("General", 0.05);
   };
   Age("11-07", N(12900, 600))
   {
    Outlier("General", 0.05);
   };
   Age("11-15", N(13600, 600))
   {
    Outlier("General", 0.05);
   };
   Age("11-09", N(13200, 600))
   {
    Outlier("General", 0.05);
   };
   Date("Date function Clovis");
  };
  Boundary("End of Clovis/Start of Paleoindian");
  Phase("Paleoindian")
  {
   Age("11-17", N(11600, 500))
   {
    Outlier("General", 0.05);
   };
   Age("11-13", N(10200, 500))
   {
    Outlier("General", 0.05);
   };
   Age("11-08", N(9900, 400))
   {
    Outlier("General", 0.05);
   };
   Age("09-06", N(9700, 400))
   {
    Outlier("General", 0.05);
   };
   Age("09-05", N(9300, 400))
   {
    Outlier("General", 0.05);
   };
   Age("11-02", N(10100, 400))
   {
    Outlier("General", 0.05);
   };
   Age("09-04", N(8800, 400))
   {
    Outlier("General", 0.05);
```

```
   };
   Age("11-16", N(9100, 400))
   {
    Outlier("General", 0.05);
   };
  };
  Boundary("end of Paleoindian/Start of Archaic");
  Phase("Archaic")
  {
   Age("09-03", N(6600, 300))
   {
    Outlier("General", 0.05);
   };
   Age("09-02", N(6100, 300))
   {
    Outlier("General", 0.05);
   };
   Age("09-01b", N(5900, 300))
   {
    Outlier("General", 0.05);
   };
   Age("09-01", N(5900, 300))
   {
    Outlier("General", 0.05);
   };
   Age("11-01", N(5700, 300))
   {
    Outlier("General", 0.05);
   };
  };
  Boundary("End of Archaic");
 };
};
```

2.2.11. Jake Bluff, Oklahoma (U.S.A.)

Jake Bluff (34HP60; at approximately 36.596874, -99.514348) is a Clovis, bison-butchering site with associated lithic tool technology[98–100]. The incorporation of five bone dates into a single `Phase`, dates the archaeological event to 12,775-12,645 cal BP (`Date` function; Fig. S20).

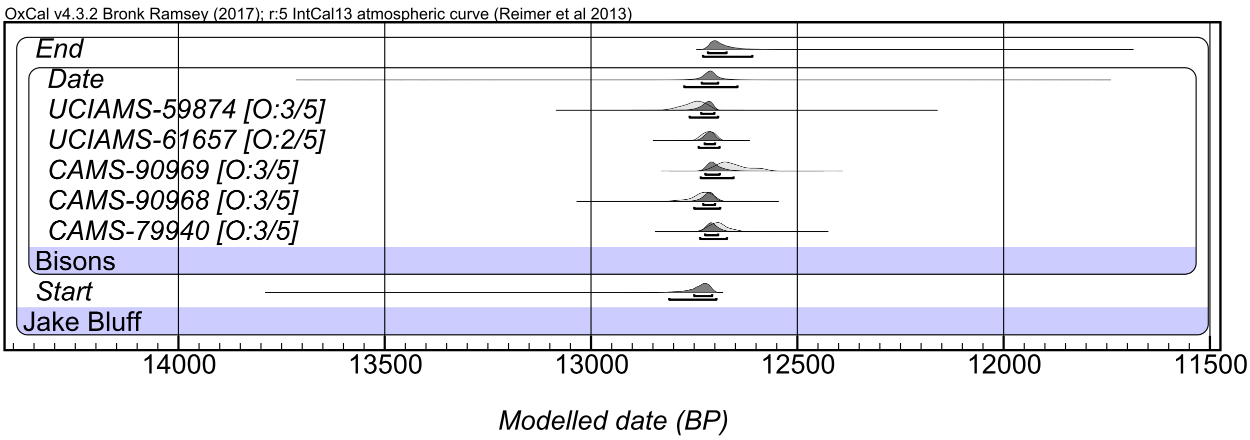

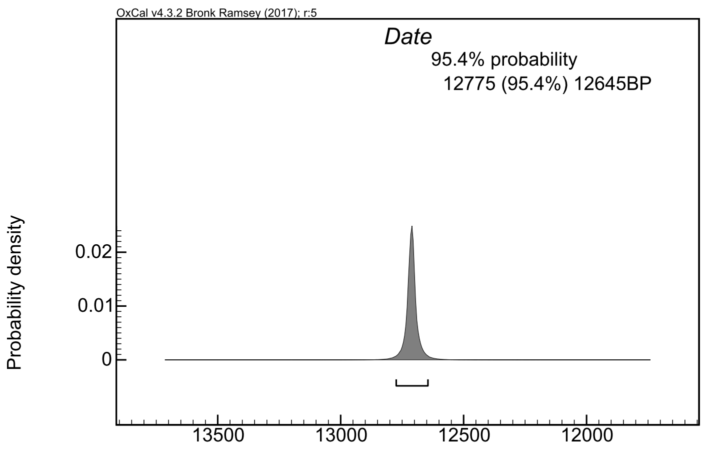

Fig. S20. Bayesian age model for Jake Bluff (above), and `Date` function (below). Brackets beneath each age estimate show 95.4% confidence interval. 'O:prior/posterior probability' reflects the outlier analysis.

```
Sequence("Jake Bluff")
{
 Outlier_Model("General",T(5),U(0,4),"t");
 Boundary("Start");
 Phase("Bisons")
 {
  R_Date("CAMS-79940", 10750, 40)
```

```
{
Outlier("General", 0.05);
};
R_Date("CAMS-90968", 10840, 45)
{
Outlier("General", 0.05);
};
R_Date("CAMS-90969", 10700, 45)
{
Outlier("General", 0.05);
};
R_Date("UCIAMS-61657", 10810, 25)
{
Outlier("General", 0.05);
};
R_Date("UCIAMS-59874", 10885, 35)
{
Outlier("General", 0.05);
};
Date("Date");
};
Boundary("End");
};
```

2.2.12. Lange/Ferguson, South Dakota (U.S.A.)

Lange/Ferguson (39SH33; at approximately 43.334567, -102.104490) is a Clovis, mammoth-butchering site with associated lithic and osseous tool technology[5,101–105]. Although geochronological data has been obtained from the site's stratified deposits[106], two XAD dates (UCIAMS-11344 and UCIAMS-11345) were measured directly from mammoth bone samples[5]. The incorporation of these into a single `Phase` model dates the Clovis component to 14,285-11,105 cal BP (`Date` function; Fig. S21).

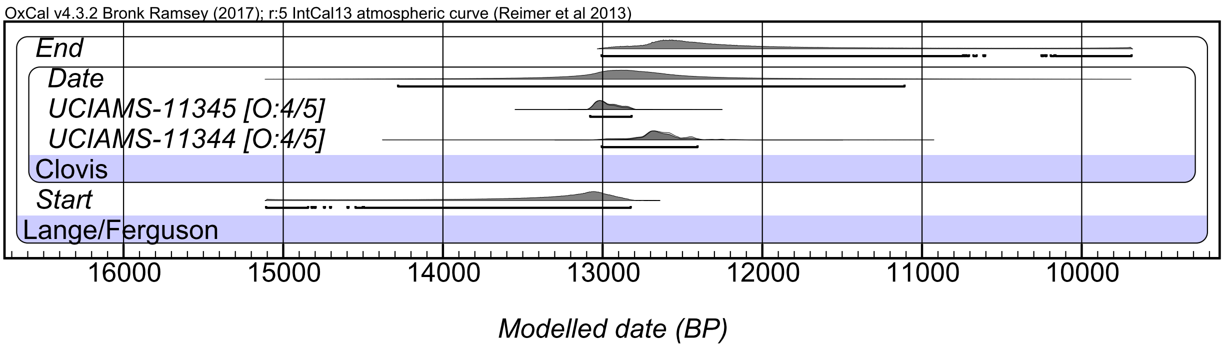

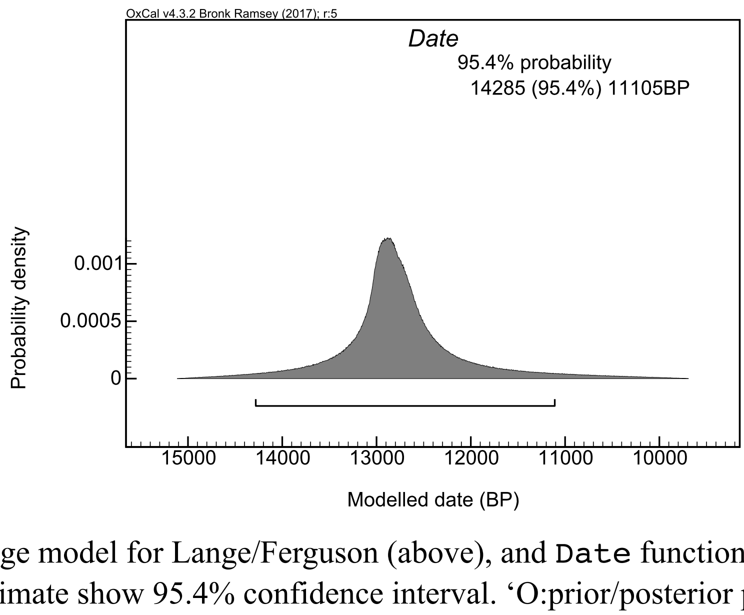

Fig. S21. Bayesian age model for Lange/Ferguson (above), and `Date` function (below). Brackets beneath each age estimate show 95.4% confidence interval. 'O:prior/posterior probability' reflects the outlier analysis.

```
Plot()
{
Outlier_Model("General",T(5),U(0,4),"t");
Sequence("Lange/Ferguson")
{
Boundary("Start");
Phase("Clovis")
{
R_Date("UCIAMS-11344", 10710, 130)
{
Outlier("General", 0.05);
};
R_Date("UCIAMS-11345", 11110, 40)
```

```
{
Outlier("General", 0.05);
};
Date("Date");
};
Boundary("End");
};
};
```

2.2.13. Lehner, Arizona (U.S.A.)

Lehner (Arizona EE:12:1; at 31.421691, -110.114805) is a Clovis, mammoth-butchering site with associated lithic tool technology and hearth features[103,107]. There are no direct bone dates, just charcoal-obtained measurements from hearth features. The incorporation of fourteen hearth-extracted, charcoal measurements into a single `Phase` model, dates the Clovis component at Lehner to 13,579-9,390 (`Date` function; Fig. S22). The span of this distribution is likely affected by five conventional radiocarbon dates—ranged from 7,205±450 (A-34) to 12,000±450 (A-40b)—which were rejected by archaeologists due to their large spread and perceived contamination[103,107].

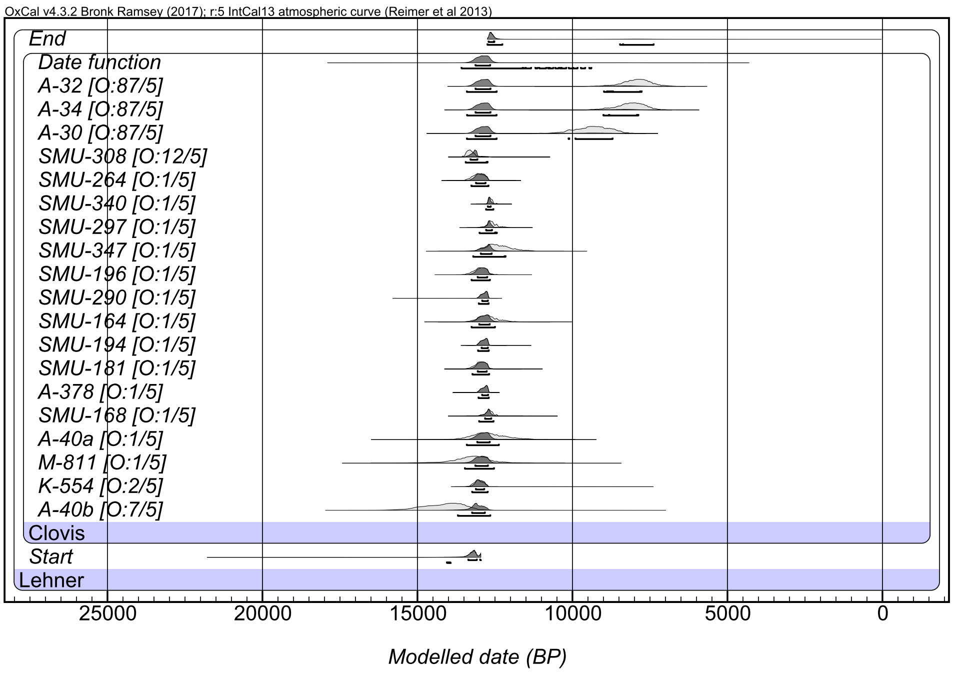

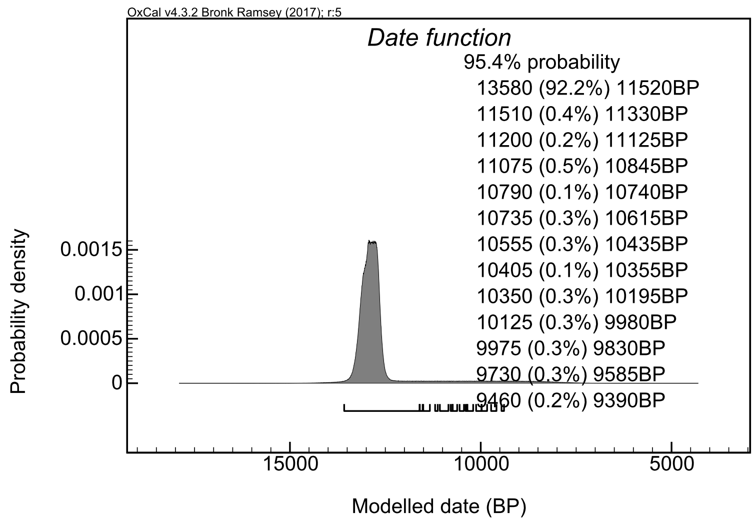

Fig. S22. Bayesian age model for Lehner (above), and `Date` function (below). Brackets beneath each age estimate show 95.4% confidence interval. 'O:prior/posterior probability' reflects the outlier analysis.

```
Plot()
{
 Outlier_Model("General",T(5),U(0,4),"t");
 Sequence(“Lehner”)
 {
  Boundary("Start");
  Phase("Clovis")
  {
   R_Date("A-40b", 12000, 450)
   {
    Outlier("General", 0.05);
   };
   R_Date("K-554", 11180, 140)
   {
    Outlier("General", 0.05);
   };
   R_Date("M-811", 11290, 500)
   {
    Outlier("General", 0.05);
   };
   R_Date("A-40a", 10900, 450)
   {
    Outlier("General", 0.05);
   };
   R_Date("SMU-168", 10770, 140)
   {
    Outlier("General", 0.05);
   };
   R_Date("A-378", 10940, 100)
   {
    Outlier("General", 0.05);
   };
   R_Date("SMU-181", 11080, 200)
   {
    Outlier("General", 0.05);
   };
   R_Date("SMU-194", 10950, 110)
   {
    Outlier("General", 0.05);
   };
   R_Date("SMU-164", 10860, 280)
   {
    Outlier("General", 0.05);
   };
   R_Date("SMU-290", 10950, 90)
   {
    Outlier("General", 0.05);
   };
   R_Date("SMU-196", 11080, 230)
   {
    Outlier("General", 0.05);
   };
   R_Date("SMU-347", 10620, 300)
   {
    Outlier("General", 0.05);
   };
   R_Date("SMU-297", 10700, 150)
   {
    Outlier("General", 0.05);
   };
   R_Date("SMU-340", 10710, 90)
   {
    Outlier("General", 0.05);
   };
   R_Date("SMU-264", 11170, 200)
   {
    Outlier("General", 0.05);
   };
   R_Date("SMU-308", 11470, 110)
   {
    Outlier("General", 0.05);
   };
   R_Date("A-30", 8330, 450)
   {
    Outlier("General", 0.05);
   };
   R_Date("A-34", 7205, 450)
   {
    Outlier("General", 0.05);
   };
   R_Date("A-32", 7022, 450)
   {
    Outlier("General", 0.05);
   };
   Date("Date function");
  };
  Boundary("End");
 };
};
```

2.2.14. Murray Springs, Arizona, (U.S.A.)

Murray Springs (Arizona EE:8:25; at approximately 32.236196, -110.330801) is a Clovis, mammoth- and bison-butchering site with associated lithic and osseous tool technology[103,108,109]. Although there are no bone dates, eight charcoal samples from the Graveyard Member (F1) have been dated and are deemed to represent the Clovis occupation at the site[108]. The incorporation of these into a single `Phase` model dates the Clovis component to 13,015-12,615 (`Date` function; Fig. S23).

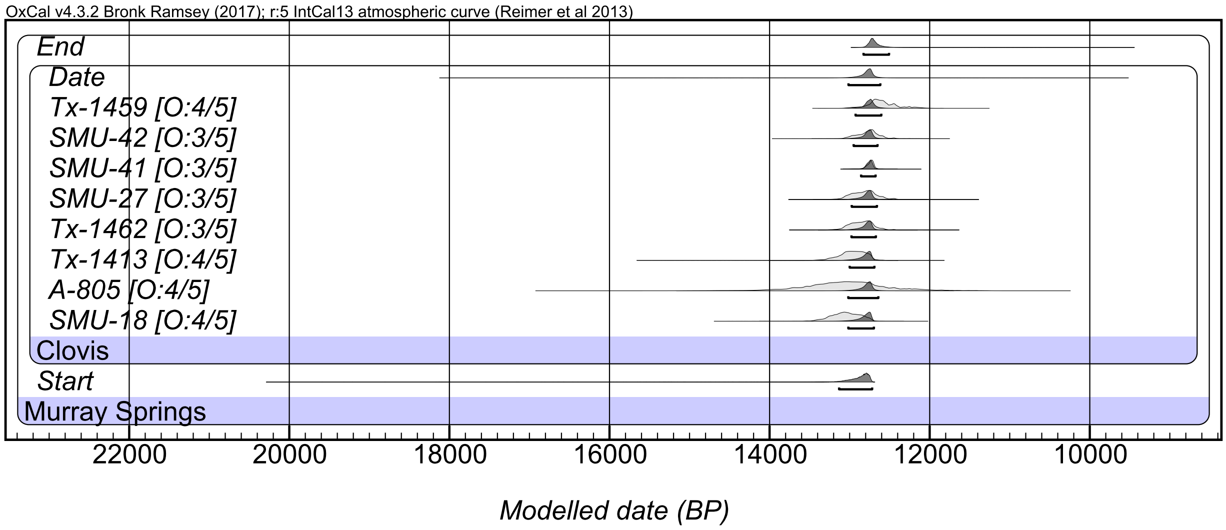

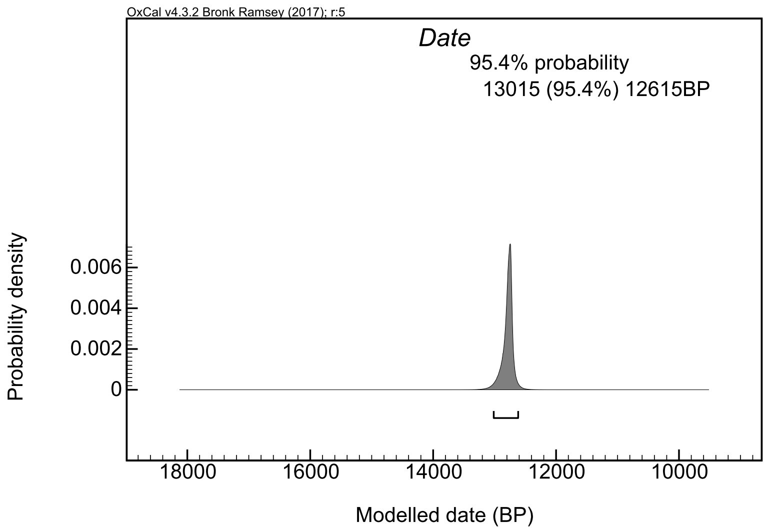

Fig. S23. Bayesian age model for Murray Springs (above), and `Date` function (below). Brackets beneath each age estimate show 95.4% confidence interval. 'O:prior/posterior probability' reflects the outlier analysis.

```
Plot()
{
 Outlier_Model("General",T(5),U(0,4),"t");
 Sequence("Murray Springs")
 {
  Boundary("Start");
  Phase("Graveyard Member F1")
  {
   R_Date("SMU-18", 11190, 180)
   {
    Outlier("General", 0.05);
   };
   R_Date("A-805", 11150, 450)
   {
    Outlier("General", 0.05);
   };
   R_Date("Tx-1413", 11080, 180)
   {
    Outlier("General", 0.05);
   };
   R_Date("Tx-1462", 10930, 170)
   {
    Outlier("General", 0.05);
   };
   R_Date("SMU-27", 10890, 180)
   {
    Outlier("General", 0.05);
   };
   R_Date("SMU-41", 10840, 70)
   {
    Outlier("General", 0.05);
   };
   R_Date("SMU-42", 10840, 140)
   {
    Outlier("General", 0.05);
   };
   R_Date("Tx-1459", 10710, 160)
   {
    Outlier("General", 0.05);
   };
   Date("Date function");
  };
  Boundary("End");
 };
};
```

2.2.15. Shawnee-Minisink, Pennsylvania, U.S.A.

Shawnee-Minisink (36MR43; at approximately 40.995474, -75.13735) is a stratified site (zones 1-4) containing Clovis, Archaic, and Woodland material[5,110–116]. Zone 4 (per ref 110), the Clovis level, includes lithic tool technology and hearth features. Apart from this layer, only the Middle Woodland has been dated[110]. Thus, all dates obtained (from hearth charcoal samples) for the Clovis component have been entered into a single `Phase` model. This dates the Clovis component to 12,910-12,650 cal BP (`Date` function; Fig. S24).

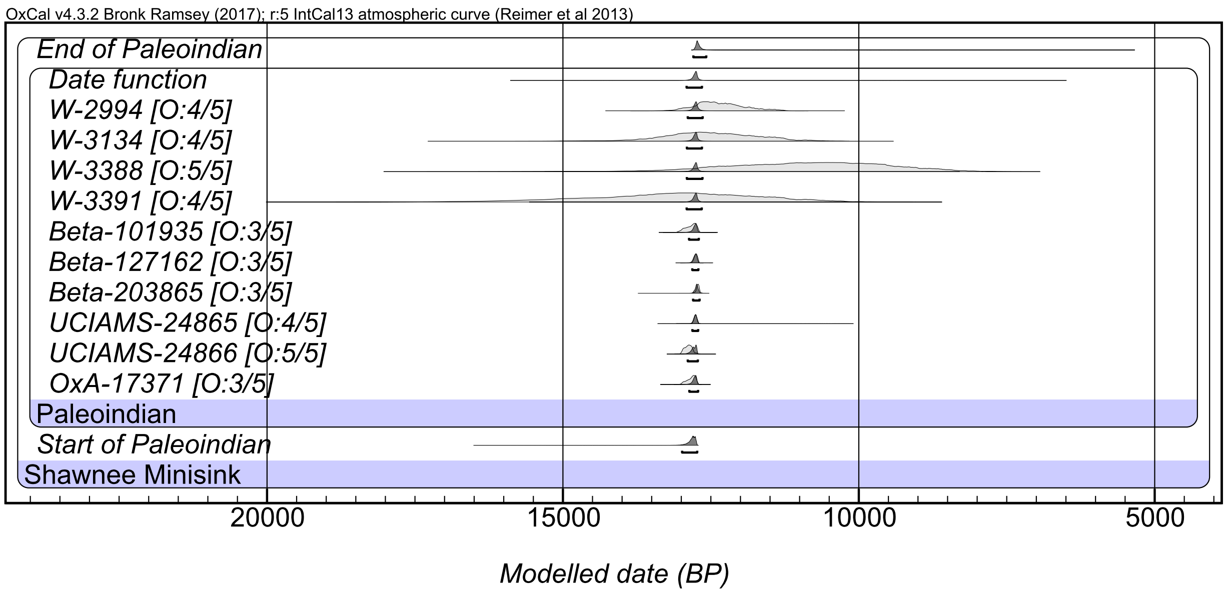

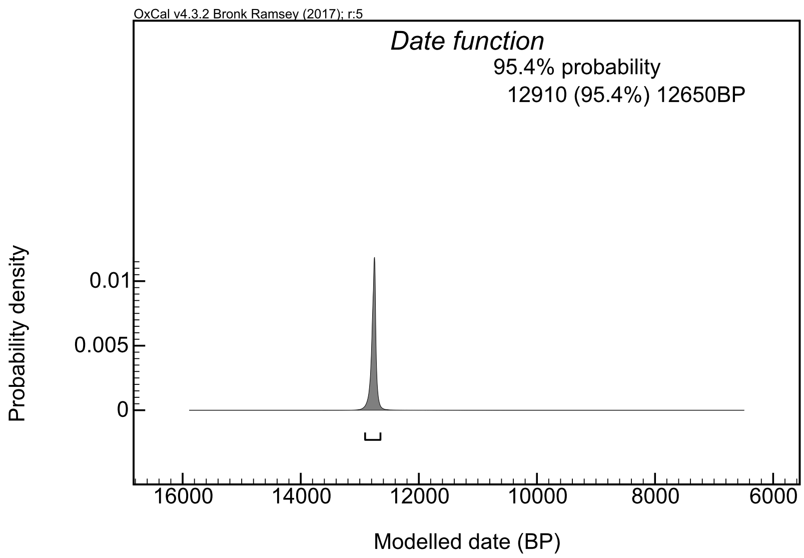

Fig. S24. Bayesian age model for Shawnee-Minisink (above), and `Date` function (below). Brackets beneath each age estimate show 95.4% confidence interval. 'O:prior/posterior probability' reflects the outlier analysis.

```
Plot()
{
 Outlier_Model("General",T(5),U(0,4),"t");
 Sequence("Shawnee-Minisink")
 {
  Boundary("Start of Paleoindian");
  Phase("Paleoindian")
  {
   R_Date("OxA-17371", 10970, 50)
   {
    Outlier("General", 0.05);
   };
   R_Date("UCIAMS-24866", 11020, 30)
   {
    Outlier("General", 0.05);
   };
   R_Date("UCIAMS-24865", 10915, 25)
```

```
   {
    Outlier("General", 0.05);
   };
   R_Date("Beta-203865", 10820, 50)
   {
    Outlier("General", 0.05);
   };
   R_Date("Beta-127162", 10900, 40)
   {
    Outlier("General", 0.05);
   };
   R_Date("Beta-101935", 10940, 90)
   {
    Outlier("General", 0.05);
   };
   R_Date("W-3391", 11050, 1000)
   {
    Outlier("General", 0.05);
   };
   R_Date("W-3388", 9310, 1000)
   {
    Outlier("General", 0.05);
   };
   R_Date("W-3134", 10750, 600)
   {
    Outlier("General", 0.05);
   };
   R_Date("W-2994", 10590, 300)
   {
    Outlier("General", 0.05);
   };
   Date("Date function");
  };
  Boundary("End of Paleoindian");
 };
};
```

2.2.16. Sheriden Cave, Ohio (U.S.A.)

Sheriden Cave (33WY252; at approximately 40.945194, -83.346083) is a stratified (units 1-6b) site containing Clovis lithic and osseous tool technology[117–123]. The Clovis assemblage was found at the upper portion of stratum 5a. Dates obtained provide stratigraphic control or date cultural features/artefacts directly, e.g., bone point (UCIAMS-38249). Using these data, the model created places the start of the Clovis component at 14,850-13,395 cal BP (Fig. S25).

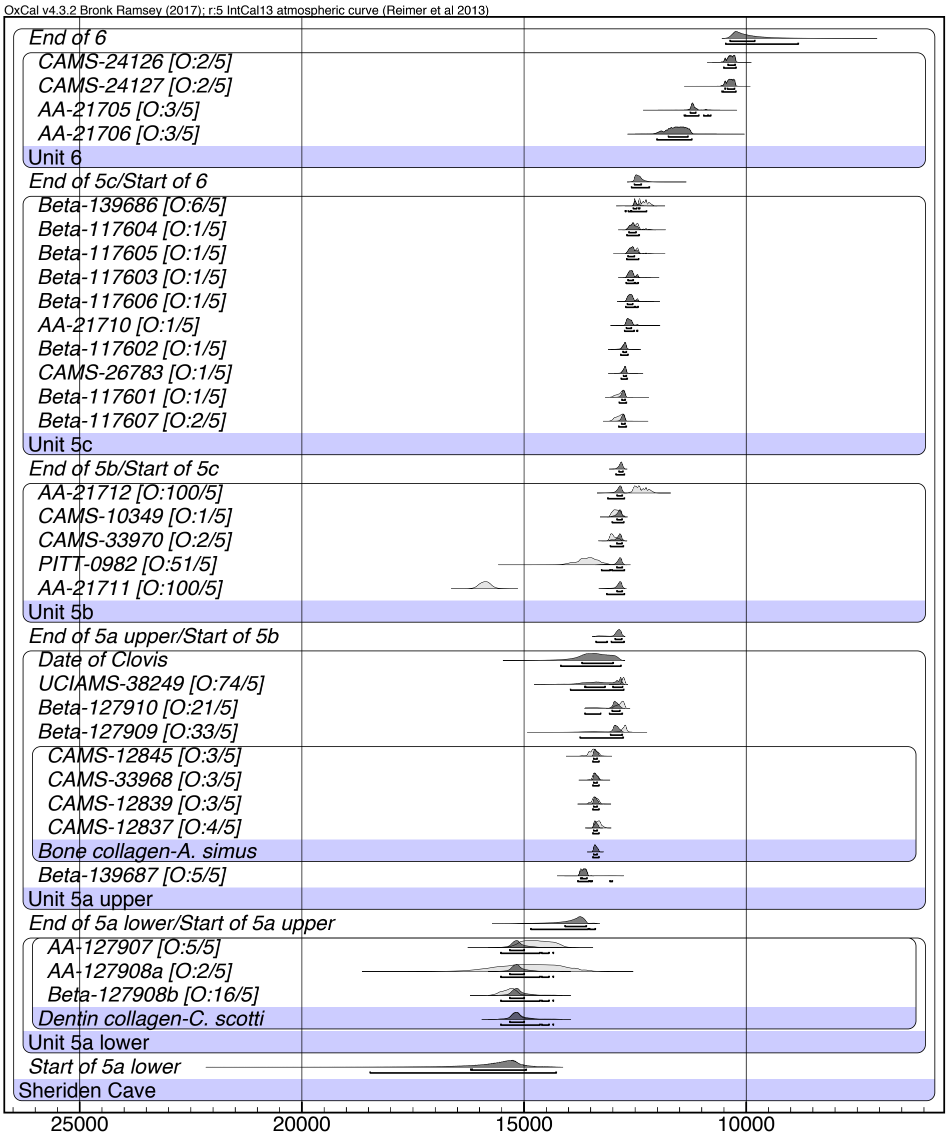

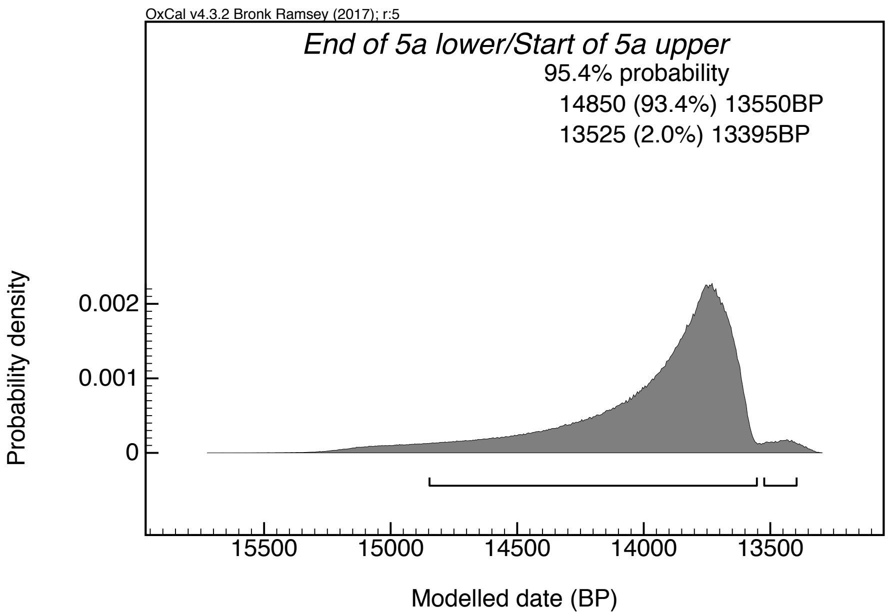

Fig. S25. Bayesian age model for Sheriden Cave (above), and start `Boundary` (below). Brackets beneath each age estimate show 95.4% confidence interval. 'O:prior/posterior probability' reflects the outlier analysis.

```
Plot()
{
 Outlier_Model("General",T(5),U(0,4),"t");
 Outlier_Model("SSimple",N(0,2),0,"s");
 Sequence("Sheriden Cave")
 {
  Boundary("Start of 5a lower");
  Phase("Unit 5a lower")
  {
   Combine("Dentin collagen-C. scotti")
   {
    R_Date("Beta-127908b", 12840, 100)
    {
     Outlier("SSimple", 0.05);
    };
    R_Date("AA-127908a", 12590, 450)
    {
     Outlier("SSimple", 0.05);
    };
    R_Date("AA-127907", 12520, 170)
    {
     Outlier("SSimple", 0.05);
    };
    Outlier("General", 0.05);
   };
  };
  Boundary("End of 5a lower/Start of 5a upper");
  Phase("Unit 5a upper")
  {
   R_Date("Beta-139687", 11860, 40)
   {
    Outlier("General", 0.05);
   };
   Combine("Bone collagen-A. simus")
   {
    R_Date("CAMS-12837", 11480, 60)
    {
     Outlier("SSimple", 0.05);
    };
    R_Date("CAMS-12839", 11570, 70)
    {
     Outlier("SSimple", 0.05);
    };
    R_Date("CAMS-33968", 11570, 50)
    {
     Outlier("SSimple", 0.05);
    };
    R_Date("CAMS-12845", 11610, 90)
    {
     Outlier("SSimple", 0.05);
    };
    Outlier("General", 0.05);
   };
   R_Date("Beta-127909", 10840, 80)
   {
    Outlier("General", 0.05);
   };
   R_Date("Beta-127910", 10960, 60)
   {
    Outlier("General", 0.05);
   };
   R_Date("UCIAMS-38249", 10915, 30)
   {
    Outlier("General", 0.05);
   };
   Date("Date of Clovis");
  };
  Boundary("End of 5a upper/Start of 5b");
  Phase("Unit 5b")
  {
   R_Date("AA-21711", 13210, 80)
   {
    Outlier("General", 0.05);
   };
   R_Date("PITT-0982", 11710, 220)
   {
    Outlier("General", 0.05);
   };
   R_Date("CAMS-33970", 11130, 60)
   {
    Outlier("General", 0.05);
   };
   R_Date("CAMS-10349", 11060, 60)
   {
    Outlier("General", 0.05);
   };
   R_Date("AA-21712", 10470, 70)
   {
    Outlier("General", 0.05);
   };
  };
  Boundary("End of 5b/Start of 5c");
  Phase("Unit 5c")
  {
   R_Date("Beta-117607", 10970, 70)
   {
    Outlier("General", 0.05);
   };
   R_Date("Beta-117601", 10940, 70)
   {
    Outlier("General", 0.05);
   };
   R_Date("CAMS-26783", 10850, 60)
   {
    Outlier("General", 0.05);
   };
   R_Date("Beta-117602", 10850, 70)
   {
    Outlier("General", 0.05);
   };
   R_Date("AA-21710", 10680, 80)
   {
    Outlier("General", 0.05);
   };
   R_Date("Beta-117606", 10620, 70)
   {
    Outlier("General", 0.05);
   };
   R_Date("Beta-117603", 10600, 60)
   {
    Outlier("General", 0.05);
   };
   R_Date("Beta-117605", 10570, 70)
   {
    Outlier("General", 0.05);
   };
   R_Date("Beta-117604", 10550, 70)
   {
    Outlier("General", 0.05);
   };
   R_Date("Beta-139686", 10440, 40)
   {
    Outlier("General", 0.05);
   };
  };
  Boundary("End of 5c/Start of 6");
  Phase("Unit 6")
  {
   R_Date("AA-21706", 10020, 115)
   {
    Outlier("General", 0.05);
   };
   R_Date("AA-21705", 9775, 70)
```

```
{
 Outlier("General", 0.05);
};
R_Date("CAMS-24127", 9190, 60)
{
 Outlier("General", 0.05);
};
R_Date("CAMS-24126", 9170, 60)
{
 Outlier("General", 0.05);
};
};
Boundary("End of 6");
};
};
```

2.3. *Clovis-coeval*

2.3.1. Arlington Springs, California (U.S.A.)

Arlington Springs (CA-SRI-173; at approximately 34.005591, -120.177117) is a Clovis-coeval site containing two human femora[124,125]. Two XAD dates were obtained on one of the femurs (CAMS-16814 and CAMS-16810). The oldest, CAMS-16810 (10,960±80 BP), was considered to be a more accurate date for the skeleton due to differences in collagen preservation within the bone[5,124]. Calibrated, the human femur dates to 13,015-12,705 cal BP.

2.3.2. Meay Channel I, Calvert Island (Canada)

Meay Channel I (EjTa-4; at approximately 51.659051, -128.098817) is a site containing several human footprints impressed into a paleosol (Stratum X)[126]. All dates obtained provide stratigraphic control. Using these data, the model created place the start of strata X/XI to 13,825-13,200 cal BP (Fig. S26). Date UCIAMS-186383 (720±15 BP), from a much younger stratum (II), was excluded as it skewed the model unnecessarily.

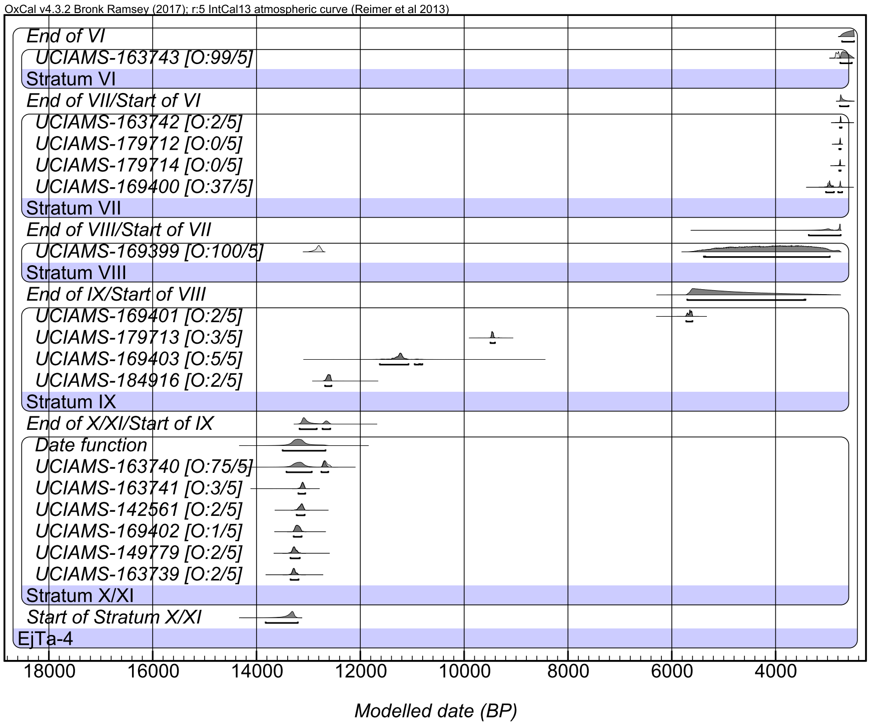

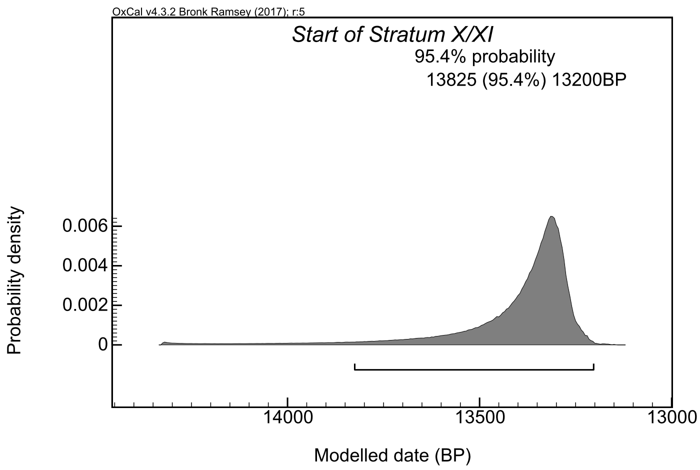

Fig. S26. Bayesian age model for Meay Channel I (above), and start `Boundary` (below). Brackets beneath each age estimate show 95.4% confidence interval. 'O:prior/posterior probability' reflects the outlier analysis.

```
Plot()
{
 Outlier_Model("General",T(5),U(0,4),"t");
 Sequence("Meay Channel I")
 {
  Boundary("Start of Stratum X/XI");
  Phase("Stratum X/XI")
  {
   R_Date("UCIAMS-163739", 11440, 25)
   {
    Outlier("General", 0.05);
   };
   R_Date("UCIAMS-149779", 11435, 30)
   {
    Outlier("General", 0.05);
   };
   R_Date("UCIAMS-169402", 11365, 25)
   {
    Outlier("General", 0.05);
   };
   R_Date("UCIAMS-142561", 11295, 30)
   {
    Outlier("General", 0.05);
   };
   R_Date("UCIAMS-163741", 11260, 25)
   {
    Outlier("General", 0.05);
   };
   R_Date("UCIAMS-163740", 10720, 60)
   {
    Outlier("General", 0.05);
   };
   Date("Date function");
  };
  Boundary("End of X/XI/Start of IX");
  Phase("Stratum IX")
  {
   R_Date("UCIAMS-184916", 10625, 20)
   {
    Outlier("General", 0.05);
```

```
   };
   R_Date("UCIAMS-169403", 9820, 80)
   {
    Outlier("General", 0.05);
   };
   R_Date("UCIAMS-179713", 8410, 20)
   {
    Outlier("General", 0.05);
   };
   R_Date("UCIAMS-169401", 4935, 25)
   {
    Outlier("General", 0.05);
   };
  };
  Boundary("End of IX/Start of VIII");
  Phase("Stratum VIII")
  {
   R_Date("UCIAMS-169399", 10980, 25)
   {
    Outlier("General", 0.05);
   };
  };
  Boundary("End of VIII/Start of VII");
  Phase("Stratum VII")
  {
   R_Date("UCIAMS-169400", 2855, 15)
   {
    Outlier("General", 0.05);
   };
   R_Date("UCIAMS-179714", 2650, 15)
   {
    Outlier("General", 0.05);
   };
   R_Date("UCIAMS-179712", 2645, 15)
   {
    Outlier("General", 0.05);
   };
   R_Date("UCIAMS-163742", 2605, 20)
   {
    Outlier("General", 0.05);
   };
  };
  Boundary("End of VII/Start of VI");
  Phase("Stratum VI")
  {
   R_Date("UCIAMS-163743", 2715, 20)
   {
    Outlier("General", 0.05);
   };
  };
  Boundary("End of VI");
 };
};
```

2.3.3. Lubbock Lake, Texas (U.S.A.)

Lubbock Lake (41LU1; at 33.622424, -101.889496) is a multi-cluster, stratified (strata 1-5) site containing Clovis-coeval, Folsom, Archaic, and Protohistoric material[127–131]. There is evidence for human predation of mammoth in the Clovis-coeval component (stratum 1)[132,133], and bison within the Folsom stratum (2). Using data from strata 1-3 (providing stratigraphic control and dating the bison directly), only, the model created places the start of the Clovis-coeval occupation at 13,790-12,765 cal BP (Fig. S27). Strata 4-5 were excluded as models struggled to reach good convergence due to large temporal gaps and inconsistencies in the upper levels. Two carbonate dates (I-246 and SMU-295) and bison bone estimates (SMU-317 and SMU-367) within Stratum 1, deemed anomalous and unreliable by the archaeologists, were given an outlier probability of 1.

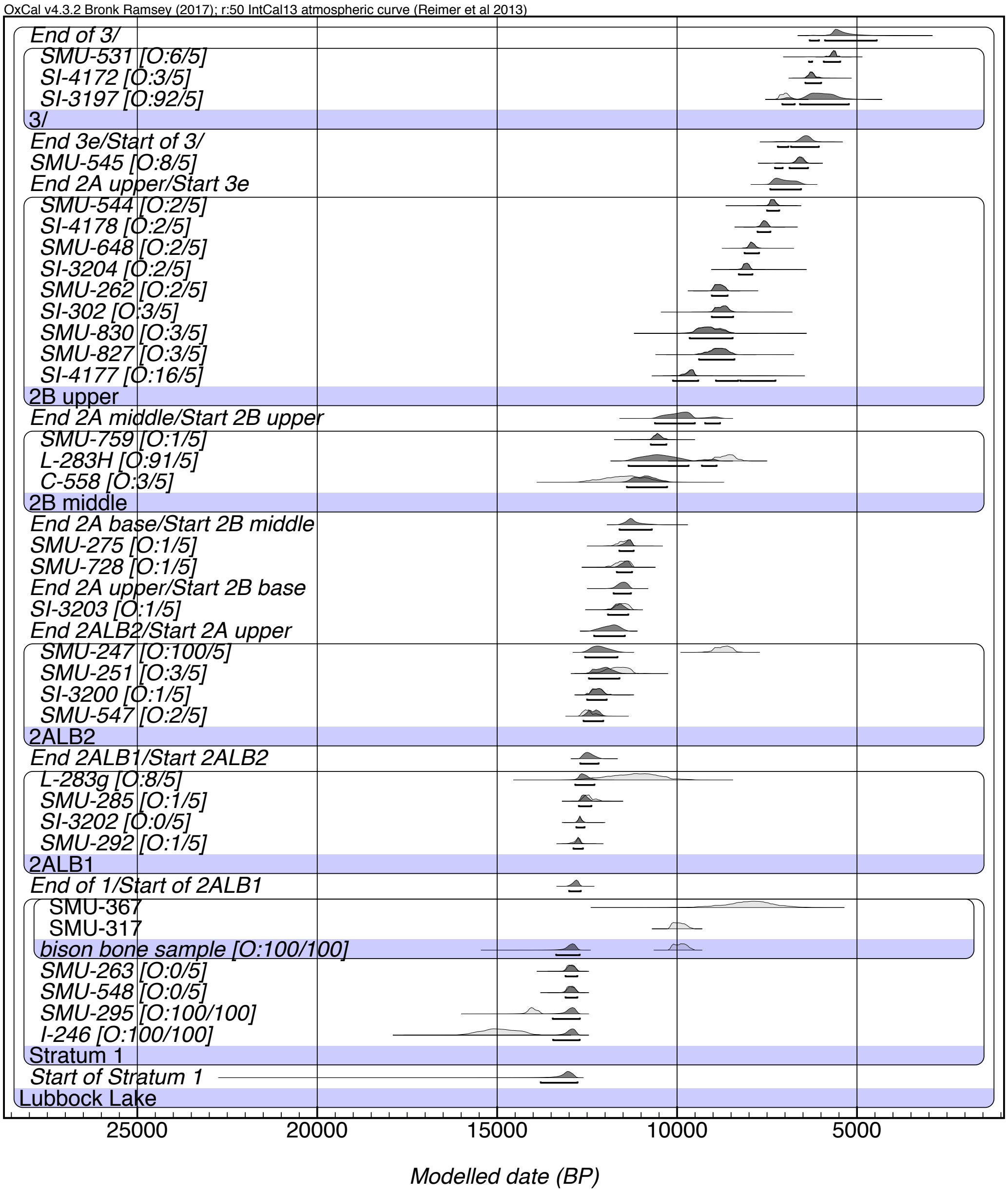

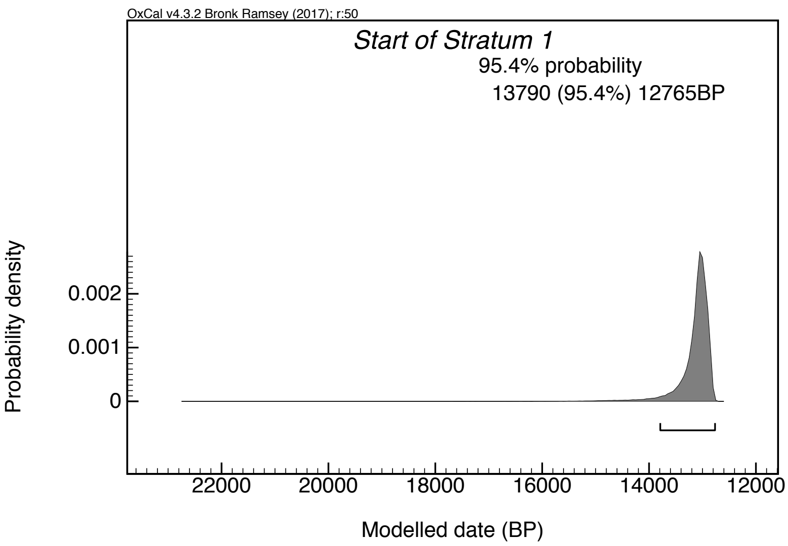

Fig. S27. Bayesian age model for Lubbock Lake (above), and start `Boundary` (below). Brackets beneath each age estimate show 95.4% confidence interval. 'O:prior/posterior probability' reflects the outlier analysis.

```
Plot()
{
 Outlier_Model("General",T(5),U(0,4),"t");
 Outlier_Model("SSimple",N(0,2),0,"s");
 Sequence("Lubbock Lake")
 {
  Boundary("Start of Stratum 1");
  Phase("Stratum 1")
  {
   R_Date("I-246", 12650, 290)
   {
    Outlier("General", 0.05);
   };
   R_Date("SMU-295", 12150, 90)
   {
    Outlier("General", 0.05);
   };
   R_Date("SMU-548", 11100, 100)
   {
    Outlier("General", 0.05);
   };
   R_Date("SMU-263", 11100, 100)
   {
    Outlier("General", 0.05);
   };
   R_Combine("bison bone sample")
   {
    R_Date("SMU-317", 8860, 90)
    {
     Outlier("SSimple", 0.05);
    };
    R_Date("SMU-367", 7040, 600)
    {
     Outlier("SSimple", 0.05);
    };
    Outlier("General", 0.05);
   };
  };
  Boundary("End of 1/Start of 2ALB1");
  Phase("2ALB1")
  {
   R_Date("SMU-292", 10880, 90)
   {
    Outlier("General", 0.05);
   };
   R_Date("SI-3202", 10780, 80)
   {
    Outlier("General", 0.05);
   };
   R_Date("SMU-285", 10530, 90)
   {
    Outlier("General", 0.05);
   };
   R_Date("L-283g", 9700, 450)
   {
    Outlier("General", 0.05);
   };
  };
  Boundary("End 2ALB1/Start 2ALB2");
  Phase("2ALB2")
  {
   R_Date("SMU-547", 10540, 100)
   {
    Outlier("General", 0.05);
   };
   R_Date("SI-3200", 10360, 80)
   {
    Outlier("General", 0.05);
   };
   R_Date("SMU-251", 10060, 170)
   {
    Outlier("General", 0.05);
   };
   R_Date("SMU-247", 7840, 170)
   {
    Outlier("General", 0.05);
   };
  };
  Boundary("End 2ALB2/Start 2A upper");
  R_Date("SI-3203", 10015, 75)
  {
   Outlier("General", 0.05);
  };
  Boundary("End 2A upper/Start 2B base");
  R_Date("SMU-728", 9990, 100)
  {
   Outlier("General", 0.05);
  };
  R_Date("SMU-275", 9960, 80)
  {
   Outlier("General", 0.05);
  };
  Boundary("End 2A base/Start 2B middle");
  Phase("2B middle")
  {
   R_Date("C-558", 9883, 350)
   {
    Outlier("General", 0.05);
   };
   R_Date("L-283H", 7765, 200)
   {
    Outlier("General", 0.05);
   };
   R_Date("SMU-759", 9330, 70)
   {
    Outlier("General", 0.05);
   };
  };
  Boundary("End 2A middle/Start 2B upper");
  Phase("2B upper")
  {
   R_Date("SI-4177", 8655, 90)
   {
    Outlier("General", 0.05);
   };
   R_Date("SMU-827", 7980, 180)
   {
    Outlier("General", 0.05);
   };
   R_Date("SMU-830", 8210, 240)
   {
    Outlier("General", 0.05);
   };
   R_Date("SI-302", 7890, 100)
   {
    Outlier("General", 0.05);
   };
   R_Date("SMU-262", 7970, 70)
   {
    Outlier("General", 0.05);
   };
   R_Date("SI-3204", 7255, 75)
   {
    Outlier("General", 0.05);
   };
   R_Date("SMU-648", 7100, 80)
   {
    Outlier("General", 0.05);
   };
   R_Date("SI-4178", 6705, 95)
   {
    Outlier("General", 0.05);
   };
   R_Date("SMU-544", 6400, 80)
```

```
   {
    Outlier("General", 0.05);
   };
  };
  Boundary("End 2A upper/Start 3e");
  R_Date("SMU-545", 5770, 80)
  {
   Outlier("General", 0.05);
  };
  Boundary("End 3e/Start of 3/");
  Phase("3/")
  {
   R_Date("SI-3197", 6115, 75)
   {
    Outlier("General", 0.05);
   };
   R_Date("SI-4172", 5475, 75)
   {
    Outlier("General", 0.05);
   };
   R_Date("SMU-531", 4900, 60)
   {
    Outlier("General", 0.05);
   };
  };
  Boundary("End of 3/");
 };
};
```

2.3.4. Wally's Beach, Alberta (Canada)

Wally's Beach (DhPg-8; at approximately 49.381404, -114.077366) is a Clovis-coeval, horse- and camel-butchering site with associated lithic tool technology[88,134–137]. Considering that XAD/HYP have been obtained for one camel, seven horses, and one muskox (nearby and unbutchered), a single `Phase` model was built. This dates the butchering events to 13,340-13,220 cal BP (`Date` function; Fig. S28).

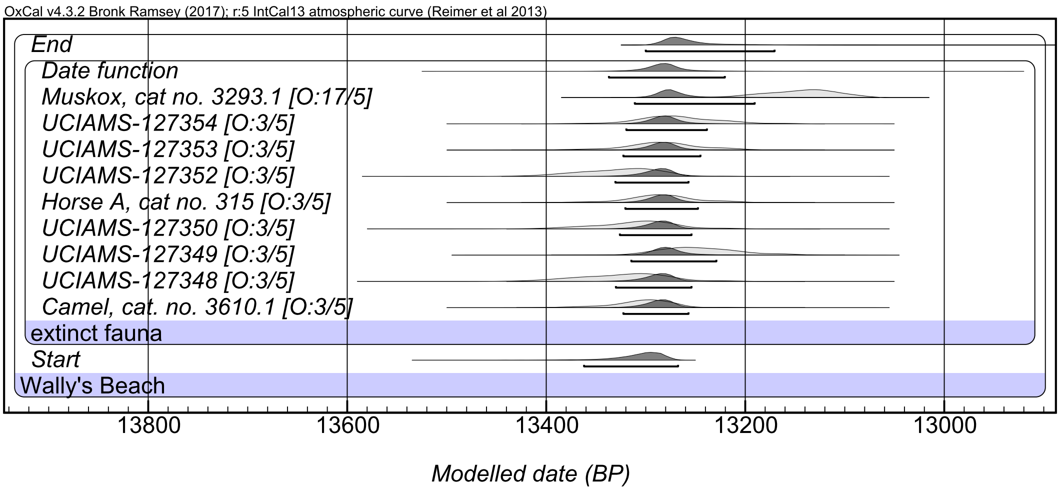

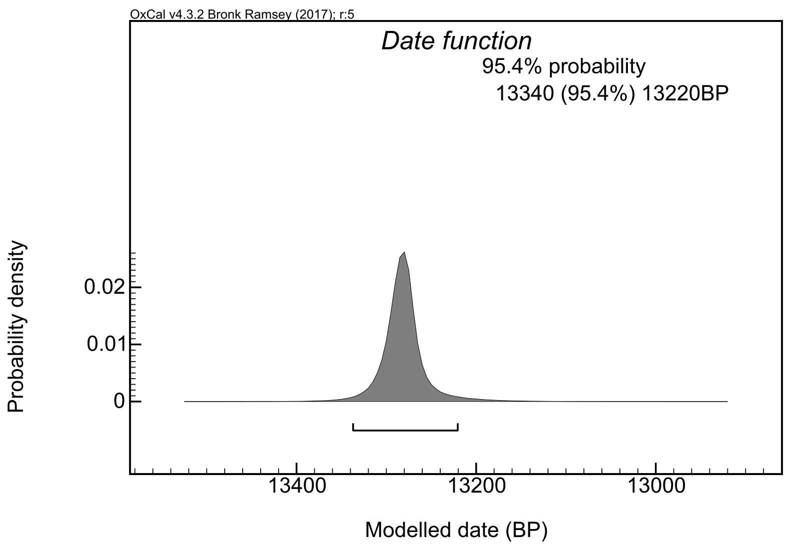

Fig. S28. Bayesian age model for Wally's Beach (above), and `Date` function (below). Brackets beneath each age estimate show 95.4% confidence interval. 'O:prior/posterior probability' reflects the outlier analysis.

```
Plot()
{
 Outlier_Model("General", T(5), U(0,4), "t");
 Outlier_Model("SSimple",N(0,2),0,"s");
 Sequence("Wally's Beach")
 {
  Boundary("Start");
  Phase("extinct fauna")
  {
   R_Combine("Camel, cat. no. 3610.1")
   {
    R_Date("UCIAMS-116400", 11465, 40)
    {
     Outlier("SSimple", 0.05);
    };
    R_Date("UCIAMS-127347", 11425, 30)
    {
     Outlier("SSimple", 0.05);
    };
    R_Date("OxA-X-2736-8", 11530, 50)
    {
     Outlier("SSimple", 0.05);
    };
    Outlier("General", 0.05);
   };
   //Horse 1, cat no.3594 XAD
   R_Date("UCIAMS-127348", 11470, 35)
   {
    Outlier("General", 0.05);
   };
   //Horse 2, cat no. 2988.1 XAD
   R_Date("UCIAMS-127349", 11410, 30)
   {
    Outlier("General", 0.05);
   };
   //Horse 3, cat no. 944 XAD
   R_Date("UCIAMS-127350", 11460, 30)
   {
    Outlier("General", 0.05);
   };
   R_Combine("Horse A, cat no. 315")
   {
    R_Date("UCIAMS-127351", 11440, 30)
    {
     Outlier("SSimple", 0.05);
    };
    R_Date("OxA-X-2736-10", 11445, 55)
    {
     Outlier("SSimple", 0.05);
    };
    Outlier("General", 0.05);
   };
   //Horse B, cat. no. 164 XAD
   R_Date("UCIAMS-127352", 11475, 30)
   {
    Outlier("General", 0.05);
   };
   //Horse C, cat. no 683 XAD
   R_Date("UCIAMS-127353", 11440, 30)
   {
    Outlier("General", 0.05);
   };
   //Horse D, cat. no 77.1 XAD
   R_Date("UCIAMS-127354", 11430, 30)
   {
    Outlier("General", 0.05);
   };
   R_Combine("Muskox, cat no. 3293.1")
   {
    R_Date("UCIAMS-127373", 11320, 30)
    {
     Outlier("SSimple", 0.05);
    };
    R_Date("OxA-X-2736-9", 11255, 50)
    {
     Outlier("SSimple", 0.05);
    };
    Outlier("General", 0.05);
   };
   Date("Date function");
  };
  Boundary("End");
 };
};
```

2.4. Pre-Clovis

In First Americans research, pre-Clovis sites are often controversial and viewed with skepticism[138]. Scrutiny is generally placed on the reliability of the archaeological evidence, rather than the chronometric data (given the relatively young age of this period, in radiocarbon dating terms, dated materials are less prone to modern carbon contamination). This study, however, considers all sites included in the analysis to provide unequivocal evidence of human activity. If there is uncertainty regarding cultural association for any given site, however, alternate views are noted. In the case of Meadowcroft Rockshelter, uncertainty regarding the cultural aspect of stratum IIa is taken into account, and a conservative modelling approach is taken (see section 2.4.9. for details).

2.4.1. Bluefish Caves, Yukon (Canada)

Bluefish Caves site (at 67.15, -140.75) is composed of three karstic cavities (Caves I, II, and III) with stratified deposits (Units A-D) and lithic technology (within Unit B)[139,140]. In 2017, six human-modified bones (but see refs 14,141) from Caves I and II were dated and published[140]. Results ranged from 10,490±55 BP (OxA-33776) to 19,650±130 BP (OxA-33778). Sample J7.8.17 (OxA-33778) is the only bone with a known stratigraphic location, however. Considering this and its antiquity, OxA-33778 (24,035-23,310 cal BP) has been used to represent the earliest human presence at Bluefish Caves.

2.4.2. Cactus Hill, Virginia (U.S.A.)

See in Clovis section.

2.4.3. Cooper's Ferry, Idaho (U.S.A.)

Cooper's Ferry (10IH73; at approximately 45.90538, -116.39751) is a multi-cluster, stratified [lithostratigraphic units (LU) 1-9] site containing lithics and faunal remains[8,12,142–145]. The oldest evidence for human activity occurs at LU3, where a number of prehistoric pit features were identified. In situ WST technology was found at the upper portion of LU3. All dates obtained provide stratigraphic control. Bayesian age modelling performed in reference 145 places the start of LU3 at 16,560-15,280 cal BP, whilst WST technology is best anchored by one date from upper LU3, OxA-X-2792-45 (13,610-13,275 cal BP). All dates directly obtained from pit features from the model were excluded as in reference 145 and not included in the sensitivity testing (section 5) due to their context.

2.4.4. Debra L. Friedkin, Texas (U.S.A.)

See Clovis section.

2.4.5. Gault, Texas (U.S.A.)

See Clovis section.

2.4.6. Hebior and Schaefer, Wisconsin (U.S.A.)

The sites of Hebior (47KN265) and Schaefer (47KN252) (both at approximately 42.643, -88.010) contain mammoth remains showing human modification and associated lithic technology[146–152]. The archaeological status of the sites has been rejected by Grayson and Meltzer, due to perceived data insufficiencies and doubts regarding the association between the mammoths and the lithic artefacts[132,133]. Although multiple dates have been obtained[146,151,153,154], XAD dates produced from mammoth bone samples are considered the most reliable. The incorporation of these into a single `Phase` model for each site dates the components to 15,615-13,975 cal BP (Hebior; `Date` function; Fig. S29) and 15,020-13,710 cal BP (Schaefer; `Date` function; Fig. S30).

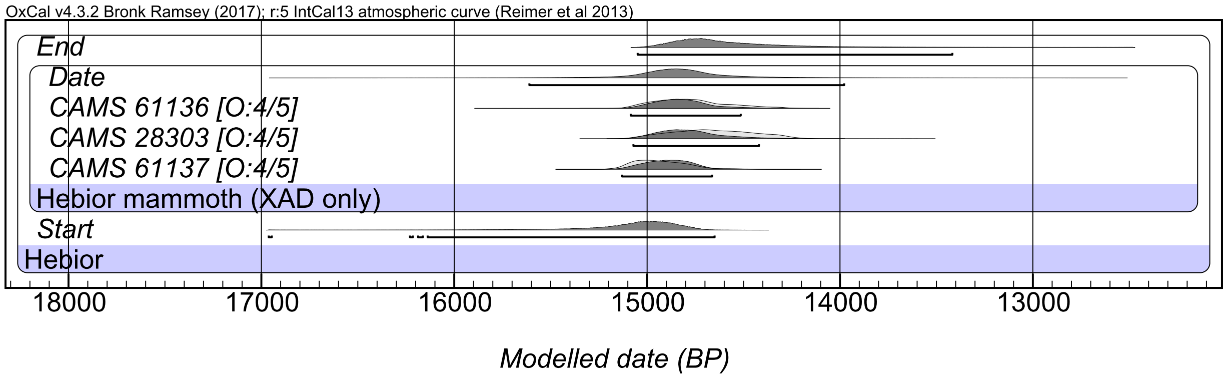

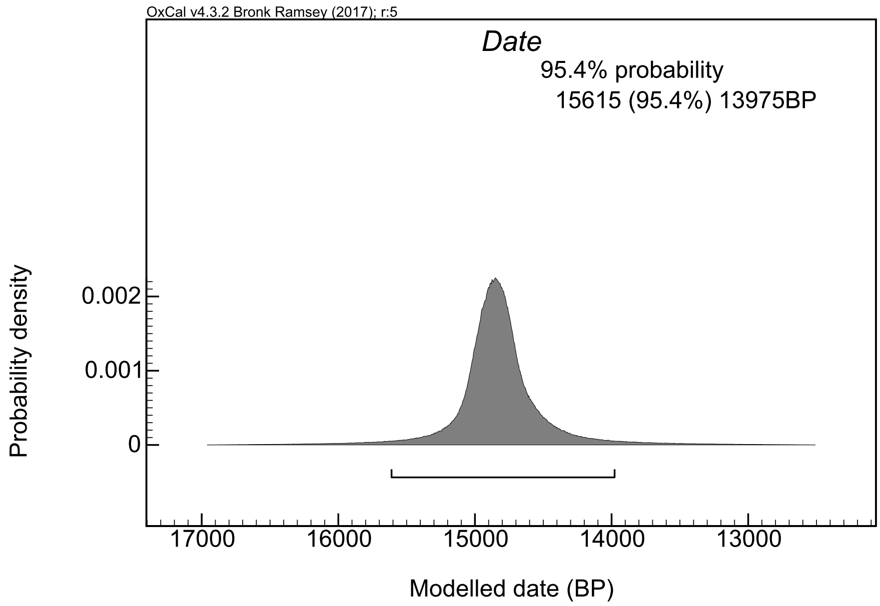

Fig. S29. Bayesian age model for Hebior (above), and `Date` function (below). Brackets beneath each age estimate show 95.4% confidence interval. 'O:prior/posterior probability' reflects the outlier analysis.

```
Sequence("Hebior")
{
 Outlier_Model("General",T(5),U(0,4),"t");
 Boundary("Start");
 Phase("Hebior mammoth (XAD only)")
 {
  R_Date("CAMS 61137", 12590, 50)
  {
   Outlier("General", 0.05);
  };
  R_Date("CAMS 28303", 12480, 60)
  {
   Outlier("General", 0.05);
  };
  R_Date("CAMS 61136", 12520, 50)
  {
   Outlier("General", 0.05);
  };
  Date("Date");
 };
 Boundary("End");
};
```

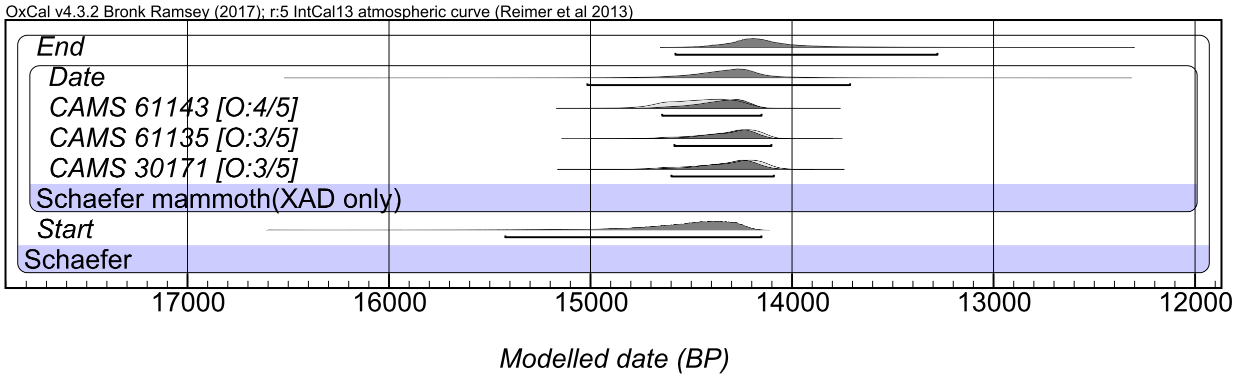

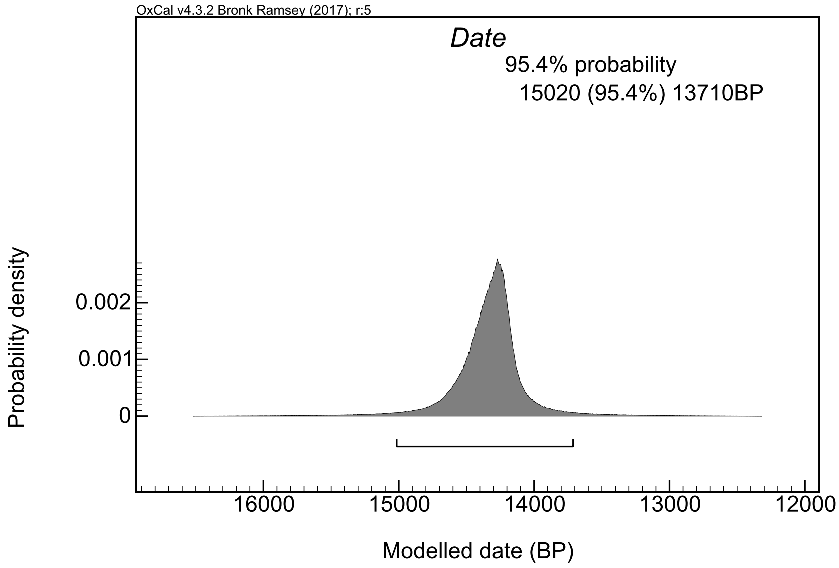

Fig. S30. Bayesian age model for Schaefer (above), and `Date` function (below). Brackets beneath each age estimate show 95.4% confidence interval. 'O:prior/posterior probability' reflects the outlier analysis.

```
Sequence("Schaefer")
{
 Outlier_Model("General",T(5),U(0,4),"t");
 Boundary("Start");
 Phase("Schaefer mammoth(XAD only)")
 {
  R_Date("CAMS 30171", 12310, 60)
  {
   Outlier("General", 0.05);
  };
  R_Date("CAMS 61135", 12320, 50)
  {
   Outlier("General", 0.05);
  };
  R_Date("CAMS 61143", 12390, 40)
  {
   Outlier("General", 0.05);
  };
  Date("Date");
 };
 Boundary("End");
};
```

2.4.7. Lindsay, Montana (U.S.A.)

Lindsay site (24DW501; also known as Deer Creek; at approximately at 47.232458, -105.128239) contains the remains of a single mammoth[88,155,156]. Cut marks on the bones suggest evidence of disarticulation and meat stripping[157] (but see reference 132). Although multiple dates have been obtained, four HYP and XAD dates produced from mammoth bone samples [88,158,159] are considered the most reliable. The incorporation of these into a single `Phase` model dates the component to 14,625-13,945cal BP (`Date` function; Fig. S31).

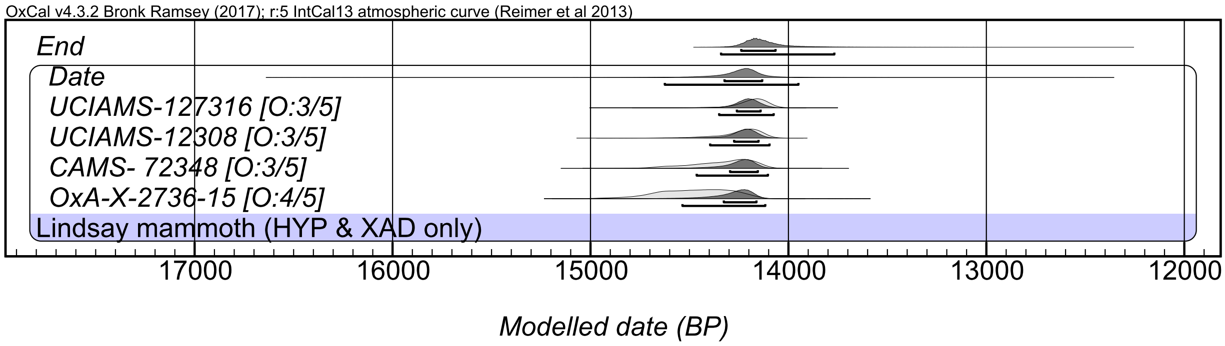

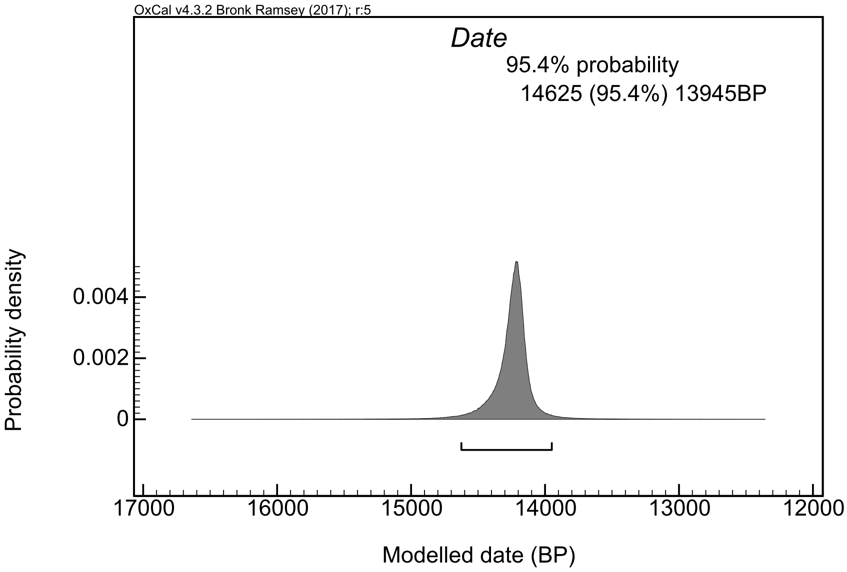

Fig. S31. Bayesian age model for Lindsay (above), and `Date` function (below). Brackets beneath each age estimate show 95.4% confidence interval. 'O:prior/posterior probability' reflects the outlier analysis.

```
Sequence("Lindsay")
{
 Outlier_Model("General",T(5),U(0,4),"t");
 Boundary("Start");
 Phase("Lindsay mammoth (HYP & XAD only)")
 {
  R_Date("OxA-X-2736-15", 12395, 55)
  {
   Outlier("General", 0.05);
  };
  R_Date("CAMS- 72348", 12330, 50)
  {
   Outlier("General", 0.05);
  };
  R_Date("UCIAMS-12308", 12300, 35)
  {
   Outlier("General", 0.05);
  };
  R_Date("UCIAMS-127316", 12270, 35)
  {
   Outlier("General", 0.05);
  };
  Date("Date");
 };
 Boundary("End");
};
```

2.4.8. Manis, Washington (U.S.A.)

Manis site (45CA218; at approximately 48.032304, -123.101320) contains the remains of a single mastodon with an osseous (mastodon bone) projectile point embedded in its rib[160–162] (but see references 132 and 163). Although multiple dates have been obtained for the site, four XAD dates produced from mastodon bone samples are considered most reliable[160]. The incorporation of these into a single `Phase` model dates the component to 13,975-13,600 cal BP (`Date` function; Fig. S32).

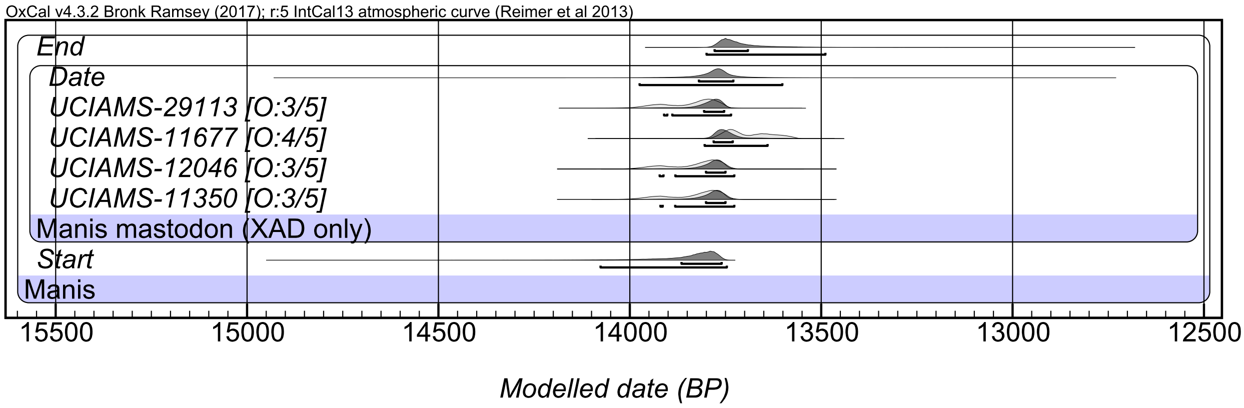

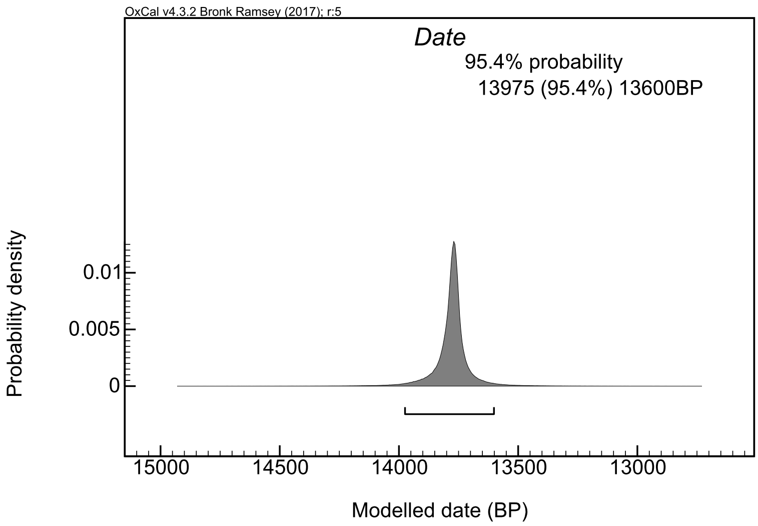

Fig. S32. Bayesian age model for Manis (above), and `Date` function (below). Brackets beneath each age estimate show 95.4% confidence interval. 'O:prior/posterior probability' reflects the outlier analysis.

```
Sequence("Manis")
 {
  Outlier_Model("General",T(5),U(0,4),"t");
  Boundary("Start");
  Phase("Manis mastodon (XAD only)")
  {
   R_Date("UCIAMS-11350",11975,35)
   {
    Outlier("General", 0.05);
   };
   R_Date("UCIAMS-12046",11975,35)
   {
    Outlier("General", 0.05);
   };
   R_Date("UCIAMS-11677",11890,35)
   {
    Outlier("General", 0.05);
   };
   R_Date("UCIAMS-29113",11990,30)
   {
    Outlier("General", 0.05);
   };
   Date("Date");
  };
  Boundary("End");
 };
```

2.4.9. Meadowcroft Rockshelter, Pennsylvania (U.S.A.)

Meadowcroft Rockshelter (36WH297; at 40.286445, -80.488813) is a multi-component, stratified (strata I-XI) site containing pre-Clovis ("Miller complex"), Archaic, Woodland, and historic material[75,164–168]. Miller technology is found within Stratum IIa and all dates obtained provide stratigraphic control[165,168]. The antiquity of the basal strata [I and IIa (deepest levels)] has caused much controversy; some argue that old-carbon contamination has overestimated the radiocarbon results[169] and others note that insufficient data has been published[170]. For this reason, the start of Stratum IIa (F-46 Lower)—instead of Stratum IIa (deepest levels)—has been used to estimate the start of the pre-Clovis component at the site, placing it at 24,335-18,620 cal BP (Fig.

S33). The imprecision of this boundary is likely due to a small temporal gap between the deepest levels of Stratum IIa and F-46 lower. Given the good agreement between chronometric data and stratigraphic evidence at this level, this, in turn, probably reflects a real taphonomic event or an artefact of sampling/dating bias.

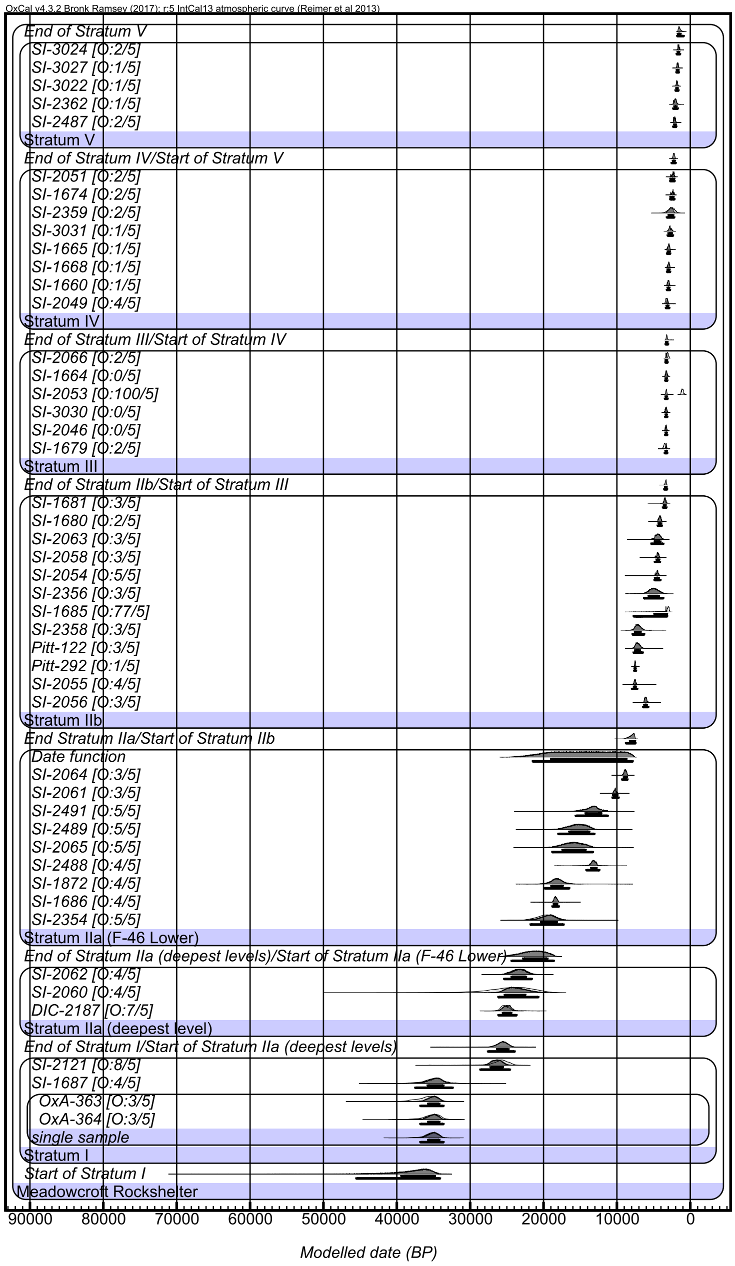

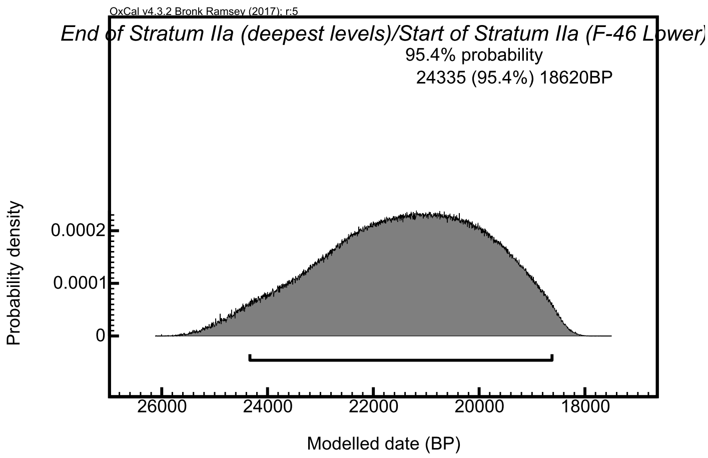

Fig. S33. Bayesian age model for Meadowcroft Rockshelter (above), and start `Boundary` (below). Brackets beneath each age estimate show 95.4% confidence interval. 'O:prior/posterior probability' reflects the outlier analysis.

```
Plot()
{
 Outlier_Model("General",T(5),U(0,4),"t");
 Outlier_Model("SSimple",N(0,2),0,"s");
 Sequence("Meadowcroft Rockshelter")
 {
  Boundary("Start of Stratum I");
  Phase("Stratum I")
  {
   R_Combine("single sample")
   {
    R_Date("OxA-364", 30900, 1100)
    {
     Outlier("SSimple", 0.05);
    };
    R_Date("OxA-363", 31400, 1200)
    {
     Outlier("SSimple", 0.05);
    };
    Outlier("General", 0.05);
   };
   R_Date("SI-1687", 30710, 1140)
   {
    Outlier("General", 0.05);
   };
   R_Date("SI-2121", 21380, 800)
   {
    Outlier("General", 0.05);
   };
  };
  Boundary("End of Stratum I/Start of Stratum IIa (deepest levels)");
  Phase("Stratum IIa (deepest level)")
  {
   R_Date("DIC-2187", 21070, 475)
   {
    Outlier("General", 0.05);
   };
   //small diluted sample
   R_Date("SI-2060", 19600, 2400)
   {
    Outlier("General", 0.05);
   };
   //small diluted sample
   R_Date("SI-2062", 19100, 810)
   {
    Outlier("General", 0.05);
   };
  };
  Boundary("End of Stratum IIa (deepest levels)/Start of Stratum IIa (F-46 Lower)");
  Phase("Stratum IIa (F-46 Lower)")
  {
   R_Date("SI-2354", 16175, 975)
   {
    Outlier("General", 0.05);
   };
   R_Date("SI-1686", 15120, 165)
   {
    Outlier("General", 0.05);
   };
   R_Date("SI-1872", 14975, 620)
   {
    Outlier("General", 0.05);
   };
   R_Date("SI-2488", 11320, 340)
   {
    Outlier("General", 0.05);
   };
   R_Date("SI-2065", 13240, 1010)
   {
    Outlier("General", 0.05);
   };
   R_Date("SI-2489", 12800, 870)
   {
    Outlier("General", 0.05);
   };
   R_Date("SI-2491", 11300, 700)
   {
    Outlier("General", 0.05);
   };
   R_Date("SI-2061", 9075, 115)
   {
    Outlier("General", 0.05);
   };
   R_Date("SI-2064", 8010, 110)
   {
    Outlier("General", 0.05);
   };
   Date("Date function");
  };
  Boundary("End Stratum IIa/Start of Stratum IIb");
  Phase("Stratum IIb")
  {
   R_Date("SI-2056", 5300, 130)
   {
    Outlier("General", 0.05);
   };
   R_Date("SI-2055", 6670, 140)
   {
    Outlier("General", 0.05);
   };
   R_Date("Pitt-292", 6630, 70)
   {
    Outlier("General", 0.05);
   };
   R_Date("Pitt-122", 6315, 280)
   {
    Outlier("General", 0.05);
   };
   R_Date("SI-2358", 6290, 355)
   {
    Outlier("General", 0.05);
   };
   R_Date("SI-1685", 2870, 85)
   {
    Outlier("General", 0.05);
   };
   R_Date("SI-2356", 4380, 500)
   {
    Outlier("General", 0.05);
   };
   R_Date("SI-2054", 4005, 85)
   {
    Outlier("General", 0.05);
   };
   R_Date("SI-2058", 3970, 85)
   {
    Outlier("General", 0.05);
   };
   R_Date("SI-2063", 3950, 240)
   {
    Outlier("General", 0.05);
   };
   R_Date("SI-1680", 3770, 90)
   {
    Outlier("General", 0.05);
   };
   R_Date("SI-1681", 3210, 95)
   {
    Outlier("General", 0.05);
   };
  };
  Boundary("End of Stratum IIb/Start of Stratum III");
  Phase("Stratum III")
  {
   R_Date("SI-1679", 3255, 115)
   {
```

```
   Outlier("General", 0.05);
  };
  R_Date("SI-2046", 3115, 70)
  {
   Outlier("General", 0.05);
  };
  R_Date("SI-3030", 3100, 90)
  {
   Outlier("General", 0.05);
  };
  R_Date("SI-2053", 1140, 115)
  {
   Outlier("General", 0.05);
  };
  R_Date("SI-1664", 3065, 80)
  {
   Outlier("General", 0.05);
  };
  R_Date("SI-2066", 2930, 75)
  {
   Outlier("General", 0.05);
  };
 };
 Boundary("End of Stratum III/Start of Stratum IV");
 Phase("Stratum IV")
 {
  R_Date("SI-2049", 3050, 85)
  {
   Outlier("General", 0.05);
  };
  R_Date("SI-1660", 2860, 80)
  {
   Outlier("General", 0.05);
  };
  R_Date("SI-1668", 2820, 75)
  {
   Outlier("General", 0.05);
  };
  R_Date("SI-1665", 2815, 80)
  {
   Outlier("General", 0.05);
  };
  R_Date("SI-3031", 2655, 120)
  {
   Outlier("General", 0.05);
  };
  R_Date("SI-2359", 2485, 350)
  {
   Outlier("General", 0.05);
  };
  R_Date("SI-1674", 2325, 75)
  {
   Outlier("General", 0.05);
  };
  R_Date("SI-2051", 2290, 90)
  {
   Outlier("General", 0.05);
  };
 };
 Boundary("End of Stratum IV/Start of Stratum V");
 Phase("Stratum V")
 {
  R_Date("SI-2487", 2155, 65)
  {
   Outlier("General", 0.05);
  };
  R_Date("SI-2362", 2075, 125)
  {
   Outlier("General", 0.05);
  };
  R_Date("SI-3022", 1880, 65)
  {
   Outlier("General", 0.05);
  };
  R_Date("SI-3027", 1790, 60)
  {
   Outlier("General", 0.05);
  };
  R_Date("SI-3024", 1665, 65)
  {
   Outlier("General", 0.05);
  };
 };
 Boundary("End of Stratum V");
};
};
```

2.4.10. Page-Ladson, Florida (U.S.A)

Page-Ladson (8JE591; at approximately 30.173805, -83.956282) is a stratified (units 2-4), underwater site containing a butchered mastodon with associated lithic tool technology. Radiocarbon data obtained from the 2013 excavations were used, where the pre-Clovis component is found within units 3c and 4[171,172]. Although the dates provide stratigraphic control, some of the measurements made on twigs are reported as mastodon digesta[171]. We built a Bayesian model based on the stratigraphic sequence of broad geological units reported by the excavators, incorporating the depths below datum in phases 3c and 4a as the relative prior within a sequence model, constrained by the units above and below. Using these data, the model yielded an age range for the start of unit 3c at 14,710-14,450 cal BP (Fig. S34).

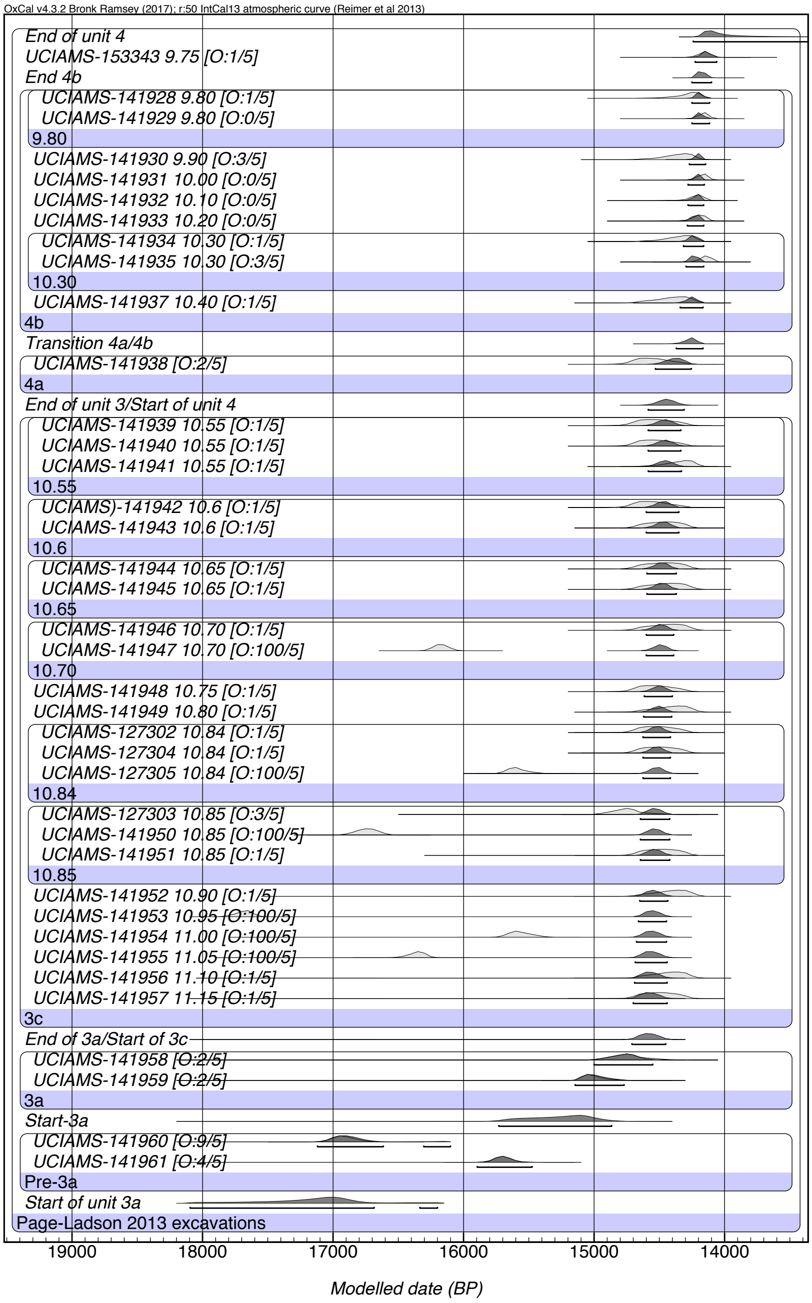

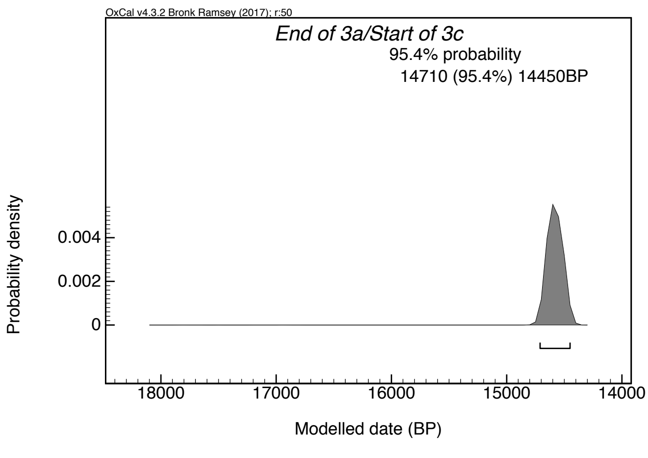

Fig. S34. Bayesian age model for Page-Ladson (above), and start `Boundary` (below). Brackets beneath each age estimate show 95.4% confidence interval. 'O:prior/posterior probability' reflects the outlier analysis.

```
Plot()
{
 Outlier_Model("General", T(5), U(0,4), "t");
 Sequence("Page-Ladson 2013 excavations")
 {
  Boundary("Start of unit 3a");
  Phase("Pre-3a")
  {
   R_Date("UCIAMS-141961", 13080, 40)
   {
    Outlier("General", 0.05);
   };
   R_Date("UCIAMS-141960", 13945, 50)
   {
    Outlier("General", 0.05);
   };
  };
  Boundary("Start-3a");
  Phase("3a")
  {
   R_Date("UCIAMS-141959", 12615, 35)
   {
    Outlier("General", 0.05);
   };
   R_Date("UCIAMS-141958", 12495, 35)
   {
    Outlier("General", 0.05);
   };
  };
  Boundary("End of 3a/Start of 3c");
  Sequence("3c")
  {
   R_Date("UCIAMS-141957 11.15", 12420, 30)
   {
    Outlier("General", 0.05);
   };
   R_Date("UCIAMS-141956 11.10", 12395, 30)
   {
    Outlier("General", 0.05);
   };
   R_Date("UCIAMS-141955 11.05", 13585, 35)
   {
    Outlier("General", 0.05);
   };
   R_Date("UCIAMS-141954 11.00", 13005, 35)
   {
    Outlier("General", 0.05);
   };
   R_Date("UCIAMS-141953 10.95", 14510, 40)
   {
    Outlier("General", 0.05);
   };
   R_Date("UCIAMS-141952 10.90", 12385, 35)
   {
    Outlier("General", 0.05);
   };
   Phase("10.85")
   {
    R_Date("UCIAMS-141951 10.85", 12415, 30)
    {
     Outlier("General", 0.05);
    };
    R_Date("UCIAMS-141950 10.85", 13830, 35)
    {
     Outlier("General", 0.05);
    };
    R_Date("UCIAMS-127303 10.85", 12495, 30)
    {
     Outlier("General", 0.05);
    };
   };
   Phase("10.84")
   {
    R_Date("UCIAMS-127305 10.84", 13015, 30)
    {
     Outlier("General", 0.05);
    };
    R_Date("UCIAMS-127304 10.84", 12420, 30)
    {
     Outlier("General", 0.05);
    };
    R_Date("UCIAMS-127302 10.84", 12425, 30)
    {
     Outlier("General", 0.05);
    };
   };
   R_Date("UCIAMS-141949  10.80", 12385, 35)
   {
    Outlier("General", 0.05);
   };
   R_Date("UCIAMS-141948  10.75", 12430, 30)
   {
    Outlier("General", 0.05);
   };
   Phase("10.70")
   {
    R_Date("UCIAMS-141947 10.70", 13440, 40)
    {
     Outlier("General", 0.05);
    };
    R_Date("UCIAMS-141946 10.70", 12400, 35)
    {
     Outlier("General", 0.05);
    };
   };
   Phase("10.65")
   {
    R_Date("UCIAMS-141945 10.65", 12400, 35)
    {
     Outlier("General", 0.05);
    };
    R_Date("UCIAMS-141944 10.65", 12410, 35)
    {
     Outlier("General", 0.05);
    };
   };
   Phase("10.6")
   {
    R_Date("UCIAMS-141943 10.6", 12410, 30)
    {
     Outlier("General", 0.05);
    };
    R_Date("UCIAMS)-141942 10.6", 12440, 30)
    {
     Outlier("General", 0.05);
    };
   };
   Phase("10.55")
   {
    R_Date("UCIAMS-141941 10.55", 12365, 30)
    {
     Outlier("General", 0.05);
    };
    R_Date("UCIAMS-141940 10.55", 12430, 30)
    {
     Outlier("General", 0.05);
    };
    R_Date("UCIAMS-141939 10.55", 12430, 35)
    {
     Outlier("General", 0.05);
    };
   };
  };
  Boundary("End of unit 3/Start of unit 4");
  Phase("4a")
  {
```

```
  R_Date("UCIAMS-141938", 12440, 30)
   {
   Outlier("General", 0.05);
   };
  };
  Boundary("Transition 4a/4b");
  Sequence("4b")
  {
   R_Date("UCIAMS-141937 10.40", 12380, 35)
   {
   Outlier("General", 0.05);
   };
   Phase("10.30")
   {
    R_Date("UCIAMS-141935 10.30", 12250, 35)
    {
    Outlier("General", 0.05);
    };
    R_Date("UCIAMS-141934 10.30", 12365, 30)
    {
    Outlier("General", 0.05);
    };
   };
   R_Date("UCIAMS-141933 10.20", 12295, 35)
   {
   Outlier("General", 0.05);
   };
   R_Date("UCIAMS-141932 10.10", 12310, 30)
   {
   Outlier("General", 0.05);
   };
   R_Date("UCIAMS-141931 10.00", 12275, 30)
   {
   Outlier("General", 0.05);
   };
   R_Date("UCIAMS-141930 9.90", 12370, 30)
   {
   Outlier("General", 0.05);
   };
   Phase("9.80")
   {
    R_Date("UCIAMS-141929 9.80", 12270, 30)
    {
    Outlier("General", 0.05);
    };
    R_Date("UCIAMS-141928 9.80", 12335, 35)
    {
    Outlier("General", 0.05);
    };
   };
  };
  Boundary("End 4b");
  R_Date("UCIAMS-153343 9.75", 12260, 35)
  {
  Outlier("General", 0.05);
  };
  Boundary("End of unit 4");
 };
};
```

2.4.11. Paisley Caves, Oregon (U.S.A.)

Paisley Caves (or Paisley Five Mile Point Caves; 35LK3400; at approximately 42.776636, -120.667361) is a multi-cluster (caves 1, 2, 3, and 5), stratified (LU 1-7) with pre-Clovis and WST components[9,173–178]. In Cave 5, human coprolites found below WST artefacts have been found in the lowest level (LU 1), whilst the earliest WST projectile point base is found within the Indurated Silt Lense (ISL) in LU 2. The latter is bounded by dated samples 2010PC-223 (on top and within the ISL) and 2010PC-224 (beneath the ISL)[174]. Although the site is stratified, modelling Paisley Caves within a bounded sequence is not straightforward; 203 radiocarbon dates have been obtained from different caves, profiles, units, and multiple, distinct archeological events[174]. These provide stratigraphic control and date cultural features directly, e.g., human coprolites. If data from Cave 5, LU's 1-3, are incorporated in a model, the order of the sequence cannot be resolved. For this reason, the age for the pre-Clovis component has been obtained through a `Date` function (14,755-13,780 cal BP) for the three earliest human coprolites (Fig. S35). Given that these date human presence directly, this is likely an accurate estimate. Moreover, considering that the age of the earliest WST artefact is extrapolated from dating done at Profile III[174], we have modelled this sequence to obtain a PDF for the start of the Western Stemmed tradition component at the site (13,110-13,015 cal BP; Fig. S36).

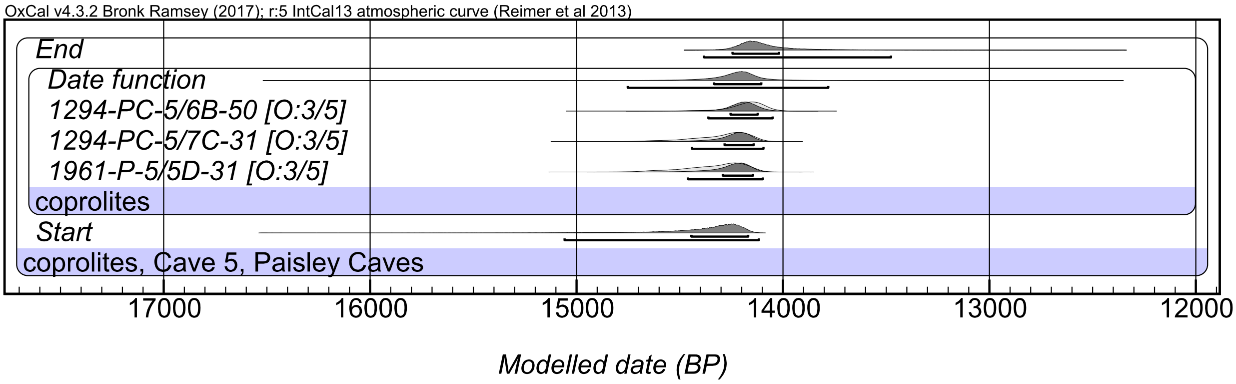

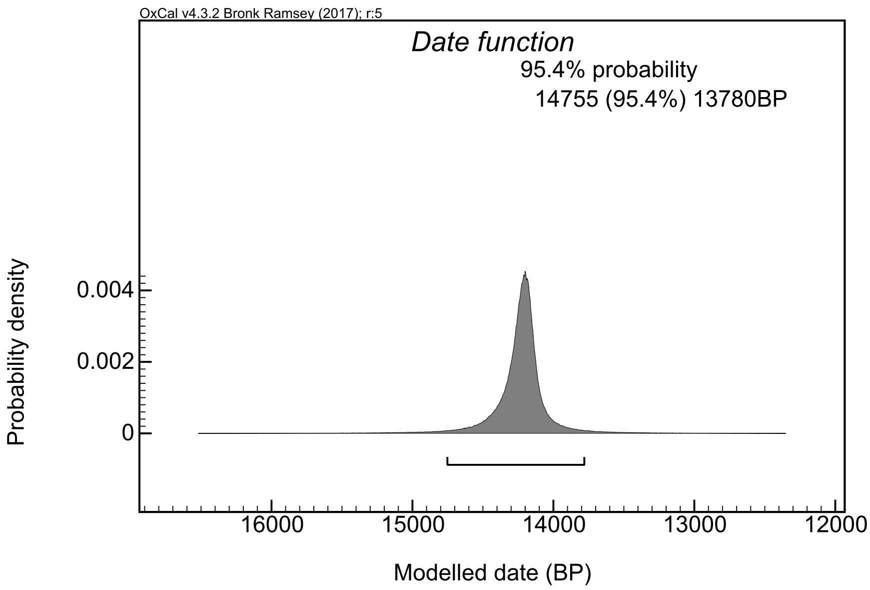

Fig. S35. Bayesian age model for Paisley Caves (coprolites; above), and `Date` function (below). Brackets beneath each age estimate show 95.4% confidence interval. 'O:prior/posterior probability' reflects the outlier analysis.

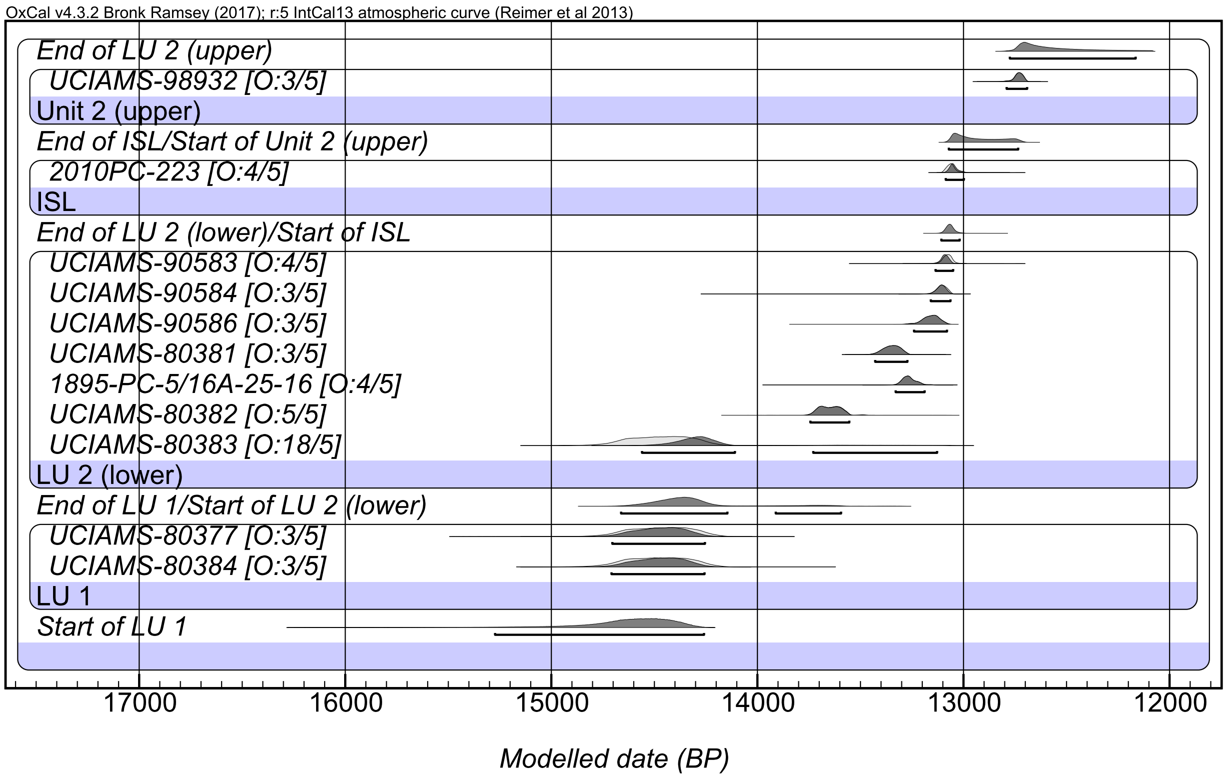

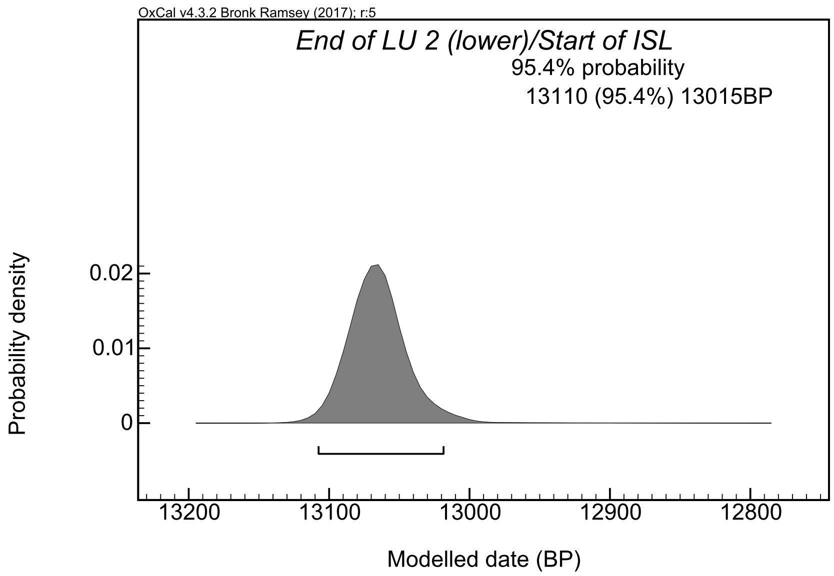

Fig. S36. Bayesian age model for Paisley Caves (Profile III; above), and start `Boundary` (below). Brackets beneath each age estimate show 95.4% confidence interval. 'O:prior/posterior probability' reflects the outlier analysis.

```
Plot()
{
 Outlier_Model("General",T(5),U(0,4),"t");
 Outlier_Model("SSimple",N(0,2),0,"s");
 Sequence("human coprolites, Cave 5, Paisley Caves")
 {
  Boundary("Start");
  Phase()
  {
   R_Combine("1961-P-5/5D-31")
   {
    R_Date("Beta-213424", 12400, 60)
    {
     Outlier("SSimple", 0.05);
    };
    R_Date("OxA-16498", 12275, 55)
    {
     Outlier("SSimple", 0.05);
    };
    Outlier("General", 0.05);
   };
   R_Combine("1294-PC-5/7C-31")
   {
```

```
    R_Date("OxA-16497", 12345, 55)
    {
     Outlier("SSimple", 0.05);
    };
    R_Date("Beta-213426", 12290, 60)
    {
     Outlier("SSimple", 0.05);
    };
    Outlier("General", 0.05);
   };
   R_Combine("1294-PC-5/6B-50")
   {
    R_Date("Beta-216474", 12260, 60)
    {
     Outlier("SSimple", 0.05);
    };
    R_Date("OxA-16495", 12140, 70)
    {
     Outlier("SSimple", 0.05);
    };
    Outlier("General", 0.05);
   };
   R_Combine("1294-PC-5/6B-40")
   {
    R_Date("Beta-213423", 10050, 50)
    {
     Outlier("SSimple", 0.05);
    };
    R_Date("OxA-16376", 10965, 50)
    {
     Outlier("SSimple", 0.05);
    };
    Outlier("General", 0.05);
   };
  };
  Boundary("End");
 };
};


Plot()
{
 Outlier_Model("General",T(5),U(0,4),"t");
 Outlier_Model("SSimple",N(0,2),0,"s");
 Sequence("Profile II, Cave 5, Paisley Caves")
 {
  Boundary("Start of LU 1");
  Phase("LU 1")
  {
   R_Date("UCIAMS-80384", 12410, 25)
   {
    Outlier("General", 0.05);
   };
   R_Date("UCIAMS-80377", 12405, 25)
   {
    Outlier("General", 0.05);
   };
  };
  Boundary("End of LU 1/Start of LU 2 (lower)");
  Phase("LU 2 (lower)")
  {
   R_Date("UCIAMS-80383", 12405, 25)
   {
    Outlier("General", 0.05);
   };
   R_Date("UCIAMS-80382", 11815, 25)
   {
    Outlier("General", 0.05);
   };
   R_Combine("1895-PC-5/16A-25-16")
   {
    R_Date("UCIAMS-90582", 11505, 30)
    {
     Outlier("SSimple", 0.05);
    };
    R_Date("UCIAMS-90581", 11340, 30)
    {
     Outlier("SSimple", 0.05);
    };
    Outlier("General", 0.05);
   };
   R_Date("UCIAMS-80381", 11500, 30)
   {
    Outlier("General", 0.05);
   };
   R_Date("UCIAMS-90586", 11315, 25)
   {
    Outlier("General", 0.05);
   };
   R_Date("UCIAMS-90584", 11250, 25)
   {
    Outlier("General", 0.05);
   };
   R_Date("UCIAMS-90583", 11205, 25)
   {
    Outlier("General", 0.05);
   };
  };
  Boundary("End of LU 2 (lower)/Start of ISL");
  Phase("ISL")
  {
   R_Combine("2010PC-223")
   {
    R_Date("UCIAMS-80379", 11295, 25)
    {
     Outlier("SSimple", 0.05);
    };
    R_Date("UCIAMS-80380", 11165, 25)
    {
     Outlier("SSimple", 0.05);
    };
    R_Date("UCIAMS-80378", 11070, 25)
    {
     Outlier("SSimple", 0.05);
    };
    Outlier("General", 0.05);
   };
  };
  Boundary("End of ISL/Start of Unit 2 (upper)");
  Phase("Unit 2 (upper)")
  {
   R_Date("UCIAMS-98932", 10855, 30)
   {
    Outlier("General", 0.05);
   };
  };
  Boundary("End of LU 2 (upper)");
 };
};
```

2.4.12. Chiquihuite Cave (Mexico)

Chiquihuite Cave (G14C6332001/ ID 44499; at 24.61666, -101.13333) is a stratified (strata 1223-1204) site located in Zacatecas, containing pre-Clovis, Paleoindian, and historic material[179,180].

Along the sequence, evidence for human occupation was found within three occupational components, labeled Stratigraphic Components (SC-) A, B, and C[180]. SC-A is the youngest, showing evidence for Colonial and pre-Columbian materials. SC-B is separated from the next component, SC-C, by a well-defined, thick clay layer that extends uniformly throughout the sequence and dates to the LGM. Lithic artefacts made from limestone were found in all strata, with increased frequency in SC-B. All dates obtained provide stratigraphic control. Bayesian age modelling performed in reference 180 places the start of SC-C to 33,150-31,405 cal BP and SC-B to 16,605-15,615 cal BP.

2.5. Western Stemmed tradition

2.5.1. Bonneville Estates Rockshelter, Nevada (U.S.A.)

Bonneville Estates Rockshelter (26EK3682; at approximately 40.294985, -114.076284) is a multi-cluster (e.g., East and West blocks), stratified (strata 1-19) site containing WST lithic technology and hearth features[8,181–186]. The earliest cultural components are represented in stratum 12, for East block, and 18b, for West block. Dates obtained provide stratigraphic control or date cultural features directly, e.g., hearth charcoal. Using these data, the models created place the start of the WST to 12,740-12,570 cal BP, at the East block, and 12,760-12,605 at cal BP, at the West block (see below for both sets of CQL code). The PDF for the start of stratum 19/18b contact for the West block (Fig. S37) was used in the tradition-level model, due to a larger sample size.

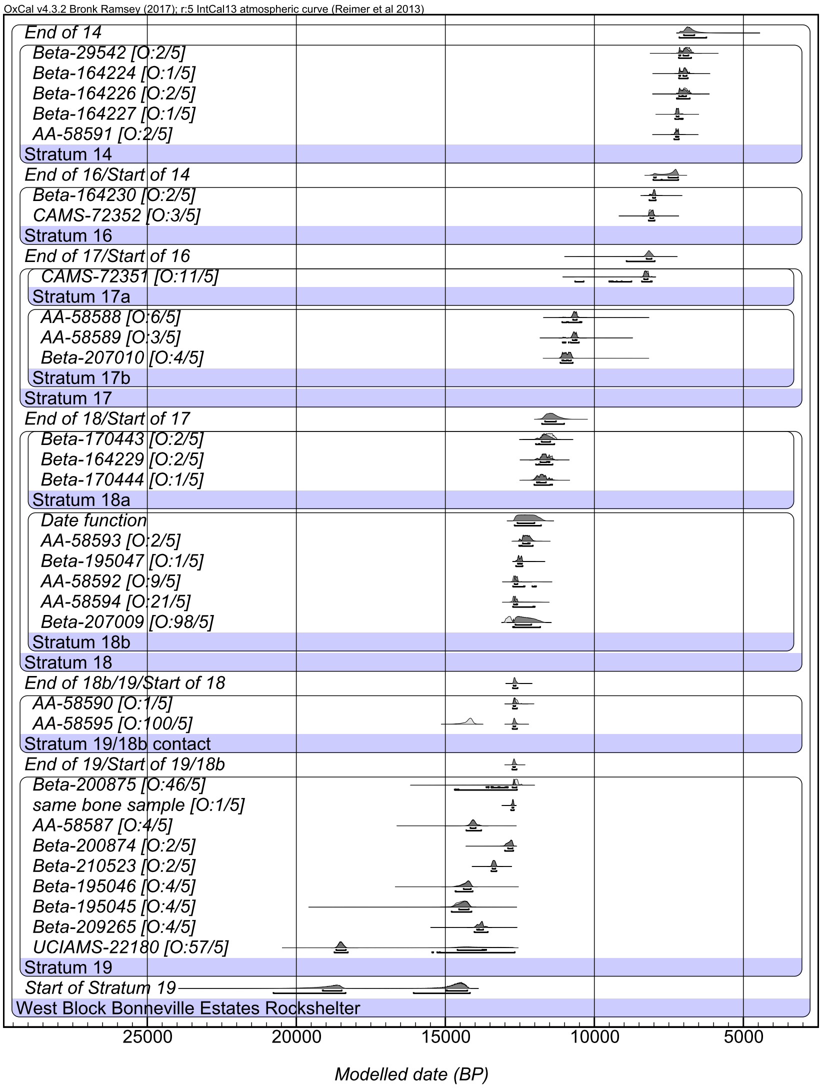

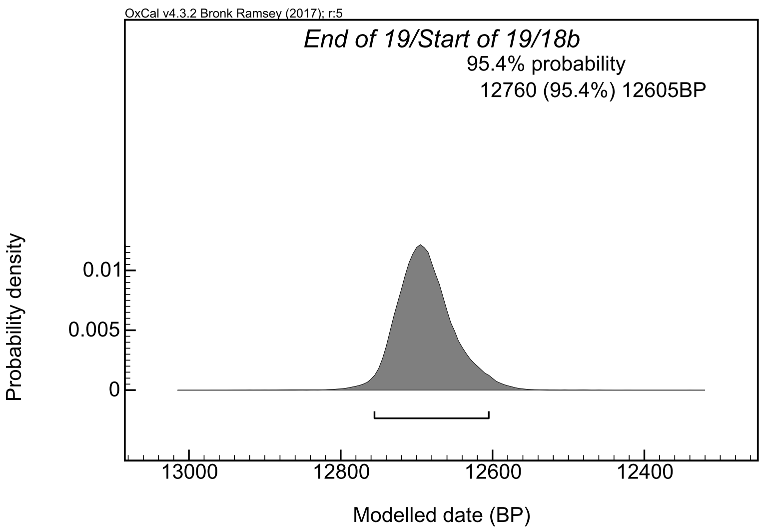

Fig. S37. Bayesian age model for Bonneville Estates Rockshelter (West block; above), and start `Boundary` (below). Brackets beneath each age estimate show 95.4% confidence interval. 'O:prior/posterior probability' reflects the outlier analysis.

```
Plot()
{
Outlier_Model("General",T(5),U(0,4),"t");
Outlier_Model("SSimple",N(0,2),0,"s");
Sequence("West Block, Bonneville Estates Rockshelter")
{
 Boundary("Start of Stratum 19");
 Phase("Stratum 19")
```

```
{
 R_Date("UCIAMS-22180", 15240, 50)
 {
  Outlier("General", 0.05);
 };
 R_Date("Beta-209265", 11960, 60)
 {
  Outlier("General", 0.05);
 };
 R_Date("Beta-195045", 12390, 40)
 {
  Outlier("General", 0.05);
 };
 R_Date("Beta-195046", 12330, 40)
 {
  Outlier("General", 0.05);
 };
 R_Date("Beta-210523", 11530, 40)
 {
  Outlier("General", 0.05);
 };
 R_Date("Beta-200874", 10970, 60)
 {
  Outlier("General", 0.05);
 };
 R_Date("AA-58587", 12180, 60)
 {
  Outlier("General", 0.05);
 };
 R_Combine("same bone sample")
 {
  R_Date("UCIAMS-22176", 10900, 50)
  {
   Outlier("SSimple", 0.05);
  };
  R_Date("Beta-210524", 10830, 40)
  {
   Outlier("SSimple", 0.05);
  };
  Outlier("General", 0.05);
 };
 R_Date("Beta-200875", 10640, 60)
 {
  Outlier("General", 0.05);
 };
};
Boundary("End of 19/Start of 19/18b");
Phase("Stratum 19/18b contact")
{
 R_Date("AA-58595", 12270, 60)
 {
  Outlier("General", 0.05);
 };
 R_Date("AA-58590", 10690, 70)
 {
  Outlier("General", 0.05);
 };
};
Boundary("End of 18b/19/Start of 18");
Sequence("Stratum 18")
{
 Phase("Stratum 18b")
 {
  R_Date("Beta-207009", 11010, 40)
  {
   Outlier("General", 0.05);
  };
  R_Date("AA-58594", 10800, 60)
  {
   Outlier("General", 0.05);
  };
  R_Date("AA-58592", 10760, 70)
  {
   Outlier("General", 0.05);
  };
  R_Date("Beta-195047", 10540, 40)
  {
   Outlier("General", 0.05);
  };
  R_Date("AA-58593", 10405, 50)
  {
   Outlier("General", 0.05);
  };
  Date("Date function");
 };
 Phase("Stratum 18a")
 {
  R_Date("Beta-170444", 10130, 60)
  {
   Outlier("General", 0.05);
  };
  R_Date("Beta-164229", 10080, 50)
  {
   Outlier("General", 0.05);
  };
  R_Date("Beta-170443", 10040, 70)
  {
   Outlier("General", 0.05);
  };
 };
};
Boundary("End of 18/Start of 17");
Sequence("Stratum 17")
{
 Phase("Stratum 17b")
 {
  R_Date("Beta-207010", 9580, 40)
  {
   Outlier("General", 0.05);
  };
  R_Date("AA-58589", 9440, 50)
  {
   Outlier("General", 0.05);
  };
  R_Date("AA-58588", 9430, 50)
  {
   Outlier("General", 0.05);
  };
 };
 Phase("Stratum 17a")
 {
  R_Date("CAMS-72351", 7420, 50)
  {
   Outlier("General", 0.05);
  };
 };
};
Boundary("End of 17/Start of 16");
Phase("Stratum 16")
{
 R_Date("CAMS-72352", 7280, 50)
 {
  Outlier("General", 0.05);
 };
 R_Date("Beta-164230", 7190, 50)
 {
  Outlier("General", 0.05);
 };
};
Boundary("End of 16/Start of 14");
Phase("Stratum 14")
{
 R_Date("AA-58591", 6315, 40)
 {
  Outlier("General", 0.05);
 };
```

```
R_Date("Beta-164227", 6280, 40)
{
Outlier("General", 0.05);
};
R_Date("Beta-164226", 6100, 80)
{
Outlier("General", 0.05);
};
R_Date("Beta-164224", 6100, 50)
{
Outlier("General", 0.05);
};
R_Date("Beta-29542", 6040, 80)
{
Outlier("General", 0.05);
};
};
Boundary("End of 14");
};
};

Plot()
{
Outlier_Model("General",T(5),U(0,4),"t");
Sequence("East Block, Bonneville Estates Rockshelter")
{
Boundary("Start of Stratum 12");
Phase("Stratum 12")
{
R_Date("Beta-195013", 10390, 40)
{
Outlier("General", 0.05);
};
R_Date("Beta-203504", 10340, 60)
{
Outlier("General", 0.05);
};
R_Date("Beta-206278", 10250, 50)
{
Outlier("General", 0.05);
};
R_Date("AA-58600", 10380, 60)
{
Outlier("General", 0.05);
};
R_Date("Beta-182935", 10050, 50)
{
Outlier("General", 0.05);
};
R_Date("Beta-182934", 10030, 50)
{
Outlier("General", 0.05);
};
R_Date("Beta-182931", 10560, 50)
{
Outlier("General", 0.05);
};
R_Date("AA-58598", 9990, 50)
{
Outlier("General", 0.05);
};
};
Boundary("End of 12/Start of 10");
Phase("Stratum 10")
{
R_Date("Beta-195042", 9580, 40)
{
Outlier("General", 0.05);
};
R_Date("Beta-195044", 9570, 40)
{
Outlier("General", 0.05);
};
R_Date("Beta-161891", 9520, 60)
{
Outlier("General", 0.05);
};
R_Date("AA-58599", 9440, 80)
{
Outlier("General", 0.05);
};
R_Date("Beta-203507", 8830, 60)
{
Outlier("General", 0.05);
};
};
Boundary("End of 10/Start of 9b");
Phase("Stratum 9b")
{
R_Date("AA-58596", 7240, 50)
{
Outlier("General", 0.05);
};
R_Date("Beta-182933", 5350, 70)
{
Outlier("General", 0.05);
};
R_Date("Beta-182928", 5160, 80)
{
Outlier("General", 0.05);
};
};
Boundary("End of Stratum 9");
};
};
```

2.5.2. Buhl, Idaho (U.S.A.)

Buhl (10TF1019; at approximately 42.658225, -114.788668) is a burial site containing the partial remains of a female individual associated with osseous artefacts and an obsidian stemmed point[8,143,187]. A direct bone (collagen) date (10,675±95 BP; Beta-43055 & ETH-7729) places the site at 12,740-12,420 cal BP.

2.5.3. Cooper's Ferry, Idaho (U.S.A.)

See pre-Clovis section.

2.5.4. Paisley Caves, Oregon (U.S.A.)

See pre-Clovis section.

3. Data tabulation

Following the analysis in section 2, two tables were compiled. The first, Table S1, is a tabulation of chronometric data included in Bayesian age models, according to each archaeological site. Provenience, material type and sources are noted. The second, Table S2, is a summary of age estimates obtained for the tradition or temporal components of interest. Where applicable, these were incorporated into tradition-level models (Extended Data Figs. 1-3).

Table S1. Chronometric data (n=767) analysed from the 42 archaeological sites included in the Bayesian age modelling (noted as in sources). Coordinates (noted as 'latitude', 'longitude'), follow the World Geodetic System (WGS84). As listed in the text (section 2) some of these are approximations. Dates ('BP' for radiocarbon measurements or 'ka' for luminescence estimates) are means and the standard deviation is 1σ.

Site name	Coordinates	Provenience	Sample material	Laboratory code	Date (BP or ka)	Source	Notes
Anzick	45.977128, -110.660209	-	human bone (Anzick-1; HYP)	OxA-X-2739-54	10915±50	62	
Anzick	45.977128, -110.660209	-	antler rod (HYP)	OxA-X-2739-55	10900±50	62	
Anzick	45.977128, -110.660209	-	antler rod (HYP)	OxA-X-2739-56	11050±55	62	
Arlington Springs	34.005591, -120.177117	-	human femur	CAMS-16810	10,960±80	5	
Aubrey	33.353936, -97.087474	surface of Unit A/ Clovis camp	charcoal	AA-5274	11590±93	63	
Aubrey	33.353936, -97.087474	surface of Unit A/ Clovis camp	charcoal	AA-5271	11542±111	63	
Aubrey	33.353936, -97.087474	Unit F	humate	SMU-2338	10718±90	63	
Aubrey	33.353936, -97.087474	Unit F	sediment	Beta-32002	10360±150	63	
Aubrey	33.353936, -97.087474	Unit G	humate	SMU-2398	10084±80	63	
Aubrey	33.353936, -97.087474	Unit G	humate	SMU-2399	9572±130	63	
Aubrey	33.353936, -97.087474	Unit G	humate	SMU-2400	8275±70	63	
Aubrey	33.353936, -97.087474	Unit G	humate	SMU-2339	7582±320	63	
Berelehk	70.500000, 144.033333	T2 profile BA1; layer1	silt with plant macro remains	Beta-269467	13390±60	19	
Berelehk	70.500000, 144.033333	T2 profile BA1; layer1	silt with plant macro remains	Beta-269468	12350±60	19	
Berelehk	70.500000, 144.033333	T2 profile BA1; layer 2	silt with plant macro remains	Beta-269469	12220±60	19	
Berelehk	70.500000, 144.033333	T2 profile BA1; layer 2	charred material screened from culture-bearing layer	Beta-269470	12100±60	19	

Site name	Coordinates	Provenience	Sample material	Laboratory code	Date (BP or ka)	Source	Notes
Berelehk	70.500000, 144.033333	T2 profile BA1; layer 2	wolf phalanx	Beta-269446	12090±60	19	
Berelehk	70.500000, 144.033333	T2 profile BA1; layer 2	twigs, material screened from culture-bearing layer	Beta-269447	11830±60	19	
Berelehk	70.500000, 144.033333	T2 profile BA1; layer 2	arctic fox	Beta-269440	11830±60	19	
Berelehk	70.500000, 144.033333	T2 profile BA1; layer 2	Pleistocene hare	Beta-271415	11890±60	19	
Berelehk	70.500000, 144.033333	T2 profile BA1; layer 2	Pleistocene hare	Beta-271416	11990±60	19	
Berelehk	70.500000, 144.033333	T2 profile BA1; layer 2	Pleistocene hare	Beta-271418	11890±60	19	
Berelehk	70.500000, 144.033333	T2 profile BA1; layer 2	bird bone/ ptarmigan (?), screened material	Beta-271420	11940±60	19	
Blackwater Locality No. 1	34.276686, -103.322134	Unit A7-8	humates	AA-7093	22930±290	66	
Blackwater Locality No. 1	34.276686, -103.322134	Unit A7-8	organic residue	AA-7092	17220±170	66	
Blackwater Locality No. 1	34.276686, -103.322134	Unit B	sediment (humates)	AA-2262	11810±90	66	
Blackwater Locality No. 1	34.276686, -103.322134	Unit B	sediment (humates)	AA-2263	12790±160	66	
Blackwater Locality No. 1	34.276686, -103.322134	Unit B	sediment (humates)	AA-1374	12330±110	66	
Blackwater Locality No. 1	34.276686, -103.322134	Unit B	sediment (humates)	AA-1375	11380±150	66	
Blackwater Locality No. 1	34.276686, -103.322134	Unit C0-1	carbonized plant remains	A-491	11630±400	66	
Blackwater Locality No. 1	34.276686, -103.322134	Unit C0-1	carbonized plant remains	A-481	11170±360	66	
Blackwater Locality No. 1	34.276686, -103.322134	Unit C0-1	soluble plant remains	A-490	11040±500	66	
Blackwater Locality No. 1	34.276686, -103.322134	Unit C0-1	carbonized wood flecks	AA-1360	10580±100	66	
Blackwater Locality No. 1	34.276686, -103.322134	Unit D	soluble plant remains	A-492	10490±200	66	
Blackwater Locality No. 1	34.276686, -103.322134	Unit D	sediment humic acids	A-386	10490±900	66	
Blackwater Locality No. 1	34.276686, -103.322134	Unit D	soluble plant remains	A-488	10170±260	66	

Site name	Coordinates	Provenience	Sample material	Laboratory code	Date (BP or ka)	Source	Notes
Blackwater Locality No. 1	34.276686, -103.322134	Unit D	sediment organic residue	A-379	9900±320	66	
Blackwater Locality No. 1	34.276686, -103.322134	Unit D	sediment organic acids from A-379	A-380	10600±320	66	
Blackwater Locality No. 1	34.276686, -103.322134	Unit D	sediment (humates)	AA-1412	9860±210	66	
Blackwater Locality No. 1	34.276686, -103.322134	Unit D	sediment	A-4701	10470±580	66	
Blackwater Locality No. 1	34.276686, -103.322134	Unit D	sediment	AA-1362	10740±100	66	
Blackwater Locality No. 1	34.276686, -103.322134	Unit D	sediment	AA-1363	10160±120	66	
Blackwater Locality No. 1	34.276686, -103.322134	Unit D	sediment	AA-1364	10210±110	66	
Blackwater Locality No. 1	34.276686, -103.322134	Unit D	charcoal flecks	AA-1371	9560±180	66	
Blackwater Locality No. 1	34.276686, -103.322134	Unit D	charcoal lump	AA-1370	10260±230	66	
Blackwater Locality No. 1	34.276686, -103.322134	Unit D	sediment (humates)	A-4702	9870±320	66	
Blackwater Locality No. 1	34.276686, -103.322134	Unit D	sediment (humates)	AA-2261	9950±100	66	
Blackwater Locality No. 1	34.276686, -103.322134	Unit D	carbonized plants (humates)	AA-1361	10640±110	66	
Blackwater Locality No. 1	34.276686, -103.322134	Unit D	bone	AA-1409	6660±160	66	
Blackwater Locality No. 1	34.276686, -103.322134	Unit D	bison bone	Y-1991	8430±200	66	
Blackwater Locality No. 1	34.276686, -103.322134	Unit D	sediment organic residue	Y-2489	9400±200	66	
Blackwater Locality No. 1	34.276686, -103.322134	Unit E/D	humates	A-1372	10250±200	66	
Blackwater Locality No. 1	34.276686, -103.322134	Unit E	sediment (humate)	A-4705	9296±320	66	
Blackwater Locality No. 1	34.276686, -103.322134	Unit E	sediment (humates)	A-4703	10000±910	66	
Blackwater Locality No. 1	34.276686, -103.322134	Unit E	sediment (humates)	A-4700	8630±310	66	
Blackwater Locality No. 1	34.276686, -103.322134	Unit E	sediment (organic residue)	AA-1365	8230±100	66	

Site name	Coordinates	Provenience	Sample material	Laboratory code	Date (BP or ka)	Source	Notes
Blackwater Locality No. 1	34.276686, -103.322134	Unit E	sediment (humates)	AA-1366	9890±100	66	
Blackwater Locality No. 1	34.276686, -103.322134	Unit E	sediment (organic residue)	AA-1367	9150±90	66	
Blackwater Locality No. 1	34.276686, -103.322134	Unit E	sediment (humates)	AA-1368	11400±190	66	
Blackwater Locality No. 1	34.276686, -103.322134	Unit E	sediment (organic residue)	AA-1358	10190±130	66	
Blackwater Locality No. 1	34.276686, -103.322134	Unit E	sediment (humates)	AA-1359	9590±120	66	
Blackwater Locality No. 1	34.276686, -103.322134	Unit E	bison bone	Y-1990	7610±160	66	
Blackwater Locality No. 1	34.276686, -103.322134	Unit E	sediment organic residue	Y-2488	8830±160	66	
Blackwater Locality No. 1	34.276686, -103.322134	Unit E	sediment organic residue	Y-2487	7020±180	66	
Blackwater Locality No. 1	34.276686, -103.322134	Unit F/E	bone	AA-1408	6190±130	66	
Blackwater Locality No. 1	34.276686, -103.322134	Unit F/E	burned bone	AA-1413	8830±120	66	
Blackwater Locality No. 1	34.276686, -103.322134	Unit F/E	bison bone	O-169	6300±150	66	
Blackwater Locality No. 1	34.276686, -103.322134	Unit F/E	bison bone	O-170	6230±150	66	
Blackwater Locality No. 1	34.276686, -103.322134	Unit F/E	soluble plant remains	A-489	9890±290	66	
Blackwater Locality No. 1	34.276686, -103.322134	Unit G	soil organic residue	SI-4585	4855±90	66	
Blackwater Locality No. 1	34.276686, -103.322134	Unit G	burned bison bone	A-512	8470±350	66	
Blackwater Locality No. 1	34.276686, -103.322134	Unit G	burned bison bone	O-157	4950±150	66	
Blackwater Locality No. 1	34.276686, -103.322134	Unit G	bison metacarpal	Y-1989	8450±280	66	
Blackwater Locality No. 1	34.276686, -103.322134	Unit G	soil organic residue	Y-2490	910±100	66	
Blackwater Locality No. 1	34.276686, -103.322134	Unit G	soil organic residue	Y-2360	680±80	66	
Blackwater Locality No. 1	34.276686, -103.322134	Unit G	charcoal	AA-2260	6720±80	66	

Site name	Coordinates	Provenience	Sample material	Laboratory code	Date (BP or ka)	Source	Notes
Blackwater Locality No. 1	34.276686, -103.322134	Unit G	charcoal (humates)	AA-2259	7850±110	66	
Blackwater Locality No. 1	34.276686, -103.322134	Unit G	burned bone	AA-1643	8230±140	66	
Blackwater Locality No. 1	34.276686, -103.322134	Unit G	burned bone (humates)	AA-2258	8730±90	66	
Blackwater Locality No. 1	34.276686, -103.322134	Unit G	brown aeolian sand (organic residue)	AA-7094	2500±60	66	
Blackwater Locality No. 1	34.276686, -103.322134	Unit G	brown aeolian sand (organic residue)	AA-7095	3800±60	66	
Bluefish Caves	67.15, -140.75	Cave II, basal loess, 142 cam below datum	bone (# J7.8.17)	OxA-33778	19650±130	140	
Bonneville Estates Rockshelter	40.294985, -114.076284	West Block, Stratum 19	bone	UCIAMS-22180	15240±50	182	
Bonneville Estates Rockshelter	40.294985, -114.076284	West Block, Stratum 19	hearth charcoal	Beta-209265	11960±60	182	
Bonneville Estates Rockshelter	40.294985, -114.076284	West Block, Stratum 19	hearth charcoal	Beta-195045	12390±40	182	
Bonneville Estates Rockshelter	40.294985, -114.076284	West Block, Stratum 19	hearth charcoal	Beta-195046	12330±40	182	
Bonneville Estates Rockshelter	40.294985, -114.076284	West Block, Stratum 19	bone	Beta-210523	11530±40	182	
Bonneville Estates Rockshelter	40.294985, -114.076284	West Block, Stratum 19	bone	Beta-200874	10970±60	182	
Bonneville Estates Rockshelter	40.294985, -114.076284	West Block, Stratum 19	hearth charcoal	AA-58587	12180±60	182	
Bonneville Estates Rockshelter	40.294985, -114.076284	West Block, Stratum 19	bone	UCIAMS-22176	10900±50;	182	
Bonneville Estates Rockshelter	40.294985, -114.076284	West Block, Stratum 19	bone	Beta-210524	10830±40;	182	
Bonneville Estates Rockshelter	40.294985, -114.076284	West Block, Stratum 19	hearth charcoal	Beta-200875	10640±60	182	
Bonneville Estates Rockshelter	40.294985, -114.076284	West Block, Stratum 19/18b contact	hearth charcoal	AA-58595	12270±60	182	
Bonneville Estates Rockshelter	40.294985, -114.076284	West Block, Stratum 19/18b contact	hearth charcoal	AA-58590	10690±70	182	
Bonneville Estates Rockshelter	40.294985, -114.076284	West Block, Stratum 18b	hearth charcoal	Beta-207009	11010±40	182	

Site name	Coordinates	Provenience	Sample material	Laboratory code	Date (BP or ka)	Source	Notes
Bonneville Estates Rockshelter	40.294985, -114.076284	West Block, Stratum 18b	hearth charcoal	AA-58594	10800±60	182	
Bonneville Estates Rockshelter	40.294985, -114.076284	West Block, Stratum 18b	hearth charcoal	AA-58592	10760±70	182	
Bonneville Estates Rockshelter	40.294985, -114.076284	West Block, Stratum 18b	hearth charcoal	Beta-195047	10540±40	182	
Bonneville Estates Rockshelter	40.294985, -114.076284	West Block, Stratum 18b	hearth charcoal	AA-58593	10405±50	182	
Bonneville Estates Rockshelter	40.294985, -114.076284	West Block, Stratum 18a	hearth charcoal	Beta-170444	10130±60	182	
Bonneville Estates Rockshelter	40.294985, -114.076284	West Block, Stratum 18a	hearth charcoal	Beta-164229	10080±50	182	
Bonneville Estates Rockshelter	40.294985, -114.076284	West Block, Stratum 18a	hearth charcoal	Beta-170443	10040±70	182	
Bonneville Estates Rockshelter	40.294985, -114.076284	West Block, Stratum 18a/17b contact	hearth charcoal	Beta-207010	9580±40	182	
Bonneville Estates Rockshelter	40.294985, -114.076284	West Block, Stratum 17b	hearth charcoal	AA-58589	9440±50	182	
Bonneville Estates Rockshelter	40.294985, -114.076284	West Block, Stratum 17b	hearth charcoal	AA-58588	9430±50	182	
Bonneville Estates Rockshelter	40.294985, -114.076284	West Block, Stratum 17a	hearth charcoal	CAMS-7235 1	7420±50	182	
Bonneville Estates Rockshelter	40.294985, -114.076284	West Block, Stratum 16	dispersed charcoal	CAMS-7235 2	7280±50	182	
Bonneville Estates Rockshelter	40.294985, -114.076284	West Block, Stratum 16	textile fragment	Beta-164230	7190±50	182	
Bonneville Estates Rockshelter	40.294985, -114.076284	West Block, Stratum 14	garbage pit charcoal	AA-58591	6315±40	182	
Bonneville Estates Rockshelter	40.294985, -114.076284	West Block, Stratum 14	hearth charcoal	Beta-164227	6280±40	182	
Bonneville Estates Rockshelter	40.294985, -114.076284	West Block, Stratum 14	hearth charcoal	Beta-164227	6280±40	182	
Bonneville Estates Rockshelter	40.294985, -114.076284	West Block, Stratum 14	cordage fragment	Beta-164224	6100±50	182	
Bonneville Estates Rockshelter	40.294985, -114.076284	West Block, Stratum 14	bulk charcoal	Beta-29542	6040±80	182	
Broken Mammoth	64.266667, -146.116667	CZ-4C	ivory artifact	CAMS-9898	15830±70	24	
Broken Mammoth	64.266667, -146.116667	CZ-4C	charcoal	WSU-4364	11770±220	24	
Broken Mammoth	64.266667, -146.116667	CZ-4C	charcoal	WSU-4351	11770±210	24	

Site name	Coordinates	Provenience	Sample material	Laboratory code	Date (BP or ka)	Source	Notes
Broken Mammoth	64.266667, -146.116667	CZ-4B	hearth charcoal	WSU-4262	11510±120	24	
Broken Mammoth	64.266667, -146.116667	CZ-4B	swan bone	CAMS-8261	11500±80	24	
Broken Mammoth	64.266667, -146.116667	CZ-4B	hearth charcoal	CAMS-5358	11420±70	24	
Broken Mammoth	64.266667, -146.116667	CZ-4B	charcoal	WSU-4265	11280±190	24	
Broken Mammoth	64.266667, -146.116667	CZ-3/4A?	charcoal	UGA-6257 D	11040±260	24	
Broken Mammoth	64.266667, -146.116667	CZ-3/4A?	wapiti bone	CAMS-7204	11060±90	24	
Broken Mammoth	64.266667, -146.116667	CZ-3/4A?	mammal bone	CAMS-7203	11040±80	24	
Broken Mammoth	64.266667, -146.116667	CZ-3	hearth charcoal	CAMS-5357	10290±70	24	
Broken Mammoth	64.266667, -146.116667	CZ-3	charcoal	WSU-4019	10790±110	24	
Broken Mammoth	64.266667, -146.116667	CZ-3	hearth charcoal	WSU-4263	10270±110	24	
Broken Mammoth	64.266667, -146.116667	CZ-3	hearth charcoal	UGA-6256 D	9690±90	24	
Broken Mammoth	64.266667, -146.116667	CZ-3A	charcoal	WSU-4266	9310±165	24	
Broken Mammoth	64.266667, -146.116667	CZ-2	charcoal	WSU-4508	7700±80	24	
Broken Mammoth	64.266667, -146.116667	CZ-2	charcoal	WSU-4264	7600±140	24	
Broken Mammoth	64.266667, -146.116667	CZ-2	charcoal	UGA-6281 D	7200±205	24	
Broken Mammoth	64.266667, -146.116667	CZ-1B	hearth charcoal	WSU-4350	4690±110	24	
Broken Mammoth	64.266667, -146.116667	CZ-1B	charcoal	WSU-4456	4540±90	24	
Broken Mammoth	64.266667, -146.116667	CZ-1B	charcoal	WSU-4457	4545±90	24	
Broken Mammoth	64.266667, -146.116667	CZ-1B	charcoal	WSU-4448	4525±90	24	
Broken Mammoth	64.266667, -146.116667	CZ-1A	charcoal	WSU-4267	2040±65	24	
Broken Mammoth	64.266667, -146.116667	CZ-1A	charcoal	UGA-6255 D	2815±180	24	
Buhl	42.658225, -114.788668	burial locale (909 masl)	human bone	Beta-43055 & ETH-7729	10675±95	187	
Cactus Hill	36.986668, -77.322360	below pre-Clovis level	sediment	UW438c	25400±1700	71	OSL
Cactus Hill	36.986668, -77.322360	below pre-Clovis level	sediment	UW438(kc)	27900±2000	71	OSL
Cactus Hill	36.986668, -77.322360	below pre-Clovis level	wood charcoal	Beta-128331	19700±130	71	
Cactus Hill	36.986668, -77.322360	below pre-Clovis level	charred organic matter	Beta-155334	19540±70	71	
Cactus Hill	36.986668, -77.322360	below pre-Clovis level	charred organic matter	Beta-156517	19310±150	71	

Site name	Coordinates	Provenience	Sample material	Laboratory code	Date (BP or ka)	Source	Notes
Cactus Hill	36.986668, -77.322360	below pre-Clovis level	charred organic matter	Beta-163608	19050±80	71	
Cactus Hill	36.986668, -77.322360	below pre-Clovis level	wood charcoal	Beta-152731	18250±80	71	
Cactus Hill	36.986668, -77.322360	below pre-Clovis level	sediment	UW618c	20600±900	71	OSL
Cactus Hill	36.986668, -77.322360	below pre-Clovis level	wood charcoal	Beta-128330	16940±50	71	
Cactus Hill	36.986668, -77.322360	pre-Clovis level	sediment	UW701	18300±1400	71	OSL
Cactus Hill	36.986668, -77.322360	pre-Clovis level	sediment	UW700	19800±3800	71	OSL
Cactus Hill	36.986668, -77.322360	pre-Clovis level	sediment	UW699	17300±1600	71	OSL
Cactus Hill	36.986668, -77.322360	pre-Clovis level	sediment	UW617c	19300±1000	71	OSL
Cactus Hill	36.986668, -77.322360	pre-Clovis level	wood charcoal	Beta-97708	16670±730	71	
Cactus Hill	36.986668, -77.322360	pre-Clovis level	wood charcoal	Beta-81590	15070±70	71	
Cactus Hill	36.986668, -77.322360	sterile zone	sediment	UW698	12500±600	71	OSL
Cactus Hill	36.986668, -77.322360	sterile zone	sediment	UW697	11800±800	71	OSL
Cactus Hill	36.986668, -77.322360	Clovis level	wood charcoal	Beta-81589	10920±250	71	
Cactus Hill	36.986668, -77.322360	Phase("Fort Nottoway working surface and fire pit"	wood charcoal	AA-15027	8920±65	71	
Cactus Hill	36.986668, -77.322360	Phase("Fort Nottoway working surface and fire pit"	wood charcoal	Beta-70127	8800±120	71	
Cactus Hill	36.986668, -77.322360	Archaic level	sediment	UW436	10300±600	71	OSL
Cactus Hill	36.986668, -77.322360	Archaic level	sediment	UW435	8000±600	71	OSL
Chiquihuite Cave	24.61666, -101.13333	Stratigraphic Component B	charcoal	LEMA-978.1.1	10513±50	180	
Chiquihuite Cave	24.61666, -101.13333	Stratigraphic Component B	charcoal	OxA-36608	12060±50	180	
Chiquihuite Cave	24.61666, -101.13333	Stratigraphic Component B	bone	LEMA-640.1.1	11403±60	180	
Chiquihuite Cave	24.61666, -101.13333	Stratigraphic Component B	charcoal	LEMA-892.1.2	11770±35	180	
Chiquihuite Cave	24.61666, -101.13333	Stratigraphic Component B	charcoal	OxA-36618	11855±50	180	
Chiquihuite Cave	24.61666, -101.13333	Stratigraphic Component B	charcoal	OxA-36621	11890±45	180	
Chiquihuite Cave	24.61666, -101.13333	Stratigraphic Component B	charcoal	OxA-36610	11895±50	180	
Chiquihuite Cave	24.61666, -101.13333	Stratigraphic Component B	charcoal	LEMA-893.1.1	11897±35	180	
Chiquihuite Cave	24.61666, -101.13333	Stratigraphic Component B	charcoal	OxA-36624	11900±50	180	
Chiquihuite Cave	24.61666, -101.13333	Stratigraphic Component B	charcoal	OxA-36753	11975±70	180	

Site name	Coordinates	Provenience	Sample material	Laboratory code	Date (BP or ka)	Source	Notes
Chiquihuite Cave	24.61666, -101.13333	Stratigraphic Component B	bone	OxA-36496	12005±55	180	
Chiquihuite Cave	24.61666, -101.13333	Stratigraphic Component B	charcoal	OxA-36619	12040±50	180	
Chiquihuite Cave	24.61666, -101.13333	Stratigraphic Component B	charcoal	OxA-36616	12050±50	180	
Chiquihuite Cave	24.61666, -101.13333	Stratigraphic Component B	charcoal	OxA-36615	12095±50	180	
Chiquihuite Cave	24.61666, -101.13333	Stratigraphic Component B	charcoal	OxA-36617	12120±50	180	
Chiquihuite Cave	24.61666, -101.13333	Stratigraphic Component B	charcoal	OxA-36609	12120±50	180	
Chiquihuite Cave	24.61666, -101.13333	Stratigraphic Component B	charcoal	OxA-36620	12140±50	180	
Chiquihuite Cave	24.61666, -101.13333	Stratigraphic Component B	charcoal	OxA-36622	12155±50	180	
Chiquihuite Cave	24.61666, -101.13333	Stratigraphic Component B	charcoal	OxA-36625	12170±50	180	
Chiquihuite Cave	24.61666, -101.13333	Stratigraphic Component B	charcoal	OxA-36633	12235±75	180	
Chiquihuite Cave	24.61666, -101.13333	Stratigraphic Component B	sediment	Oxford X-7233	10960±1,610	180	OSL
Chiquihuite Cave	24.61666, -101.13333	Stratigraphic Component B	charcoal	OxA-36623	13010±55	180	
Chiquihuite Cave	24.61666, -101.13333	Stratigraphic Component B	charcoal	Beta-436710	12880±50	180	
Chiquihuite Cave	24.61666, -101.13333	Stratigraphic Component B	charcoal	OxA-36612	12885±50	180	
Chiquihuite Cave	24.61666, -101.13333	Stratigraphic Component B	charcoal	LEMA-573.1.1	12916±58	180	
Chiquihuite Cave	24.61666, -101.13333	Stratigraphic Component B	charcoal	OxA-36634	12990±55	180	
Chiquihuite Cave	24.61666, -101.13333	Stratigraphic Component B	charcoal	LEMA-574.1.1	13092±63	180	
Chiquihuite Cave	24.61666, -101.13333	Stratigraphic Component B	charcoal	OxA-36611	13050±55	180	
Chiquihuite Cave	24.61666, -101.13333	Stratigraphic Component B	charcoal	LEMA-635.1.1	13054±60	180	
Chiquihuite Cave	24.61666, -101.13333	Stratigraphic Component B	Bone	OxA-36359	13525±35	180	
Chiquihuite Cave	24.61666, -101.13333	Stratigraphic Component B	charcoal	LEMA-635.1.2	13142±60	180	
Chiquihuite Cave	24.61666, -101.13333	Stratigraphic Component B	charcoal	OxA-36613	13630±55	180	
Chiquihuite Cave	24.61666, -101.13333	Stratigraphic Component B/C transit	sediment	Beta-436709	13010±50	180	
Chiquihuite Cave	24.61666, -101.13333	Stratigraphic Component B/C transit	charcoal	LEMA-636.1.1	13569±60	180	
Chiquihuite Cave	24.61666, -101.13333	Stratigraphic Component B/C transit	charcoal	LEMA-636.1.2	13788±90	180	
Chiquihuite Cave	24.61666, -101.13333	Stratigraphic Component B/C transit	sediment	LEMA-575.1.2	14107±64	180	
Chiquihuite Cave	24.61666, -101.13333	Stratigraphic Component B/C transit	charcoal	LEMA-575.1.3	14778±77	180	

Site name	Coordinates	Provenience	Sample material	Laboratory code	Date (BP or ka)	Source	Notes
Chiquihuite Cave	24.61666, -101.13333	Stratigraphic Component B/C transit	sediment	Oxford X-7231	15560±1,740	180	OSL
Chiquihuite Cave	24.61666, -101.13333	Stratigraphic Component B/C transit	sediment	Oxford X-7232	13870±2250	180	OSL
Chiquihuite Cave	24.61666, -101.13333	Stratigraphic Component C	sediment	Oxford X-7227	11620±2000	180	OSL
Chiquihuite Cave	24.61666, -101.13333	Stratigraphic Component C	charcoal	OxA-36614	20860±100	180	
Chiquihuite Cave	24.61666, -101.13333	Stratigraphic Component C	bone	OxA-36360	21140±130	180	
Chiquihuite Cave	24.61666, -101.13333	Stratigraphic Component C	bone	OxA-34965	21990±170	180	
Chiquihuite Cave	24.61666, -101.13333	Stratigraphic Component C	bone	OxA-36530	22170±140	180	
Chiquihuite Cave	24.61666, -101.13333	Stratigraphic Component C	charcoal	LEMA-576.1.1	20896±80	180	
Chiquihuite Cave	24.61666, -101.13333	Stratigraphic Component C	charcoal	LEMA-577.1.1	21401±95	180	
Chiquihuite Cave	24.61666, -101.13333	Stratigraphic Component C	sediment	ICA-16OS/0510	20220±80	180	
Chiquihuite Cave	24.61666, -101.13333	Stratigraphic Component C	bone	Beta-345055	27830±150	180	
Chiquihuite Cave	24.61666, -101.13333	Stratigraphic Component C	charcoal	PRI-5414	27929±82	180	
Chiquihuite Cave	24.61666, -101.13333	Stratigraphic Component C	sediment	Oxford X-7229	23940±2,950	180	OSL
Chiquihuite Cave	24.61666, -101.13333	Stratigraphic Component C	sediment	Oxford X-4135	27790±4,340	180	OSL; (minimum age)
Colby	44.020499, -107.854297	Bone Pile 2	mammoth bone (XAD)	UCIAMS-11342	10790±30	5	
Colby	44.020499, -107.854297	Bone Pile 2	mammoth bone (XAD)	UCIAMS-11343	10950±30	5	
Cooper's Ferry	45.90538, -116.39751	Mid LU5	bone	OxA-37169	8141±38	13	
Cooper's Ferry	45.90538, -116.39751	Mid LU5	sediment	CFA019	12170±2320	13	OSL
Cooper's Ferry	45.90538, -116.39751	Upper LU4	bone	OxA-38048	9775±50	13	
Cooper's Ferry	45.90538, -116.39751	Upper LU4	bone	OxA-X-2792-41	9110±50	13	
Cooper's Ferry	45.90538, -116.39751	Mid LU4	bone	OxA-38103	10055±55	13	
Cooper's Ferry	45.90538, -116.39751	Mid LU4	sediment	CFA018	12730±2400	13	OSL
Cooper's Ferry	45.90538, -116.39751	Mid LU4	bone	OxA-X-2792-42	13165±70	13	
Cooper's Ferry	45.90538, -116.39751	Lower LU4	bone	OxA-37171	10005±40	13	
Cooper's Ferry	45.90538, -116.39751	Lower LU4	charcoal	D-AMS 029850	9714±57	13	
Cooper's Ferry	45.90538, -116.39751	Lower LU4	bone	OxA-X-2792-43	10050±60	13	
Cooper's Ferry	45.90538, -116.39751	Lower LU4	charcoal	D-AMS 029851	7944±39	13	
Cooper's Ferry	45.90538, -116.39751	Near surface of LU3	charcoal	TO-7349	11410±120	13	

Site name	Coordinates	Provenience	Sample material	Laboratory code	Date (BP or ka)	Source	Notes
Cooper's Ferry	45.90538, -116.39751	Upper LU3	bone	OxA-X-2792-45	11630±80	13	
Cooper's Ferry	45.90538, -116.39751	Mid LU3	bone	OxA-38104	7605±40	13	
Cooper's Ferry	45.90538, -116.39751	Mid LU3	sediment	CFA017	13710±2620	13	OSL
Cooper's Ferry	45.90538, -116.39751	Mid LU3 (F129)	charcoal	D-AMS 029846	12348±71	13	
Cooper's Ferry	45.90538, -116.39751	Mid LU3	charcoal	OxA-38050	7831±40	13	
Cooper's Ferry	45.90538, -116.39751	Mid LU3 (F129)	charcoal	D-AMS 029749	12598±54	13	
Cooper's Ferry	45.90538, -116.39751	Mid LU3 (F129)	charcoal	D-AMS 029847	12472±61	13	
Cooper's Ferry	45.90538, -116.39751	Mid LU3	charcoal	D-AMS 029848	12363±49	13	
Cooper's Ferry	45.90538, -116.39751	Lower LU3	bone	OxA-37284	12475±60	13	
Cooper's Ferry	45.90538, -116.39751	Lower LU3	charcoal	OxA-38051	13070±80	13	
Cooper's Ferry	45.90538, -116.39751	Lower LU3	bone	OxA-X-2792-48	12830±65	13	
Cooper's Ferry	45.90538, -116.39751	Lower LU3	bone	OxA-38106	7985±40	13	
Cooper's Ferry	45.90538, -116.39751	Within pit (F144)	bone	OxA-38197	11720±80	13	excluded from models (see site description for further information)
Cooper's Ferry	45.90538, -116.39751	Within first pit (PFA2)	charcoal	Beta-114949	11370±40	13	excluded from models (see site description for further information)
Cooper's Ferry	45.90538, -116.39751	Within second pit (F134)	bone	OxA-38049	10010±50	13	excluded from models (see site description for further information)
Cooper's Ferry	45.90538, -116.39751	Within second pit (F134)	bone	OxA-38052	13335±75	13	excluded from models (see site description for further information)
Cooper's Ferry	45.90538, -116.39751	Within third pit (F135)	bone	OxA-38105	9955±50	13	excluded from models (see site description for further information)
Debra L. Friedkin (Block A)	30.892283, -97.709742	Pre-Occupation Floodplain deposits	sediment	UIC2351Q	27650±1800	82	OSL
Debra L. Friedkin (Block A)	30.892283, -97.709742	Pre-Occupation Floodplain deposits	sediment	UIC235	26090±1670	82	OSL
Debra L. Friedkin (Block A)	30.892283, -97.709742	Pre-Occupation Floodplain deposits	sediment	BG4079	24145±1635	82	OSL

Site name	Coordinates	Provenience	Sample material	Laboratory code	Date (BP or ka)	Source	Notes
Debra L. Friedkin (Block A)	30.892283, -97.709742	Pre-Occupation Floodplain deposits	sediment	UIC2358	25185±1640	82	OSL
Debra L. Friedkin (Block A)	30.892283, -97.709742	Pre-Occupation Floodplain deposits	sediment	UIC2057	24420±1580	82	OSL
Debra L. Friedkin (Block A)	30.892283, -97.709742	Pre-Occupation Floodplain deposits	sediment	BG4078	22950±1445	82	OSL
Debra L. Friedkin (Block A)	30.892283, -97.709742	Pre-Occupation Floodplain deposits	sediment	UIC2357S	23150±1600	82	OSL
Debra L. Friedkin (Block A)	30.892283, -97.709742	Pre-Occupation Floodplain deposits	sediment	UIC2357	22710±1450	82	OSL
Debra L. Friedkin (Block A)	30.892283, -97.709742	Pre-Occupation Floodplain deposits	sediment	UIC2058	20330±1320	82	OSL
Debra L. Friedkin (Block A)	30.892283, -97.709742	Pre-Occupation Floodplain deposits	sediment	UIC2370	20565±1325	82	OSL
Debra L. Friedkin (Block A)	30.892283, -97.709742	Pre-Occupation Floodplain deposits	sediment	UIC2370Q	20490±1305	82	OSL
Debra L. Friedkin (Block A)	30.892283, -97.709742	Pre-Occupation Floodplain deposits	sediment	BG4077	20250±1340	82	OSL
Debra L. Friedkin (Block A)	30.892283, -97.709742	Pre-Occupation Floodplain deposits	sediment	BG3993	19750±1245	82	OSL
Debra L. Friedkin (Block A)	30.892283, -97.709742	Pre-Occupation Floodplain deposits	sediment	UIC2348	18930±1210	82	OSL
Debra L. Friedkin (Block A)	30.892283, -97.709742	Pre-Occupation Floodplain deposits	sediment	BG4076	19680±1320	82	OSL
Debra L. Friedkin (Block A)	30.892283, -97.709742	Pre-Occupation Floodplain deposits	sediment	BG3994	19650±1230	82	OSL
Debra L. Friedkin (Block A)	30.892283, -97.709742	Boundary Date	sediment	UIC2368	17530±1140	82	OSL
Debra L. Friedkin (Block A)	30.892283, -97.709742	Boundary Date	sediment	UIC2553	16270±1040	82	OSL
Debra L. Friedkin (Block A)	30.892283, -97.709742	Boundary Date	sediment	UIC2183	15110±960	82	OSL
Debra L. Friedkin (Block A)	30.892283, -97.709742	Boundary Date	sediment	UIC2062	16170±1030	82	OSL
Debra L. Friedkin (Block A)	30.892283, -97.709742	Pre-Clovis	sediment	UIC2355	16515±1075	82	OSL
Debra L. Friedkin (Block A)	30.892283, -97.709742	Pre-Clovis	sediment	BG4069	15725±1030	82	OSL
Debra L. Friedkin (Block A)	30.892283, -97.709742	Pre-Clovis	sediment	BG4239	16650±1110	82	OSL

Site name	Coordinates	Provenience	Sample material	Laboratory code	Date (BP or ka)	Source	Notes
Debra L. Friedkin (Block A)	30.892283, -97.709742	Pre-Clovis	sediment	UIC2044	16400±1040	82	OSL
Debra L. Friedkin (Block A)	30.892283, -97.709742	Pre-Clovis	sediment	BG2044	15800±1080	82	OSL
Debra L. Friedkin (Block A)	30.892283, -97.709742	Pre-Clovis	sediment	BG4238	15500±1020	82	OSL
Debra L. Friedkin (Block A)	30.892283, -97.709742	Pre-Clovis	sediment	UIC2356	14710±940	82	OSL
Debra L. Friedkin (Block A)	30.892283, -97.709742	Pre-Clovis	sediment	BG3995	15020±1010	82	OSL
Debra L. Friedkin (Block A)	30.892283, -97.709742	Pre-Clovis	sediment	UIC2043	15210±960	82	OSL
Debra L. Friedkin (Block A)	30.892283, -97.709742	Pre-Clovis	sediment	BG4236	15400±1015	82	OSL
Debra L. Friedkin (Block A)	30.892283, -97.709742	Pre-Clovis	sediment	UIC2359	15730±1010	82	OSL
Debra L. Friedkin (Block A)	30.892283, -97.709742	Pre-Clovis	sediment	BG4018	15265±1000	82	OSL
Debra L. Friedkin (Block A)	30.892283, -97.709742	Pre-Clovis	sediment	BG4235	14965±985	82	OSL
Debra L. Friedkin (Block A)	30.892283, -97.709742	Pre-Clovis	sediment	BG4234	14790±985	82	OSL
Debra L. Friedkin (Block A)	30.892283, -97.709742	Pre-Clovis	sediment	UIC2350S	14580±1030	82	OSL
Debra L. Friedkin (Block A)	30.892283, -97.709742	Pre-Clovis	sediment	UIC2350Q	14480±920	82	OSL
Debra L. Friedkin (Block A)	30.892283, -97.709742	Pre-Clovis	sediment	UIC2350	14000±890	82	OSL
Debra L. Friedkin (Block A)	30.892283, -97.709742	Pre-Clovis	sediment	UIC2047	15270±960	82	OSL
Debra L. Friedkin (Block A)	30.892283, -97.709742	Pre-Clovis	sediment	UIC2369	14370±930	82	OSL
Debra L. Friedkin (Block A)	30.892283, -97.709742	Pre-Clovis	sediment	BG4017	13960±965	82	OSL
Debra L. Friedkin (Block A)	30.892283, -97.709742	Pre-Clovis	sediment	UIC2367	14080±920	82	OSL
Debra L. Friedkin (Block A)	30.892283, -97.709742	Pre-Clovis	sediment	BG4220	13595±930	82	OSL
Debra L. Friedkin (Block A)	30.892283, -97.709742	Boundary Date	sediment	UIC2046	14350±910	82	OSL

Site name	Coordinates	Provenience	Sample material	Laboratory code	Date (BP or ka)	Source	Notes
Debra L. Friedkin (Block A)	30.892283, -97.709742	Boundary Date	sediment	BG4019	13620±880	82	OSL
Debra L. Friedkin (Block A)	30.892283, -97.709742	Boundary Date	sediment	UIC2354	14070±910	82	OSL
Debra L. Friedkin (Block A)	30.892283, -97.709742	Boundary Date	sediment	BG4219	13010±905	82	OSL
Debra L. Friedkin (Block A)	30.892283, -97.709742	Clovis and Folsom	sediment	UIC2059Q	13780±885	82	OSL
Debra L. Friedkin (Block A)	30.892283, -97.709742	Clovis and Folsom	sediment	UIC2059	13090±830	82	OSL
Debra L. Friedkin (Block A)	30.892283, -97.709742	Clovis and Folsom	sediment	UIC2045Q	12925±845	82	OSL
Debra L. Friedkin (Block A)	30.892283, -97.709742	Clovis and Folsom	sediment	UIC2045	12240±800	82	OSL
Debra L. Friedkin (Block A)	30.892283, -97.709742	Clovis and Folsom	sediment	BG4218	13020±870	82	OSL
Debra L. Friedkin (Block A)	30.892283, -97.709742	Clovis and Folsom	sediment	BG4209	12560±830	82	OSL
Debra L. Friedkin (Block A)	30.892283, -97.709742	Clovis and Folsom	sediment	UIC2366A	12100±860	82	OSL
Debra L. Friedkin (Block A)	30.892283, -97.709742	Clovis and Folsom	sediment	UIC2366	12000±770	82	OSL
Debra L. Friedkin (Block A)	30.892283, -97.709742	Clovis and Folsom	sediment	BG4068	12940±855	82	OSL
Debra L. Friedkin (Block A)	30.892283, -97.709742	Clovis and Folsom	sediment	BG4208	12170±820	82	OSL
Debra L. Friedkin (Block A)	30.892283, -97.709742	Paleoindian	sediment	UIC2050	12970±830	82	OSL
Debra L. Friedkin (Block A)	30.892283, -97.709742	Late Paleoindian	sediment	UIC2048	12690±955	82	OSL
Debra L. Friedkin (Block A)	30.892283, -97.709742	Late Paleoindian	sediment	BG4075	11060±735	82	OSL
Debra L. Friedkin (Block A)	30.892283, -97.709742	Late Paleoindian	sediment	UIC2365	11870±760	82	OSL
Debra L. Friedkin (Block A)	30.892283, -97.709742	Late Paleoindian	sediment	BG4206	10785±715	82	OSL
Debra L. Friedkin (Block A)	30.892283, -97.709742	Late Paleoindian	sediment	BG4207	10530±750	82	OSL
Debra L. Friedkin (Block A)	30.892283, -97.709742	Late Paleoindian	sediment	BG4341	10830±695	82	OSL

Site name	Coordinates	Provenience	Sample material	Laboratory code	Date (BP or ka)	Source	Notes
Debra L. Friedkin (Block A)	30.892283, -97.709742	Late Paleoindian	sediment	BG4074	10375±740	82	OSL
Debra L. Friedkin (Block A)	30.892283, -97.709742	Late Paleoindian	sediment	UIC2051	10480±675	82	OSL
Debra L. Friedkin (Block A)	30.892283, -97.709742	Late Paleoindian	sediment	UIC2364	9930±640	82	OSL
Debra L. Friedkin (Block A)	30.892283, -97.709742	Late Paleoindian	sediment	BG4340	10360±705	82	OSL
Debra L. Friedkin (Block A)	30.892283, -97.709742	Late Paleoindian	sediment	BG4067	10100±695	82	OSL
Debra L. Friedkin (Block A)	30.892283, -97.709742	Late Paleoindian	sediment	BG4339	10095±655	82	OSL
Debra L. Friedkin (Block A)	30.892283, -97.709742	Late Paleoindian	sediment	UIC2052	9250±600	82	OSL
Debra L. Friedkin (Block A)	30.892283, -97.709742	Late Paleoindian	sediment	UIC2363	9405±610	82	OSL
Debra L. Friedkin (Block A)	30.892283, -97.709742	Early Archaic	sediment	UIC2061	9215±620	82	OSL
Debra L. Friedkin (Block A)	30.892283, -97.709742	Early Archaic	sediment	BG4338	8655±550	82	OSL
Debra L. Friedkin (Block A)	30.892283, -97.709742	Early Archaic	sediment	UIC2060Q	8490±560	82	OSL
Debra L. Friedkin (Block A)	30.892283, -97.709742	Early Archaic	sediment	UIC2060	8070±520	82	OSL
Debra L. Friedkin (Block A)	30.892283, -97.709742	Early Archaic	sediment	UIC2362	8160±540	82	OSL
Debra L. Friedkin (Block A)	30.892283, -97.709742	Early Archaic	sediment	BG4066	8315±540	82	OSL
Debra L. Friedkin (Block A)	30.892283, -97.709742	Early Archaic	sediment	UIC2360	7160±470	82	OSL
Debra L. Friedkin (Block A)	30.892283, -97.709742	Early Archaic	sediment	UIC2360s	7030±470	82	OSL
Dent	40.319080, -104.829562	mammoth bone bed	mammoth bone (HYP)	OxA-X-2736-11	11055±50	88	
Dent	40.319080, -104.829562	mammoth bone bed	mammoth bone (HYP)	OxA-X-2736-12	11155±50	88	
Domebo	34.957529, -98.271482	Clovis mammoth bone bed	mammoth bone	UCIAMS-11341	10960±30	5	
Dry Creek	63.883333, -149.033333	Loess 2; component I; feature 11.02	hearth charcoal (Salix sp.)	Beta-315411	11530±50	33	
Dry Creek	63.883333, -149.033333	Loess 2; component I; feature 11.02	hearth charcoal (Salix sp.)	UCIAMS-135114	11510±40	33	

Site name	Coordinates	Provenience	Sample material	Laboratory code	Date (BP or ka)	Source	Notes
Dry Creek	63.883333, -149.033333	Loess 2; component I; feature 11.03	hearth charcoal (Salix sp.)	UCIAMS-135112	11635±40	33	
Dry Creek	63.883333, -149.033333	Loess 2; component I; feature 11.03	hearth charcoal (Salix sp.)	UCIAMS-135113	11580±40	33	
Dry Creek	63.883333, -149.033333	Loess 3; component II; feature 11.01	hearth charcoal (Salix sp.)	Beta-315410	9460±60	33	
Dry Creek	63.883333, -149.033333	Loess 3; component II; feature 11.01	hearth charcoal (Salix sp.)	UCIAMS-135115	9480±35	33	
El Fin del Mundo	29.733406, -111.760384	Stratum 3 (A)	shell (Planorbid)	AA-90707	12180±40	91	
El Fin del Mundo	29.733406, -111.760384	Stratum 3 (B)	tooth enamel	AA-95550	9755±92	91	
El Fin del Mundo	29.733406, -111.760384	Stratum 3 (B)	organic matter	AA-83272B	11040±580	91	
El Fin del Mundo	29.733406, -111.760384	Stratum 3 (B)	tooth enamel	AA-95550 (duplicate)	9804±93	91	
El Fin del Mundo	29.733406, -111.760384	Stratum 3 (B)	charcoal	AA-100182B	11880±200	91	
El Fin del Mundo	29.733406, -111.760384	Stratum 3 (B)	charcoal	AA-100181B	10650±250	91	
El Fin del Mundo	29.733406, -111.760384	Stratum 3 (B)	charcoal	AA-100181A	11550±60	91	
El Fin del Mundo	29.733406, -111.760384	Stratum 4 (D)	organic matter	AA-14896A	6185±115	91	
El Fin del Mundo	29.733406, -111.760384	Stratum 4 (D)	organic matter	AA-80078A	6921±58	91	
El Fin del Mundo	29.733406, -111.760384	Stratum 4 (D)	organic matter	AA-80076A	7570±93	91	
El Fin del Mundo	29.733406, -111.760384	Stratum 4 (D.E)	charcoal	AA-80084A	9715±64	91	
El Fin del Mundo	29.733406, -111.760384	Stratum 4 (D.E)	charcoal	AA-80671B	9560±120	91	
El Fin del Mundo	29.733406, -111.760384	Stratum 4 (D.E)	charcoal	AA-80085B	9290±290	91	
El Fin del Mundo	29.733406, -111.760384	Stratum 4 (D.E)	organic matter	A-14850	9030±75	91	
El Fin del Mundo	29.733406, -111.760384	Stratum 4 (D.E)	organic matter	A-14836	9465±100	91	
El Fin del Mundo	29.733406, -111.760384	Stratum 4 (D.E)	organic matter	A-14837	8375±110	91	
El Fin del Mundo	29.733406, -111.760384	Stratum 4 (D.E)	shell (Succinid)	AA-88886	8470±50	91	
El Fin del Mundo	29.733406, -111.760384	Stratum 4 (D.E)	shell (Succinid)	AA-81350	8030±50	91	
El Fin del Mundo	29.733406, -111.760384	Stratum 4 (D.E)	shell (Succinid)	AA-88885	8770±60	91	
Gault	30.892283, -97.709742	Gault Assemblage	sediment	11-06	21700±1400	97	OSL
Gault	30.892283, -97.709742	Gault Assemblage	sediment	11-18	16900±1100	97	OSL
Gault	30.892283, -97.709742	Gault Assemblage	sediment	11-20	16700±1100	97	OSL
Gault	30.892283, -97.709742	Gault Assemblage	sediment	11-05b	18700±1200	97	OSL

Site name	Coordinates	Provenience	Sample material	Laboratory code	Date (BP or ka)	Source	Notes
Gault	30.892283, -97.709742	Clovis	sediment	11-03	11900±800	97	OSL
Gault	30.892283, -97.709742	Clovis	sediment	11-07	12900±600	97	OSL
Gault	30.892283, -97.709742	Clovis	sediment	11-15	13600±600	97	OSL
Gault	30.892283, -97.709742	Clovis	sediment	11-09	13200±600	97	OSL
Gault	30.892283, -97.709742	Paleoindian	sediment	11-17	11600±500	97	OSL
Gault	30.892283, -97.709742	Paleoindian	sediment	11-13	10200±500	97	OSL
Gault	30.892283, -97.709742	Paleoindian	sediment	11-08	9900±400	97	OSL
Gault	30.892283, -97.709742	Paleoindian	sediment	09-06	9700±400	97	OSL
Gault	30.892283, -97.709742	Paleoindian	sediment	09-05	9300±400	97	OSL
Gault	30.892283, -97.709742	Paleoindian	sediment	11-02	10100±400	97	OSL
Gault	30.892283, -97.709742	Paleoindian	sediment	09-04	8800±400	97	OSL
Gault	30.892283, -97.709742	Paleoindian	sediment	11-16	9100±400	97	OSL
Gault	30.892283, -97.709742	Archaic	sediment	09-03	6600±300	97	OSL
Gault	30.892283, -97.709742	Archaic	sediment	09-02	6100±300	97	OSL
Gault	30.892283, -97.709742	Archaic	sediment	09-01b	5900±300	97	OSL
Gault	30.892283, -97.709742	Archaic	sediment	09-01	5900±300	97	OSL
Gault	30.892283, -97.709742	Archaic	sediment	11-01	5700±300	97	OSL
Hebior	42.643, -88.010	Paleoindian	mammoth bone (XAD)	CAMS-61137	12590±50	151	
Hebior	42.643, -88.010	Paleoindian	mammoth bone (XAD)	CAMS-28303	12480±60	153	
Hebior	42.643, -88.010	Paleoindian	mammoth bone (XAD)	CAMS-61136	12520±50	151	Although they might not be the same, this same date is noted as CAMS 24943 in ref 153.
Jake Bluff	36.596874, -99.514348	Clovis bison bone bed	bison bone (XAD)	CAMS-79940	10750±40	98	
Jake Bluff	36.596874, -99.514348	Clovis bison bone bed	bison bone (XAD)	CAMS-90968	10840±45	98	
Jake Bluff	36.596874, -99.514348	Clovis bison bone bed	bison bone (XAD)	CAMS-90969	10700±45	98	
Jake Bluff	36.596874, -99.514348	Clovis bison bone bed	bison bone (XAD)	UCIAMS-61657	10810±25	99	
Jake Bluff	36.596874, -99.514348	Clovis bison bone bed	bison bone (XAD)	UCIAMS-59874	10885±35	99	
Lange/ Ferguson	43.334567, -102.104490	Clovis mammoth bone bed	mammoth bone (XAD)	UCIAMS-11344	10710±130	5	
Lange/ Ferguson	43.334567, -102.104490	Clovis mammoth bone bed	mammoth bone (XAD)	UCIAMS-11345	11110±40	5	

Site name	Coordinates	Provenience	Sample material	Laboratory code	Date (BP or ka)	Source	Notes
Lehner	31.421691, -110.114805	hearth 2	hearth charcoal	K-554	11180±140	107	
Lehner	31.421691, -110.114805	hearth 2	hearth charcoal	M-811	11290±500	107	
Lehner	31.421691, -110.114805	F1	hearth charcoal	SMU-168	10770±140	103	
Lehner	31.421691, -110.114805	F1	hearth charcoal	A-378	10940±100	103	
Lehner	31.421691, -110.114805	F1	hearth charcoal	SMU-181	11080±200	103	
Lehner	31.421691, -110.114805	F2/D,Z	hearth charcoal	SMU-194	10950±110	103	
Lehner	31.421691, -110.114805	F2/D,Z	hearth charcoal	SMU-164	10860±280	103	
Lehner	31.421691, -110.114805	F2/D,Z	hearth charcoal	SMU-290	10950±90	103	
Lehner	31.421691, -110.114805	F2/D,Z	hearth charcoal	SMU-196	11080±230	103	
Lehner	31.421691, -110.114805	F2/F0	hearth charcoal	SMU-347	10620±300	103	
Lehner	31.421691, -110.114805	F2/F0	hearth charcoal	SMU-297	10700±150	103	
Lehner	31.421691, -110.114805	F2/F0	hearth charcoal	SMU-340	10710±90	103	
Lehner	31.421691, -110.114805	F2/F0	hearth charcoal	SMU-264	11170±200	103	
Lehner	31.421691, -110.114805	F2/F0	hearth charcoal	SMU-308	11470±110	103	
Lehner	31.421691, -110.114805	hearth 1	hearth charcoal	A-34	7205±450	107	
Lehner	31.421691, -110.114805	hearth 2	hearth charcoal	A-32	7022±450	107	
Lehner	31.421691, -110.114805	hearth 2	hearth charcoal	A-30	8330±450	107	
Lehner	31.421691, -110.114805	hearth 2	hearth charcoal	A-40a	10900±450	107	
Lehner	31.421691, -110.114805	hearth 2	hearth charcoal	A-40b	12000±450	107	
Lindsay	47.232458, -105.128239	late-Pleistocene loess	mammoth bone (HYP)	OxA-X-2736-15	12395±55	88	
Lindsay	47.232458, -105.128239	late-Pleistocene loess	mammoth bone (XAD)	CAMS-72348	12330±50	159	
Lindsay	47.232458, -105.128239	late-Pleistocene loess	mammoth bone (XAD)	UCIAMS-12308	12300±35	158	
Lindsay	47.232458, -105.128239	late-Pleistocene loess	mammoth bone (XAD)	UCIAMS-127316	12270±35	158	
Lubbock Lake	33.622424, -101.889496	Stratum 1	clams (Sphaerium and Psidium), carbonate	I-246	12650±290	128	
Lubbock Lake	33.622424, -101.889496	Stratum 1	clams (Sphaerium and Psidium), carbonate	SMU-295	12150±90	128	
Lubbock Lake	33.622424, -101.889496	Stratum 1	wood	SMU-548	11100±100	128	
Lubbock Lake	33.622424, -101.889496	Stratum 1	wood	SMU-263	11100±80	128	

Site name	Coordinates	Provenience	Sample material	Laboratory code	Date (BP or ka)	Source	Notes
Lubbock Lake	33.622424, -101.889496	Stratum 1	bison bone apatite, same as SMU-367	SMU-317	8860±90	128	
Lubbock Lake	33.622424, -101.889496	Stratum 1	bison bone collagen, same as SMU-317	SMU-367	7040±600	128	
Lubbock Lake	33.622424, -101.889496	Stratum 2 (2ALB1)	snails (Helisoma trivolis, Lymnaea reflaxa), carbonate	SMU-292	10880±90	128	
Lubbock Lake	33.622424, -101.889496	Stratum 2 (2ALB1)	organic mud, humin	SI-3202	10780±80	128	
Lubbock Lake	33.622424, -101.889496	Stratum 2 (2ALB1)	diatomite, humic acid	SMU-285	10530±90	128	
Lubbock Lake	33.622424, -101.889496	Stratum 2 (2ALB1)	snails, carbonate, solid carbon	L-283g	9700±450	128	
Lubbock Lake	33.622424, -101.889496	Stratum 2 (2ALB2)	charcoal	SMU-547	10540±100	128	
Lubbock Lake	33.622424, -101.889496	Stratum 2 (2ALB2)	cienaga, humin	SI-3200	10360±80	128	
Lubbock Lake	33.622424, -101.889496	Stratum 2 (2ALB2)	diatomite, humic acid, same as SMU-247	SMU-251	10060±170	128	
Lubbock Lake	33.622424, -101.889496	Stratum 2 (2ALB2)	diatomite, humin acid, same as SMU-251	SMU-247	7840±170	128	
Lubbock Lake	33.622424, -101.889496	Stratum 2 (2A upper)	organic mud, humin	SI-3203	10015±75	128	
Lubbock Lake	33.622424, -101.889496	Stratum 2 (2B base)	cienaga, humic acid	SMU-728	9990±100	128	
Lubbock Lake	33.622424, -101.889496	Stratum 2 (2B base)	diatomite, humic acid	SMU-275	9960±80	128	
Lubbock Lake	33.622424, -101.889496	Stratum 2 (2B middle)	charred bison bone, solid carbon	C-558	9883±350	128	
Lubbock Lake	33.622424, -101.889496	Stratum 2 (2B middle)	charred bison bone, solid carbon	L-283H	7765±200	128	
Lubbock Lake	33.622424, -101.889496	Stratum 2 (2B middle)	organic mud, humic acid	SMU-759	9330±70	128	
Lubbock Lake	33.622424, -101.889496	Stratum 2 (2B upper)	organic mud, humin	SI-4177	8655±90	128	
Lubbock Lake	33.622424, -101.889496	Stratum 2 (2B upper)	cienaga, humic acid	SMU-827	7980±180	128	
Lubbock Lake	33.622424, -101.889496	Stratum 2 (2B upper)	cienaga, humic acid	SMU-830	8210±240	128	
Lubbock Lake	33.622424, -101.889496	Stratum 2 (2B upper)	organic mud, humic acid	SI-302	7890±100	128	
Lubbock Lake	33.622424, -101.889496	Stratum 2 (2B upper)	cienaga, humic acid	SMU-262	7970±70	128	
Lubbock Lake	33.622424, -101.889496	Stratum 2 (2B upper)	organic mud, humin	SI-3204	7255±75	128	
Lubbock Lake	33.622424, -101.889496	Stratum 2 (2B upper)	cienaga, humic acid	SMU-648	7100±80	128	

Site name	Coordinates	Provenience	Sample material	Laboratory code	Date (BP or ka)	Source	Notes
Lubbock Lake	33.622424, -101.889496	Stratum 2 (2B upper)	cienaga, humin	SI-4178	6705±95	128	
Lubbock Lake	33.622424, -101.889496	Stratum 2 (2B upper)	cienaga, humic acid	SMU-544	6400±80	128	
Lubbock Lake	33.622424, -101.889496	Stratum 3 (3e)	humic acid	SMU-545	5770±80	128	
Lubbock Lake	33.622424, -101.889496	Stratum 3 (3/)	buried A horizon, humin	SI-3197	6115±75	128	
Lubbock Lake	33.622424, -101.889496	Stratum 3 (3/)	buried A horizon, humin, check on SI-3197	SI-4172	5475±75	128	
Lubbock Lake	33.622424, -101.889496	Stratum 3 (3/)	buried A horizon, humic acid	SMU-531	4900±60	128	
Lubbock Lake	33.622424, -101.889496	Stratum 4 (4/)	marsh, humin	SI-3205	5545±100	128	excluded from models (see site description for further information)
Lubbock Lake	33.622424, -101.889496	Stratum 4 (4/)	marsh, humin, check on SI-3205	SI-4176	4355±80	128	excluded from models (see site description for further information)
Lubbock Lake	33.622424, -101.889496	Stratum 4 (4/)	marsh, humin	SI-3206	3925±80	128	excluded from models (see site description for further information)
Lubbock Lake	33.622424, -101.889496	Stratum 4 (4/)	marsh, humin, check on SI-3206	SI-4175	3175±85	128	excluded from models (see site description for further information)
Lubbock Lake	33.622424, -101.889496	Stratum 4 (4/)	marsh, humic acid	SMU-697	2600±50	128	excluded from models (see site description for further information)
Lubbock Lake	33.622424, -101.889496	Stratum 4 (4/)	marsh, humin	SI-4588	980±60	128	excluded from models (see site description for further information)
Lubbock Lake	33.622424, -101.889496	Stratum 4 (4A)	bison bone collagen (average of several dates)	SMU-332/333	4910±50	128	excluded from models (see site description for further information)
Lubbock Lake	33.622424, -101.889496	Stratum 4 (4A)	bison bone apatite, same as SMU-367	SMU-309	4470±50	128	excluded from models (see site description for further information)
Lubbock Lake	33.622424, -101.889496	Stratum 4 (4B)	ash and humic acid, same as SI-4171	SMU-492	4960±50	128	excluded from models (see site description for further information)

Site name	Coordinates	Provenience	Sample material	Laboratory code	Date (BP or ka)	Source	Notes
Lubbock Lake	33.622424, -101.889496	Stratum 4 (4B)	ash and humic acid, same as SMU-492	SI-4171	4700±65	128	excluded from models (see site description for further information)
Lubbock Lake	33.622424, -101.889496	Stratum 4 (4B)	buried A horizon, humin	SI-4174	1955±75	128	excluded from models (see site description for further information)
Lubbock Lake	33.622424, -101.889496	Stratum 4 (4B)	buried A horizon, humin	SI-3201	1215±65	128	excluded from models (see site description for further information)
Lubbock Lake	33.622424, -101.889496	Stratum 4 (4B)	buried A horizon, humic acid	SMU-651	890±70	128	excluded from models (see site description for further information)
Lubbock Lake	33.622424, -101.889496	Stratum 4 (4B)	buried A horizon, humin	SI-4169	880±70	128	excluded from models (see site description for further information)
Lubbock Lake	33.622424, -101.889496	Stratum 4 (4B)	buried A horizon, humic acid	SMU-534	870±40	128	excluded from models (see site description for further information)
Lubbock Lake	33.622424, -101.889496	Stratum 5 (5A/)	marsh, humic acid	SMU-698	600±50	128	excluded from models (see site description for further information)
Lubbock Lake	33.622424, -101.889496	Stratum 5 (5A)	buried A horizon, humic acid	SMU-314	720±40	128	excluded from models (see site description for further information)
Lubbock Lake	33.622424, -101.889496	Stratum 5 (5A)	buried A horizon, humin	SI-3208	640±75	128	excluded from models (see site description for further information)
Lubbock Lake	33.622424, -101.889496	Stratum 5 (5A)	charcoal, lower FA8-6	SI-2701	505±55	128	excluded from models (see site description for further information)
Lubbock Lake	33.622424, -101.889496	Stratum 5 (5A)	charcoal, upper FA8-6, same as SMU-345	SI-2700	380±40	128	excluded from models (see site description for further information)
Lubbock Lake	33.622424, -101.889496	Stratum 5 (5A)	charcoal	SMU-546	320±60	128	excluded from models (see site description for further information)

Site name	Coordinates	Provenience	Sample material	Laboratory code	Date (BP or ka)	Source	Notes
Lubbock Lake	33.622424, -101.889496	Stratum 5 (5A)	charcoal	SI-2704	315±50	128	excluded from models (see site description for further information)
Lubbock Lake	33.622424, -101.889496	Stratum 5 (5A)	charcoal, upper FA8-6, same as SI-2700	SMU-345	300±60	128	excluded from models (see site description for further information)
Lubbock Lake	33.622424, -101.889496	Stratum 5 (5A)	charcoal	SI-2703	285±60	128	excluded from models (see site description for further information)
Lubbock Lake	33.622424, -101.889496	Stratum 5 (5A)	buried A horizon, humic acid	SMU-555	220±50	128	excluded from models (see site description for further information)
Lubbock Lake	33.622424, -101.889496	Stratum 5 (5A)	modern A horizon, humic acid	SMU-343	160±60	128	excluded from models (see site description for further information)
Lubbock Lake	33.622424, -101.889496	Stratum 5 (5A)	charred bison bone	I-208	160±90	128	excluded from models (see site description for further information)
Lubbock Lake	33.622424, -101.889496	Stratum 5 (5A)	charred bison bone	I-140	70±70	128	excluded from models (see site description for further information)
Lubbock Lake	33.622424, -101.889496	Stratum 5 (5B/)	wood	SMU-715	400±110	128	excluded from models (see site description for further information)
Lubbock Lake	33.622424, -101.889496	Stratum 5 (5B/)	marsh, humic acid	SMU-831	390±50	128	excluded from models (see site description for further information)
Lubbock Lake	33.622424, -101.889496	Stratum 5 (5B/)	wood	SI-716	210±40	128	excluded from models (see site description for further information)
Lubbock Lake	33.622424, -101.889496	Stratum 5 (5B)	buried A horizon, humic acid	SMU-650	50±50	128	excluded from models (see site description for further information)
Manis	48.032304, -123.101320	colluvium	mastodon tusk ivory sample no. 1 (XAD)	UCIAMS-11350	11975±35	160	

Site name	Coordinates	Provenience	Sample material	Laboratory code	Date (BP or ka)	Source	Notes
Manis	48.032304, -123.101320	colluvium	mastodon tusk ivory sample no. 1 (XAD)	UCIAMS-12046	11975±35	160	
Manis	48.032304, -123.101320	colluvium	mastodon tusk ivory sample no. 2 (XAD)	UCIAMS-11677	11890±35	160	
Manis	48.032304, -123.101320	colluvium	mastodon rib bone (XAD)	UCIAMS-29113	11990±30	160	
Mead	64.271001, -146.075173	CZ1	charcoal	Beta-312937	3780±30	35	
Mead	64.271001, -146.075173	CZ1	charcoal	Beta-264529	4940±40	34, 35	
Mead	64.271001, -146.075173	CZ2	charcoal	Beta-264525	4580±40	35	
Mead	64.271001, -146.075173	CZ2	charcoal	Beta-264524	6050±40	34, 35	
Mead	64.271001, -146.075173	CZ3	charcoal	Beta-264528	7790±50	34, 35	
Mead	64.271001, -146.075173	CZ3	charcoal	Beta-264526	10140±50	35	
Mead	64.271001, -146.075173	CZ3	charcoal	Beta-264527	10160±50	35	
Mead	64.271001, -146.075173	CZ3	charcoal (Betula sp.)	Beta-337171	10220±40	35	
Mead	64.271001, -146.075173	CZ3	charcoal (Populus sp.)	Beta-342449	10560±40	35	
Mead	64.271001, -146.075173	CZ4	Wapiti antler tool	Beta-342930	11050±40	17	
Mead	64.271001, -146.075173	CZ4	hearth charcoal (Betula sp.)	Beta-337174	11080±50	35	
Mead	64.271001, -146.075173	CZ4	hearth charcoal (Populus/ Salix)	Beta-337172	11100±50	35	
Mead	64.271001, -146.075173	CZ4	hearth charcoal	Beta-264530	11210±60	34, 35	
Mead	64.271001, -146.075173	CZ4	charcoal (Populus/ Salix)	Beta-337181	11030±50	17, 34	
Mead	64.271001, -146.075173	CZ4	charcoal (stratigraphic)	Beta-59121	11560±80	17, 34	
Mead	64.271001, -146.075173	CZ4	charcoal (stratigraphic)	Beta-59120	11600±60	17, 34	
Mead	64.271001, -146.075173	CZ5	bone collagen (Bison sp.)	Beta-264522	11460±50	17, 34	
Meadowcroft Rockshelter	40.286445, -80.488813	Stratum IIa (F-46 lower)	charcoal	SI-2354"±16175±975	16175±975	17, 34	
Meadowcroft Rockshelter	40.286445, -80.488813	Stratum IIa (F-46 lower)	charcoal	SI-1686	15120±165	164	
Meadowcroft Rockshelter	40.286445, -80.488813	Stratum IIa (F-46 lower)	charcoal	SI-1872	14975±620	164	
Meadowcroft Rockshelter	40.286445, -80.488813	Stratum IIa (F-46 lower)	charcoal	SI-2488	11320±340	164	

Site name	Coordinates	Provenience	Sample material	Laboratory code	Date (BP or ka)	Source	Notes
Meadowcroft Rockshelter	40.286445, -80.488813	Stratum IIa (F-46 lower)	charcoal	SI-2065	13240±1010	164	
Meadowcroft Rockshelter	40.286445, -80.488813	Stratum IIa (F-46 lower)	charcoal	SI-2489	12800±870	164	
Meadowcroft Rockshelter	40.286445, -80.488813	Stratum IIa (F-46 lower)	charcoal	SI-2491	11300±700	164	
Meadowcroft Rockshelter	40.286445, -80.488813	Stratum IIa (F-46 lower)	charcoal	SI-2061	9075±115	164	
Meadowcroft Rockshelter	40.286445, -80.488813	Stratum IIa (F-46 lower)	charcoal	SI-2064	8010±110	164	
Meadowcroft Rockshelter	40.286445, -80.488813	Stratum IIb	charcoal	SI-2056	5300±130	164	
Meadowcroft Rockshelter	40.286445, -80.488813	Stratum IIb	charcoal	SI-2055	6670±140	164	
Meadowcroft Rockshelter	40.286445, -80.488813	Stratum IIb	black walnut charcoal	Pitt-292	6630±70	164	
Meadowcroft Rockshelter	40.286445, -80.488813	Stratum IIb	charcoal	SI-2358	6290±355	164	
Meadowcroft Rockshelter	40.286445, -80.488813	Stratum IIb	charcoal	SI-1685	2870±85	164	
Meadowcroft Rockshelter	40.286445, -80.488813	Stratum IIb	charcoal	SI-2356	4380±500	164	
Meadowcroft Rockshelter	40.286445, -80.488813	Stratum IIb	charcoal	SI-2054	4005±85	164	
Meadowcroft Rockshelter	40.286445, -80.488813	Stratum IIb	charcoal	SI-2058	3970±85	164	
Meadowcroft Rockshelter	40.286445, -80.488813	Stratum IIb	charcoal	SI-2063	3950±240	164	
Meadowcroft Rockshelter	40.286445, -80.488813	Stratum IIb	carbonized basketry fragments	SI-1680	3770±90	164	
Meadowcroft Rockshelter	40.286445, -80.488813	Stratum IIb	charcoal	SI-1681	3210±95	164	
Meadowcroft Rockshelter	40.286445, -80.488813	Stratum III	charcoal	SI-1679	3255±115	164	
Meadowcroft Rockshelter	40.286445, -80.488813	Stratum III	charcoal	SI-2046	3115±70	164	
Meadowcroft Rockshelter	40.286445, -80.488813	Stratum III	charcoal	SI-3030	3100±90	164	
Meadowcroft Rockshelter	40.286445, -80.488813	Stratum III	charcoal	SI-2053	1140±115	164	
Meadowcroft Rockshelter	40.286445, -80.488813	Stratum III	charcoal	SI-1664	3065±80	164	
Meadowcroft Rockshelter	40.286445, -80.488813	Stratum III	charcoal	SI-2066	2930±75	164	
Meadowcroft Rockshelter	40.286445, -80.488813	Stratum IV	charcoal	SI-2049	3050±85	164	
Meadowcroft Rockshelter	40.286445, -80.488813	Stratum IV	charcoal	SI-1660	2860±80	164	
Meadowcroft Rockshelter	40.286445, -80.488813	Stratum IV	charcoal	SI-1668	2820±75	164	
Meadowcroft Rockshelter	40.286445, -80.488813	Stratum IV	charcoal	SI-1665	2815±80	164	
Meadowcroft Rockshelter	40.286445, -80.488813	Stratum IV	charcoal	SI-3031	2655±120	164	
Meadowcroft Rockshelter	40.286445, -80.488813	Stratum IV	charcoal	SI-2359	2485±350	164	
Meadowcroft Rockshelter	40.286445, -80.488813	Stratum IV	charcoal	SI-1674	2325±75	164	

Site name	Coordinates	Provenience	Sample material	Laboratory code	Date (BP or ka)	Source	Notes
Meadowcroft Rockshelter	40.286445, -80.488813	Stratum IV	charcoal	SI-2051	2290±90	164	
Meadowcroft Rockshelter	40.286445, -80.488813	Stratum V	charcoal	SI-2487	2155±65	164	
Meadowcroft Rockshelter	40.286445, -80.488813	Stratum V	charcoal	SI-2362	2075±125	164	
Meadowcroft Rockshelter	40.286445, -80.488813	Stratum V	charcoal	SI-3022	1880±65	164	
Meadowcroft Rockshelter	40.286445, -80.488813	Stratum V	charcoal	SI-3027	1790±60	164	
Meadowcroft Rockshelter	40.286445, -80.488813	Stratum V	charcoal	SI-3024	1665±65	164	
Meay Channel I	51.659051, -128.098817	Stratum X/XI	Pinus contorta wood	UCIAMS-163739	11440±25	126	
Meay Channel I	51.659051, -128.098817	Stratum X	wood	UCIAMS-149779	11435±30	126	
Meay Channel I	51.659051, -128.098817	Stratum X	Pinus contorta wood	UCIAMS-169402	11365±25	126	
Meay Channel I	51.659051, -128.098817	Stratum X	wood	UCIAMS-142561	11295±30	126	
Meay Channel I	51.659051, -128.098817	Stratum X	Pinus contorta wood	UCIAMS-163741	11260±25	126	
Meay Channel I	51.659051, -128.098817	Stratum X	Pinus contorta wood	UCIAMS-163740	10720±60	126	
Meay Channel I	51.659051, -128.098817	Stratum IX	Pinus contorta wood	UCIAMS-184916	10625±20	126	
Meay Channel I	51.659051, -128.098817	Stratum IX	unidentified organic material	UCIAMS-169403	9820±80	126	
Meay Channel I	51.659051, -128.098817	Stratum IX	Malus seed + wood	UCIAMS-179713	8410±20	126	
Meay Channel I	51.659051, -128.098817	Stratum IX	unidentified organic material-root	UCIAMS-169401	4935±25	126	
Meay Channel I	51.659051, -128.098817	Stratum VIII	Pinus contorta wood	UCIAMS-169399	10980±25	126	
Meay Channel I	51.659051, -128.098817	Stratum VII	unidentified organic material-root	UCIAMS-169400	2855±15	126	
Meay Channel I	51.659051, -128.098817	Stratum VII	charcoal	UCIAMS-179714	2650±15	126	
Meay Channel I	51.659051, -128.098817	Stratum VII	unidentified plant material	UCIAMS-179712	2645±15	126	
Meay Channel I	51.659051, -128.098817	Stratum VII	charcoal	UCIAMS-163742	2605±20	126	
Meay Channel I	51.659051, -128.098817	Stratum VI	charcoal	UCIAMS-163743	2715±20	126	
Meay Channel I	51.659051, -128.098817	Stratum II	charcoal	UCIAMS-186383	720±15	126	excluded from models (see site description for further information)

Site name	Coordinates	Provenience	Sample material	Laboratory code	Date (BP or ka)	Source	Notes
Mesa	68.439857, -155.813683	"B"	hearth charcoal	DIC-1589	7620±95	36	
Mesa	68.439857, -155.813683	"B"	hearth charcoal	Beta-55286	11660±80	37	
Mesa	68.439857, -155.813683	"B"	hearth charcoal	Beta-57430/ CAMS-4147	11190±70	37	
Mesa	68.439857, -155.813683	"Saddle"	hearth charcoal	Beta-50429	10980±280	36	
Mesa	68.439857, -155.813683	"B"	hearth charcoal	Beta-55283/ CAMS-3569	10240±80	37	
Mesa	68.439857, -155.813683	"A"	hearth charcoal	Beta50428/ ETH-9086	10090±85	37	
Mesa	68.439857, -155.813683	"Saddle"	hearth charcoal	Beta-69898/ CAMS-11035	10070±60	36	
Mesa	68.439857, -155.813683	"B"	hearth charcoal	Beta-52606/ CAMS-2688	10060±70	37	
Mesa	68.439857, -155.813683	"B"	hearth charcoal	Beta-69900/ CAMS-11037	10050±90	36	
Mesa	68.439857, -155.813683	"B"	hearth charcoal	Beta-55285/ CAMS-3571	10000±80	37	
Mesa	68.439857, -155.813683	"B"	hearth charcoal	Beta-69899/ CAMS-11036	9900±80	36	
Mesa	68.439857, -155.813683	"Saddle"	hearth charcoal	Beta-55282/ CAMS-3568	9990±80	37	
Mesa	68.439857, -155.813683	"B"	hearth charcoal	Beta-57429/ CAMS-4146	9900±70	37	
Mesa	68.439857, -155.813683	"Saddle"	hearth charcoal	Beta-50430/ ETH-9087	9945±75	37	
Mesa	68.439857, -155.813683	"B"	hearth charcoal	Beta-55284/ CAMS-3570	9930±80	37	
Mesa	68.439857, -155.813683	"Saddle"	soil charcoal	Beta-36805/ ETH-6570	9730±80	37	
Mesa	68.439857, -155.813683	"B"	hearth charcoal	Beta-55284/ CAMS-3570	9930±80	37	
Moose Creek	64.066667, -149.100000	Component I/ lower paleosol complex/Nenana	hearth charcoal	Beta-96627	11190±60	41	
Moose Creek	64.066667, -149.100000	Transition between Component I and II (soil organics)	soil organics	GX-6281	11730±250	43	
Moose Creek	64.066667, -149.100000	Transition between Component I and II (soil organics)	soil organics	I-11227	10640±280	43	
Moose Creek	64.066667, -149.100000	Transition between Component I and II (soil organics)	soil organics	A-2144	8940±270	43	
Moose Creek	64.066667, -149.100000	Transition between Component I and II (soil organics)	soil organics	A-2168	8160±260	43	
Moose Creek	64.066667, -149.100000	Component II// Denali I	hearth charcoal	Beta-106040	10500±60	41	

Site name	Coordinates	Provenience	Sample material	Laboratory code	Date (BP or ka)	Source	Notes
Moose Creek	64.066667, -149.100000	Component III/ Denali II	hearth charcoal	Beta-106041	5680±50	41	
Murray Springs		Graveyard Member (F1)	charcoal (Fraxinus sp.)	SMU-18	11190±180	103	
Murray Springs	32.236196, -110.330801	Graveyard Member (F1)	charcoal	A-805	11150±450	103	
Murray Springs	32.236196, -110.330801	Graveyard Member (F1)	charcoal	Tx-1413	11080±180	103	
Murray Springs	32.236196, -110.330801	Graveyard Member (F1)	charcoal	Tx-1462	10930±170	103	
Murray Springs	32.236196, -110.330801	Graveyard Member (F1)	charcoal	SMU-27	10890±180	103	
Murray Springs	32.236196, -110.330801	Graveyard Member (F1)	charcoal	SMU-41	10840±70	103	
Murray Springs	32.236196, -110.330801	Graveyard Member (F1)	charcoal	SMU-42	10840±140	103	
Murray Springs	32.236196, -110.330801	Graveyard Member (F1)	charcoal	Tx-1459	10710±160	103	
Owl Ridge	64.0125, -149.556944	Stratum 2/ Component 1/ Square N88E110	charcoal (*Salix* sp.)	AA-86969	11060±60	46	
Owl Ridge	64.0125, -149.556944	Stratum 4/ Component 2/ Square N85E103	charcoal (*Salix* sp.)	UCIAMS-71261	10485±25	46	
Owl Ridge	64.0125, -149.556944	Stratum 4/ Component 2/ Square N85E103	charcoal (*Salix* sp.)	AA-86968	10440±60	46	
Owl Ridge	64.0125, -149.556944	Stratum 4/ Component 2/ Square N86E104	charcoal (*Salix* sp.)	AA-86964	10420±60	46	
Owl Ridge	64.0125, -149.556944	Stratum 4/ Component 2/ Square N86E103	charcoal (*Salix* sp.)	AA-86960	10415±60	46	
Owl Ridge	64.0125, -149.556944	Stratum 4/ Component 2/ Square N86E103	charcoal (*Salix* sp.)	AA-86962	10335±60	46	
Owl Ridge	64.0125, -149.556944	Stratum 4/ Component 2/ Square N86E103	charcoal (*Salix* sp.)	AA-86963	10340±75	46	
Owl Ridge	64.0125, -149.556944	Stratum 4/ Component 2/ Square N86E103	charcoal (*Salix* sp.)	AA-86961	10330±70	46	
Owl Ridge	64.0125, -149.556944	Stratum 4/ Component 2/ Square N86E104	charcoal (*Salix* sp.)	AA-86965	10295±60	46	
Owl Ridge	64.0125, -149.556944	Stratum 4/ Component 2/ Square N86E106	charcoal (*Salix* sp.)	AA-86966	10290±75	46	
Owl Ridge	64.0125, -149.556944	Stratum 4/ Component 2/ Square N88E105	charcoal (*Salix* sp.)	UCIAMS-71260	10125±20	46	
Owl Ridge	64.0125, -149.556944	Stratum 4/ Component 2/ Square N88E105	charcoal (*Salix* sp.)	AA-86967	10120±75	46	
Owl Ridge	64.0125, -149.556944	Stratum 4/ Component 2/ Square N88E108	charcoal (*Salix* sp.)	Beta-289378	10020±40	46	
Owl Ridge	64.0125, -149.556944	Stratum 4/ Component 2/ Square N95E98	charcoal (*Picea* sp.)	Beta-289382	80±40	46	

Site name	Coordinates	Provenience	Sample material	Laboratory code	Date (BP or ka)	Source	Notes
Owl Ridge	64.0125, -149.556944	Strata 6/5/4/ Component 3/2/ Square N83E105	charcoal (*Salix* sp.)	Beta-289377	10080±40	46	
Owl Ridge	64.0125, -149.556944	Strata 6/5/4/ Component 3/2/ Square N83E105	charcoal (*Salix* sp.)	Beta-289376	9550±40	46	
Owl Ridge	64.0125, -149.556944	Stratum 5/ Component 3/ Square N92E110	charcoal (*Salix* sp.)	Beta-330172	9880±40	46	
Owl Ridge	64.0125, -149.556944	Stratum 5/ Component 3/ Square N92E110	charcoal (*Salix* sp.)	Beta-289379	9790±40	46	
Page-Ladson	30.173805, -83.956282	Stratum 3a	wood (Taxonium distichum)	UCIAMS-141961	13080±40	171	
Page-Ladson	30.173805, -83.956282	Stratum 3a	wood (Taxonium distichum)	UCIAMS-141960	13945±50	171	
Page-Ladson	30.173805, -83.956282	Stratum 3a	twig (Taxonium distichum)	UCIAMS-141959	12615±35	171	
Page-Ladson	30.173805, -83.956282	Stratum 3a	twig (Taxonium distichum)	UCIAMS-141958	12495±35	171	
Page-Ladson	30.173805, -83.956282	Stratum 3c	twig (Quercus sp.)	UCIAMS-141957	12420±30	171	
Page-Ladson	30.173805, -83.956282	Stratum 3c	twig (Taxonium distichum)	UCIAMS-141956	12395±30	171	
Page-Ladson	30.173805, -83.956282	Stratum 3c	wood (Taxonium distichum)	UCIAMS-141955	13585±35	171	
Page-Ladson	30.173805, -83.956282	Stratum 3c	wood (Taxonium distichum)	UCIAMS-141954	13005±35	171	
Page-Ladson	30.173805, -83.956282	Stratum 3c	wood (Taxonium distichum)	UCIAMS-141953	14510±40	171	
Page-Ladson	30.173805, -83.956282	Stratum 3c	wood (Quercus-Leucobalanus group)	UCIAMS-141952	12385±35	171	
Page-Ladson	30.173805, -83.956282	Stratum 3c	wood (Quercus-Leucobalanus group)	UCIAMS-141951	12415±30	171	
Page-Ladson	30.173805, -83.956282	Stratum 3c	wood (Taxonium distichum)	UCIAMS-141950	13830±35	171	
Page-Ladson	30.173805, -83.956282	Stratum 3c	wood (Fraxinus sp.)	UCIAMS-127303	12495±30	171	
Page-Ladson	30.173805, -83.956282	Stratum 3c	bark (unknown peridem)	UCIAMS-127305	13015±30	171	
Page-Ladson	30.173805, -83.956282	Stratum 3c	wood (Abies)	UCIAMS-127304	12420±30	171	
Page-Ladson	30.173805, -83.956282	Stratum 3c	wood (Acer)	UCIAMS-127302	12425±30	171	
Page-Ladson	30.173805, -83.956282	Stratum 3c	twig (Quercus sp.)	UCIAMS-141949	12385±35	171	

Site name	Coordinates	Provenience	Sample material	Laboratory code	Date (BP or ka)	Source	Notes
Page-Ladson	30.173805, -83.956282	Stratum 3c	wood (Fraxinus sp.)	UCIAMS-141948	12430±30	171	
Page-Ladson	30.173805, -83.956282	Stratum 3c	wood (Taxonium distichum)	UCIAMS-141947	13440±40	171	
Page-Ladson	30.173805, -83.956282	Stratum 3c	twig (Fraxinus sp.)	UCIAMS-141946	12400±35	171	
Page-Ladson	30.173805, -83.956282	Stratum 3c	twig (Taxonium distichum)	UCIAMS-141945	12400±35	171	
Page-Ladson	30.173805, -83.956282	Stratum 3c	twig (Taxonium distichum)	UCIAMS-141944	12410±35	171	
Page-Ladson	30.173805, -83.956282	Stratum 3c	twig (Quercus sp.)	UCIAMS-141943	12410±30	171	
Page-Ladson	30.173805, -83.956282	Stratum 3c	twig (unidentified hardwood)	UCIAMS-141942	12440±30	171	
Page-Ladson	30.173805, -83.956282	Stratum 3c	twig (unidentified hardwood)	UCIAMS-141941	12365±30	171	
Page-Ladson	30.173805, -83.956282	Stratum 3c	twig (Fraxinus sp.)	UCIAMS-141940	12430±30	171	
Page-Ladson	30.173805, -83.956282	Stratum 3c	twig (unidentified hardwood)	UCIAMS-141939	12430±35	171	
Page-Ladson	30.173805, -83.956282	Stratum 4a	wood (unidentified hardwood)	UCIAMS-141938	12440±30	171	
Page-Ladson	30.173805, -83.956282	Stratum 4b	wood (Morus rubra)	UCIAMS-141937	12380±35	171	
Page-Ladson	30.173805, -83.956282	Stratum 4b	twig (unidentified hardwood)	UCIAMS-141935	12250±35	171	
Page-Ladson	30.173805, -83.956282	Stratum 4b	wood (Fagus grandifolia)	UCIAMS-141934	12365±30	171	
Page-Ladson	30.173805, -83.956282	Stratum 4b	wood (Taxonium distichum)	UCIAMS-141933	12295±35	171	
Page-Ladson	30.173805, -83.956282	Stratum 4b	twig (Carya sp.)	UCIAMS-141932	12310±30	171	
Page-Ladson	30.173805, -83.956282	Stratum 4b	wood (Fagus grandifolia)	UCIAMS-141931	12275±30	171	
Page-Ladson	30.173805, -83.956282	Stratum 4b	twig (Carya sp. aquatic)	UCIAMS-141930	12370±30	171	
Page-Ladson	30.173805, -83.956282	Stratum 4b	twig (unidentified hardwood, ring-porous)	UCIAMS-141929	12270±30	171	
Page-Ladson	30.173805, -83.956282	Stratum 4b	twig (unidentified hardwood, diffuse-porous)	UCIAMS-141928	12335±35	171	
Page-Ladson	30.173805, -83.956282	Stratum 4b	twig (unidentified hardwood)	UCIAMS-153343	12260±35	171	

Site name	Coordinates	Provenience	Sample material	Laboratory code	Date (BP or ka)	Source	Notes
Paisley Caves	42.776636, -120.667361	Cave 5, LU 1b, excavation unit 5/5D	human coprolite (1961-P-5/5D-31)	Beta-213424 4	12400±60	175	
Paisley Caves	42.776636, -120.667361	Cave 5, LU 1b, excavation unit 5/5D	human coprolite (1961-P-5/5D-31)	OxA-16498	12275±55	175	
Paisley Caves	42.776636, -120.667361	Cave 5, LU 1b, excavation unit 5/7C	human coprolite (1294-PC-5/7C-31)	OxA-16497	12345±55	175	
Paisley Caves	42.776636, -120.667361	Cave 5, LU 1b, excavation unit 5/7C	human coprolite (1294-PC-5/7C-31)	Beta-213426 3	12290±60	175	
Paisley Caves	42.776636, -120.667361	Cave 5, LU 1a or b, excavation unit 5/6B	human coprolite (1294-PC-5/6B-50)	Beta-216474 2	12260±60	175	
Paisley Caves	42.776636, -120.667361	Cave 5, LU 1a or b, excavation unit 5/6B	human coprolite (1294-PC-5/6B-50)	OxA-16495	12140±70	175	
Paisley Caves	42.776636, -120.667361	Cave 5, Profile III, LU 1; excavation unit 5/16A	Artemisa twig (geo stratigraphic)	UCIAMS-8 0384	12410±25	9	
Paisley Caves	42.776636, -120.667361	Cave 5, Profile III, LU 1; excavation unit 5/16A	Artemisa twig (geo stratigraphic)	UCIAMS-8 0377	12405±25	9	
Paisley Caves	42.776636, -120.667361	Cave 5, Profile III, LU 2; ; excavation unit 5/16A	Ericacaea twig (geo stratigraphic; 2010PC-224)	UCIAMS-8 0381	11500±30	9	entered as "Unit 2 (lower)" in the model
Paisley Caves	42.776636, -120.667361	Cave 5, Profile III, LU 2; ; excavation unit 5/16A	Camelid coprolite (water soluble)	UCIAMS-9 0586	11315±25	9	entered as "Unit 2 (lower)" in the model
Paisley Caves	42.776636, -120.667361	Cave 5, Profile III, LU 2; ; excavation unit 5/16A	Human coprolite (water soluble)	UCIAMS-9 0584	11250±25	9	entered as "Unit 2 (lower)" in the model
Paisley Caves	42.776636, -120.667361	Cave 5, Profile III, LU 2; ; excavation unit 5/16A	Human coprolite (macro)	UCIAMS-9 0583	11205±25	9	entered as "Unit 2 (lower)" in the model
Paisley Caves	42.776636, -120.667361	Cave 5, Profile III, LU 2, excavation unit 5/16A	Artemisa twig (water soluble proteins; 2010PC-223)	UCIAMS-8 0379	11295±25	9	entered as "ISL" in the model
Paisley Caves	42.776636, -120.667361	Cave 5, Profile III, LU 2, excavation unit 5/16A	Artemisa twig (water soluble salts; 2010PC-223)	UCIAMS-8 0380	11165±25	9	entered as "ISL" in the model
Paisley Caves	42.776636, -120.667361	Cave 5, Profile III, LU 2, excavation unit 5/16A	Artemisa twig (2010PC-223)	UCIAMS-8 0378	11070±25	9	entered as "ISL" in the model

Site name	Coordinates	Provenience	Sample material	Laboratory code	Date (BP or ka)	Source	Notes
Paisley Caves	42.776636, -120.667361	Cave 5, Profile III, LU 2, excavation unit 5/18A	Unidentified macroflora in sediment	UCIAMS-98932	10855±30	9	entered as "Unit 2 (upper)" in the model
Schaefer	42.643, -88.010	Paleoindian	mammoth bone (XAD)	CAMS-30171	12310±60	153	
Schaefer	42.643, -88.010	Paleoindian	mammoth bone (XAD)	CAMS-61135	12320±50	151	
Schaefer	42.643, -88.010	Paleoindian	mammoth bone (XAD)	CAMS-61143	12390±40	151	
Shawnee Minisink	40.995474, -75.13735	hearth 2 (feature 9), sq. 4/4E (2006 excavations)	charred hawthorne seeds	OxA-17371	10970±50	114	incorrectly noted as "OxA-1731" in Gingerich , 2007, 2013
Shawnee Minisink	40.995474, -75.13735	hearth 1 (feature 12), sq. 4/4E (2006 excavations)	hearth charcoal	UCIAMS-24866	11020±30	5	
Shawnee Minisink	40.995474, -75.13735	hearth 1 (feature 12), sq. 4/4E (2006 excavations)	hearth charcoal	UCIAMS-24865	10915±25	5	
Shawnee Minisink	40.995474, -75.13735	hearth 1 (feature 12), sq. 4/4E (2006 excavations)	hearth charcoal	Beta-203865	10820±50	114	
Shawnee Minisink	40.995474, -75.13735	Zone 4 (1972 excavations)	hearth charcoal	Beta-127162	10900±40	114	
Shawnee Minisink	40.995474, -75.13735	Zone 4 (1972 excavations)	hearth charcoal	Beta-101935	10940±90	114	
Shawnee Minisink	40.995474, -75.13735	Zone 4 (1974 excavations)	charcoal (humates)	W-3391	11050±1000	110	
Shawnee Minisink	40.995474, -75.13735	Zone 4 (1974 excavations)	charcoal	W-3388	9310±1000	110	
Shawnee Minisink	40.995474, -75.13735	Zone 4 (1974 excavations)	hearth charcoal	W-3134	10750±600	110	
Shawnee Minisink	40.995474, -75.13735	Zone 4 (1972 excavations)	hearth charcoal	W-2994	10590±300	110	
Sheriden Cave	40.945194, -83.346083	Unit 5a	dentin collagen (C. scotti)	Beta-127908b	12840±100	118	
Sheriden Cave	40.945194, -83.346083	Unit 5a	dentin collagen (C. scotti)	AA-127908a	12590±450	118	
Sheriden Cave	40.945194, -83.346083	Unit 5a	dentin collagen (C. scotti)	AA-127907	12520±170	118	
Sheriden Cave	40.945194, -83.346083	Unit 5a	bone collagen (M.nasutus)	Beta-139687	11860±40	118	
Sheriden Cave	40.945194, -83.346083	Unit 5a	bone collagen (A. simus)	CAMS-12837	11480±60	119	
Sheriden Cave	40.945194, -83.346083	Unit 5a	bone collagen (A. simus)	CAMS-12839	11570±70	118	
Sheriden Cave	40.945194, -83.346083	Unit 5a	bone collagen (A. simus)	CAMS-33968	11570±50	119	
Sheriden Cave	40.945194, -83.346083	Unit 5a	bone collagen (A. simus)	CAMS-12845	11610±90	119	
Sheriden Cave	40.945194, -83.346083	Unit 5a	wood charcoal	Beta-127909	10840±80	118	

Site name	Coordinates	Provenience	Sample material	Laboratory code	Date (BP or ka)	Source	Notes
Sheriden Cave	40.945194, -83.346083	Unit 5a	wood charcoal	Beta-127910	10960±60	118	
Sheriden Cave	40.945194, -83.346083	Unit 5a	bone point (XAD)	UCIAMS-38249	10915±30	117	
Sheriden Cave	40.945194, -83.346083	Unit 5b	wood charcoal	AA-21711	13210±80	118	
Sheriden Cave	40.945194, -83.346083	Unit 5b	wood charcoal	PITT-0982	11710±220	119	
Sheriden Cave	40.945194, -83.346083	Unit 5b	bone collagen (P. compressus)	CAMS-33970	11130±60	118	
Sheriden Cave	40.945194, -83.346083	Unit 5b	bone collagen (P. compressus)	CAMS-10349	11060±60	119	
Sheriden Cave	40.945194, -83.346083	Unit 5b	wood charcoal	AA-21712	10470±70	118	
Sheriden Cave	40.945194, -83.346083	Unit 5c	wood charcoal	Beta-117607	10970±70	118	
Sheriden Cave	40.945194, -83.346083	Unit 5c	wood charcoal	Beta-117601	10940±70	118	
Sheriden Cave	40.945194, -83.346083	Unit 5c	bone collagen (C. ohioensis)	CAMS-26783	10850±60	118	
Sheriden Cave	40.945194, -83.346083	Unit 5c	wood charcoal	Beta-117602	10850±70	118	
Sheriden Cave	40.945194, -83.346083	Unit 5c	wood charcoal	AA-21710	10680±80	118	
Sheriden Cave	40.945194, -83.346083	Unit 5c	wood charcoal	Beta-117606	10620±70	118	
Sheriden Cave	40.945194, -83.346083	Unit 5c	wood charcoal	Beta-117603	10600±60	118	
Sheriden Cave	40.945194, -83.346083	Unit 5c	wood charcoal	Beta-117605	10570±70	118	
Sheriden Cave	40.945194, -83.346083	Unit 5c	wood charcoal	Beta-117604	10550±70	118	
Sheriden Cave	40.945194, -83.346083	Unit 5c	bone collagen (R. tarandus)	Beta-139686	10440±40	118	
Sheriden Cave	40.945194, -83.346083	Unit 6	wood charcoal	AA-21706	10020±115	118	
Sheriden Cave	40.945194, -83.346083	Unit 6	wood charcoal	AA-21705	9775±70	118	
Sheriden Cave	40.945194, -83.346083	Unit 6	wood charcoal	CAMS-24127	9190±60	119	
Sheriden Cave	40.945194, -83.346083	Unit 6	wood charcoal	CAMS-24126	9170±60	119	
Swan Point	63.300000, -146.033333	CZ4b	mammoth ivory tusk collagen	NSRL-2001/CAMS-17045	12060±70	50	
Swan Point	63.300000, -146.033333	CZ4b	mammoth ivory tusk collagen	AA-98488	12500±150	17	
Swan Point	63.300000, -146.033333	CZ4b	mammoth ivory tusk collagen	Beta-365062	12170±50	49	
Swan Point	63.300000, -146.033333	CZ4b	mammoth molar collagen	AA-74250	12110±120	49	

Site name	Coordinates	Provenience	Sample material	Laboratory code	Date (BP or ka)	Source	Notes
Swan Point	63.300000, -146.033333	CZ4b	hearth charcoal (Populus/ Salix)	Beta-209882	12290±40	49	
Swan Point	63.300000, -146.033333	CZ4b	residue (carbonized fat/grease)	Beta-209884	12220±40	49	
Swan Point	63.300000, -146.033333	CZ4b	residue (carbonized fat/grease)	Beta-209883	12100±40	49	
Swan Point	63.300000, -146.033333	CZ4b	mammoth ivory tusk collagen	AA-74251	12050±120	49	
Swan Point	63.300000, -146.033333	CZ4b	horse molar collagen	AA-74249	11950±100	49	
Swan Point	63.300000, -146.033333	CZ4b	residue (carbonized fat/grease)	Beta-170457	12360±60	49	
Swan Point	63.300000, -146.033333	CZ4b	hearth charcoal (Populus/ Salix)	Beta-QA-619	12040±40	49	
Swan Point	63.300000, -146.033333	CZ4b	residue (carbonized fat/grease)	Beta-175491	12110±50	49	
Swan Point	63.300000, -146.033333	CZ4b	artifact residue	AA-19322	11770±140	49	
Swan Point	63.300000, -146.033333	CZ4b	charcoal (Salix sp.)	Beta-71372/ CAMS-12389	11660±60	50	
Swan Point	63.300000, -146.033333	CZ4b	charcoal (Populus/ Salix)	Beta-56667/ CAMS-4252	11660±70	50	
Swan Point	63.300000, -146.033333	CZ4a	burned bone collagen	Beta-175489 (KOH)	11360±50	47	
Swan Point	63.300000, -146.033333	CZ4a	hearth	Beta-355852	11350±50	47	
Swan Point	63.300000, -146.033333	CZ3b	Populus/Salix from hearth with burnt bone	Beta-401126	10620±40	47	
Swan Point	63.300000, -146.033333	CZ3b	hearth charcoal	Beta-209885	10570±40	48	
Swan Point	63.300000, -146.033333	CZ3b	charcoal	Beta-56666/ CAMS-4251	10230±80	50	
Swan Point	63.300000, -146.033333	CZ3a	hearth bulk sample	Beta-355867	10160±50	47	
Swan Point	63.300000, -146.033333	CZ3a	hearth stain	Beta-357816	10070±40	47	
Swan Point	63.300000, -146.033333	CZ3a	hearth charcoal	Beta-170458	10050±60	48	
Swan Point	63.300000, -146.033333	CZ3a	hearth charcoal	Beta-190578	10010±90	48	
Swan Point	63.300000, -146.033333	CZ2	charcoal	WSU-4426	7400±80	48	
Swan Point	63.300000, -146.033333	CZ2	charcoal	Beta-209886	6610±40	48	
Swan Point	63.300000, -146.033333	CZ1b	cf. Larix from hearth?/ reddish stain	Beta-401125	4480±30	47	

Site name	Coordinates	Provenience	Sample material	Laboratory code	Date (BP or ka)	Source	Notes
Swan Point	63.300000, -146.033333	CZ1b	hearth charcoal	Beta-190580	4260±40	48	
Swan Point	63.300000, -146.033333	CZ1b	Picea assoc. w/calcined bone	Beta-401124	3060±30	47	
Swan Point	63.300000, -146.033333	CZ1a	charcoal from hearth?/fcr	Beta-401123	1860±30	47	
Swan Point	63.300000, -146.033333	CZ1a	charcoal/resin	WSU-4521	1750±80	50	
Swan Point	63.300000, -146.033333	CZ1a	charcoal	WSU-4522	1670±60	50	
Swan Point	63.300000, -146.033333	CZ1a	charcoal (Picea sp.)	WSU-4524	1570±70	50	
Swan Point	63.300000, -146.033333	CZ1a	charcoal (Betula sp.)	WSU-4523	1220±70	50	
Swan Point	63.300000, -146.033333	CZ1a	hearth charcoal	Beta-223302	860±40	48	
Swan Point	63.300000, -146.033333	CZ1a	hearth bulk sample	Beta-340993	810±30	47	
Ushki	56.206208, 159.994846	Below Component 7	charcoal	AA-45718	11820±100	53	
Ushki	56.206208, 159.994846	Below Component 7	charcoal	AA-45712	11200±160	53	
Ushki	56.206208, 159.994846	Below Component 7	charcoal	AA-45711	11870±90	53	
Ushki	56.206208, 159.994846	Component 7	charcoal	AA-45716	11050±75	53	
Ushki	56.206208, 159.994846	Component 7	charcoal	AA-45710	10675±75	53	
Ushki	56.206208, 159.994846	Component 7	charcoal	AA-45708	10810±75	53	
Ushki	56.206208, 159.994846	Component 7	charcoal	AA-45709	10850±320	53	
Ushki	56.206208, 159.994846	Component 7	charcoal	SR-5810/ CAMS-74639	11330±50	53	
Ushki	56.206208, 159.994846	Component 7	charcoal	AA-1388	11005±115	53	
Ushki	56.206208, 159.994846	Component 7	humates	AA-41389	11050±75	53	
Ushki	56.206208, 159.994846	Component 6	charcoal	AA-45720	10230±70	53	
Ushki	56.206208, 159.994846	Component 6	charcoal	AA-45719	10385±90	53	
Ushki	56.206208, 159.994846	Component 6	charcoal	AA-45717	11130±100	53	
Ushki	56.206208, 159.994846	Component 6	charcoal	AA-45713	10040±130	53	
Ushki	56.206208, 159.994846	Component 6	charcoal	AA-45715	10160±75	53	
Ushki	56.206208, 159.994846	Component 6	charcoal	AA-45714	10800±175	53	
Ushki	56.206208, 159.994846	Component 6	charcoal	SR-5811/ CAMS-74640	10460±80	53	
Ushki	56.206208, 159.994846	Component 6	charcoal	AA-41386	10240±75	53	
Ushki	56.206208, 159.994846	Component 6	humates	AA-41387	9485±275	53	

Site name	Coordinates	Provenience	Sample material	Laboratory code	Date (BP or ka)	Source	Notes
Walker Road	63.966667, -149.083333	Loess 1 & 2	hearth charcoal	Beta-11254	11820±200	54	
Walker Road	63.966667, -149.083333	Loess 1 & 2	hearth charcoal	AA-2264	11300±120	54	
Walker Road	63.966667, -149.083333	Loess 1 & 2	hearth charcoal	AA-1681	11170±180	54	
Walker Road	63.966667, -149.083333	Loess 1 & 2	hearth charcoal	AA-1683	11010±230	54	
Walker Road	63.966667, -149.083333	Loess 4	charcoal	AA-1692	8720±250	54	
Walker Road	63.966667, -149.083333	Loess 5	charcoal	GX-12875	4415±95	54	
Walker Road	63.966667, -149.083333	Loess 5	charcoal	AA-1693	3816±79	54	
Wally's Beach	49.381404, -114.077366	aeolian sand	camel bone (cat. no. 3610.1; XAD)	UCIAMS-116400	11465±40	134	
Wally's Beach	49.381404, -114.077366	aeolian sand	camel bone (cat. no. 3610.1; XAD)	UCIAMS-127347	11425±30	134	
Wally's Beach	49.381404, -114.077366	aeolian sand	camel bone (cat. no. 3610.1; HYP)	OxA-X-2736-8	11530±50	88	
Wally's Beach	49.381404, -114.077366	aeolian sand	horse bone (1; cat no. 3594; XAD)	UCIAMS-127348	11470±35	134	
Wally's Beach	49.381404, -114.077366	aeolian sand	horse bone (2; cat no. 2988.1; XAD)	UCIAMS-127349	11410±30	134	
Wally's Beach	49.381404, -114.077366	aeolian sand	horse bone (3; cat no. 944; XAD)	UCIAMS-127350	11460±30	134	
Wally's Beach	49.381404, -114.077366	aeolian sand	horse bone (A; cat no. 315; XAD)	UCIAMS-127351	11440±30	134	
Wally's Beach	49.381404, -114.077366	aeolian sand	horse bone (A; cat no. 315; XAD)	OxA-X-2736-10	11445±55	88	
Wally's Beach	49.381404, -114.077366	aeolian sand	horse bone (B; cat. no. 164 XAD)	UCIAMS-127352	11475±30	134	
Wally's Beach	49.381404, -114.077366	aeolian sand	horse bone (C; cat. no 683; XAD)	UCIAMS-127353	11440±30	134	
Wally's Beach	49.381404, -114.077366	aeolian sand	horse bone (D, cat. no 77.1; XAD)	UCIAMS-127354	11430±30	134	
Wally's Beach	49.381404, -114.077366	aeolian sand	muskox bone (cat no. 3293.1; XAD)	UCIAMS-127373	11320±30	134	
Wally's Beach	49.381404, -114.077366	aeolian sand	muskox bone (cat no. 3293.1; HYP)	OxA-X-2736-9	11255±50	88	

Table S2. Age estimates obtained for archaeological components analysed, at 95.4% and 68.2% confidence or credible intervals (CI). These are represented by start Boundaries, Date functions, or calibrated dates. For more information on each site, see Supplementary Information, section 2.

Tradition or temporal category	**Archaeological site**	**Type of age estimate**	**cal BP (68.2% CI)**	**cal BP (95.4% CI)**
Beringian tradition	Berelekh	start Boundary	14190-13970	14315-13835
	Broken Mammoth	start Boundary	13615-13305	14130-13255
	Dry Creek	start Boundary	13525-13405	13700-13350
	Mead	start Boundary	13425-13310	13520-13010
	Mesa	Date within a Phase	13145-11135	13910-9355
	Moose Creek	start Boundary	13735-12980	15195-12865
	Owl Ridge	start Boundary	1338512820	14315-12745
	Swan Point	start Boundary	14430-14205	14650-14150
	Ushki	start Boundary	13290-13095	13435-12855
	Walker Road	start Boundary	13950-13220	14950-13075
Clovis	Anzick	Date within a Phase	12880-12710	13175-12485
	Aubrey	start Boundary	13760-13330	14750-13245
	Blackwater Locality No.1	start Boundary	13285-12855	13440-12675
	Cactus Hill	start Boundary	13140-12320	13605-11390
	Colby	Date within a Phase	12835-12650	13165-12350
	Debra L. Friedkin	start Boundary	14370-13515	14755-13120
	Dent	Date within a Phase	13125-12815	13545-12415
	Domebo	calibrated date (R_Date)	12825-12740	12910-12710
	El Fin del Mundo	start Boundary	14070-13705	14135-13470
	Gault	start Boundary	15180-13110	16895-12705
	Jake Bluff	Date within a Phase	12735-12690	12775-12645
	Lange/Ferguson	Date within a Phase	13270-12355	14285-11105
	Lehner	Date within a Phase	13130-12654	13579-9390
	Murray Springs	Date within a Phase	12840-12700	13015-12615
	Shawnee-Minisink	Date within a Phase	12805-12720	12910-12650

Tradition or temporal category	Archaeological site	Type of age estimate	cal BP (68.2% CI)	cal BP (95.4% CI)
	Sheriden Cave	start `Boundary`	14075-13595	14850-13395
Clovis-coeval	Arlington Springs	calibrated date (`R_Date`)	12915-12730	13015-12705
	Meay Channel I	start `Boundary`	13425-13255	13825-13205
	Lubbock Lake	start `Boundary`	13205-12860	13790-12765
	Wally's Beach	`Date` within a `Phase`	13305-13265	13340-13220
pre-Clovis	Bluefish Caves	calibrated date (`R_Date`)	23860-23505	24035-23310
	Cactus Hill	start `Boundary`	20470-19775	20585-18970
	Chiquihuite Cave (SC-C)	start `Boundary`	32000-31490	33150-31405
	Chiquihuite Cave (SC-B)	start `Boundary`	16440-15680	16605-15615
	Cooper's Ferry	start `Boundary`	16020-15445	16560-15285
	Debra L. Friedkin	start `Boundary`	15920-15060	16330-14690
	Gault	start `Boundary`	22835-18815	26435-17385
	Hebior	`Date` within a `Phase`	15055-14640	15615-13975
	Lindsay	`Date` within a `Phase`	14325-14130	14625-13945
	Manis	`Date` within a `Phase`	13820-13725	13795-13600
	Meadowcroft Rockshelter	start `Boundary`	22740-19485	24335-18620
	Page-Ladson	start `Boundary`	14655-14510	14710-14450
	Paisley Caves	`Date` within a `Phase`	14335-14105	14755-13780
	Schaefer	`Date within a Phase`	14495-14145	15020-13710
Western Stemmed tradition	Bonneville Estates	start `Boundary`	12715-12635	12760-12605
	Buhl	calibrated date (`R_Date`)	12705-12560	12740-12420
	Cooper's Ferry	calibrated date (`R_Date`)	13555-13385	13610-13275
	Paisley Caves	start `Boundary`	13090-13045	13110-13015

4. Archaeological sites excluded

4.1. Cerutti Mastodon site, San Diego (U.S.A.)

The Cerutti Mastodon site is reported as a 130,000 year-old archaeological site containing hammerstones and stone anvils, associated with the remains of a single mastodon[188]. The cultural aspect of the site and the methodology applied in the study have been questioned and criticised, however[189–194]. As such, pending future research, the site was excluded.

4.2. El Pit I, Quintana Roo (Mexico)

The El Pit I individual was found in a submerged sinkhole and directly dated to 11,332±64 BP (KIA-43524)[195]. Given the depositional environment and fraction dated (bone apatite; see reference 196), this measurement is likely a minimum-age estimate. As such, this individual and site was excluded from the analysis pending future chronometric work.

4.3. Healy Lake, Alaska (U.S.A.)

Healy Lake Village is a stratified site containing three Cultural Stages—Chindadn (earliest), Transitional and Athapaskan—within ten stratigraphic levels[197]. The chronological dataset for Healy Lake is highly incongruent[197]. As such, the site was excluded.

4.4. La Prele, Wyoming (U.S.A.)

In 1986, the La Prele Mammoth locality (formerly known as Hinrichs or Fetterman) produced the remains of a mammoth and a small lithic assemblage. The association between the two, however, was deemed equivocal[198]. In 2014, the site was re-excavated and the discovery of new cultural material reported[199]. Given that the results of the most current efforts have yet to be published, La Prele was excluded from this analysis.

4.5. Miami, Texas (U.S.A.)

Miami (41RB1) is a Clovis, mammoth-butchering site with associated lithic tool technology[200]. There no direct bone dates for the site. Instead, the bone bed (loess layer), dated to 11,415±125 BP (AA-7086), is bracketed by four sediment dates (obtained from two separate samples) from under- and over-lying deposits. Considering that the limited number of dates do not warrant a model and the cultural event itself is not directly dated, this site was excluded.

4.6. Naharon individual, Quintana Roo (Mexico)

The Naharon individual, known as 'Naharon Woman', was found in a submerged sinkhole and directly dated to 11,670 ± 60 BP (UCR-4000A/CAMS-87301; total amino acid fraction)[195,201]. This measurement is regarded as problematic and preliminary, however, since biochemical examination of the bone determined organic carbon content to be extremely low[201]. As such, this site was excluded from the analysis pending future chronometric work.

4.7. Paleo Crossing, Ohio (U.S.A.)

Paleo Crossing (33ME274) is stratified site containing Clovis, Archaic, Woodland, and Late Prehistoric material[202–213]. Within the Clovis (lithic) assemblage layer, charcoal and organic fragments extracted from a cylindrical pit (containing a Clovis point base) and post molds were dated. The resulting dataset was conflicting, however, with ages ranging from 9,230±80 BP (AA-8252; above a cylindrical pit) to 13,100±100 BP (AA-8251; inside the cylindrical pit). Later efforts at dating two burned Clovis stone tools using luminescence methods resulted in a weighted average of 9.1±1.8 ka[213]. Considering that archaeological and chronometric investigations at the site are ongoing[213], this site was excluded.

4.8. Topper, South Carolina (U.S.A.)

Topper (38AL23) is a stratified site reported to contain a pre-Clovis and Clovis assemblage. Given that the human origin of the pre-Clovis component is equivocal[214], this site was excluded.

5. Sensitivity testing and `Difference` query results

To determine the reproducibility of the of Clovis and Beringian tradition models presented in the main text (models 'A'; Extended Data Figs. 1 and 3), Clovis and Beringian tradition models were run using start boundaries, instead of `Date` functions, for all single-phase, site-specific models (models 'B'; where applicable; Figs. 38-39). To test whether this led to significant variations between models A and B, we used the `Difference` query within OxCal[215] on the start boundaries for each tradition (Fig. S40). Given that these overlap zero at 95.4% probability, the use of `Date` functions in models A had no significant impact on the modelled output. In other words, different approaches to site-specific model building (priors) had negligible impact on the output of tradition-level models (posteriors).

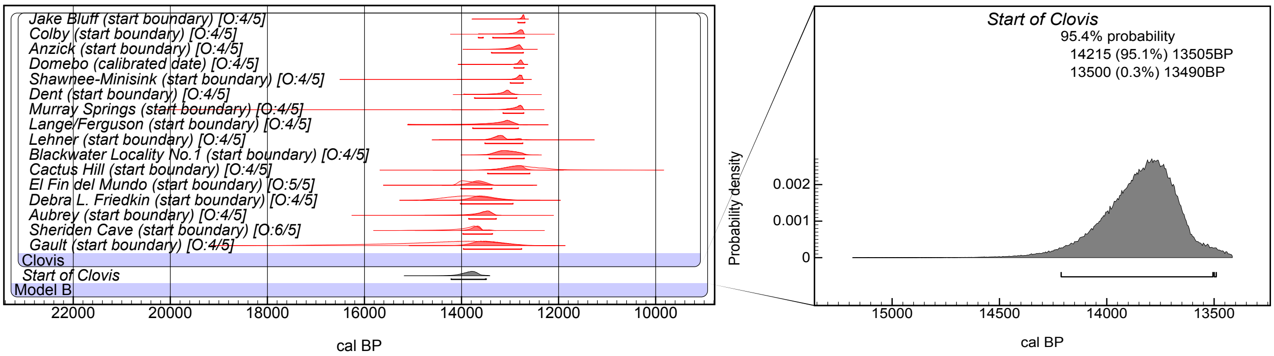

Fig. S38. Bayesian age model B for the start of Clovis (using start boundaries). Outlier analysis output is noted as 'O:posterior probability/prior probability'.

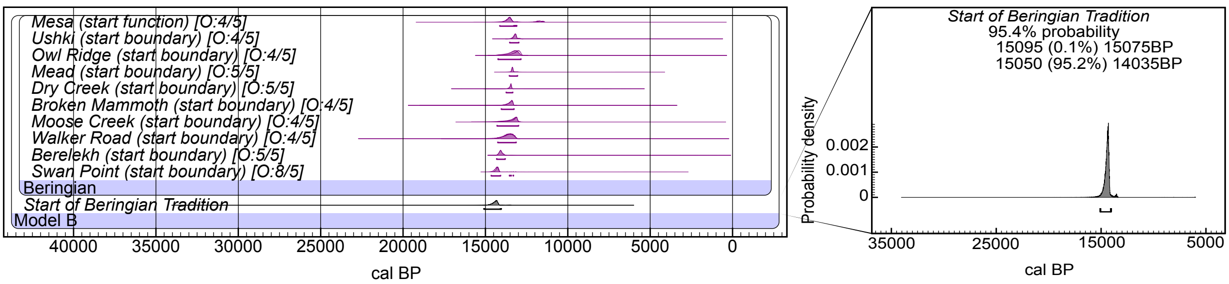

Fig. S39. Bayesian age model B for the start of the Beringian tradition (using start boundaries). Outlier analysis output is noted as 'O:posterior probability/prior probability'.

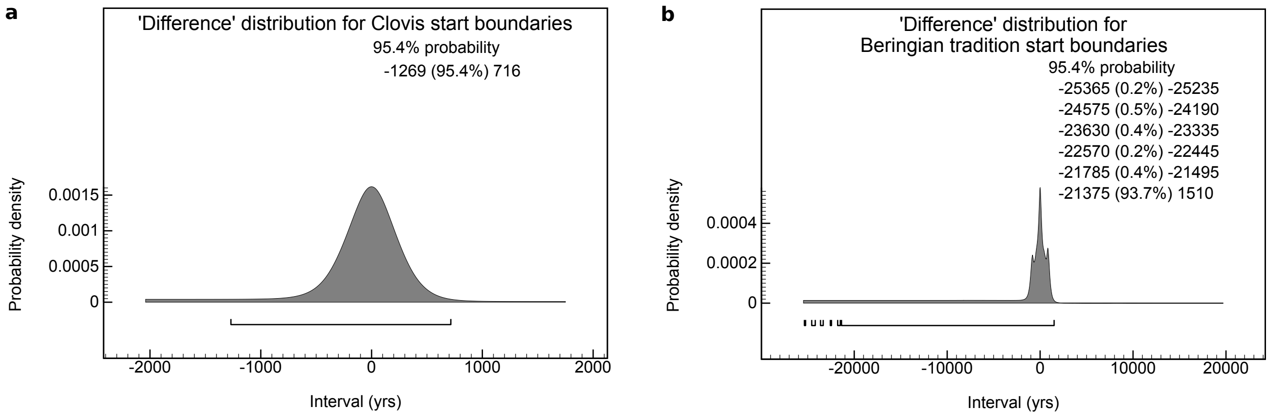

Fig. S40. **a**. Probability density function (PDF) for the difference between the start of Clovis in model A (Extended Data Fig. 3), compared with that of model B (Fig. S38). **b**. PDF for the difference between the start of Beringian tradition in model A (Extended Data Fig. 1), compared with that of model B (Fig. S39). These results suggest that there is no significant difference between the modelled outputs, as the distributions overlap zero at 95.4% probability.

In the main text, we note that the start dates of the Beringian, Western Stemmed and Clovis traditions are statistically indistinguishable. This is based on the result of a `Difference` query, which shows that all three overlap zero at 95.4% (Fig. S41).

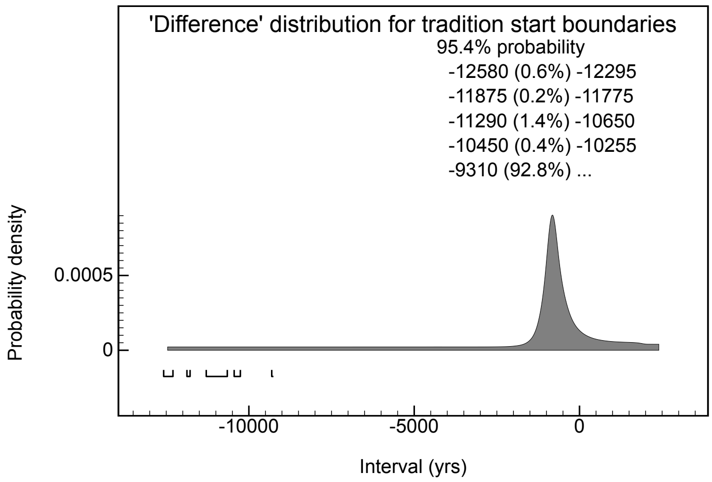

Fig. S41. Probability density function for the difference between the start of Beringian, Western Stemmed and Clovis traditions (Extended Data Figs. 1-3). These results suggest that there is no significant difference between the modelled outputs, as the distributions overlap zero at 95.4% probability.

References

1. Smallwood, A. M. & Jennings, T. A. *Clovis: On the Edge of a New Understanding*. (Texas A&M University Press, 2014).
2. Haynes, C. V., Jr. Fluted Projectile Points: Their Age and Dispersion: Stratigraphically controlled radiocarbon dating provides new evidence on peopling of the New World. *Science* **145**, 1408–1413 (1964).
3. Haynes, G. *The Early Settlement of North America: The Clovis Era*. (Cambridge University Press, 2002).
4. Stanford, D., Bonnichsen, R., Meggers, B. & Steele, D. G. Paleoamerican origins: Models, evidence, and future directions. *Paleoamerican Origins: Beyond Clovis* 313–353 (2005).

5. Waters, M. R. & Stafford, T. W., Jr. Redefining the age of Clovis: implications for the peopling of the Americas. *Science* **315**, 1122–1126 (2007).
6. Howard, C. D. The Clovis Point: Characteristics and Type Description. *Plains Anthropol.* **35**, 255–262 (1990).
7. Goebel, T. Clovis culture update. *Clovis: On the edge of a new understanding* 325–352 (2015).
8. Goebel, T. & Keene, J. L. Are Great Basin stemmed points as old as Clovis in the Intermountain West? A review of the geochronological evidence. *Archaeology in the Great Basin and Southwest: Papers in Honor of Don D. Fowler* 35–60 (2014).
9. Jenkins, D. L. *et al.* Clovis age Western Stemmed projectile points and human coprolites at the Paisley Caves. *Science* **337**, 223–228 (2012).
10. Bryan, A. L. The stemmed point tradition: An early technological tradition in western North America. *Anthropological Papers in Memory of Earl H. Swanson, Jr* 77–107 (1980).
11. Beck, C. & Jones, G. T. Clovis and Western Stemmed: Population Migration and the Meeting of Two Technologies in the Intermountain West. *Am. Antiq.* **75**, 81–116 (2010).
12. Davis, L. G., Nyers, A. J. & Willis, S. C. Context, Provenance and Technology of a Western Stemmed Tradition Artifact Cache from the Cooper's Ferry Site, Idaho. *Am. Antiq.* **79**, 596–615 (2014).
13. Davis, L. G. *et al.* Late Upper Paleolithic occupation at Cooper's Ferry, Idaho, USA, ~16,000 years ago. *Science* **365**, 891–897 (2019).
14. Graf, K. E. & Buvit, I. Human Dispersal from Siberia to Beringia: Assessing a Beringian Standstill in Light of the Archaeological Evidence. *Curr. Anthropol.* **58**, S583–S603 (2017).
15. Agenbroad, L. D. *et al. American Beginnings: The Prehistory and Palaeoecology of Beringia*. (University of Chicago Press, 1996).
16. Holmes, C. E. Tanana River Valley Archaeology circa 14,000 to 9000 B.P. *Arctic Anthropol.* **38**, 154–170 (2001).
17. Potter, B. A., Holmes, C. E. & Yesner, D. R. Technology and economy among the earliest prehistoric foragers in interior eastern Beringia. in *Paleoamerican Odyssey* (eds. Graf, K. E., Ketron, C. V. & Waters, M. R.) 81–103 (Center for the Study of the First Americans, Texas A&M University College Station, 2014).
18. Pitulko, V. V. The Berelekh quest: A review of forty years of research in the mammoth graveyard in northeast Siberia. *Geoarchaeology* **26**, 5–32 (2011).
19. Pitulko, V. V., Basilyan, A. E. & Pavlova, E. Y. The Berelekh Mammoth 'Graveyard': New Chronological and Stratigraphical Data from the 2009 Field Season. *Geoarchaeology* **29**, 277–299 (2014).
20. Mocanov, Y. A. & Fedoseeva, S. A. Berelekh, Allakhovsk Region. in *American Beginnings: The Prehistory and Paleoecology of Beringia* (ed. West, F. H.) 218–221 (The University of Chicago Press, 1996).
21. Dilley, T. E. Late quaternary loess stratigraphy, soils, and environments of the Shaw Creek flats Paleoindian sites, Tanana Valley, Alaska. (1998).
22. Yesner, D. R., Holmes, C. E. & Crossen, K. J. Archaeology and paleoecology of the Broken Mammoth site, central Tanana Valley, interior Alaska, USA. *Current Research in the Pleistocene* **9**, 12 (1992).
23. Krasinski, K. E. & Yesner, D. R. Late Pleistocene/early Holocene site structure in Beringia: a case study from the Broken Mammoth site, interior Alaska. *Alaska Journal of Anthropology* **6**, 27–41 (2008).
24. Holmes, C. E. Broken Mammoth. in *American Beginnings: The Prehistory and Palaeoecology of Beringia* (ed. West, F. H.) 313–317 (University of Chicago Press, 1996).
25. Thorson, R. M. & Hamilton, T. D. Geology of the Dry Creek Site; a Stratified Early Man Site in Interior Alaska. *Quat. Res.* **7**, 149–176 (1977).
26. Goebel, T., Powers, R. & Bigelow, N. The Nenana Complex of Alaska and Clovis Origins. in *Clovis Origins and Adaptations* (eds. Bonnichsen, R. & Turnmire, K.) 49–79 (Center for the Study of the First Americans, 1991).
27. Powers, W. R. & Hamilton, T. D. *Dry Creek: A late Pleistocene human occupation in central Alaska*. (1978).
28. Powers, W. R. & Hoffecker, J. F. Late Pleistocene Settlement in the Nenana Valley, Central Alaska. *Am. Antiq.* **54**, 263–287 (1989).
29. Bigelow, N. H. & Powers, W. R. New AMS dates from the Dry Creek Paleoindian site, central Alaska. *Current Research in the Pleistocene* **11**, 114–116 (1994).
30. Bigelow, N. H. & Powers, W. R. Climate, Vegetation, and Archaeology 14,000–9000 Cal Yr B.P. in Central Alaska. *Arctic Anthropol.* **38**, 171–195 (2001).

31. Powers, W. R., Guthrie, R. D. & Hoffecker, J. F. *Dry Creek: Archaeology and paleoecology of a late Pleistocene Alaskan hunting camp*. (Texas A&M University Press, 2017).
32. Hoffecker, J. F., Powers, W. R. & Bigelow, N. H. Dry Creek. in *American Beginnings: The Prehistory and Paleoecology of Beringia* (ed. West, F. H.) 343–352 (The University of Chicago Press, 1996).
33. Graf, K. E. *et al.* Dry Creek Revisited: New Excavations, Radiocarbon Dates, and Site Formation Inform on the Peopling of Eastern Beringia. *Am. Antiq.* **80**, 671–694 (2015).
34. Potter, B. A., Gilbert, P. J., Holmes, C. E. & Crass, B. A. The Mead Site, a late Pleistocene - Holocene stratified site in Central Alaska. *Current Research in the Pleistocene* **28**, 73–75 (2011).
35. Little, A. A. Lithic Analysis at the Mead Site, Central Alaska. (University of Alaska Fairbanks, 2013).
36. Kunz, M. L. & Reanier, R. E. The Mesa Site: A Paleoindian Hunting Lookout in Arctic Alaska. *Arctic Anthropol.* **32**, 5–30 (1995).
37. Kunz, M. L. & Reanier, R. E. Paleoindians in beringia: evidence from arctic alaska. *Science* **263**, 660–662 (1994).
38. Reanier, R. E. The Antiquity of Paleoindian Materials in Northern Alaska. *Arctic Anthropol.* **32**, 31–50 (1995).
39. Bever, M. R. Stone Tool Technology and the Mesa Complex: Developing a Framework of Alaskan Paleoindian Prehistory. *Arctic Anthropol.* **38**, 98–118 (2001).
40. Bever, M. R. Distinguishing Holocene Microblades from a Paleoindian Component at the Mesa Site, Alaska. *J. Field Archaeol.* **33**, 133–150 (2008).
41. Pearson, G. A. Early Occupations and Cultural Sequence at Moose Creek: A Late Pleistocene Site in Central Alaska. *Arctic* **52**, 332–345 (1999).
42. Hoffecker, J. F. Moose Creek. in *American Beginnings: The Prehistory and Palaeoecology of Beringia* (ed. West, F. H.) 363–366 (University of Chicago Press, 1996).
43. Hoffecker, J. F. The Moose Creek site. *National Geographic Society Research Reports* **19**, 33–48 (1985).
44. Phippen, P. G. Archaeology at Owl Ridge: A Pleistocene-Holocene boundary age site in central Alaska. (University of Alaska Fairbanks, 1988).
45. Hoffecker, J. F., Powers, R. & Phippen, P. G. Owl Ridge. in *American Beginnings: The Prehistory and Palaeoecology of Beringia* (ed. West, F. H.) 353–356 (University of Chicago Press, 1996).
46. Graf, K. E. *et al.* Recent excavations at Owl Ridge, interior Alaska: Site stratigraphy, chronology, and site formation and implications for late Pleistocene archaeology and peopling of eastern Beringia. *Geoarchaeology* **35**, 3–26 (2019).
47. Hirasawa, Y. & Holmes, C. E. The relationship between microblade morphology and production technology in Alaska from the perspective of the Swan Point site. *Quat. Int.* **442**, 104–117 (2017).
48. Holmes, C. E. The Taiga period: Holocene archaeology of the northern boreal forest, Alaska. *Alaska Journal of Anthropology* **6**, 69–81 (2008).
49. Holmes, C. E. The Beringian and transitional periods in Alaska: technology of the east Beringian tradition as viewed from Swan point. in *From the Yenisei to the Yukon: Interpreting Lithic Assemblage Variability in Late Pleistocene/Early Holocene Beringia* (eds. Goebel, T. & Buvit, I.) 179–198 (Texas A&M University Press, 2011).
50. Holmes, C. E., VanderHoek, R. & Dilley, T. E. Swan Point. in *American Beginnings: The Prehistory and Palaeoecology of Beringia* (ed. West, F. H.) 319–323 (University of Chicago Press, 1996).
51. Coutouly, Y. A. G. & Holmes, C. E. The Microblade Industry from Swan Point Cultural Zone 4b: Technological and Cultural Implications from the Earliest Human Occupation in Alaska. *Am. Antiq.* **83**, 735–752 (2018).
52. Mochanov, Y. A. & Fedoseeva, S. A. Dyuktai Cave. in *American Beginnings: The Prehistory and Paleoecology of Beringia* (ed. West, F. H.) 164–174 (The University of Chicago Press, 1996).
53. Goebel, T., Waters, M. R. & Dikova, 2. Margarita. The Archaeology of Ushki Lake, Kamchatka, and the Pleistocene Peopling of the Americas. *Science* **301**, (2003).
54. Goebel, T., Powers, R., Bigelow, N. H. & Higgs, A. S. Walker Road. in *American Beginnings: The Prehistory and Palaeoecology of Beringia* (ed. West, F. H.) 356–363 (University of Chicago Press, 1996).
55. Morrow, J. E. & Fiedel, S. New radiocarbon dates for the Clovis component of the Anzick Site, Park County, Montana. in *Paleoindian archaeology: a hemispheric perspective* (eds. Morrow, J. E. & Gnecco, C.) 123–138 (University Press of Florida, 2006).
56. Rasmussen, M. *et al.* The genome of a Late Pleistocene human from a Clovis burial site in western Montana. *Nature* **506**, 225–229 (2014).

57. Stafford, T. W., Jull, A. J. T., Brendel, K., Duhamel, R. C. & Donahue, D. Study of Bone Radiocarbon Dating Accuracy at the University of Arizona NSF Accelerator Facility for Radioisotope Analysis. *Radiocarbon* **29**, 24–44 (1987).
58. Stafford, T. W., Hare, P. E., Currie, L., Jull, A. J. T. & Donahue, D. J. Accelerator radiocarbon dating at the molecular level. *J. Archaeol. Sci.* **18**, 35–72 (1991).
59. Lahren, L. & Bonnichsen, R. Bone Foreshafts From a Clovis Burial in Southwestern Montana. *Science* **186**, 147–150 (1974).
60. Wilke, P. J., Flenniken, J. J. & Ozbun, T. L. Clovis Technology at the Anzick Site, Montana. *J. Calif. Gt. Basin Anthropol.* **13**, 242–272 (1991).
61. Owsley, D. W., Hunt, D. R., Macintyre, I. G. & Logan, M. A. Clovis and Early Archaic Crania from the Anzick Site (24PA506), Park County, Montana. *Plains Anthropol.* **46**, 115–124 (2001).
62. Becerra-Valdivia, L. *et al.* Reassessing the chronology of the archaeological site of Anzick. *Proc. Natl. Acad. Sci. U. S. A.* **115**, 7000–7003 (2018).
63. Ferring, C. R. *The archaeology and paleoecology of the Aubrey Clovis site (41DN479) Denton County, Texas*. http://www.dtic.mil/docs/citations/ADA391588 (2001).
64. Ferring, C. R. The 1989 investigations at the Aubrey Clovis site, Texas. *Current Research in the Pleistocene* **7**, 0–12 (1990).
65. Haynes, C. V. & Agogino, G. A. Prehistoric Springs and Geochronology of the Clovis Site, New Mexico. *Am. Antiq.* **31**, 812–821 (1966).
66. Haynes, C. V. Geochronology of paleoenvironmental change, clovis type site, Blackwater draw, New Mexico. *Geoarchaeology* **10**, 317–388 (1995).
67. Howard, E. B. Association of artifacts with mammoth and bison in eastern New Mexico. *Science* **78**, 524 (1933).
68. Howard, E. B. The Occurrence of Flints and Extinct Animals in Pluvial Deposits near Clovis, New Mexico. Part I: Introduction. *Proceedings of the Academy of Natural Sciences of Philadelphia* **87**, 299–303 (1935).
69. Saunders, J. J., Agogino, G. A., Boldurian, A. T. & Haynes, C. V. A Mammoth-Ivory Burnisher-Billet from the Clovis Level, Blackwater Locality No. 1, New Mexico. *Plains Anthropol.* **36**, 359–363 (1991).
70. McAvoy, J. M. & McAvoy, L. D. *Archaeological Investigations of Site 44SX202, Cactus Hill, Sussex County, Virginia*. (Department of Historic Resources, 1997).
71. Feathers, J. K., Rhodes, E. J., Huot, S. & Mcavoy, J. M. Luminescence dating of sand deposits related to late Pleistocene human occupation at the Cactus Hill Site, Virginia, USA. *Quat. Geochronol.* **1**, 167–187 (2006/8).
72. Wagner, D. P. & McAvoy, J. M. Pedoarchaeology of Cactus Hill, a sandy Paleoindian site in southeastern Virginia, USA. *Geoarchaeology* **19**, 297–322 (2004).
73. Wagner, D. P. Cactus Hill, Virginia. in *Encyclopedia of Geoarchaeology* (ed. Gilbert, A. S.) 95–95 (Springer Netherlands, 2017).
74. Macphail, R. I. & McAvoy, J. M. A micromorphological analysis of stratigraphic integrity and site formation at Cactus Hill, an Early Paleoindian and hypothesized pre-Clovis occupation in south-central Virginia, USA. *Geoarchaeology* **23**, 675–694 (2008).
75. Goodyear, A. C. Evidence of Pre-Clovis Sites in the Eastern United States. in *Paleoamerican Origins: Beyond Clovis* (eds. Bonnichesen, R., Lepper, B. T., Standford, D. & Waters, M. R.) 103–112 (2005).
76. Frison, G. C. & Todd, L. C. *The Colby mammoth site: taphonomy and archaeology of a Clovis kill in northern Wyoming*. (University of New Mexico Press, 1986).
77. Walker, D. N. & Frison, G. C. The late Pleistocene mammalian fauna from the Colby Mammoth Kill site, Wyoming. *Rocky Mt Geol.* **19**, 69–79 (1980).
78. Morrow, J. E. *et al.* Pre-Clovis in Texas? A critical assessment of the 'Buttermilk Creek Complex'. *J. Archaeol. Sci.* **39**, 3677–3682 (2012).
79. Waters, M. R. *et al.* The Buttermilk Creek complex and the origins of Clovis at the Debra L. Friedkin site, Texas. *Science* **331**, 1599–1603 (2011).
80. Jennings, T. A. Clovis, Folsom, and Midland components at the Debra L. Friedkin site, Texas: context, chronology, and assemblages. *J. Archaeol. Sci.* **39**, 3239–3247 (2012).
81. Jennings, T. A. & Michael, R. Pre-Clovis Lithic Technology at the Debra L. Friedkin Site, Texas: Comparisons to Clovis Through Site-Level Behavior, Technological Trait-List, and Cladistic Analyses. *American Antiquity* **79**, 25–44 (2014).
82. Waters, M. R. *et al.* Pre-Clovis projectile points at the Debra L. Friedkin site, Texas—Implications for the Late Pleistocene peopling of the Americas. *Science Advances* **4**, eaat4505 (2018).

83. Haynes, C. V., Jr, McFaul, M., Brunswig, R. H. & Hopkins, K. D. Kersey--Kuner terrace investigations at the Dent and Bernhardt sites, Colorado. *Geoarchaeology: An International Journal* **13**, 201–218 (1998).
84. Brunswig, R. H. New interpretations of the Dent mammoth site. *Frontiers in Colorado Paleoindian archaeology* 87–121 (2007).
85. Saunders, J. J. Morphometrical analyses of Mammuthus columbi from the Dent site, Weld county, Colorado. *Deinsea* **6**, 55–78 (1999).
86. Agogino, G. Progress Report on the Chemical Removal of Preservative from Radiocarbon Samples. *La Conquista* **2**, (1963).
87. Agogino, G. An Early Attempt to Remove Preservatives from Bone. *Southwestern Lore* **63**, 42–43 (1997).
88. Deviѐse, T. *et al.* Increasing accuracy for the radiocarbon dating of sites occupied by the first Americans. *Quaternary Science Research* **198**, 171–180 (2018).
89. Leonhardy, F. C. *Domebo: A Paleo-Indian mammoth kill in the prairie-plains*. (Great Plains Historical Association, 1966).
90. Hofman, J. L. Dating the lower member of the Domebo Formation in western Oklahoma. *Current Research in the Pleistocene* **5**, 86–88 (1988).
91. Sanchez, G. *et al.* Human (Clovis)-gomphothere (Cuvieronius sp.) association ~ 13,390 calibrated yBP in Sonora, Mexico. *Proc. Natl. Acad. Sci. U. S. A.* **111**, 10972–10977 (2014).
92. Collins, M. B. The Gault Site, Texas, and Clovis research. *Athena Review* **3**, 31–42 (2002).
93. Vilsack, L. E. Investigations of Area 12: Gault Site. (Texas State University, San Marcos, 2016).
94. Gilmer, A. Geoarchaeological Investigations of Site Formation Processes in Area 15 at the Gault Site, Bell County, Texas. (Texas State University, San Marcos, 2013).
95. Gandy, J. L. Analysis of the lithic debitage from the older-than-Clovis stratigraphic layers of the Gault site, Texas. (Texas State University, San Marcos, 2013).
96. Williams, T. J. *et al.* Evidence of an early projectile point technology in North America at the Gault Site, Texas, USA. *Sci Adv* **4**, eaar5954 (2018).
97. Rodrigues, K. *et al.* OSL ages of the Clovis, Late Paleoindian, and Archaic components at Area 15 of the Gault Site, Central Texas, U.S.A. *Journal of Archaeological Science: Reports* **7**, 94–103 (2016).
98. Bement, L. C. & Carter, B. J. Clovis bison hunting at the Jake Bluff site, NW Oklahoma. *Current Research in the Pleistocene* **20**, 5–7 (2003).
99. Bement, L. C. & Carter, B. J. Jake Bluff: Clovis Bison Hunting on the Southern Plains of North America. *Am. Antiq.* **75**, 907–933 (2010).
100. Bement, L. C. & Carter, B. J. From Mammoth to bison: Changing Clovis Prey Availability at the End of the. *Clovis: On the Edge of a New Understanding* 263 (2014).
101. Hannus, L. A. The Lange/Ferguson Site: an event of Clovis mammoth butchery with the associated bone tool technology: the mammoth and its track. (Department of Anthropology, University of Utah, 1985).
102. Hannus, L. A. Flaked mammoth bone from the Lange/Ferguson site, White River badlands area, South Dakota. *Bone modification* 395–412 (1989).
103. Haynes, C. V. Contributions of Radiocarbon Dating to the Geochronology of the Peopling of the New World. in *Radiocarbon After Four Decades* 355–374 (Springer New York, 1992).
104. Taylor, R. E., Vance Haynes, C. & Stuiver, M. Clovis and Folsom age estimates: stratigraphic context and radiocarbon calibration. *Antiquity* **70**, 515–525 (1996).
105. Hannus, L. A. *Clovis Mammoth Butchery: The Lange/Ferguson Site and Associated Bone Tool Technology*. (Texas A&M University Press, 2018).
106. Haynes, C. V. Geochronology of the Lange/Ferguson Clovis Site. in *The Lange/Ferguson Site: An Event of Clovis Mammoth Butchery with an Associated Bone Tool Technology* (eds. Hannus, L. A. et al.) 29–59 (Texas A&M University Press, 2018).
107. Haury, E. W., Sayles, E. B. & Wasley, W. W. The Lehner Mammoth Site, Southeastern Arizona. *Am. Antiq.* **25**, 2–30 (1959).
108. Haynes, C. V. & Huckell, B. B. *Murray Springs: A Clovis Site with Multiple Activity Areas in the San Pedro Valley, Arizona*. (University of Arizona Press, 2007).
109. Haynes, C. V. & Hemmings, E. T. Mammoth-bone shaft wrench from murray springs, Arizona. *Science* **159**, 186–187 (1968).
110. McNett, C. W., McMillan, B. A. & Marshall, S. B. The Shawnee-Minisink Site. *Ann. N. Y. Acad. Sci.* **288**, 282–296 (1977).
111. McNett, C. W. *Shawnee Minisink: A Stratified Paleoindian–Archaic Site in the Upper Delaware Valley of Pennsylvania*. (Academic Press, 1985).

112. Gingerich, J. A. M. Revisiting Shawnee-Minisink. in *In the Eastern Fluted Point Tradition: Volume I* (ed. Gingerich, J. A. M.) vol. 1 218–256 (University of Utah Press, 2013).
113. Dent, R. J. Shawnee Minisink: new dates on the Paleoindian component. in *Poster presented at the 64th Annual Meeting of the Society for American Archaeology* (1999).
114. Gingerich, J. A. M. Shawnee-Minisink revisited: Re-evaluating the Paleoindian occupation. (University of Wyoming, 2007).
115. Gingerich, J. A. M. Down to Seeds and Stones: A New Look at the Subsistence Remains From Shawnee-Minisink. *Am. Antiq.* **76**, 127–144 (2011).
116. Gingerich, J. A. M., Whyte, T. R. & Whittaker, S. Misidentified Clovis-age fish bone at Shawnee-Minisink and the problem with single case studies in Late Pleistocene archaeology. *Journal of Archaeological Science: Reports* **25**, 94–99 (2019).
117. Waters, M. R., Stafford, T. W., Redmond, B. G. & Tankersley, K. B. The Age of the Paleoindian Assemblage at Sheriden Cave, Ohio. *Am. Antiq.* **74**, 107–111 (2009).
118. Redmond, B. G. & Tankersley, K. B. Evidence of Early Paleoindian Bone Modification and Use at the Sheriden Cave Site (33WY252), Wyandot County, Ohio. *Am. Antiq.* **70**, 503–526 (2005).
119. Tankersley, K. B. Sheriden: A Clovis cave site in eastern North America. *Geoarchaeology: An International Journal* **12**, 713–724 (1997).
120. Tankersley, K. B. & Landefeld, C. S. Geochronology of Sheriden Cave, Ohio: the 1997 field season. *Current Research in the Pleistocene* **15**, 136–138 (1998).
121. Tankersley, K. B. & Redmond, B. G. Radiocarbon dating of a Paleoindian projectile point from Sheriden Cave, Ohio. *Current Research in the Pleistocene* **16**, 76–77 (1999).
122. Tankersley, K. B., Ford, K. M., McDonald, H. G., Genheimer, R. A. & Hendricks, R. Late Pleistocene archaeology of Sheriden Cave, Wyandot County, Ohio. *Current Research in the Pleistocene* **14**, 81–83 (1997).
123. Tankersley, K. B., Redmond, B. G. & Grove, T. E. Radiocarbon dates associated with a single-beveled bone projectile point from Sheriden Cave, Ohio. *Current Research in the Pleistocene* **18**, 62–64 (2001).
124. Johnson, J. R., Stafford, T. W., Jr, Ajie, H. O. & Morris, D. P. Arlington springs revisited. in *Proceedings of the fifth California Islands symposium* vol. 23 541–545 (Santa Barbara, CA: Santa Barbara Museum of Natural History, 2002).
125. Orr, P. C. Arlington Springs man. *Science* **135**, 219 (1962).
126. McLaren, D. *et al.* Terminal Pleistocene epoch human footprints from the Pacific coast of Canada. *PLoS One* **13**, e0193522 (2018).
127. Johnson, E. & Holliday, V. T. Lubbock Lake: Late Quaternary cultural and environmental change on the Southern High Plains, USA. *J. Quat. Sci.* **4**, 145–165 (1989).
128. Holliday, V. T., Johnson, E., Haas, H. & Stuckenrath, R. Radiocarbon ages from the Lubbock Lake Site, 1950-1980: framework for cultural and ecological change on the Southern High Plains. *Plains Anthropologist* **28**, 165–182 (1983).
129. Knudson, R., Johnson, E. & Holliday, V. T. The 10,000-Year-Oid Lubbock Artifact Assemblage. *Plains Anthropol.* **43**, 239–256 (1998).
130. Johnson, E. & Holliday, V. T. Late Paleo-Indian Activity At The Lubbock Lake Site. *Plains Anthropol.* **26**, 173–193 (1981).
131. Johnson, E. & Holliday, V. T. A Plainview Kill/Butchering Locale On The Llano Est Acado-The Lubbock Lake Site. *Plains Anthropol.* **25**, 89–111 (1980).
132. Grayson, D. K. & Meltzer, D. J. Revisiting Paleoindian exploitation of extinct North American mammals. *J. Archaeol. Sci.* **56**, 177–193 (2015).
133. Grayson, D. K. & Meltzer, D. J. Clovis Hunting and Large Mammal Extinction: A Critical Review of the Evidence. *Journal of World Prehistory* **16**, 313–359 (2002).
134. Waters, M. R., Stafford, T. W., Jr, Kooyman, B. & Hills, L. V. Late Pleistocene horse and camel hunting at the southern margin of the ice-free corridor: reassessing the age of Wally's Beach, Canada. *Proc. Natl. Acad. Sci. U. S. A.* **112**, 4263–4267 (2015).
135. Kooyman, B., Hills, L. V., McNeil, P. & Tolman, S. Late Pleistocene Horse Hunting at the Wally's Beach Site (DhPg-8), Canada. *Am. Antiq.* **71**, 101–121 (2006).
136. McNeil, P., Hills, L. V., Kooyman, B. & Tolman, M. S. Late Pleistocene geology and fauna of the Wally's Beach Site (DhPg-8), Alberta, Canada. *Archaeology on the edge: new perspectives from the Northern Plains. Edited by B. Kooyman and J. Kelley. University of Calgary Press, Calgary, Alta. , Canadian Archaeological Association, Paper* 79–94 (2004).
137. Kooyman, B., Hills, L. V., Tolman, S. & McNeil, P. Late Pleistocene Western Camel (Camelops Hesternus) Hunting in Southwestern Canada. *Am. Antiq.* **77**, 115–124 (2012).

138. Wheat, A. D. Survey of professional opinions regarding the peopling of the Americas. *The SAA Archaeological Record* **12**, 10–14 (2012).
139. Cinq-Mars, J. & Morlan, R. E. Bluefish Caves and Old Crow Basin: A New Rapport. in *Ice Age People of North America: Environments, Origins, and Adaptations* (eds. Bonnichsen, R. & Turnmire, K. L.) 200–212 (Oregon State University Press, 1999).
140. Bourgeon, L., Burke, A. & Higham, T. Earliest Human Presence in North America Dated to the Last Glacial Maximum: New Radiocarbon Dates from Bluefish Caves, Canada. *PLoS One* **12**, e0169486 (2017).
141. Potter, B. A. *et al.* Current evidence allows multiple models for the peopling of the Americas. *Sci Adv* **4**, eaat5473 (2018).
142. Davis, L. G. & Schweger, C. E. Geoarchaeological context of late Pleistocene and early Holocene occupation at the Cooper's Ferry site, western Idaho, USA. *Geoarchaeology* **19**, 685–704 (2004).
143. Goebel, T., Hockett, B., Adams, K. D., Rhode, D. & Graf, K. Climate, environment, and humans in North America's Great Basin during the Younger Dryas, 12,900–11,600 calendar years ago. *Quat. Int.* **242**, 479–501 (2011).
144. Davis, L. G., Macfarlan, S. J. & Henrickson, C. N. A PXRF-based chemostratigraphy and provenience system for the Cooper's Ferry site, Idaho. *J. Archaeol. Sci.* **39**, 663–671 (2012).
145. Davis, L. G. *et al.* Late Upper Paleolithic Occupation at Cooper's Ferry, Idaho, USA Shows Americas Settled Before ~16,000 Years Ago. *Science* **365(6456)**, 891–897 (2019).
146. Overstreet, D. F. & Kolb, M. F. Geoarchaeological contexts for Late Pleistocene archaeological sites with human-modified woolly mammoth remains in southeastern Wisconsin, U.S.A. *Geoarchaeology* **18**, 91–114 (2003).
147. Johnson, E. Along the ice margin—The cultural taphonomy of Late Pleistocene mammoth in southeastern Wisconsin (USA). *Quat. Int.* **169-170**, 64–83 (2007).
148. Joyce, D. J. Chronology and new research on the Schaefer mammoth (?Mammuthus primigenius) site, Kenosha County, Wisconsin, USA. *Quat. Int.* **142**, 44–57 (2006).
149. Johnson, E. The taphonomy of mammoth localities in southeastern Wisconsin (USA). *Quat. Int.* **142**, 58–78 (2006).
150. Overstreet, D. F. Still more on cultural contexts of mammoth and mastodon in the southwestern Lake Michigan basin. *Current Research in the Pleistocene* **13**, 36–38 (1996).
151. Overstreet, D. F. Late Pleistocene geochronology and the Paleoindian penetration of the southwestern Lake Michigan Basin. *The Wisconsin Archeologist* **79**, 28–52 (1998).
152. Joyce, D. J. Pre-Clovis megafauna butchery sites in the western Great Lakes region, USA. in *Paleoamerican Oddysey* (eds. Graf, K. E., Ketron, C. V. & Waters, M. R.) 467–483 (Center for the Study of the First Americans, Texas A&M University College Station, 2014).
153. Overstreet, D. F. & Stafford, T. W., Jr. Additions to a revised chronology for cultural and non-cultural mammoth and mastodon fossils in the southwestern Lake Michigan Basin. *Current Research in the Pleistocene* **14**, (1997).
154. Dallman, J. E., Overstreet, D. F. & Stafford, T. W., Jr. A revised chronology for cultural and non-cultural mammoth and mastodon fossils in the southwestern Lake Michigan Basin. *Current Research in the Pleistocene* **13**, 10–13 (1996).
155. Davis, L. B. & Wilson, M. C. The late Pleistocene Lindsay mammoth (24DW501), eastern Montana: Possible man-mammoth association. *Current Research in the Pleistocene* **2**, 97–98 (1985).
156. Hill, C. L. & Davis, L. B. Stratigraphy, AMS radiocarbon age, and stable isotope biogeochemistry of the Lindsay Mammoth, eastern Montana. *Current Research in the Pleistocene* **15**, 109–112 (1998).
157. Krasinski, K. E. Broken bones and cutmarks: Taphonomic analyses and implications for the peopling of North America. (University of Nevada, Reno, 2010).
158. Waters, M. R. & Stafford, T. W. The first Americans: A review of the evidence for the Late-Pleistocene peopling of the Americas. *Paleoamerican odyssey* 543–562 (2013).
159. Huber, J. K. & Hill, C. L. Paleoecological inferences based on pollen and stable isotopes for mammoth-bearing deposits of the Oahe Formation (Aggie Brown Member), eastern Montana. *Current Research in the Pleistocene* **20**, 95–97 (2003).
160. Waters, M. R. *et al.* Pre-Clovis Mastodon Hunting 13,800 Years Ago at the Manis Site, Washington. *Science* **334**, 351–353 (2011).
161. Gustafson, C. E., Gilbow, D. W. & Daugherty, R. D. The Manis Mastodon Site: Early Man on the Olympic Peninsula. *Canadian Journal of Archaeology / Journal Canadien d'Archéologie* 157–164 (1979).
162. Petersen, K. L., Mehringer, P. J. & Gustafson, C. E. Late-Glacial Vegetation and Climate at the Manis Mastodon site, Olympic Peninsula, Washington. *Quat. Res.* **20**, 215–231 (1983).

163. Haynes, C. V. & Huckell, B. B. The Manis Mastodon: An Alternative Interpretation. *PaleoAmerica* **2**, 189–191 (2016).
164. Goldberg, P. & Arpin, T. L. Micromorphological Analysis of Sediments from Meadowcroft Rockshelter, Pennsylvania: Implications for Radiocarbon Dating. *J. Field Archaeol.* **26**, 325–342 (1999).
165. Adovasio, J. M., Pedler, D. R., Donahue, J. & Stuckenrath, R. Two Decades of Debate on Meadowcroft Rockshelter. *North American Archaeologist* **19**, 317–341 (1998).
166. Adovasio, J. M., Gunn, J. D., Donahue, J. & Stuckenrath, R. Excavations at Meadowcroft Rockshelter, 1973-1974: A Progress Report. *Pennsylvania Archaeologist* **45**, 1–30 (1975).
167. Adovasio, J. M., Donahue, J. & Stuckenrath, R. The Meadowcroft Rockshelter Radiocarbon Chronology 1975-1990. *Am. Antiq.* **55**, 348–354 (1990).
168. Adovasio, J. M., Gunn, J. D., Donahue, J. & Stuckenrath, R. Meadowcroft Rockshelter, 1977: An Overview. *Am. Antiq.* **43**, 632–651 (1978).
169. Haynes, C. V. Paleoindian Charcoal from Meadowcroft Rockshelter: Is Contamination a Problem? *Am. Antiq.* **45**, 582–587 (1980).
170. Kelly, R. L. A Comment on the Pre-Clovis Deposits at Meadowcroft Rockshelter. *Quat. Res.* **27**, 332–334 (1987).
171. Halligan, J. J. *et al.* Pre-Clovis occupation 14,550 years ago at the Page-Ladson site, Florida, and the peopling of the Americas. *Sci Adv* **2**, e1600375 (2016).
172. Webb, S. D. *First Floridians and Last Mastodons: The Page-Ladson Site in the Aucilla River*. (Springer Science & Business Media, 2006).
173. Jenkins, D. L. Distribution and dating of cultural and paleontological remains at the Paisley Five Mile Point Caves in the northern Great Basin. *Paleoindian or Paleoarchaic* 57e81 (2007).
174. Jenkins, D. L. *et al.* Geochronology, archaeological context, and DNA at the Paisley Caves. in *Paleoamerican Odyssey* (eds. Graf, K. E., Ketron, C. V. & Waters, M. R.) 485–510 (Center for the Study of the First Americans, Texas A&M University College Station, 2014).
175. Gilbert, M. T. P. *et al.* DNA from pre-Clovis human coprolites in Oregon, North America. *Science* **320**, 786–789 (2008).
176. Hockett, B. & Jenkins, D. L. Identifying Stone Tool Cut Marks and the Pre-Clovis Occupation of the Paisley Caves. *Am. Antiq.* **78**, 762–778 (2013).
177. Sistiaga, A., Berna, F., Laursen, R. & Goldberg, P. Steroidal biomarker analysis of a 14,000 years old putative human coprolite from Paisley Cave, Oregon. *J. Archaeol. Sci.* **41**, 813–817 (2014).
178. Shillito, L. M. *et al.* New Research at Paisley Caves: Applying New Integrated Analytical Approaches to Understanding Stratigraphy, Taphonomy, and Site Formation Processes. *PaleoAmerica* **4**, 82–86 (2018).
179. Ardelean, C. F. Archaeology of Early Human Occupations and the Pleistocene-Holocene Transition in the Zacatecas Desert, Northern Mexico. (University of Exeter, 2013).
180. Ardelean, C. F. *et al.* Evidence of human occupation in Mexico around the Last Glacial Maximum. *Nature* https://doi.org/10.1038/s41586-020-2509-0 (2020).
181. Goebel, T., Graf, K. & Rhode, D. The Paleoindian occupations at Bonneville Estates Rockshelter, Danger Cave, and Smith Creek Cave (eastern Great Basin, USA): Interpreting their radiocarbon chronologies. *British Archaeological Reports (BAR) International Series* **1655**, 147 (2007).
182. Graf, K. E. Stratigraphy and chronology of the Pleistocene to Holocene transition at Bonneville Estates Rockshelter, eastern Great Basin. in *Paleoindian or Archaic? Great Basin Human Ecology at the Pleistocene-Holocene Transition* (eds. Graf, K. E. & Schmitt, D. N.) 82–104 (The University of Utah Press, 2007).
183. Goebel, T., Graf, K. E., Hockett, B. & Rhode, D. Late-Pleistocene humans at Bonneville Estates Rockshelter, eastern Nevada. *Current Research in the Pleistocene* **20**, 3 (2003).
184. Goebel, T., Holmes, A., Keene, J. L. & Coe, M. M. Technological Change from the Terminal Pleistocene Through Early Holocene in the Eastern Great Basin, USA: The Record from Bonneville Estates Rockshelter. in *Lithic Technological Organization and Paleoenvironmental Change: Global and Diachronic Perspectives* (eds. Robinson, E. & Sellet, F.) 235–261 (Springer International Publishing, 2018).
185. Hockett, B. Nutritional ecology of late Pleistocene to middle Holocene subsistence in the Great Basin: zooarchaeological evidence from Bonneville Estates Rockshelter. *Paleoindian or paleoarchaic* 204–230 (2007).
186. Rhode, D. & Louderback, L. A. Dietary plant use in the Bonneville basin during the terminal Pleistocene/early Holocene transition. *Paleoindian or Paleoarchaic* 231–247 (2007).
187. Green, T. J. *et al.* The Buhl Burial: A Paleoindian Woman from Southern Idaho. *Am. Antiq.* **63**, 437–456 (1998).

188. Holen, S. R. *et al.* A 130,000-year-old archaeological site in southern California, USA. *Nature* **544**, 479–483 (2017).
189. Braje, T. J. *et al.* Were Hominins in California ~130,000 Years Ago? *PaleoAmerica* vol. 3 200–202 (2017).
190. Haynes, G. The Cerutti Mastodon. *PaleoAmerica* **3**, 196–199 (2017).
191. Ferraro, J. V. *et al.* Contesting early archaeology in California. *Nature* **554**, E1–E2 (2018).
192. Magnani, M. *et al.* Evaluating claims for an early peopling of the Americas: experimental design and the Cerutti Mastodon site. *Antiquity* **93**, 789–795 (2019).
193. Ferrell, P. M. The Cerutti Mastodon Site Reinterpreted with Reference to Freeway Construction Plans and Methods. *PaleoAmerica* **5**, 1–7 (2019).
194. Sutton, M. Q., Parkinson, J. & Rosen, M. D. Observations Regarding the Cerutti Mastodon. *PaleoAmerica* **5**, 8–15 (2019).
195. González, A. *et al.* The first human settlers on the Yucatán Peninsula: evidence from drowned caves in the state of Quintana Roo (South Mexico). in *Paleoamerican Odyssey* (eds. Graf, K. E., Ketron, C. V. & Waters, M. R.) 323–337 (Center for the Study of the First Americans, Texas A&M University College Station, 2014).
196. Zazzo, A. & Saliège, J.-F. Radiocarbon dating of biological apatites: A review. *Palaeogeogr. Palaeoclimatol. Palaeoecol.* **310**, 52–61 (2011).
197. Cook, J. P. Healy Lake. in *American Beginnings: The Prehistory and Palaeoecology of Beringia* (ed. West, F. H.) 323–327 (University of Chicago Press, 1996).
198. Byers, D. A. Taphonomic analysis, associational integrity, and depositional history of the Fetterman mammoth, eastern Wyoming, USA. *Geoarchaeology: An International Journal* **17**, 417–440 (2002).
199. Mackie, M. M., Surovell, T. A., Kelly, R. L. & O'Brien, M. J. New Excavations at the La Prele Mammoth Site, Converse County, Wyoming. (2017).
200. Holliday, V. T., Haynes, C. V., Jr, Hofman, J. L. & Meltzer, D. J. Geoarchaeology and geochronology of the Miami (Clovis) site, southern High Plains of Texas. *Quat. Res.* **41**, 234–244 (1994).
201. Taylor, R. E. Six Decades of Radiocarbon Dating in New World Archaeology 1. *Radiocarbon* **51**, 173–212 (2009).
202. Brose, D. S. Archaeological investigations at the Paleo Crossing site, a Paleoindian occupation in Medina County, Ohio. *The first discovery of America: Archaeological evidence of the early inhabitants of the Ohio area* 61–76 (1994).
203. Boulanger, M. T. *et al.* Neutron activation analysis of 12,900-year-old stone artifacts confirms 450–510+ km Clovis tool-stone acquisition at Paleo Crossing (33ME274), northeast Ohio, U.S.A. *J. Archaeol. Sci.* **53**, 550–558 (2015).
204. Eren, M. I. & Redmond, B. G. Clovis Blades at Paleo Crossing (33ME274), Ohio. *MidCont. J. Archaeol.* **36**, 173–194 (2011).
205. Eren, M. I. *et al.* Paleo Crossing (33ME274): a Clovis site in northeastern Ohio. in *In the Eastern Fluted Point Tradition: Volume II* (ed. Gingerich, J. A. M.) vol. 2 187–210 (University of Utah Press, 2018).
206. Miller, G. L. Illuminating activities at Paleo Crossing (33ME274) through microwear analysis. Lithic Technol 38 (2): 108--197. *Lithic Technology* **38**, 108–197 (2013).
207. Eren, M. I., Redmond, B. G. & Kollecker, M. A. Unifacial stone tool analyses from the Paleo Crossing site (33-ME-274), Ohio. *Current Research in the Pleistocene* **22**, 43–45 (2005).
208. Eren, M. I. The Paleo Crossing (33-ME-274) non-projectile point biface assemblage. *Current Research in the Pleistocene* **23**, 95–97 (2006).
209. Eren, M. I. Anvil Reduction at the Early-Paleoindian Site of Paleo Crossing (33ME274), Northeast Ohio. *Current Research in the Pleistocene* **27**, 75–77 (2010).
210. Eren, M. I., Redmond, B. G. & Kollecker, M. A. The Paleo Crossing (33-ME-274) fluted point assemblage. *Current Research in the Pleistocene* **21**, 38–39 (2004).
211. Tankersley, K. B. & Holland, J. D. Lithic Procurement Patterns at the Paleo Crossing Site, Medina County, Ohio. *Current Research in the Pleistocene* **11**, 61–63 (1994).
212. Eren, M. I. & Kollecker, M. A. Data on the post-Paleoindian projectile point assemblage from the Paleo Crossing Site (33-ME-274). *Ohio Archaeol* **54**, (2004).
213. Eren, M. I. *et al.* Thermoluminescence (TL) and Optically Stimulated Luminescence (OSL) Dating of Two Burned Clovis Wyandotte Chert Lithic Specimens from Paleo Crossing (33ME274), Ohio, USA. *Lithic Technology* **43**, 18–25 (2018).
214. Waters, M. R., Forman, S. L., Stafford, T. W., Jr. & Foss, J. Geoarchaeological investigations at the Topper and Big Pine Tree sites, Allendale County, South Carolina. *J. Archaeol. Sci.* **36**, 1300–1311 (2009/7).

215. Bronk Ramsey, C. Development of the radiocarbon program OxCal. *Radiocarbon* **43**, 355–363 (2001).